

A46

Mechanisms of cell death in energy depleted cardiomyocytes

Role of calcium overload, calpain and phospholipase

Douwe E. Atsma

TNO Preventie en Gezondheid
Gaubius-bibliotheek
Zernikedreef 9
Postbus 2215, 2301 CE Leiden

16573

STELLINGEN

Mechanisms of cell death in energy depleted
cardiomyocytes

Role of calcium overload, calpain and phospholipase

Douwe E. Atsma

Stellingen bij het proefschrift "Mechanisms of cell death in energy depleted cardiomyocytes".

1. Calcium overload is een belangrijke determinant voor celdood van de anoxische hartcel. (dit proefschrift)
2. Calcium Activated Neutral Protease (CANP) is geen essentiële determinant voor het ontstaan van celdood in hartcellen tijdens anoxie. (dit proefschrift)
3. Zure incubatie van anoxische hartcellen vermindert of voorkomt celdood van deze cellen. (dit proefschrift, Bond *et al. Biochem Biophys Res Comm* 1991;179:798-803)
4. Een rol voor fosfolipase A₂ bij het ontstaan van celdood in anoxische hartcellen kan niet worden uitgesloten. (dit proefschrift, Van der Vusse *et al. NIPS* 1989;4:49-53)
5. De rol van apoptose bij reperfusieschade van het hart en bij het ontstaan van decompensatio cordis verdient nadere aandacht. (Bing. *J Moll Cell Cardiol.* 1994; 26:943-948)
6. Oxidatief gemodificeerd low-density lipoproteïn gemerkt met een radiofarmaca kan van grote waarde zijn bij de non-invasieve detectie van atherosclerose. (Atsma *et al. Arterios Thromb.* 1993;13: 78-83)
7. De discipline en het uithoudingsvermogen opgedaan tijdens wedstrijdroeien is van grote waarde tijdens het uitvoeren en voltooiën van promotieonderzoek. Om deze reden dient wedstrijdroeien te worden opgenomen in het curriculum van de AIO.
8. Veel farmaca hebben vele andere werkingen naast de werking waarvoor deze stoffen worden aanbevolen en verkocht. Conclusies over biologische werkingsmechanismen op grond van experimenten met farmaca met een vermeende "specifieke" activiteit dienen met terughoudendheid getrokken te worden.
9. Medisch wetenschappelijk onderzoek moet klinisch relevant zijn.
10. Het noorden van ons land wordt nog gekenmerkt als oord voor rust en ruimte. Het dienen als overloop van de economische activiteiten van de Randstad heeft een betwistbaar nut.
11. De Friese taal is klankrijker dan het Nederlands.

12. W.H.O. cares? (*Lancet* 1995;345:203)
13. De snelle technologische ontwikkelingen van computergeheugens bevorderen het ontwikkelen van het menselijk geheugen niet.
14. Een carrière als medicus is meer een renbaan dan een loopbaan.

D.E. Atsma
Leiden, 25 september 1996

Mechanisms of cell death in energy depleted cardiomyocytes

Role of calcium overload, calpain and phospholipase

Proefschrift
ter verkrijging van de graad van Doctor
aan de Rijksuniversiteit te Leiden,
op gezag van de Rector Magnificus Dr. L. Leertouwer,
hoogleraar in de faculteit der Godgeleerdheid,
volgens besluit van het College van Dekanen
te verdedigen op woensdag 25 september 1996
te klokke 16.15 uur

door

Douwe Ekke Atsma

geboren te Rijswijk in 1961

Promotiecommissie

Promoter Prof. dr. A. van der Laarse

Referent: Prof. dr. G.J. van der Vusse (Rijksuniversiteit Limburg)

Overige leden: Prof. dr. P. Brakman
 Prof. dr. A.V.G Brusckhe
 Prof. dr. C. Ince (Universiteit van Amsterdam)

Financial support by the Netherlands Heart Foundation and the '3A-out gelden', Department of Internal Medicine, University Hospital Leiden, for the publication of this thesis is gratefully acknowledged.

Boaskjen en bargeslachtsjen, it hat syn útfallen
(siswize)

Oan Hait en Mem
Aan Marjolijn

Contents

| | | |
|-----------|--|-----|
| Chapter 1 | Introduction | 1 |
| Chapter 2 | Measurement of intracellular Ca^{2+} concentration using fluorescent probes and fluorescence videomicroscopy | 33 |
| Chapter 3 | A novel two-compartment culture dish allows microscopic evaluation of two different treatments in one cell culture simultaneously: Influence of external pH on $\text{Na}^+/\text{Ca}^{2+}$ exchanger activity in cultured rat cardiomyocytes <i>Pflügers Archiv</i> . 1994;428:296-299 | 53 |
| Chapter 4 | Role of Calcium Activated Neutral Protease (Calpain) in cell death in cultured neonatal rat cardiomyocytes during metabolic inhibition <i>Circ Res</i> . 1995;76:1071-1078 | 63 |
| Chapter 5 | I. Role of phospholipid degradation in death of anoxic cardiomyocytes. Effect of purported PLA_2 inhibitors on calcium overload and phospholipid degradation | 85 |
| Chapter 6 | II. Role of phospholipid degradation in death of anoxic cardiomyocytes. Effect of halo-enol lactone, an inhibitor of plasmalogen-selective phospholipase A_2 | 109 |
| Chapter 7 | Low external pH limits cell death in energy depleted cardiomyocytes by decreasing Ca^{2+} overload via $\text{Na}^+/\text{Ca}^{2+}$ exchange inhibition <i>Am J Physiol</i> . 1996; 270:H2149-H2156 | 123 |
| Chapter 8 | Summary and general discussion | 141 |
| Chapter 9 | Samenvatting en algemene discussie | 147 |

| | | |
|----------|--|-----|
| | Nawoord | 153 |
| | List of publications | 155 |
| | Curriculum vitae | 159 |
| Appendix | Cyclic-GMP and nitric oxide modulate thrombin-induced endothelial permeability. Regulation via different pathways in human aortic and umbilical vein endothelial cells <i>Circ Res.</i> 1995;76:199-208 | 161 |

Chapter 1

Introduction

The basic mechanism responsible for myocardial ischemic cell death is unclear. Many manifestations of ischemic cell injury, which precede actual cell death, have been reported, including a depletion of high-energy nucleotides, development of contracture, loss of ion homeostasis, bleb formation, cellular swelling, formation of contraction bands, mitochondrial swelling, and formation of granular mitochondrial dense bodies.¹⁻⁴ However, the single decisive factor responsible for the transition of reversible cell injury to cell death has not yet been identified.

Detailed knowledge of the mechanism of cell death would facilitate the conception of treatments aimed to salvage ischemic myocardium from cell death. Many hypotheses on the mechanism of myocardial cell death have been postulated, including the lysosomal, mitochondrial, metabolic end product, calcium overload, phospholipase and lipid peroxidation hypotheses.³⁻⁸ Despite considerable effort, these theories have remained unproven.

The research described in this thesis is aimed to provide insight into the mechanism of the development of cell death in cardiomyocytes, and specifically investigates the hypothesis schematically depicted in figure 1. This hypothesis links the development of calcium overload during ischemia to the activation of intracellular proteases and phospholipases, which by their degradative actions damage the sarcolemmal membrane to such an extent that cell death follows inevitably.

This chapter provides background information on the various aspects involved in the hypothesis under investigation, namely I) calcium overload, II) Calcium Activated Neutral Protease (CANP) and III) phospholipase A₂.

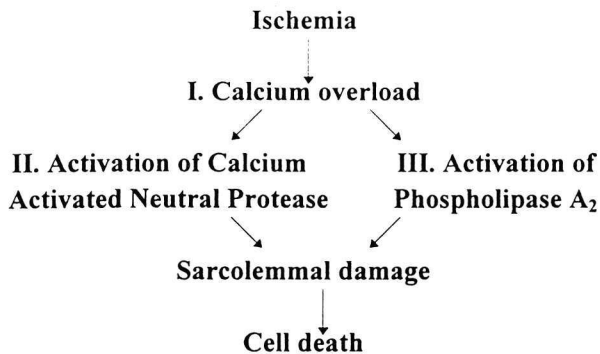


Figure 1. Hypothesis for the development of cell death in heart cells during ischemia, which is the subject of the research described in this thesis.

I. Calcium overload

In recent years, the alterations in ion homeostasis in anoxic, ischemic or energy-depleted heart cells have drawn strong attention. It has been observed that under these conditions the intracellular free calcium concentration ($[Ca^{2+}]_i$) rises dramatically, leading to a condition referred to as 'calcium overload'.⁹⁻¹¹ This phenomenon has also been observed in reoxygenated or reperfused myocardium.¹²⁻¹⁴ As calcium overload was found to occur in a variety of pathological states prior to cell damage and cell death, calcium overload was proposed to play a causal role in the development of cell damage and cell death.⁹

Calcium homeostasis in the normal cell

In the heart, Ca^{2+} has a pivotal role in excitation-contraction coupling, and in signal transduction. As intracellular Ca^{2+} is a powerful mediator between extracellular events (e.g. action potential, hormones binding to receptors) and the intracellular sequelae (contraction, protein synthesis), its intracellular concentration ($[Ca^{2+}]_i$) must be strictly controlled in order to tightly regulate the various Ca^{2+} -mediated processes. Under normal conditions, $[Ca^{2+}]_i$ in the cardiomyocyte is maintained at a diastolic level of 60-100 nM, with transients during each contraction of 400-800 nM.¹⁵ This concentration is 10,000 fold (diastolic) to 1000 fold (systolic) lower than the extracellular Ca^{2+} concentration, which is in the order of 2.5 mM, of which approximately 50% is bound to proteins. The powerful regulatory systems involved in the regulation of $[Ca^{2+}]_i$ comprise of ion channels, ion pumps and ion exchangers, situated in the sarcolemma, sarcoplasmic reticulum (SR) and mitochondria. Figure 2 shows a schematic representation of the various cellular components involved in cellular calcium homeostasis. It is estimated that the maintenance of the steep transsarcollemmal Ca^{2+} gradient consumes approximately 25 % of the cell's total energy expenditure.¹⁶ Each of the components of the $[Ca^{2+}]_i$ regulatory system will be briefly discussed here (for extensive reviews on myocardial calcium homeostasis see references¹⁵⁻¹⁷).

1. Ca^{2+} channels. Upon depolarization, Ca^{2+} influx from the extracellular compartment takes place along its concentration gradient via sarcolemmal transient (T)-type channels and long-lasting (L)-type Ca^{2+} channels, which are activated at a more negative and less negative membrane potential, respectively.¹⁶ The extent of Ca^{2+} influx through the sarcolemmal channels can be graded over a wide range with high maximal flux values.¹⁶

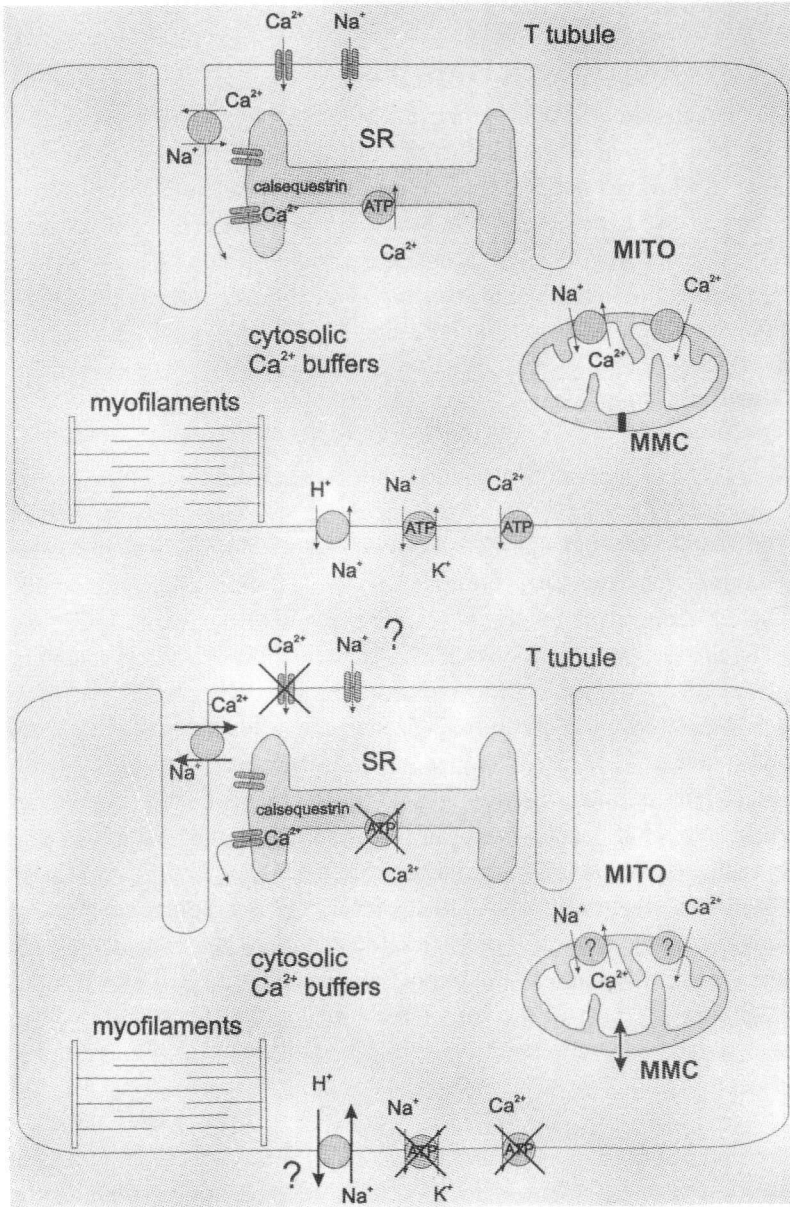


Figure 2. Schematic representation of cellular components involved in calcium homeostasis in cardiomyocytes, during control conditions (top), and during ischemia or energy depletion (bottom) (SR=sarcoplasmic reticulum, MITO=mitochondrion, MMC=mitochondrial megachannel). Adapted from Silverman *et al.*¹

2. *Na⁺/Ca²⁺ exchanger*. The sarcolemmal Na⁺/Ca²⁺ exchanger is situated on the entire myocyte surface, but is especially concentrated in the T-tubule region of the myocyte.^{18,19} Because of its stoichiometry of 3 Na⁺ : 1 Ca²⁺, the exchanger is an electrogenic transporter. The Na⁺/Ca²⁺ exchanger is the major Ca²⁺ efflux mechanism of the cell, responsible for 75% of the Ca²⁺ efflux under control conditions.²⁰ Its direction of operation and level of activity is dictated by the transsarcolemmal gradients of Na⁺ ions and of Ca²⁺ ions, and by the membrane potential.¹⁵ At resting membrane potential, the Na⁺/Ca²⁺ exchanger is in the 'forward' mode, extruding Ca²⁺ ions in return for Na⁺ ion uptake. As [Na⁺]_i is controlled largely by Na⁺/K⁺-ATPase, this latter pump is an important indirect control mechanism for Na⁺/Ca²⁺ exchange activity.

3. *Ca²⁺-ATPase*. The sarcolemmal Ca²⁺-ATPase requires the free energy of the hydrolysis of one ATP molecule to extrude one Ca²⁺ ion against its concentration gradient. In cultured cells, its rate of Ca²⁺ extrusion appears to be one tenth that of Na⁺/Ca²⁺ exchange.²¹ As its K_m for Ca²⁺ is approximately 0.5 μM, the sarcolemmal Ca²⁺-ATPase is thought to be involved in the regulation of the diastolic [Ca²⁺]_i. The activity of the sarcolemmal Ca²⁺-ATPase is complexly regulated and under calmodulin control.¹⁶

4. *Sarcoplasmic reticulum*. The sarcoplasmic reticulum is an important dynamic intracellular storage site for the Ca²⁺ ions which are released during excitation-contraction coupling. Uptake of Ca²⁺ into the sarcoplasmic reticulum is mediated by the sarcoplasmic Ca²⁺-ATPase, which transports, in contrast to the sarcolemmal Ca²⁺-ATPase, two Ca²⁺ ions into the SR for each ATP molecule hydrolyzed. This Ca²⁺-ATPase is controlled by phospholamban. Ca²⁺ which has been transported into the SR is bound to the calcium-binding protein calsequestrin, which binds approx. 50 Ca²⁺ ions per protein molecule. During each excitation-contraction cycle, Ca²⁺ is released from the sarcoplasmic reticulum into the cytosol via ryanodine-sensitive Ca²⁺ release channels, which are controlled by a variety of factors including ATP, calmodulin and phosphorylation of the channel.

5. *Cytosolic Ca²⁺ buffers*. In addition to the above mentioned transport mechanisms involved in calcium homeostasis, [Ca²⁺]_i is also regulated by binding of Ca²⁺ to intracellular Ca²⁺ buffers.²²⁻²⁴ These buffers include troponin C, calmodulin, ATP, creatine phosphate, and the mitochondrial outer membrane. Of particular interest is the assumption of a large buffering role of the sarcolemmal inner membrane, where Ca²⁺ is thought to bind to negatively charged phospholipids.^{22,25,26}

6. *Mitochondria.* The regulation of the mitochondrial Ca^{2+} concentration ($[\text{Ca}^{2+}]_m$) is intimately linked to the regulation of mitochondrial enzyme activities, including pyruvate dehydrogenase, NAD^+ -isocitrate dehydrogenase and α -ketoglutarate dehydrogenase,^{16,27} in order to accommodate changes in energy demand. Under normal conditions, $[\text{Ca}^{2+}]_m$ is lower than $[\text{Ca}^{2+}]_i$,¹ and does not show beat-to-beat variation.^{16,28} However, physiological increases in $[\text{Ca}^{2+}]_i$ which take place over a longer period, e.g. after adrenergic stimulation, result in an increased $[\text{Ca}^{2+}]_m$ and consequently in increased dehydrogenase activities.²⁸ Uptake of Ca^{2+} into the mitochondria is mediated by a Ca^{2+} -uniporter and is driven by the mitochondrial membrane potential (-150 mV to -180 mV as compared to cytosol), which results from active outward H^+ pumping coupled to electron transport.²⁹ Efflux of Ca^{2+} occurs via a $\text{Na}^+/\text{Ca}^{2+}$ exchanger,³⁰ the maximum capacity of which is approximately one tenth of the Ca^{2+} uniporter. Another regulatory pathway is referred to as the 'mitochondrial megachannel' or 'permeability transition pore', and seems to be a megachannel activated by large increases in $[\text{Ca}^{2+}]_m$.³¹

$[\text{Ca}^{2+}]_i$ during excitation-contraction coupling

The interplay between the various components involved in calcium homeostasis becomes apparent during the excitation-contraction coupling. The action potential causes depolarization of the cell membrane as a result of Na^+ influx through Na^+ -channels and Ca^{2+} influx through voltage-operated Ca^{2+} -channels. Recently it has been proposed that Ca^{2+} influx during cell depolarization can also occur via the $\text{Na}^+/\text{Ca}^{2+}$ exchanger,³² but this notion is still controversial. The small quantity of Ca^{2+} that enters the cell upon depolarization induces the release of larger quantities of Ca^{2+} from the sarcoplasmic reticulum, by binding to and subsequent activation of SR Ca^{2+} release channels.¹⁵ This phenomenon is known as the 'calcium-induced calcium release'. There is evidence that not all sarcoplasmic Ca^{2+} is released through this mechanism, but rather that the magnitude of Ca^{2+} release from the SR can be modulated by the amount of trigger Ca^{2+} entering the cell during depolarization,²⁴ thereby regulating inotropy. Upon its release, the Ca^{2+} from the SR induces a conformational change of troponin C, thereby relieving its inhibition of actin and myosin interaction, leading to contraction.

The decay of the Ca^{2+} transient is mediated by the re-uptake of Ca^{2+} by the SR, and extrusion of Ca^{2+} from the myocyte by the sarcolemmal $\text{Na}^+/\text{Ca}^{2+}$ exchanger and the sarcolemmal Ca^{2+} -ATPase. Uptake of Ca^{2+} in the SR is carried out by the sarcoplasmic Ca^{2+} -ATPase, which is activated by phosphorylation of its regulatory protein phospholamban. Although competition for Ca^{2+} exists between the sarcolemmal $\text{Na}^+/\text{Ca}^{2+}$ exchanger and the sarcoplasmic Ca^{2+} -ATPase, the quantity of

Ca^{2+} which is extruded by the $\text{Na}^+/\text{Ca}^{2+}$ exchanger balances the amount of Ca^{2+} that entered the cell upon depolarization, when the cell is in the steady state.

Mechanism of calcium overload

Studies in isolated hearts and in myocardial cells have shown that reduction or removal of extracellular Ca^{2+} ions leads to a reduction or absence of calcium overload during ischemia or hypoxia.^{33,34} These results indicate that calcium overload is mainly the result of entry of extracellular Ca^{2+} ions into the cytosol. The current opinion is that the rise in $[\text{Ca}^{2+}]_i$ upon ischemia is not caused by physical leaks in the sarcolemma, but by perturbations in the calcium homeostasis pathways. Only during prolonged ischemia $[\text{Ca}^{2+}]_i$ may increase further due to extracellular Ca^{2+} ions entering the cell through sarcolemmal defects.^{3,35}

Entry pathways for extracellular Ca^{2+} ions include Ca^{2+} channels and the sarcolemmal $\text{Na}^+/\text{Ca}^{2+}$ exchanger. However, increased influx of Ca^{2+} ions during ischemia does not appear to occur through the voltage-dependent calcium channels, as the calcium current is reduced or has disappeared after 15 min of ischemia due to depolarization, ATP depletion and acidosis.³⁶ In addition, the Ca^{2+} channel blockers verapamil and nifedipine have no effect on Ca^{2+} entry in hypoxic/reoxygenated cardiomyocytes.^{13,37}

Several studies which employ a variety of methodologies indicate that the major part of Ca^{2+} entry during ischemia and anoxia occurs via the sarcolemmal $\text{Na}^+/\text{Ca}^{2+}$ exchanger.³⁸⁻⁴¹ In the normal situation, the exchanger operates in the *forward mode*, extruding one Ca^{2+} ion in return for three Na^+ ions. However, if a relatively modest increase in the intracellular Na^+ concentration ($[\text{Na}^+]_i$) is present, the exchanger switches direction and operates in *reversed mode*, extruding Na^+ ions while loading the cell with extracellular Ca^{2+} ions, leading to calcium overload.^{16,40} In addition, as cellular ATP levels fall, Ca^{2+} extrusion via the sarcolemmal Ca^{2+} -ATPase and Ca^{2+} uptake in the sarcoplasmic reticulum slows down, further contributing to the rise in $[\text{Ca}^{2+}]_i$. Also, redistribution of cellular Ca^{2+} ions during ischemia and energy depletion may contribute to the development of calcium overload.⁴²⁻⁴⁴

The rise in $[\text{Na}^+]_i$ during ischemia, anoxia or metabolic inhibition which is required for uptake of extracellular Ca^{2+} ions via reversed $\text{Na}^+/\text{Ca}^{2+}$ exchange, has been reported by several investigators.⁴⁵⁻⁴⁷ Potential mechanisms responsible for the ischemia-induced increase in $[\text{Na}^+]_i$ include: 1) failure of the Na^+/K^+ -ATPase to extrude Na^+ ions as a result of ATP depletion and/or decreased intracellular pH (pH_i),⁴⁸ 2) Na^+ influx via Na^+/H^+ exchange, driven by the increase in H^+ ions during ischemia,⁴⁹ or 3) Na^+ influx via voltage gated Na^+ channels, as inhibitors of these channels such as lignocaine, R56865 or tetrodotoxin^{46,50-52} attenuate Na^+ overload.

Previously, Na⁺ channels were thought to be inactivated during ischemia because of prolonged membrane depolarization. Recent findings, however, suggest that ischemic metabolites including lysophosphatidylcholine⁵³ and long chain acylcarnitines⁵⁴ induce Na⁺ channel activation and/or slow inactivation, leading to an increased open probability of the Na⁺ channel. Determination of the relative contribution of each of the above mentioned mechanisms to the development of Na⁺ overload during ischemia awaits further experimental work.

In addition to cytoplasmic calcium overload, excessive Ca²⁺ loading in mitochondria has also been held responsible for cellular dysfunction and cell damage.⁵⁵ Upon anoxia a rise in [Ca²⁺]_m is observed which may be reversible upon reoxygenation in reversibly injured cells,⁵⁶ whereas in hypercontracting cells a persistent elevation of [Ca²⁺]_m is observed.²⁷ Prevention of mitochondrial Ca²⁺ uptake during anoxia by ruthenium Red appears to have beneficial effects on myocyte function and viability.^{56,57} Also, prevention of the opening of the mitochondrial megachannel by cyclosporin A, an inhibitor of the mitochondrial megachannel, leads to attenuated cell damage in anoxic heart cells.⁵⁸ However, these studies do not provide a definite answer concerning the role of mitochondrial dysfunction due to mitochondrial calcium overload in the development of ischemic myocardial cell damage.

An intriguing new concept in the pathogenesis of calcium overload is the involvement of the so-called 'calcium leak channel'.^{59,60} This channel, present in various cell types including cardiomyocytes, has been partially characterized: 1) it is selective for divalent ions, 2) it is not blocked by classic L-type calcium blockers, but polycationic protamine blocks the channel completely, and 3) its activity is increased upon energy depletion.^{59,60} The channel is constitutively present in cells, but is inhomogeneously distributed over the entire cell population. It is tempting to attribute at least some of the heterogeneity in the response of cardiomyocytes to states of energy depletion to this inhomogeneous distribution of the channel. Further detailed research is required to establish the role of calcium leak channels in the development of myocardial calcium overload during ischemia, anoxia and energy depletion.

II. Calcium Activated Neutral Protease (CANP)

Calcium Activated Neutral Protease (CANP), also known as Calpain, was first described 30 years ago.⁶¹ Since then CANP activity has been found in practically all eukaryotic cells in various species. The cysteine protease (EC 3.4.22.17) actually exists in two distinct isoforms.⁶² Together with two specific regulatory proteins, one inhibitory and one stimulatory, CANP is part of a complex and highly regulated

Ca²⁺-dependent proteolytic system. The enzymes exist as pro-enzymes and are, at least *in vitro*, regulated by Ca²⁺ ions and autoproteolysis.

The physiological role of CANP in cellular protein metabolism is proposed to be regulatory rather than degradative, as the enzymatic action of CANP results in modification, rather than degradation of its substrates. This way CANP is involved in modulating activity, structure and function of regulatory enzymes including protein kinase C, structural proteins such as ankyrin, and receptor proteins like the steroid hormone receptor.⁶³

In addition to its role in cellular physiology, CANP has been implicated in several pathological states. CANP is thought to play a harmful role in a variety of pathologic states, such as in Duchenne muscular dystrophy,⁶⁴ in neurodegenerative conditions including Alzheimer disease,⁶⁵ ischemia,⁶⁶ and multiple sclerosis;⁶⁷ in toxic⁶⁸ and anoxic^{69, 70} injury in hepatocytes, in oxidative stress in endothelial cells,⁷¹ and in the development of cataract.⁷²

Several studies have addressed the involvement of CANP in anoxic or ischemic cell death in heart cells. In these studies conflicting results have been reported as to the activation of CANP during anoxia or ischemia, and the effects of inhibitors of CANP on cell injury. An *increased* CANP activity was found in regionally ischemic rat hearts *in vivo*,⁷³ in Langendorff-perfused rat hearts after ischemia/reperfusion⁷⁴ and in anoxic rat cardiomyocytes.⁷⁵ In contrast, a *decreased* CANP activity was found in ischemic dog heart.⁷⁶ In addition, a CANP inhibitor temporarily protected the ischemic rabbit heart in one study,⁷⁶ whereas in another study no effect of inhibitors of CANP on infarct size in ischemic rat hearts was found.⁷⁷

The involvement of CANP in cell death as an effector of irreversible cell injury constitutes an attractive hypothesis, as the proteolytic action of CANP is Ca²⁺-dependent and among its purported substrates are several key cytoskeletal proteins.⁶³ Thus, massive supraphysiological activation of CANP during ischemia would link the developing calcium overload with the subsequent degradation of the sarcolemmal membrane, thereby causing myocardial cell death.⁷⁸

This hypothesis has been subject of the research described in chapter 4 of this thesis.

1. Biochemistry. Originally, Ca²⁺-dependent proteolytic activity was thought to be caused by a single CANP which required high concentrations of Ca²⁺ (>1 mM) for activity.⁷⁹ Later it was discovered that a second enzyme exists, which has many similarities with the original CANP in terms of biochemical and catalytic properties, but differs notably in its Ca²⁺ requirement. The enzyme described originally, now known as CANP II, mCANP or Calpain II, required millimolar concentrations of Ca²⁺ ions for full proteolytic activity, whereas the enzyme described later, known as CANP

I, μ CANP or Calpain I, requires only micromolar concentrations of Ca^{2+} ions for full proteolytic activity.⁶³

Most mammalian (and probably most avian) cells contain both CANP I and CANP II, with the exception of erythrocytes, which appear to contain only CANP I. Both enzymes have the form of a heterodimer, consisting of a large subunit (~80 kD) and a small subunit (~30 kD)^{80,81} (Figure 3). Minor variations in molecular weight of each subunit exist between different cell types. Within a single cell type, the size of the small subunits of CANP I and CANP II is identical, whereas the large subunits can differ by as much as ~5 kD.⁸² Several reports have described monomeric CANPs with a molecular weight ranging from 96 to 150 kD.^{83,84}

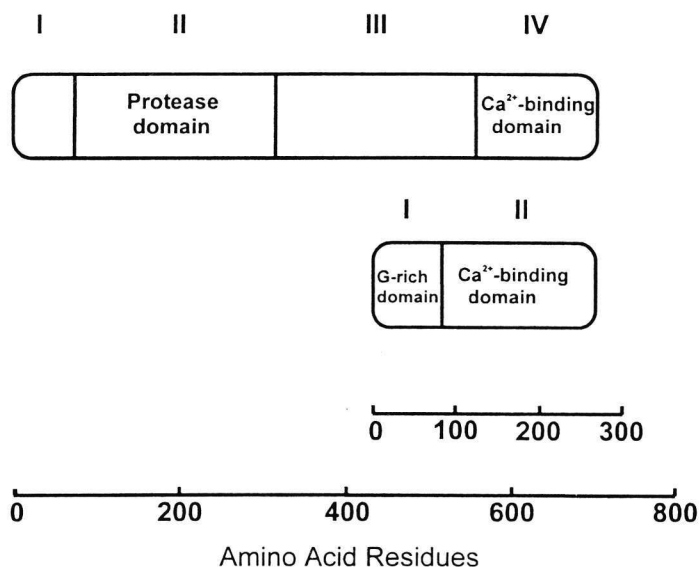


Figure 3. Schematic representation of the general structure of CANP I and CANP II. It shows the large subunit (80 kD), containing four domains, on top and the small subunit (30 kD), containing two domains, below. The large and small subunits are linked at their Ca^{2+} binding domain to form a heterodimer. Adapted from ref. ⁶³

2. *Characterization of CANP I and CANP II.* Although originally CANP I and CANP II were considered to be two forms of the same enzyme, extensive studies on the amino acid composition,^{80,85} immunological properties,^{86,87} and amino acid sequence information obtained from cDNA cloning experiments have established that CANP I and CANP II are two distinct enzymes.^{88,89}

The 80 kD subunit of both enzymes consists of four domains (Figure 3). Domain II (amino acids 77-316, ~35% of the sequence) is the proteolytic domain and has similarities to other sulphhydryl proteases such as papain, cathepsin B and cathepsin H.^{90,91} Domain IV (amino acids 556-699, ~20% of the sequence at the COOH

terminus) is the Ca^{2+} -binding domain and has marked similarity to Ca^{2+} binding proteins such as calmodulin and troponin C. The domain contains four Ca^{2+} binding sites, so called EF-hand structures, which are characteristic for Ca^{2+} binding proteins.^{91,92} The function of domain I (amino acids 1-76, ~10 % at the NH_2 terminus of the sequence) and domain III (amino acids 317-555, ~35% of the sequence) is less clear. These domains may be involved in the interaction with regulatory proteins such as the inhibitor or the stimulator protein of the CANPs. The NH_2 terminal end of the sequence (domain I) probably has a regulatory role, as it is autoproteolytically cleaved during activation of the protease.^{93,94}

The 30 kD subunit of CANP I and II (Figure 3) consists of 266 amino acids, as deduced from the sequence of the cDNA encoding the protein.⁹⁴ This subunit consists of two domains, connected by a proline-rich sequence (amino acids 76-81). Domain I (amino acids 1-75) contains ~50% glycine and other hydrophobic residues. This finding suggests that this domain is involved in the interaction with cellular membranes.^{95, 96} Domain II (amino acids 81-266) is homologous to domain IV of the large subunit, and therefore also resembles Ca^{2+} binding proteins such as calmodulin. The COOH terminal region of the 30 kD subunit is considered important in the interaction with the 80 kD subunit.⁹³

Each heterodimer of the enzyme binds 5-6 moles Ca^{2+} per mole CANP.⁹⁷ Of the eight possible Ca^{2+} binding sites in each CANP heterodimer, it was found that in the large subunit the first, second and fourth EF-hand structure are the most likely Ca^{2+} binding sites, whereas in the small regulatory subunit the first and the fourth EF-hand loop exhibited the highest affinity for Ca^{2+} ions.^{92, 98}

3. Catalytic properties. No major differences exist between CANP I and CANP II with respect to their catalytic properties. The main distinction between the two isoforms is their requirement for Ca^{2+} ions. *In vitro*, CANP I needs 1-20 μM Ca^{2+} for half-maximal proteolytic activity, whereas CANP II needs 250-750 μM Ca^{2+} for half-maximal activity.^{80,99,100} In the absence of Ca^{2+} ions, neither enzyme exhibits any proteolytic activity. The enzymes have a pH optimum of about 7.5. They belong to the cysteine class of proteases due to the involvement of a cysteine residue at the active catalytic site. Therefore, the proteases are irreversibly inhibited by alkylating agents such as iodoacetamide, iodoacetate and N-ethylmaleimide.¹⁰¹ Other sulfhydryl protease inhibitors, such as leupeptin, E64 and antipain (see below), are also potent inhibitors with inhibitory constants (K_i) of approximately 1 μM .¹⁰²

Table 1. Proteins cleaved by calcium-activated neutral proteases (CANP)

Myofibrillar and nonmuscle cytoskeletal proteins

| | |
|-----------------------|---------------------------------|
| Tropomyosin | Filamin (actin-binding protein) |
| Troponin I and C | Talin |
| Myosin light chain | Frodin/Spectrin |
| C protein | Ankyrin |
| Vimentin/Desmin | Platelet α -actinin |
| NF200, NF160 and NF68 | α -Crystallin |
| MAP-I and -II | Myelin basic protein |
| Tubulin | |

Enzymes and receptors

| | |
|-------------------------------|--------------------------|
| Phosphorylase b kinase | Ca ²⁺ -ATPase |
| Protein kinase C | Transglutaminase |
| Myosin light-chain kinase | Calcineurin |
| EGF receptor | Glycogen synthase |
| PDGF receptor | Phospholipase C |
| Steroid hormone receptors | HMG-CoA reductase |
| α -adrenergic receptor | Tyrosine hydroxylase |
| Aromatic hydrocarbon receptor | Tryptophan hydroxylase |

From: D.E. Croall, *Physiol Rev* 1991;71:813.

4. *Substrate specificity.* *In vitro*, a large number of proteins and peptides are proteolyzed by CANP I and CANP II in cell free systems (Table 1). Whether these proteins and peptides are also substrates for CANP in intact cells, is unclear. The extent of substrate proteolysis by CANP ranges from extensive, as with casein,¹⁰³ to limited as with talin,¹⁰⁴ spectrin,¹⁰⁵ frodrin,¹⁰⁶ 3-hydroxy-3-methylglutamyl (HMG)-CoA reductase,¹⁰⁷ and protein kinase C.¹⁰⁸ As to the specificity of the cleavage sites, the two CANPs do not differ. The amino acid composition adjacent to the cleaved peptide bond is slightly variable, implying that substrate susceptibility to proteolysis by CANP could be determined by the amino acid sequence near the peptide bond to be cleaved. Of the small substrates, the peptides with a basic or bulky group (arginine, lysine, tyrosine and methionine) at the P1 position, and hydrophobic groups (leucine and valine) at the P2 position are the best substrates for CANP. The observed cleavage site specificities correlate well with the actions of several peptidyl protease inhibitors for CANP. Leupeptin (propionyl(or acetyl)-L-leucyl-L-leucyl-L-

argininal) and antipain (S-(1-carboxy-2-phenylethyl)carbonyl-L-arginyl-L-valylargininal) are powerful inhibitors of CANP. The leucyl-containing peptide epoxide E64 (N-[N-(L-3-trans-carboxy oxiran-2-carbonyl)-L-leucyl]-amido-(4-guanidino)butane) is also an effective CANP inhibitor. The identification of the cleavage site specificity of CANP, combined with the observed efficacy of the above mentioned biological CANP inhibitors, allowed synthesis of several new inhibitors. Several tripeptidyl chloromethyl ketones synthesized by Sasaki *et al.*¹⁰⁹ are effective at less than micromolar concentrations. The newly synthesized benzoylcarbonyl leucyl-norleucinal (calpeptin) and benzyloxycarbonyl leucyl-methioninal proved effective at concentrations of approximately 50 nM.¹¹⁰ In addition to its potent CANP inhibitory action, calpeptin is cell permeable, which allows the study of CANP in intact cells.

5. *Autoproteolytic activation of CANP in vitro.* Limited Ca^{2+} -induced autoproteolysis of CANP plays an essential role in the regulation of CANP proteolytic activity.^{111,112} The function of autoproteolysis of CANP is to convert the inactive proenzyme into its active form.^{85,113} As a result of autoproteolysis, the molecular weight of the small subunit decreases from 30 kD through several intermediate steps to approximately 17 kD.^{94,111} After autoproteolysis, the small subunit remains associated with the large subunit. Also in the large 80 kD catalytic subunit of CANP autoproteolysis takes place. In this subunit, approximately 4-7 kD is removed from the NH_2 -terminus (domain I) during Ca^{2+} -dependent autoproteolysis.^{80,85}

Another consequence of autoproteolytic processing of the two CANP isoforms is a significant decrease in the Ca^{2+} concentration required for activity. This is especially true for CANP II, for which the Ca^{2+} requirement is lowered 20-50 fold to $\sim 10\mu\text{M}$ for half maximal activity.

The physiological consequences of this reduced Ca^{2+} requirement following autoproteolysis is unclear, as the concentrations of Ca^{2+} needed for the lowering of the Ca^{2+} requirement are similar to the Ca^{2+} concentrations needed for CANP proteolytic activity *in vitro*, i.e. micromolar and millimolar concentrations of Ca^{2+} ions for CANP I and CANP II, respectively. However, there may be additional mechanisms *in vivo* which are able to lower the Ca^{2+} requirement of CANP, such as the interaction of CANP II with phosphatidylinositol.^{95,96} This latter mechanism is attractive in view of the various proposed CANP-membrane interactions, and the known signal transduction pathways which involve phosphatidylinositol. The phosphorylation-dephosphorylation mechanism which regulates the activity of many cellular enzymes does not regulate CANP activity directly, but may regulate its function indirectly at the level of the substrate.

Phosphorylated forms of troponin¹¹⁴ and of HMG-CoA reductase¹¹⁵ are degraded more rapidly by CANP than their dephosphorylated forms. In contrast, the phosphorylated form of filamin is degraded more slowly by CANP as compared to its dephosphorylated form.¹¹⁶

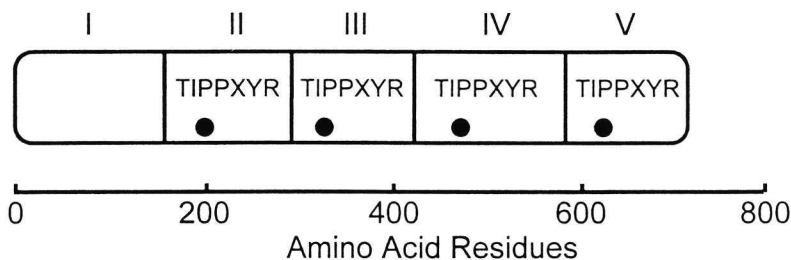


Figure 4. General structure of the CANP inhibitor calpastatin. It consists of five domains, four of which have a repeating structure of approximately 140 amino acids. Each of these four domains have inhibitory activity. Adapted from ref.⁶³

6. *Endogenous CANP-regulating proteins: calpastatin.* The endogenous inhibitor of CANP, calpastatin, is co-distributed with CANP in all cells.^{117,118} The absolute quantity of the inhibitor and the relative concentration with respect to CANP differs widely among cell types.^{63,118} However, in crude cell extracts of many cell types including heart, the concentration of calpastatin is sufficiently high to completely block the activity of CANP *in vitro*.^{119,120} Whether this means that CANP activity is also completely inhibited in intact cells is unclear.

The exact biochemical characteristics of calpastatin have not yet been defined. Its reported molecular weight ranges from 34 to 400 kD,⁶³ with the most commonly reported values of ~120 kD and ~70 kD. The inhibitory action is directed exclusively to both CANPs, with no other proteases affected. Calpastatin interacts with the CANPs only if Ca^{2+} is bound to CANP, suggesting that a Ca^{2+} -induced conformational change of the CANP isoforms is necessary to interact with the inhibitor.^{117,121} Upon addition of Ca^{2+} -chelating agents, the binding between the inhibitor and CANP is reversed. A remarkable characteristic of the interaction of calpastatin with CANP is its unusual stoichiometry. One molecule of calpastatin has been reported to inhibit multiple CANP molecules, the latter number ranging from 3 to 12.⁶³

The primary sequence of calpastatin, as deduced from analysis of cloned cDNA, consists of 718 and 713 amino acids in rabbit and porcine tissue, respectively.^{122,123}

The amino acid sequence of calpastatin contains four similar domains with homologous repeating regions of ~140 amino acids (Figure 4). The presence of these four repeated, homologous structures could explain the observed inhibition of multiple

CANP molecules by a single calpastatin molecule. This hypothesis is further supported by the finding that fragments of calpastatin as small as 15 kD retain inhibitory activity, with a concomitant decrease in stoichiometry.¹²¹ Although calpastatin was previously thought to be distributed exclusively in the cytosol, recent evidence suggests that a considerable fraction (up to 30%) may be associated with the membrane.^{124,125} This finding is significant as it is compatible with today's view that CANP exerts its function primarily at the cell membrane.⁶³

7. *Endogenous CANP-regulating proteins: Stimulatory protein.* Recently, a specific stimulatory protein has been isolated which enhances CANP activity *in vitro* up to 25-fold. The protein is present in several tissues, and was isolated from both cytosolic and membrane fractions.^{126,127} The finding that the membrane appears to contain the highest fraction of the CANP stimulatory protein is in agreement with the hypothesis that CANP functions at the cellular membrane. Further research is needed to elucidate the role of the stimulatory protein in CANP regulation *in vivo*.

8. *Physiological functions of CANP.* In contrast to the extensive knowledge about the biochemical characteristics of CANP, little is known about its physiological role(s). The reasons for this are: a) the lack of knowledge about the physiological substrate(s) of CANP *in vivo* hampers the study of CANP activity in intact cells, b) as the interaction of CANP with calpastatin and its stimulatory protein *in vivo* is not well understood, the extrapolation of results from *in vitro* experiments to CANP's physiological roles *in vivo* is difficult, and c) there is a lack of specific cell-permeable inhibitors for CANP.

Firstly, it is not clear whether CANP should be categorized as a degradative enzyme, mediating extensive protein breakdown, or a regulatory enzyme, catalyzing only limited proteolysis of selected substrates, hereby altering the biological function of the substrate.^{128,129} Some investigators interpret the degradation of cytoskeletal proteins and protein kinases by CANP as a degradative breakdown of the substrates,^{129,130} whereas others look upon the proteolytic processing of cytoskeletal proteins and protein kinases by CANP as a regulatory event. In favor of the latter hypothesis, CANP was found to modulate the sensitivity of phosphorylase b kinase,¹³¹ protein kinase C,¹⁰⁸ plasma membrane Ca^{2+} -ATPase,¹³² and myosin light-chain kinase,¹³³ for their physiological regulatory molecules, rather than to degrade the substrates substantially.

Secondly, the site of CANP activity is unknown. Immunohistochemical studies have revealed the selective localization of CANP to Z-lines in skeletal muscle,¹³⁴ to adhesion sites in certain cell lines,¹³⁵ and to a sub-plasma membrane region in myoblasts.¹²⁸ However, the earlier mentioned finding that CANPs are present in the form of inactive proenzymes throughout the cells, may frustrate attempts to link localization of CANP, usually determined by the use of antibodies, mostly polyclonal, to any physiological role of activated CANP.

Several factors point to the plasma membrane as the primary site of CANP activity: 1) CANP interacts with phosphatidylinositol and other phospholipids,^{96,136} 2) CANP is also associated with Ca^{2+} -dependent signal transduction pathways,⁶³ the components of which are located mainly at the cytoplasmic side of the plasma membrane, 3) the plasma membrane contains Ca^{2+} channels which can provide the Ca^{2+} ions needed for CANP activation and several putative substrates for CANP, such as talin, fodrin, ankyrin, and Ca^{2+} -ATPase, 4) the interaction between CANP and the plasma membrane is facilitated by the fact that CANP molecules in their proenzyme form are slightly hydrophobic,⁸⁰ and 5) the Ca^{2+} -induced conformational change of CANP increases its hydrophobicity, further favoring membrane association.¹³⁷

III. Phospholipase A_2

Myocardial cell membranes

Numerous studies which investigated the development of ischemic myocardial cell death have focused on the ischemia-induced perturbations in the cardiomyocyte membranes, as proper membrane functioning is of vital importance to the maintenance of cellular homeostasis. Hence, damage of the cellular membranes is liable to result in cellular dysfunction, and eventually, cell death.

The myocardium contains three major, functionally distinct membrane systems: the sarcolemma (containing 2-4% of cellular lipids), sarcoplasmic reticulum, and mitochondria (containing >75% of cellular lipids).¹³⁸

The sarcolemmal membrane serves simultaneously as: 1) a semipermeable barrier between the cytoplasm and the interstitial space, allowing the existence of the specialized milieu interieure, 2) an active surface where many biochemical conversions take place, and 3) a solvent for proteins involved in signal transduction, substrate transport and ion homeostasis. The sarcoplasmic reticulum is a dynamic Ca^{2+} storage and release reservoir which plays a pivotal role in calcium homeostasis during excitation/contraction coupling. The mitochondria are the sites for energy production and have a double bilayer membrane which is tailored for this task.

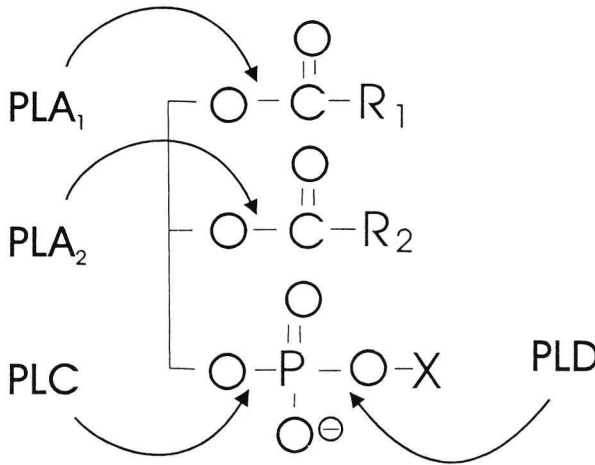


Figure 5. General chemical structure of phospholipids and the site of action of various phospholipases. R_1 and R_2 : aliphatic tails of fatty acyl moieties connected to the sn-1 and sn-2 positions of the glycerol backbone, respectively. X represents polar head group, linked via a phosphodiester linkage to the sn-3 position of the glycerol backbone. PLA₁, PLA₂, PLC and PLD represent phospholipase A₁, A₂, C and D, respectively.

Myocardial phospholipids

Myocardial membranes consist of polar lipids, including phospholipids, which are arranged in a bilayer configuration, interspersed with nonpolar lipids such as cholesterol, and proteins, such as ion channels.

The myocardial phospholipids are comprised of a glycerol backbone, with typically two long-chain fatty acids covalently bound to the sn-1 and sn-2 positions of the glycerol backbone (Figure 5). At the sn-3 position, a polar headgroup is covalently bound via a phosphodiester linkage.

Phospholipids are divided into a) classes, based on the chemical nature of the polar head group (e.g. choline, inositol, ethanolamine), b) subclasses, based on the nature of the covalent linkage to the sn-1 position (e.g. ester vs. ether bonds), and c) molecular species, based on the chain length and degree of unsaturation of the aliphatic constituents at the sn-1 and sn-2 positions.

In myocardial cells, the classes of phospholipids are asymmetrically distributed over the inner and outer leaflet of the sarcolemma, with the negatively charged phosphatidylinositol (PI) and phosphatidylserine (PS) almost exclusively located in the inner leaflet.¹³⁹ Phosphatidylethanolamine (PE) is predominantly present in the inner leaflet (75%) and sphingomyelin (Sph) predominantly (93%) located in the outer leaflet. Phosphatidylcholine (PC) is equally distributed over the inner and outer leaflets.¹³⁹

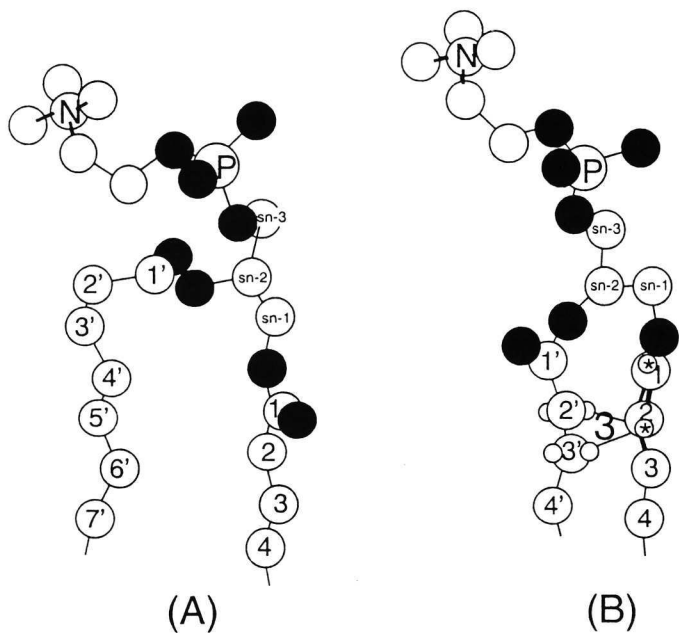


Figure 6. Structure of phosphatidylcholine (A) and the predicted structure of plasmenylcholine (B). The difference between the two molecules lies in the nature of the covalent linkage of the acyl moiety at the sn-1 position: an ester bond in phosphatidylcholine vs. a vinyl-ether linkage in plasmenylcholine. The model predicts a closer relation between the sn-1 and sn-2 aliphatic chains in the plasmalogen phospholipid, influencing its behaviour in membrane systems. (P and N: phosphorus and nitrogen atoms, resp. Solid circles: oxygen atoms; open circles: carbon atoms). Adapted from ref.¹³⁸

In contrast to most mammalian cells which contain mostly diacyl phospholipids (phosphatidylcholine and phosphatidylethanolamine), myocardial sarcolemma and sarcoplasmic reticulum contain sizable fractions of plasmalogen species (plasmenylcholine and plasmenylethanolamine),¹⁴⁰ i.e. phospholipids containing a vinyl ether linkage rather than an ester bond at the sn-1 position. The fraction of sarcolemmal plasmalogen phospholipids in different species is highly variable, ranging from approximately 12 % of sarcolemmal phospholipids in rat,^{141, 142} to 40 % in rabbit and 45 % in dog.¹³⁸ Plasmalogens have different dynamics and different geometry (Figure 6) as compared to diacyl phospholipids. They appear to be exclusively confined to heart, brain and nerves, and their structure probably reflects the specialized role of these phospholipids in electroresponsive membranes.¹⁴³ Cholesterol influences plasmalogen dynamics,¹⁴⁴ and possibly its propensity to phospholipase A₂ (PLA₂) mediated hydrolysis.¹⁰⁷

Biochemical phospholipid degradation theory

During myocardial ischemia, an accelerated turnover of cellular phospholipids has been observed.¹⁴⁵⁻¹⁴⁸ The sarcolemma appears to be the selective target for accelerated phospholipid degradation in energy-depleted cardiomyocytes.^{1,148} Several authors have proposed that activation of cellular phospholipases including

PLA₂, which catalyzes the hydrolysis of acyl moieties from the sn-2 position of phospholipids, is a critical event in the development of ischemic cell death.

The involvement of PLA₂ in the ischemia-induced degradation of cardiac phospholipids during ischemia has been inferred from several (experimental) observations:

1) In ischemic myocardium, various phospholipid degradation products accumulate, including arachidonic acid and lysophospholipids.^{147,149-152} As arachidonic acid is predominantly (approximately 99.3%) located at the sn-2 position of myocardial phospholipids,¹³⁸ its liberation is conceivably due to PLA₂ activity. In addition to damage due to degradation of constitutive membranous phospholipid components, the accumulation of the degradation products may also lead to cellular dysfunction. The accumulation of arachidonic acid in ischemic heart cells may lead to altered electrophysiological characteristics of ion channels and gap junctions in myocytes.^{153,154} In addition, transport of liberated arachidonic acid from the myocytes to endothelial cells and circulating blood cells may influence vascular reactivity, thrombosis and leukocyte margination. The accumulation of lysophospholipids may have detrimental effects on cellular function as well, as lysophospholipids influence action potentials in Purkinje fibers and ventricular myocytes,¹⁴⁵ alter ligand-receptor coupling,¹⁴⁰ and modulate the activity of transmembrane ion pumps.¹⁵⁵ They also have marked effects on the biophysical properties of cellular membranes, which may alter the activity of many membrane proteins, whose function is influenced by the molecular dynamics of the membrane domains surrounding their membrane spanning elements.^{140,156}

2). Various purported chemical inhibitors of PLA₂ have been reported to have protective effects on ischemic, anoxic or energy depleted cardiomyocytes, further lending support to the concept of ischemic cell death due to PLA₂-induced phospholipid degradation.^{146,151,157-160} In addition, monoclonal antibodies directed against myocardial PLA₂ reduced ischemia-induced phospholipid degradation and myocardial cell death in isolated rat hearts.¹⁶¹

Although an ischemia-induced increase in PLA₂ activity may well explain the observed accumulation of arachidonic acid, it should be stressed that net arachidonic acid liberation during ischemia may theoretically also result from other mechanisms, such as: 1) impaired reacylation of lysophospholipids with arachidonic acid due to ischemia-induced damage to the reacylation mechanism,¹⁵⁷ 2) the consecutive action of phospholipase C and diacylglycerol lipase or monoacylglycerol lipase, or 3) the consecutive action of phospholipase D, phosphatidic acid phosphatase and diacylglycerol lipase.¹³⁸

Recently, a unique PLA₂ activity was identified in canine, rabbit and human myocardium, which is Ca²⁺-independent and selective for a plasmalogen

substrate.^{140,162,163} This PLA₂ has a molecular weight of 40 kD and a pH optimum of 6.4. The purified enzyme selectively hydrolyzed ether-containing phospholipids (1-alkenyl-2-acyl PC > 1-alkyl-2-acyl PC > 1,2 diacyl PC). Phospholipids with arachidonic acid at the sn-2 position were preferentially hydrolyzed, as with 'ordinary' PLA₂. It appears that this plasmalogen-selective PLA₂ activity is regulated by ATP.¹⁴⁰

Already 5 min after start of ischemia in a Langendorff-perfused rabbit heart, membrane-associated calcium-independent plasmalogen-selective PLA₂ activity was increased 10-fold, whereas no increase in diacyl selective PLA₂ activity was detected.¹⁶⁴ Plasmalogen-selective PLA₂ activation paralleled lactate accumulation. Upon reperfusion, plasmalogen-selective PLA₂ activity decreased in parallel with the decrease in lactate accumulation.¹⁶⁴ Accumulation of lyso-plasmalogen phospholipids results in an alteration in membrane dynamics that is five times greater than those observed with lyso-phospholipids,¹⁴⁰ potentially contributing greatly to ischemia-induced membrane perturbations.

Despite the above mentioned factors supporting an important role for PLA₂ in ischemia-induced myocardial cell death, it is still not clear whether phospholipid degradation is a causal factor in ischemic myocardial cell death, or whether it is merely the consequence of it, reflecting autolysis of necrotic heart cells. In this respect, it has been reported that loss of cell membrane integrity during ischemia can occur before substantial accumulation of lysophospholipids takes place, challenging the concept of phospholipase-induced cell death.¹⁶⁵

In addition, it has been reported that PLA₂ activity during ischemia is depressed rather than enhanced, further contesting a causal role for PLA₂ in ischemia-induced cell death.^{166,167}

Physico-chemical phospholipid perturbation theory

In contrast to the above described theory on the biochemical degradation of cardiac phospholipids during ischemia by increased phospholipase activity and/or impaired phospholipid resynthesis, another promising hypothesis explains the sarcolemmal perturbations during ischemia in terms of alterations in the biophysical interactions of the sarcolemmal phospholipids.

The lipids of biological membranes, including the sarcolemma, are organized in a fluid bilayer configuration, the so-called 'Singer and Nicholson fluid-mosaic model'.¹⁶⁸ Within the plane of the membrane the lipids are highly mobile, whereas the membranous proteins move more slowly due to their higher mass, or due to anchoring to components of the cytoskeleton or gap junctions.

As already stated, the various phospholipid classes are not randomly distributed over the inner and outer leaflets of the sarcolemmal membrane, but rather show an asymmetric distribution. The negatively charged phosphatidylinositol (PI) and phosphatidylserine (PS), as well as phosphatidylethanolamine (PE) are almost exclusively confined to the inner leaflet,¹³⁹ whereas sphingomyelin (Sph) is predominantly located in the outer leaflet. Phosphatidylcholine is equally distributed over the inner and outer leaflets. The imbalance in fluidity resulting from the asymmetric phospholipid distribution is corrected by a relatively higher content of cholesterol in the outer sarcolemmal leaflet. The sarcolemmal phospholipid asymmetry is maintained by the action of an ATP-dependent translocase, which action (in red blood cells) is impaired by a low ATP, a rise in $[Ca^{2+}]_i$, and an oxidation of sulfhydryl groups.¹⁶⁹

In ischemic and reperfused hearts, major ultrastructural changes were identified in the sarcolemmal membrane, including 1) an aggregation of intramembranous particles (IMP), most likely membranous proteins, and 2) an extrusion of membranous phospholipids in the form of multilamellar liposome-like structures (blebs).¹⁷⁰

Prior to actual cell death, a rearrangement of the normally asymmetrically distributed sarcolemmal phospholipids takes place.¹⁷¹ It is conceivable that this rearrangement is due to a decreased action of the ATP-dependent translocase as a consequence of ATP depletion and a rise in $[Ca^{2+}]_i$. Due to the rearrangement in sarcolemmal phospholipid distribution, in combination with the increase in $[Ca^{2+}]_i$ during ischemia, negatively charged PS and PI are no longer prevented from transforming from their original liquid-crystalline phase to the gel phase.¹⁷² This change from liquid-crystalline to gel phase is known as 'lateral phase shift', and leads to the formation of domains of 'frozen' lipids. As a result of this 'freezing' of certain membrane domains, previously dissolved proteins are excluded and aggregate in the still fluid lipid domains, forming IMP aggregates.

There are indications that the occurrence of lateral phase shift is facilitated by an increased $[Ca^{2+}]_i$ and a decreased pH_i , both prominent features of ischemic cardiomyocytes. *In vivo*, the time course of lateral phase separation in energy depleted cardiomyocytes correlates with the time course of the rise in $[Ca^{2+}]_i$.¹⁷³ Also *in vitro*, an increase in $[Ca^{2+}]_i$ and a decrease in pH_i are able to induce lateral phase transition from gel phase to liquid-crystalline phase in vesicles composed of PE and PS or of PE and PI.^{172,174}

In addition to IMP aggregation, bleb formation and lipid extrusion occur. This indicates that the stability of the membrane is lost. This is attributed to the propensity of PE to adopt a non-bilayer configuration in an aqueous environment, hereby inducing uncontrolled fusion events and extrusion of lipid particles. This non-bilayer

configuration is referred to as the hexagonal_{II} (H_{II}) phase, consisting of cylindrical tubes or inverted micelles with an aqueous core.¹⁷²

In the healthy membrane, the tendency of PE to adopt the H_{II} phase is suppressed by 'bilayer-preferring' phospholipids, such as PI and PS, and proteins. However during ischemia, loss of membrane asymmetry and the rise in $[Ca^{2+}]_i$ may lead to lateral phase separation of PS¹⁷⁵ and PI,¹⁷⁶ lifting their bilayer-preferring influence from sarcolemmal PE, which tends to adopt the H_{II} phase, leading to an unstable membrane configuration. The ensuing tendency of the compromised sarcolemma to uncontrolled random fusion events may then lead to extrusion of blebs and ultimately to the loss of sarcolemmal integrity and cell death.

Although the two theories on phospholipid perturbations during ischemia are presented as two separate entities, it is possible that ischemia-induced phospholipid alterations in myocardial membranes are the result of the combined effect of physico-chemical phospholipid alterations and biochemical phospholipid degradation. It is conceivable that a redistribution of membranous phospholipids renders them more susceptible to biochemical digestion by phospholipase, whereas hydrolysis of sarcolemmal phospholipids may alter the interaction of the various phospholipid classes, facilitating derangements in membrane architecture.

Aim and outline of this thesis

This thesis aims to investigate the hypothesis schematically depicted in figure 1. It seeks to answer the question whether cell death in ischemic myocardium is caused by the degradative action of massively activated intracellular CANP and/or PLA₂. These enzymes are thought to be inappropriately activated by the extreme rise in the concentration of the second messenger Ca^{2+} during ischemia, a situation referred to as 'calcium overload'.

In chapter 2 the background and practical considerations regarding the measurement of $[Ca^{2+}]_i$ with fluorescent probes in digital imaging fluorescence microscopy are described.

In chapter 3 the two-compartment culture dish developed by us is described. It was designed to cope with the natural variability between individual cultures, which phenomenon complicates the discrimination of cellular responses to interventions from natural variability. To illustrate its application, we investigated the effect of external pH on the activity of the sarcolemmal Na^+/Ca^{2+} exchanger in intact rat cardiomyocytes.

In chapter 4 the role of CANP in the development of cell death in neonatal rat cardiomyocytes during metabolic inhibition is investigated. To this end we measured

CANP activity *in vitro* and *in vivo* with fluorogenic substrates for CANP, and we assessed the effect of several CANP inhibitors on cell death and CANP activity during metabolic inhibition.

In chapter 5 the role of PLA₂ in cell death of neonatal rat cardiomyocytes during metabolic inhibition was studied, with the aid of the (purported) PLA₂ inhibitors chlorpromazine (CPZ) and trifluoperazine (TFP). In metabolically inhibited cells, we measured [Ca²⁺]_i, cell death, ATP depletion and phospholipid degradation during metabolic inhibition, and the effect of CPZ and TFP on these parameters. As we found that CPZ and TFP influenced the development of calcium overload as well, we studied their effect on the sarcolemmal Na⁺/Ca²⁺ exchanger activity.

In chapter 6 we investigated the role of plasmalogen-selective PLA₂ in cell death in neonatal rat cardiomyocytes during metabolic inhibition using a specific synthetic inhibitor of the enzyme, termed halo-enol lactone suicide substrate (HELSS). In metabolically inhibited cardiomyocytes, we measured [Ca²⁺]_i, cell death, ATP depletion and phospholipid degradation and the effect of HELSS on these parameters.

In chapter 7 we studied the influence of external pH on calcium overload, cell death, ATP depletion, intracellular Na⁺ concentration and intracellular pH during metabolic inhibition in neonatal rat cardiomyocytes.

References

1. Silverman HS, Stern MD. Ionic basis of ischaemic cardiac injury: Insights from cellular studies. *Cardiovasc Res.* 1994;28:581-597.
2. Shen AC, Jennings RB. Myocardial calcium and magnesium in acute ischemic injury. *Am J Pathol.* 1972;67:417-440.
3. Jennings RB, Reimer KA. Lethal myocardial ischemic injury. *Am J Pathol.* 1981;102:241-255.
4. Steenbergen C, Murphy E, Watts JA, London RE. Correlation between cytosolic free calcium, contracture, ATP, and irreversible ischemic injury in perfused rat hearts. *Circ Res.* 1990;66:135-146.
5. Wildenthal K. Lysosomal alterations in ischemic myocardium: result or cause of myocellular damage? *J Mol Cell Cardiol.* 1978;10:595-603.
6. Nayler WG. The role of oxygen radicals during reperfusion. *J Cardiovasc Pharmacol.* 1992;20:S14-S17.
7. Buja LM, Eigenbrodt ML, Eigenbrodt EH. Apoptosis and necrosis - Basic types and mechanisms of cell death. *Arch Pathol Lab Med.* 1993;117:1208-1214.
8. Nayler WG. The role of calcium in the ischemic myocardium. *Am J Pathol.* 1981;102:262-270.
9. Steenbergen C, Murphy E, Levy L, London RE. Elevation of cytosolic free calcium concentration early in myocardial ischemia in perfused rat heart. *Circ Res.* 1987;60:700-707.
10. Murphy E, Aiton JF, Horres CR, Lieberman M. Calcium elevation in cultured heart cells: its role in cell injury. *Am J Physiol.* 1983;14:316-321.

11. Ishida H, Kohmoto O, Bridge JHB, Barry WH. Alterations in cation homeostasis in cultured chick ventricular cells during and after recovery from adenosine triphosphate depletion. *J Clin Invest.* 1988;81:1173-1181.
12. Stern MD, Chien AM, Capogrossi MC, Pelto DJ, Lakatta EG. Direct observation of the "oxygen paradox" in single rat ventricular myocytes. *Circ Res.* 1985;56:899-903.
13. Murphy JG, Smith TW, Marsh JD. Mechanisms of reoxygenation-induced calcium overload in cultured chick embryo heart cells. *Am J Physiol.* 1988;254:1133-1141.
14. Piper HM, Siegmund B, Ladilov YV, Schluter KD. Calcium and sodium control in hypoxic-reoxygenated cardiomyocytes. *Basic Res Cardiol.* 1993;88:471-482.
15. Barry WH, Bridge JHB. Intracellular calcium homeostasis in cardiac myocytes. *Circulation.* 1993;87:1806-1815.
16. Langer GA. Calcium and the heart: exchange at the tissue, cell and organelle levels. *FASEB J.* 1992;6:893-902.
17. Carafoli E. Intracellular calcium homeostasis. *Annu Rev Biochem.* 1987;56:395-433.
18. Frank JS, Mottino G, Reid D, Molday RS, Philipson KD. Distribution of the Na^+ - Ca^{2+} exchange protein in mammalian cardiomyocytes: An immunofluorescence and immunocolloidal gold-labeling study. *J Cell Biol.* 1992;117:337-345.
19. Iwata Y, Hanada H, Takahashi M, Shigekawa M. Ca^{2+} -ATPase distributes differently in cardiac sarcolemma than dihydropyridine receptor alpha 1 subunit and Na^+ / Ca^{2+} exchanger. *FEBS Lett.* 1994;355:65-68.
20. Cannell MB. Contribution of sodium-calcium exchange to calcium regulation in cardiac muscle. *Ann N Y Acad Sci.* 1991;639:428-443.
21. Barry WH, Rasmussen CAF, Ishida H, Bridge JHB. External Na^+ -independent Ca^{2+} extrusion in cultured cells. *J Gen Physiol.* 1985;88:394-411.
22. Hovemadsen L, Bers DM. Passive Ca^{2+} buffering and SR Ca^{2+} uptake in permeabilized rabbit ventricular myocytes. *Am J Physiol.* 1993;264:C677-C686.
23. Pierce GN, Philipson KD, Langer GA. Passive calcium-buffering capacity of a rabbit ventricular homogenate preparation. *Am J Physiol.* 1985;249:C248-C255.
24. Fabiato A. Calcium-induced release of calcium from the cardiac sarcoplasmic reticulum. *Am J Physiol.* 1983;245:C1-C14.
25. Post JA, Kuwata JH, Langer GA. A discrete Na^+ / Ca^{2+} exchange dependent, Ca^{2+} compartment in cultured neonatal rat heart cells. Characteristics, localization and possible physiological function. *Cell Calcium.* 1993;14:61-71.
26. Langer GA. Myocardial calcium compartmentation. *Trends Cardiovasc Med.* 1994;4:103-109.
27. Miyata H, Lakatta EG, Stern MD, Silverman HS. Relation of mitochondrial and cytosolic free calcium to cardiac myocyte recovery after exposure to anoxia. *Circ Res.* 1992;71:605-613.
28. Miyata H, Silverman HS, Sollott SJ, Lakatta EG, Stern MD and Hansford RG. Measurement of mitochondrial free Ca^{2+} concentration in living single rat cardiac myocytes. *Am J Physiol.* 1991;
29. Cox DA, Matlib MA. A role for the mitochondrial Na^+ / Ca^{2+} exchanger in the regulation of oxidative phosphorylation in isolated heart mitochondria. *J Biol Chem.* 1993;268:938-947.
30. Cox DA, Matlib MA. Modulation of intramitochondrial free Ca^{2+} concentration by antagonists of Na^+ / Ca^{2+} exchange. *Trends in Pharmacol Sci.* 1993;14:408-413.
31. Duchon MR, Mcguinness O, Brown LA, Crompton M. On the involvement of a cyclosporin-A sensitive mitochondrial pore in myocardial reperfusion injury. *Cardiovasc Res.* 1993;27:1790-1794.

32. Leblanc N, Hume JR. Sodium current-induced release of calcium from cardiac sarcoplasmic reticulum. *Science*. 1990;248:372-376.
33. Koomen JM, Schevers JAM, Noordhoek J. Myocardial recovery from global ischemia and reperfusion: effects of pre- and/or post-ischemic reperfusion with low-Ca²⁺. *J Mol Cell Cardiol*. 1983;15:383-392.
34. Allshire A, Piper HM, Cuthbertson K, Cobbold PH. Cytosolic free Ca²⁺ in single rat heart cells during anoxia and reoxygenation. *Biochem J*. 1987;244:381-385.
35. Bourdillion PDV, Poole-Wilson PA. Effects of ischemia and reperfusion on calcium exchange and mechanical function in isolated rabbit myocardium. *Cardiovasc Res*. 1981;15:121-130.
36. Sperelakis N. Regulation of calcium slow channels of cardiac muscle by cyclic nucleotides and phosphorylation. *J Mol Cell Cardiol*. 1988;20:76-106.
37. Hano O, Silverman HS, Blank PS, Mellits ED, Baumgardner R, Lakatta EG, Stern MD. Nicardipine prevents calcium loading and "oxygen paradox" in anoxic single rat myocytes by a mechanism independent of calcium channel blockade. *Circ Res*. 1991;69:1500-1505.
38. Kihara Y, Sasayama S, Inoko M, Morgan JP. Sodium/calcium exchange modulates intracellular calcium overload during posthypoxic reoxygenation in mammalian working myocardium - Evidence from aequorin-loaded ferret ventricular muscles. *J Clin Invest*. 1994;93:1275-1284.
39. Ziegelstein RC, Zweier JL, Mellits ED, Younes A, Lakatta EG, Stern MD, Silverman HS. Dimethylthiourea, an oxygen radical scavenger protects isolated cardiac myocytes from hypoxic injury by inhibition of Na⁺-Ca²⁺ exchange and not by its antioxidant effects. *Circ Res*. 1992;70:804-811.
40. Haigney MCP, Miyata H, Lakatta EG, Stern MD, Silverman HS. Dependence of hypoxic cellular calcium loading on Na⁺/Ca²⁺ exchange. *Circ Res*. 1992;71:547-557.
41. Murphy E, Perlman M, London RE, Steenbergen C. Amiloride delays the ischemia-induced rise in cytosolic free calcium. *Circ Res*. 1991;68:1250-1258.
42. Borgers M, Piper HM. Calcium-shifts in anoxic cardiac myocytes. A cytochemical study. *J Mol Cell Cardiol*. 1986;18:439-448.
43. Jimenez E, Delnido P, Feinberg H, Levitsky S. Redistribution of myocardial calcium during ischemia - Relationship to onset of contracture. *J Thorac Cardiovasc Surg*. 1993;105:988-994.
44. Borgers M, Guo Shu L, Xhonneux R, Thone F, Van Overloop P. Changes in ultrastructure and Ca²⁺ distribution in the isolated working rabbit heart after ischemia. A time related study. *Am J Pathol*. 1987;126:92-102.
45. Guarnieri T. Intracellular sodium-calcium dissociation in early contractile failure in hypoxic ferret papillary muscles. *J Physiol (Lond)*. 1987;388:449-465.
46. Butwell NB, Ramasamy R, Lazar I, Sherry AD, Malloy CR. Effect of lidocaine on contracture, intracellular sodium, and pH in ischemic rat hearts. *Am J Physiol*. 1993;264:H1884-H1889.
47. Van Echteld CJA, Kirkels JH, Eijgelshoven MHJ, Van der Meer P, Ruigrok TJC. Intracellular sodium during ischemia and calcium-free perfusion: A ²³Na NMR study. *J Mol Cell Cardiol*. 1991;23:297-307.
48. Sperelakis N, Lee EC. Characterization of (Na⁺,K⁺)-ATPase isolated from embryonic chick hearts and cultured chick heart cells. *Biochim Biophys Acta*. 1971;233:562-579.
49. Dennis SC, Gevers W, Opie LH. Protons in ischemia: where do they come from; where do they go? *J Mol Cell Cardiol*. 1991;23:1077-1086.
50. Karmazyn M, Ray M, Haist JV. Comparative effects of Na⁺/H⁺ exchange inhibitors against cardiac injury produced by ischemia/reperfusion, hypoxia/reoxygenation, and the calcium paradox. *J Cardiovas Pharmacol*. 1993;21:172-178.

Chapter 1

51. Verdonck L, Borgers M, Verdonck F. Inhibition of sodium and calcium overload pathology in the myocardium - A new cytoprotective principle. *Cardiovasc Res.* 1993;27:349-357.
52. Haigney MCP, Lakatta EG, Stern MD, Silverman HS. Sodium channel blockade reduces hypoxic sodium loading and sodium-dependent calcium loading. *Circulation.* 1994;90:391-399.
53. Undrovinas AI, Fleidervish IA, Makielski JC. Inward sodium current at resting potentials in single cardiac myocytes induced by the ischemic metabolite lysophosphatidylcholine. *Circ Res.* 1992;71:1231-1241.
54. Bassani JWM, Bassani RA, Bers DM. Ca^{2+} cycling between sarcoplasmic reticulum and mitochondria in rabbit cardiac myocytes. *J Physiol (Lond).* 1993;460:603-621.
55. Silverman HS. Mitochondrial free calcium regulation in hypoxia and reoxygenation - relation to cellular injury. *Basic Res Cardiol.* 1993;88:483-494.
56. Allen SP, Darleyusmar VM, McCormack JG, Stone D. Changes in mitochondrial matrix free calcium in perfused rat hearts subjected to hypoxia reoxygenation. *J Mol Cell Cardiol.* 1993;25:949-958.
57. Park Y, Bowles DK, Kehrer JP. Protection against hypoxic injury in isolated-perfused rat heart by ruthenium red. *J Pharmacol Exp Ther.* 1990;253:628-635.
58. Griffiths EJ, Halestrap AP. Protection by cyclosporin a of ischemia reperfusion-induced damage in isolated rat hearts. *J Mol Cell Cardiol.* 1993;25:1461-1469.
59. Wang S-Y, Clague JR, Langer GA. Increase in calcium leak channel activity by metabolic inhibition or hydrogen peroxide in rat ventricular myocytes and its inhibition by polycations. *J Mol Cell Cardiol.* 1995;27:211-222.
60. Clague JR, Harvey R, Langer GA. Protamine and other polycationic drugs inhibit calcium leak in cardiac cells during metabolic inhibition and free radical exposure. *J Pharmacol Exp Therap.* 1993;267:1349-1354.
61. Guroff GA. A neutral calcium-activated proteinase from the soluble fraction of rat brain. *J Biol Chem.* 1964;239:149-155.
62. Mellgren RL. Canine cardiac calcium-dependent proteases: resolution of two forms with different requirements for calcium. *FEBS Lett.* 1980;109:129-133.
63. Croall DE, Demartino GN. Calcium-activated neutral protease (calpain) system: structure, function and regulation. *Physiol Rev.* 1991;71:813-847.
64. Reddy PA, Anandavalli TE, Anandaraj MPJS. Calcium activated neutral protease (milli- and microCANP) and endogenous CANP inhibitor of muscle in Duchenne muscular dystrophy (DMD). *Clin Chim Acta.* 1986;160:281-288.
65. Saito KI, Elce JS, Hamos JE, Nixon RA. Widespread activation of calcium-activated neutral proteinase (Calpain) in the brain in Alzheimer disease - A potential molecular basis for neuronal degeneration. *Proc Natl Acad Sci USA.* 1993;90:2628-2632.
66. Hong SC, Goto Y, Lanzino G, Soleau S, Kassell NF, Lee KS. Neuroprotection with a calpain inhibitor in a model of focal cerebral ischemia. *Stroke.* 1994;25:663-669.
67. Zimmerman U-JP, Schlaepfer A. Calcium-activated neutral protease (CANP) in brain and other tissues. *Prog Neurobiol.* 1984;23:63-78.
68. Nicotera P, Hartzell P, Davis G, Orrenius S. The formation of plasma membrane blebs in hepatocytes exposed to agents that increase cytosolic Ca^{2+} is mediated by the activation of a non-lysosomal proteolytic system. *FEBS Lett.* 1986;209:139-144.
69. Bronk SF, Gores GJ. pH-Dependent nonlysosomal proteolysis contributes to lethal anoxic injury of rat hepatocytes. *Am J Physiol.* 1993;264:G744-G751.

70. Nichols JC, Bronk SF, Mellgren RL, Gores GJ. Inhibition of nonlysosomal calcium-dependent proteolysis by glycine during anoxic injury of rat hepatocytes. *Gastroenterology*. 1994;106:168-176.
71. Geeraerts MD, Ronveauw-Dupal MF, Lemasters JJ, Herman B. Cytosolic free Ca^{2+} and proteolysis in lethal oxidative injury in endothelial cells. *Am J Physiol*. 1991;261:C889-C896.
72. Lampi KJ, Kadoya K, Azuma M, David LL, Shearer TR. Comparison of cell-permeable calpain inhibitors and E64 in reduction of cataract in cultured rat lenses. *Toxicol Appl Pharmacol*. 1992;117:53-57.
73. Tolnai S, Korecky B. Calcium-dependent proteolysis and its inhibition in the ischemic rat myocardium. *Can J Cardiol*. 1986;2:42-47.
74. Yoshida K, Yamasaki Y, Kawashima S. Calpain activity alters in rat myocardial subfractions after ischemia or reperfusion. *Biochim Biophys Acta*. 1993;1182:215-220.
75. Iizuka K, Kawaguchi H, Kitabatake A. Effects of thiol protease inhibitors on fodrin degradation during hypoxia in cultured myocytes. *J Mol Cell Cardiol*. 1993;25:1101-1109.
76. Toyooka T, Kamishiro T, Gotoh Y, Fumino H, Masaki T, Hosoda S. Temporary salvage of ischemic myocardium by the protease inhibitor bis[ethyl(2R,3R)-3-[(S)-methyl-1-[4-(2,3,4-trimethoxy-phenyl-methyl)piperazin-1-ylcarbonyl]butyl-carbonyl]oxiran-2-carboxylate]sulfate. *Arzneimittelforschung*. 1986;36:671-675.
77. Bolli R, Cannon RO, Speir E, Goldstein RE, Epstein SE. Role of cellular proteinases in acute myocardial infarction. II. Influence of in vivo suppression of myocardial proteolysis by antipain, leupeptin and pepstatin on myocardial infarct size in the rat. *J Am Coll Cardiol*. 1983;2:681-686.
78. Deutsch N, Weiss JN. ATP-Sensitive K^{+} channel modification by metabolic inhibition in isolated guinea-pig ventricular myocytes. *J Physiol (Lond)*. 1993;465:163-179.
79. Dayton WR, Reville WJ, Goll DE, Stromer MH. A Ca^{2+} activated protease possibly involved in myofibrillar turnover, Partial characterization of the purified enzyme. *Biochemistry*. 1976;15:2159-2167.
80. Croall DE, Demartino GN. Comparison of two calcium-dependent proteases from bovine heart. *Biochim Biophys Acta*. 1984;788:348-355.
81. Hatanaka MN, Yumoto N, Sakihama T, Murachi T. Evidence for heterodimeric nature of calpain molecules as studied by cross-linking modification. *Biochem Int*. 1985;10:187-193.
82. Croall DE, Demartino GN. Purification and characterization of calcium-dependent proteases from rat heart. *J Biol Chem*. 1983;258:5660-5665.
83. Ikeda U, Toyooka T, Hosoda S. Identification of two new calcium dependent hydrolases in the human heart. *Biochem Biophys Res Commun*. 1986;136:773-777.
84. Melloni E, Pontremoli S, Salamino F, Sparatore B, Michetti M, Horecker BL. Two cytosolic Ca^{2+} -dependent neutral proteinases from rabbit liver: purification and properties of the proenzymes. *Arch Biochem Biophys*. 1984;232:505-512.
85. Inomata M, Hayashi M, Nakamura M, Kawashima S. Hydrolytic and autolytic behaviour of two forms of calcium-activated neutral protease (CANP). *J Biochem*. 1985;98:407-416.
86. Barth R, Elce JS. Immunofluorescent localization of a Ca^{2+} -dependent neutral proteinase in hamster muscle. *Am J Physiol*. 1981;240:E493-E498.
87. Yoshimura N, Hatanaka M, Kitahara A, Kawaguchi N, Murachi T. Intracellular localization of two distinct Ca^{2+} -proteases (calpain I and calpain II) as demonstrated by using discriminative antibodies. *J Biol Chem*. 1984;259:7168-7174.

88. Aoki K, Imajoh S, S. O, Emori Y, Koike M, Kosaki G, Kannagi R. Complete amino acid sequence of the large subunit of the low Ca^{2+} -requiring form of human Ca^{2+} -activated neutral protease (μCANP) deduced from its cDNA sequence. *FEBS Lett.* 1986;205:313-317.
89. Emori Y, Kawasaki H, Sugihara H, Imajoh S, Kawashima S, Suzuki K. Isolation and sequence analysis of cDNA clones for the large subunits of two isozymes of rabbit calcium-dependent protease. *J Biol Chem.* 1986;261:9465-9471.
90. Mettrioni RM. On the relationship of calpains to the papain family. *Trends Biochem Sci.* 1986;11:117-118.
91. Ohno S, Emori Y, Imajoh S, Kawasaki S, Kisaragi M, Suzuki K. Evolutionary origin of calcium-dependent protease by fusion of genes for a thiol protease and a calcium-binding protein? *Nature.* 1984;312:566-570.
92. Minami Y, Emori Y, Imajoh-Ahmi S, Kawasaki H, Suzuki K. Carboxyl-terminal truncation and site-directed mutagenesis of the EF hand structure domain of the small subunit of rabbit calcium-dependent protease. *J Biochem.* 1988;104:927-933.
93. Imajoh S, Kawasaki H, Suzuki K. Limited autolysis of calcium-activated neutral protease (CANP): reduction of the Ca^{2+} requirement is due to the NH_2 -terminal processing of the large subunit. *J Biochem.* 1986;100:633-642.
94. McClelland P, Lash JA, Hathaway DR. Identification of major autolytic cleavage sites in the regulatory subunit of vascular calpain II. A comparison of partial amino-terminal sequences to deduced sequence from complementary DNA. *J Biol Chem.* 1989;264:17428-17431.
95. Imajoh S, Kawasaki H, Suzuki K. The amino-terminal hydrophobic region of the small subunit of calcium-activated neutral protease (CANP) is essential for its activation by phosphatidyl inositol. *J Biochem.* 1986;99:1281-1284.
96. Garret C, Cottin P, Dufourcq J, Ducastaing A. Evidence for a Ca^{2+} -independent association between Calpain II and phospholipid vesicles. *FEBS Lett.* 1988;227:209-214.
97. Suzuki K, Ishiura S. Effects of metal ions on the structure and activity of calcium-activated neutral protease (CANP). *J Biochem.* 1983;93:1463-1471.
98. Minami Y, Emori Y, Kawasaki H, Suzuki K. E-F hand structure-domain of calcium-activated neutral protease (CANP) can bind Ca^{2+} ions. *J Biochem.* 1987;101:889-895.
99. Dayton WR, Schollmeier JV, Lepley RA, Cortes LR. A calcium-activated protease possibly involved in myofibrillar protein turnover. Isolation of a low-calcium-requiring form of the protease. *Biochim Biophys Acta.* 1981;659:48-61.
100. Inomata M, Kasai Y, Nkamura M, Kawashima S. Comparison of low and high calcium requiring forms of the calcium-activated neutral protease (CANP) from rabbit skeletal muscle. *J Biochem.* 1984;95:1661-1670.
101. Azanza J-L, Raymond J, Robin J-M, Cottin P, Ducastaing A. Purification and some physico-chemical and enzymatic properties of a calcium-ion activated neutral proteinase from rabbit skeletal muscle. *Biochem J.* 1979;183:339-347.
102. Wang KKW. Developing selective inhibitors of calpain. *Trends Pharmacol Sci.* 1990;11:139-142.
103. Demartino GN. Calcium-dependent proteolytic activity in rat liver: identification of two proteases with different calcium requirements. *Arch Biochem Biophys.* 1981;211:253-257.
104. Beckerle MC, O'Halloran T, Burridge K. Demonstration of a relationship between talin and P235, a major substrate of calcium-dependent protease in platelets. *J Cell Biochem.* 1986;30:259-270.
105. Croall DE, Morrow JS, Demartino GN. Limited proteolysis of the erythrocyte membrane skeleton by calcium-dependent proteinases. *Biochim Biophys Acta.* 1986;882:287-296.

106. Siman R, Baudry M, Lynch G. Brain fodrin: substrate for calpain I, an endogenous calcium-activated proteinase. *Proc Natl Acad Sci USA*. 1984;81:3572-3576.
107. Gross RW. High plasmalogen and arachidonic acid content of canine myocardial sarcolemma: a fast atom bombardment spectroscopic and gas chromatography-mass spectroscopic characterization. *Biochemistry*. 1984;23:158-165.
108. Kishimoto A, Kajikawa N, Shiota M, Nishizuka Y. Proteolytic activation of calcium-activated, phospholipid-dependent protein kinase by calcium-dependent neutral protease. *J Biol Chem*. 1983;258:1156-1164.
109. Sasaki T, Kikuchi T, Fukui I, Murachi T. Inactivation of calpain I and calpain II by specificity-oriented tripeptidyl chloromethyl ketones. *J Biochem*. 1986;99:173-179.
110. Tsujinaka T, Kajiwana Y, Kambayashi J, Sakon M, Higuchi N, Tanaka T, Mori T. Synthesis of a new cell penetrating calpain inhibitor (calpeptin). *Biochem Biophys Res Commun*. 1988;153:1201-1208.
111. DeMartino GN, Huff CA, Croall DE. Autoproteolysis of the small subunit of the subunit of calcium-dependent protease II activates and regulates enzyme activity. *J Biol Chem*. 1986;262:12047-12052.
112. Hathaway DR, Werth DK, Haeberle JR. Limited autolysis reduces the Ca^{2+} -requirement of a smooth muscle Ca^{2+} -activated protease. *J Biol Chem*. 1982;257:9072-9077.
113. Mellgren RL, Lane RD. Myocardial calpain is inhibited by monoclonal antibodies specific for the small, noncatalytic subunit. *Biochim Biophys Acta*. 1988;954:154-169.
114. Toyo-oka T. Phosphorylation with cyclic adenosine 3',5'-monophosphate-dependent protein kinase renders bovine cardiac troponin sensitive to the degradation by calcium-activated neutral protease. *Biochem Biophys Res Commun*. 1982;107:44-50.
115. Parker RA, Miller SJ, Gibson DM. Phosphorylation of microsomal HMG CoA reductase increases susceptibility to proteolytic degradation in vitro. *Biochem Biophys Res Commun*. 1984;125:629-635.
116. Zhang Z, Lawrence J, Stracher A. Phosphorylation of platelet actin binding protein protects against proteolysis by calcium-dependent sulfhydryl protease. *Biochem Biophys Res Commun*. 1988;151:355-360.
117. Cottin P, Vidalenc PL, Ducastaing A. Ca^{2+} -dependent association between a Ca^{2+} -activated neutral proteinase (CANP) and its specific inhibitor. *FEBS Lett*. 1981;136:221-224.
118. Murachi T, Hatanaka M, Yasumoto Y, Nakayama N, Tanaka KA. A quantitative distribution study on calpain and calpastatin in rat tissues and cells. *Biochem Int*. 1981;2:651-656.
119. Blomgren K, Nilsson E, Karlsson JO. Calpain and calpastatin levels in different organs of the rabbit. *Comp Biochem Physiol*. 1989;93:403-407.
120. Clark AF, Demartino GN, Croall DE. Fractionation and quantification of calcium-dependent proteinase activity from small tissue samples. *Biochem J*. 1986;235:279-282.
121. Mellgren RL, Mericle MT, Lane RD. Proteolysis of the calcium-dependent protease inhibitor by myocardial calcium-dependent protease. *Arch Biochem Biophys*. 1986;246:233-239.
122. Emori Y, Kawasaki H, Imajoh S, Imahori K, Suzuki K. Endogenous inhibitor for calcium-dependent cysteine protease contains four internal repeats that could be responsible for its multiple reactive sites. *Proc Natl Acad Sci USA*. 1987;84:3590-3594.
123. Takano E, Maki M, Hori H, Hatanaka M, Marto T, Titani K, Murachi T. Pig heart calpastatin: identification of repetitive domain structures and anomalous behaviour in polyacrylamide gel electrophoresis. *Biochemistry*. 1988;27:1964-1972.
124. Lane RD, Mellgren RL, Mericle MT. Subcellular localization of bovine heart calcium-dependent protease inhibitor. *J Mol Cell Cardiol*. 1985;17:863-872.

125. Mellgren RL. Calcium-dependent proteases: an enzyme system active at cellular membranes. *FASEB J*. 1987;1:110-115.
126. Demartino GN, Blumenthal DK. Identification and partial purification of a factor that stimulates calcium-dependent proteases. *Biochemistry*. 1982;21:4297-4303.
127. Pontremoli S, Melloni E, Michetti M, Salamino F, Sparatore B, Horecker BL. An endogenous activator of the Ca^{2+} -dependent proteinase of human neutrophils that increases its affinity for Ca^{2+} . *Proc Natl Acad Sci USA*. 1988;85:1740-1743.
128. Schollmeyer JE. Calpain II involvement in mitosis. *Science*. 1988;240:911-913.
129. Watanabe N, Van de Woude GF, Ikawa I, Sagat N. Specific proteolysis of the *c-mos* proto-oncogene product by calpain on fertilization of xenopus eggs. *Nature*. 1989;324:505-511.
130. Nelson WJ, Traub P. Properties of a Ca^{2+} -activated protease specific for the intermediate size filament protein vimentin in Ehrlich-ascites-tumour cells. *Eur J Biochem*. 1981;116:51-57.
131. Huston RB, Krebs EG. Activation of skeletal muscle phosphorylase kinase by Ca^{2+} : identification of the kinase activating factor as a proteolytic enzyme. *Biochemistry*. 1968;7:2116-2122.
132. Wang KK, Villalobo A, Roufogalis BD. Activation of the Ca^{2+} -ATPase of human erythrocyte membrane by an endogenous Ca^{2+} -dependent neutral proteinase. *Arch Biochem Biophys*. 1988;260:696-706.
133. Ito M, Tanaka T, Nunoki K, Hidaka H, Suzuki K. The Ca^{2+} -activated protease (calpain) modulates Ca^{2+} /calmodulin dependent activity of smooth muscle myosin light chain kinase. *Biochem Biophys Res Commun*. 1987;145:1321-1328.
134. Dayton WR, Schollmayer JV. Immunocytochemical localization of a calcium-activated protease in skeletal muscle cells. *Exp Cell Res*. 1981;136:423-433.
135. Beckerle M, Burrige K, Demartino GN, Croall DE. Colocalization of calcium-dependent protease II and one of its substrates at sites of cell adhesion. *Cell*. 1987;51:569-577.
136. Pontremoli S, Melloni E, Sparatore B, Salamino F, Michetti M, Sacco O, Hirecker BL. Binding to erythrocyte membrane is the physiological mechanism for activation of Ca^{2+} -dependent neutral proteinase. *Biochem Biophys Res Commun*. 1985;128:331-338.
137. Harris AS, Croall DE, Morrow JS. The calmodulin-binding site in alpha-frodrin is near the calcium-dependent protease 1 cleavage site. *J Biol Chem*. 1988;263:15754-15761.
138. Hazen SL, Gross RW. Principles of membrane biochemistry and their application to the pathophysiology of cardiovascular disease. In: Fozzard *et al*, eds. *The heart and cardiovascular system*. 2nd edition. New York. Raven Press. 1992:839-860.
139. Post JA, Langer GA, Op den Kamp JAF, Verkleij AJ. Phospholipid asymmetry in cardiac sarcolemma. Analysis of intact cells and 'gas-dissected' membranes. *Biochim Biophys Acta*. 1988;943:256-266.
140. Gross RW. Myocardial phospholipases A_2 and their membrane substrates. *Trends Cardiovasc Med*. 1992;2:115-121.
141. Post JA, Verkleij AJ, Roelofsen B, Op den Kamp JAF. Plasmalogen content and distribution in the sarcolemma of cultured neonatal rat cardiomyocytes. *FEBS Lett*. 1988;240:78-82.
142. Schulz R, Strynadka KD, Panas DL, Olley PM, Lopaschuk GD. Analysis of myocardial plasmalogen and diacyl phospholipids and their arachidonic acid content using high-performance liquid chromatography. *Anal Biochem*. 1993;213:140-146.
143. Han X, Gross RW. Plasmenylcholine and phosphatidylcholine membrane bilayers possess distinct conformational motifs. *Biochemistry*. 1990;29:4992-4996.

144. Pak JH, Bork VP, Norberg RE, Creer MH, Wolf RA, Gross RW. Disparate molecular dynamics of plasmenylcholine and phosphatidylcholine bilayers. *Biochemistry*. 1987;26:4824-4830.
145. Corr PB, Gross RW, Sobel BE. Amphipathic metabolites and membrane dysfunction in ischemic myocardium. *Circ Res*. 1984;55:135-154.
146. Chien KR, Sen A, Reynolds R, Chang A, Kim Y, Gunn MD, Buja LM, Willerson JT. Release of arachidonate from membrane phospholipids in cultured neonatal rat myocardial cells during adenosine triphosphate depletion. *J Clin Invest*. 1985;75:1770-1780.
147. Van der Vusse GJ, Roemen THM, Prinzen FW, Coumans WA, Reneman RS. Uptake and tissue content of fatty acids content in dog myocardium under normoxic and ischemic conditions. *Circ Res*. 1982;50:538-546.
148. Miyazaki Y, Gross RW, Sobel BE, Saffitz JE. Selective turnover of sarcolemmal phospholipids with lethal cardiac myocyte injury. *Am J Physiol*. 1990;259:C325-C331.
149. Chien KR, Han A, Sen A, Buja LM, Willerson JT. Accumulation of unesterified arachidonic acid in ischemic canine myocardium. *Circ Res*. 1984;54:313-322.
150. Prinzen FW, Van der Vusse GJ, Arts T, Roemen THM, Coumans WA, Reneman RS. Accumulation of nonesterified fatty acids in ischemic canine myocardium. *Am J Physiol*. 1984;247:H264-H272.
151. Jones RL, Miller JC, Hagler HK, Chien KR, Willerson JT, Buja LM. Association between inhibition of arachidonic acid release and prevention of calcium loading during ATP depletion in cultured rat cardiac myocytes. *Am J Pathol*. 1989;135:541-556.
152. Otani H, Engelman RM, Rousou JA, Bryer RH, Das DK. Enhanced prostaglandin synthesis due to phospholipid breakdown in ischemic-reperfused myocardium. *J Mol Cell Cardiol*. 1986;18:953-961.
153. Kim D, Clapham DE. Potassium channels in cardiac cells activated by arachidonic acid and phospholipids. *Science*. 1989;1174-1176.
154. Moore LK, Beyer EC, Burt JM. Characterization of gap junction channels in A7r5 vascular smooth muscle cells. *Am J Physiol*. 1991;C975-C981.
155. Karli JN, Karikas GA, Hatzipavlou PK, Levis GM, Mouloupoulos SN. The inhibition of Na^+/K^+ -ATPase activity of rabbit and dog heart sarcolemma by lysophosphatidylcholine. *Life Sci*. 1979;24:1869-1875.
156. Vemuri R, Philipson KD. Phospholipid composition modulates the $\text{Na}^+/\text{Ca}^{2+}$ exchange activity. *Am J Physiol*. 1989;256:C1273-C1276.
157. Das DK, Engelman RM, Rousou JA, Breyer RH, Otani H, Lemeshow S. Role of membrane phospholipids in myocardial injury induced by ischemia and reperfusion. *Am J Physiol*. 1986;251:H71-H79.
158. Zalewski A, Goldberg S, Maroko PR. The effects of phospholipase A_2 inhibition on experimental infarct size, left ventricular hemodynamics and regional myocardial blood flow. *Int J Cardiol*. 1988;21:247-257.
159. Van Bilsen M, Van der Vusse GJ, Willemsen PHM, Coumans WA, Roemen THM, Reneman RS. Effects of nicotinic acid and mepacrine on fatty acid accumulation and myocardial damage during ischemia and reperfusion. *J Mol Cell Cardiol*. 1990;22:155-163.
160. Moffat MP, Tsushima RG. Functional and electrophysiological effects of quinacrine on the response of ventricular tissues to hypoxia and reoxygenation. *Can J Physiol Pharmacol*. 1988;67:929-935.

161. Prasad MR, Popescu LM, Moraru II, Liu X, Maity S, Engelman RM, Das DK. Role of phospholipases A₂ and C in myocardial ischemic reperfusion injury. *Am J Physiol.* 1991;260:H877-H883.
162. Hazen SL, Stuppy RJ, Gross RW. Purification and characterization of canine myocardial cytosolic phospholipase A₂. *J Biol Chem.* 1990;265:10622-10630.
163. Hazen SL, Gross RW. Identification and characterization of myocardial phospholipase A₂ from transplant recipients suffering from end-stage ischemic heart disease. *Circ Res.* 1992;70:486-495.
164. Ford DA, Hazen SL, Saffitz JE, Gross RW. The rapid and reversible activation of a calcium-independent plasmalogen-selective phospholipase A₂ during myocardial ischemia. *J Biol Chem.* 1991;260:7295-7303.
165. Steenbergen C, Jennings RB. Relationship between lysophospholipid accumulation and plasma membrane injury during total in vitro ischemia in dog heart. *J Mol Cell Cardiol.* 1984;16:605-621.
166. Grynberg A, Nalbone G, Leonardi J, Lafont H, Athias P. Eicosapentanoic and docosahexanoic acids in cultured rat ventricular myocytes and hypoxia-induced alterations in phospholipase-A activity. *Mol Cell Biochem.* 1992;116:75-78.
167. Bentham JM, Higgins AJ, Woodward B. The effects of ischemia, lysophosphatidylcholine and palmitoylcarnitine on rat heart phospholipase A₂ activity. *Basic Res Cardiol.* 1987;82 (Suppl I):127-137.
168. Singer SJ, Nicholson GL. The fluid mosaic model of the structure of cell membranes. *Science.* 1972;175:720-731.
169. Comfurius P, Senden JMG, Tilly RHJ, Schroit AJ, Bevers EM, Zwaal RFA. Loss of membrane phospholipid asymmetry in platelets and red cells may be associated with calcium-induced shedding of plasma membrane and inhibition of aminophospholipid translocase. *Biochim Biophys Acta.* 1990;1026:153-160.
170. Post JA, Leunissen-Bijvelt J, Ruigrok TJC, Verkleij AJ. Ultrastructural changes in sarcolemma and mitochondria in the isolated rabbit heart during ischemia and reperfusion. *Biochim Biophys Acta.* 1985;845:119-123.
171. Musters RJP, Otten E, Biegelmann E, Bijvelt J, Keijzer JJH, Post JA, Op Den Kamp JAF, Verkleij AJ. Loss of asymmetric distribution of sarcolemmal phosphatidylethanolamine during simulated ischemia in the isolated neonatal rat cardiomyocyte. *Circ Res.* 1993;73:514-523.
172. Verkleij AJ, Post JA. Physico-chemical properties and organization of lipids in membranes: their possible role in myocardial injury. *Basic Res Cardiol.* 1987;82 (Suppl. I):85-91.
173. Post JA, Clague JR, Langer GA. Sarcolemmal phospholipid asymmetry and Ca²⁺ fluxes on metabolic inhibition of neonatal rat heart cells. *Am J Physiol.* 1993;265:H461-H468.
174. Van Dijk PWM, De Kruiff B, Verkleij AJ, Van Deenen LLM, De Gier J. Comparative studies on the effects of pH and Ca²⁺ on bilayers of various negatively charged phospholipids and their mixtures with phosphatidylcholine. *Biochim Biophys Acta.* 1978;512:84-96.
175. Tilcock CPS, Cullis PR. The polymorphic phase behaviour of mixed phosphatidylserine-phosphatidylethanolamine model systems as detected by 31-P-NMR. Effects of divalent cations and pH. *Biochim Biophys Acta.* 1981;641:189-201.
176. Nayar R, Schmid S, Hope MJ, Cullis PR. Structural preferences of phosphatidylinositol and phosphatidylinositol-phosphatidylethanolamine model membranes. Influence of Ca²⁺ and Mg²⁺. *Biochim Biophys Acta.* 1982;688:169-176.

Chapter 2

Measurement of the intracellular Ca^{2+} concentration using fluorescent probes and fluorescence videomicroscopy

Douwe E. Atsma

Introduction

Since the recognition of the pivotal role of Ca^{2+} in the regulation and effectuation of a wide range of cell processes, the search for a simple and reliable means to measure the intracellular Ca^{2+} concentration ($[\text{Ca}^{2+}]_i$) has been without end.

Before the introduction of fluorescent Ca^{2+} probes, the role of Ca^{2+} in cell physiology was studied using Ca^{2+} -selective electrodes, $^{45}\text{Ca}^{2+}$, or the luminescent probe aequorin, a protein isolated from the coelenterate *Aequorea Victoria*, which must be introduced into cells by microinjection.

The development of fura-2 by Grynkiewicz *et al.*¹ in 1985 spurred a stream of publications on the role of Ca^{2+} as a second messenger in various cell types. Fura-2 has also been used in the work described in this thesis. This chapter describes the fundamental and practical considerations for the development of an experimental set-up to measure $[\text{Ca}^{2+}]_i$ with fluorescent Ca^{2+} probes in intact living cells in general, with emphasis on fura-2 (Part I) and on the microscope set-up that was used in our research (Part II). To illustrate the versatility of the system, we have included the Appendix to describe the use of the system in the measurement of rapid Ca^{2+} kinetics in endothelial cells upon thrombin stimulation.

Table 1. Characteristics of fluorescent Ca^{2+} probes that are derived from BAPTA

| Probe: | Fura-2 | Indo-1 | Fluo-3 |
|----------------------------|--|--|--|
| wavelengths | $\lambda_{\text{ex}} = 340 \text{ nm}$ $\lambda_{\text{ex}} = 380 \text{ nm}$ $\lambda_{\text{em}} = 490 \text{ nm}$ | $\lambda_{\text{ex}} = 355 \text{ nm}$ $\lambda_{\text{em}} = 405 \text{ nm}$ $\lambda_{\text{em}} = 485 \text{ nm}$ | $\lambda_{\text{ex}} = 488 \text{ nm}$ $\lambda_{\text{em}} = 530 \text{ nm}$ |
| Ratio measurement possible | Yes: excitation shift | Yes: emission shift | No |
| reported K_D * | 224 nM | 250 nM | 860 nM |
| loading via: | | | |
| micro-injection | + (as free salt) | + (as free salt) | + (as free salt) |
| AM-ester | + | + | + |

* As pointed out in the text, the K_D may differ in various experimental situations, depending upon viscosity, polarity, ionic strength, pH and temperature of the solutions.

Part I. Optical $[\text{Ca}^{2+}]_i$ probes

The present family of fluorescent Ca^{2+} probes, which includes fura-2, indo-1 and fluo-3 (Table 1), is derived from the Ca^{2+} -chelating molecule BAPTA² (Fig. 1). This compound is an aromatic derivative of the well-known divalent cation chelator

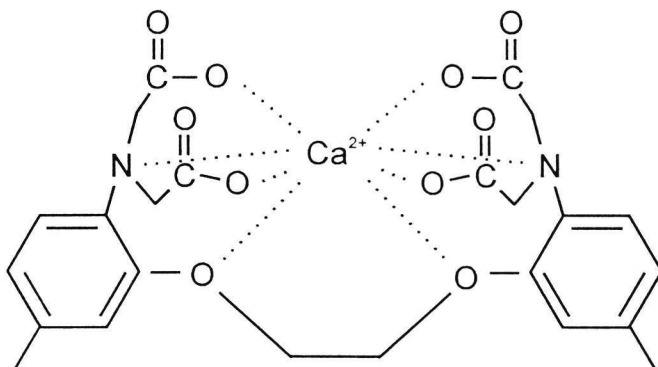


Figure 1. Structure of BAPTA, which forms the backbone of a family of fluorescent Ca^{2+} indicator dyes. BAPTA provides the fluorescent Ca^{2+} indicators with their ion selectivity and Ca^{2+} binding properties through its single high affinity octa-coordinate Ca^{2+} binding site.

EGTA (ethylene glycol-bis(β -aminoethyl ether) N,N,N',N' -tetraacetic acid). BAPTA has one high affinity Ca^{2+} -binding site, at which Ca^{2+} is bound to eight ligands on the BAPTA molecule. This yields a straightforward 1:1 stoichiometry with Ca^{2+} , which greatly simplifies the interpretation of the spectral changes of the fluorescent Ca^{2+} indicators upon binding with Ca^{2+} . As compared to EGTA, BAPTA has a better selectivity of Ca^{2+} over Mg^{2+} (10^4 vs. 1). Also, its Ca^{2+} binding is less pH dependent in the physiological pH range, as the aromatic amino groups in BAPTA are not protonated at physiological pH, whereas in EGTA they are (BAPTA: pK_a of the two amino groups 5.47 and 6.36, versus EGTA: pK_a 9.58 and 8.96). This same property makes Ca^{2+} binding to BAPTA faster than to EGTA, as Ca^{2+} -binding to the unprotonated amino groups of BAPTA is faster than the deprotonation/ Ca^{2+} -binding sequence needed for the amino groups of EGTA. The fast Ca^{2+} -binding characteristics of BAPTA allows the study of fast Ca^{2+} transients. Since the BAPTA molecule itself is not fluorescent, a fluorophore must be conjugated to BAPTA in order to use the compound as a fluorescent Ca^{2+} probe. The effects of the binding of Ca^{2+} to BAPTA are then relayed to the fluorescent moiety, causing changes in its fluorescent properties. In case of fura-2, Ca^{2+} binding causes a shift in the excitation spectrum from 362 to 335 nm (see Fig. 2). Indo-1 also shows an excitation shift upon binding with Ca^{2+} , but in addition has a shift in the emission spectrum. These spectral shifts permits the use of fura-2 and indo-1 as ratiometric Ca^{2+} indicators (see below). Fluo-3 does not show a sufficiently large spectral shift to be suitable as a ratiometric Ca^{2+} indicator, but rather increases its fluorescence up to 40-fold upon binding of Ca^{2+} . This vast increase in brightness, combined with its ability to be excited by visible light, can make fluo-3 an attractive choice.

Ratiometric measurement of $[Ca^{2+}]_i$

In the ratiometric measurement method, the $[Ca^{2+}]_i$ is not derived from the fluorescence intensity of the Ca^{2+} probe at just one excitation or emission wavelength, but rather from the ratio of fluorescence intensities at two different excitation or emission wavelengths. This way, a number of (unknown) factors that may influence fluorescence intensity are cancelled out, because these factors have similar effects on fluorescence intensities at both wavelengths. These perturbing factors include fluorescence properties of the dye, the extent of dye loading in the cell, heterogeneous distribution of the dye within the cell, leakage of the dye from the cell, dye bleaching, cell thickness, and several equipment related parameters such as illumination intensity, collection efficiency and sensitivity. Both fura-2 and indo-1 are suitable probes to be used as ratiometric indicators due to their spectral shifts upon Ca^{2+} binding (see above). However, the lack of spectral shift makes fluo-3 suitable for single-wavelength measurement only, and its use as a quantitative indicator of $[Ca^{2+}]_i$ is dependent upon the careful determination of, and correction for, the disturbing factors described above.

Fura-2

Fura-2 is the most commonly used fluorescent $[Ca^{2+}]_i$ indicator in imaging studies. The reason for this is: 1) its excitation spectrum shifts upon binding with calcium, making it suitable for ratio imaging, 2) it has a high quantum yield, resulting in a strong fluorescence signal, 3) it has low Mg^{2+} sensitivity, and 4) it is relatively resistant to photobleaching. Due to the high fluorescent yield, the intracellular concentration needed for a good fluorescence signal is in the order of several micromolar, as opposed to the millimolar concentrations needed for its predecessor quin-2. This lower intracellular fura-2 concentration minimises the $[Ca^{2+}]_i$ buffering effect of the dye. The K_D is such (224 nM),¹ that fura-2 can be used to measure $[Ca^{2+}]_i$ in the physiological range, between 10^{-8} M and 10^{-5} M.

1. Basic characteristics. Fura-2 is composed of the BAPTA backbone described above and the fura-2 fluorochrome which gives it its fluorescence properties. Figure 2 shows the emission intensity at 510 nm during excitation of fura-2 with a spectrum from 250 to 450 nm, in the presence of various concentrations of Ca^{2+} . As compared to the excitation spectrum with no Ca^{2+} present (0 μ M), the excitation spectra upon the addition of Ca^{2+} show an increase in emission intensity at wavelengths below

360 nm (with maximal dynamic range at 340 nm), and a decrease in emission intensity at wavelengths above 360 nm (with maximal dynamic range at 380 nm).

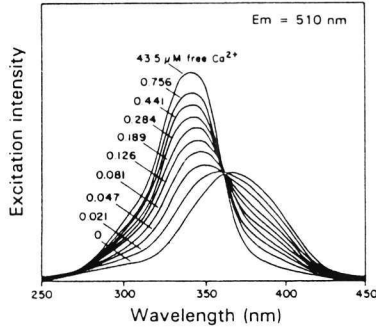


Figure 2. Excitation spectrum of fura-2 in the presence of various concentrations of Ca^{2+} . Emission wavelength is 510 nm. Numbers in the figure refer to the Ca^{2+} concentrations present (in μM) (From the Molecular Probes catalogue).

At 360 nm, emission intensity is independent of Ca^{2+} , and is called the isosbestic wavelength. At the isosbestic wavelength, fluorescence intensity is dependent upon the concentration of fura-2 only, and therefore it can be used to monitor the fura-2 concentration in cells. The opposite response of fura-2 fluorescence at 340 nm and at 380 nm to changes in $[Ca^{2+}]_i$ is of great importance in the ratiometric use of fura-2. As described above, the use of the ratio of the fura-2 fluorescence at 340 nm (F_{340}) and at 380 nm excitation (F_{380}) eliminates the influence of a variety of perturbing factors which affect fura-2 fluorescence at each individual wavelength. In addition, the ratio of two parameters which have a significant dynamic range in *opposite* direction, yields a value that exhibits an even greater dynamic range. This allows the detection of even very small changes in $[Ca^{2+}]_i$.

The intracellular concentration of free calcium ($[Ca^{2+}]_i$) (in nM) can be calculated from the fura-2 fluorescence values using equation [1]:

$$[Ca^{2+}]_i = K_D * \beta * \frac{(R - R_{min})}{(R_{max} - R)} \quad [1]$$

in which K_D is the dissociation constant of the Ca^{2+} - fura-2 complex (taken to be 224 nM¹), β is the ratio of the maximal fura-2 fluorescence at 380 nm excitation ($F_{380_{max}}$) and the minimal fluorescence at 380 nm ($F_{380_{min}}$), and R is the ratio of the fluorescence at 340 nm excitation (F_{340}) and the fluorescence at 380 nm excitation (F_{380}) measured in cells. R_{min} and R_{max} are the minimal and the maximal ratios

which can be obtained. These two values, together with β are obtained during the calibration procedure, described below.

The kinetics of Ca^{2+} binding to fura-2 have proven to be sufficiently fast to track Ca^{2+} transients on a time scale of 7-10 ms,³ although several reports claim that under certain conditions Ca^{2+} binding to fura-2 is slowed down considerably.^{4,5} Therefore, although it is theoretically possible to track Ca^{2+} transients of 3-4 ms duration, one should be aware that this time resolution is not always achieved during the experiment.

2. *Loading.* Introduction of the fura-2 molecule into the cells under study can be performed either via microinjection of the free salt of fura-2, or by incubation with the acetoxymethylester form (AM form) of the dye. Microinjection requires specialized equipment and may be difficult in small cells, such as the neonatal rat heart cells we use. Also, only a limited number of cells can be loaded this way.

An alternative method, which is most often used, is loading of fura-2 using the AM-ester form (fura-2/AM) of the dye. In this method, the lipophilic AM-ester passively crosses the plasma membrane, and once intracellularly, the ester bonds in the molecule are readily cleaved by cellular esterases. This step yields the free fura-2 that is capable of chelating Ca^{2+} . Since the gradient of fura-2/AM is always directed towards the intracellular space, high intracellular concentrations of the dye can be obtained. A too high intracellular concentration of fura-2 is to be avoided as this can lead to phototoxicity and/or buffering of intracellular Ca^{2+} (see below: *Problems*). In addition, each hydrolysed AM-ester yields one toxic formaldehyde molecule which may have adverse effects on the cells, especially if high fura-2/AM concentrations are used. However, due to the favourable quantum yield of fura-2, only relatively small intracellular concentrations of the dye (0.1-2 μM) are required to obtain a good signal, thus minimising the effects of formaldehyde. A further protective measure against the deleterious effects of formaldehyde was reported to be the addition of pyruvate (1 mM).⁶

In our experiments, the cardiomyocytes were loaded with fura-2 by incubation with 2 μM fura-2/AM (Molecular Probes) in 1 ml of a N-2-hydroxyethyl piperazine-N'-2-ethanesulfonic acid (HEPES) buffered balanced salt solution (HBSS), containing in mM: NaCl 125, KCl 5, MgSO_4 1, KH_2PO_4 1, CaCl_2 2.5, NaHCO_3 10, HEPES 20, pyruvate 5, probenecid 2.5, pH 7.4, for 30 min at 37°C. After loading, the coverslip with the cardiomyocytes is rinsed three times, and mounted in the two-compartment culture dish used for the microscope experiments (see Chapter 3). The poor solubility of fura-2/AM in water may limit adequate loading of cells with the dye, as the concentration of fura-2/AM in the medium can not be increased indefinitely. In that case, dispersing agents such as Pluronic F127, bovine serum albumin or

cyclodextrins may be useful, as they allow a higher fura-2/AM concentration to be used in the incubation medium.⁷

3. *Calibration.* In order to calculate $[Ca^{2+}]_i$ from the fura-2 fluorescence values, the fura-2 fluorescence signals should be calibrated. To this end, the factors, K_D , β , R_{min} and R_{max} which appear in equation [1], need to be determined.

There are two different opinions on how to obtain these calibration factors. Several investigators prefer to perform the calibration procedure *in vitro*, whereas others favour the calibration to be performed *in vivo*, i.e. in cells.

In the *in vitro* calibration, the fluorescence of the free salt of fura-2 is measured in solutions mimicking the intracellular environment, with various known concentrations of Ca^{2+} . The resulting ratio values can be plotted against pCa to form a calibration curve (see Fig. 3) which can be used to derive $[Ca^{2+}]_i$ from the ratio values obtained in the experiments with cells.

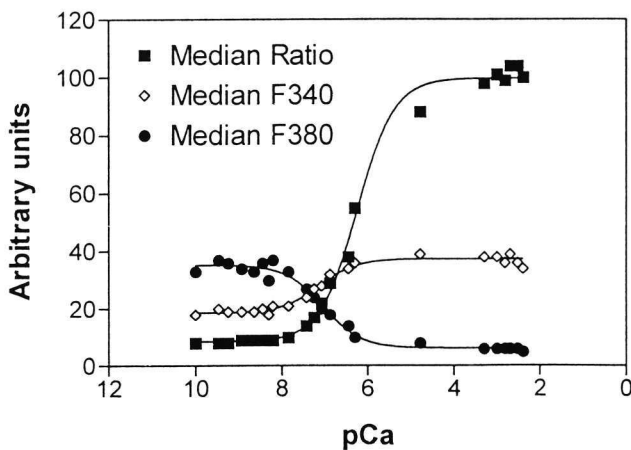


Figure 3. *In vitro* calibration curve of fura-2 fluorescence in the presence of various concentrations of Ca^{2+} . Shown are individual F340 (open diamonds) and F380 values (closed circles), and the ratio value (closed squares) derived from these parameters. Ratio data are multiplied by 16 to scale the results in a suitable range.

In the *in vivo* calibration procedure, which is usually performed at the end of the experiment, the maximally obtainable ratio R_{max} and $F380_{min}$ are determined after addition of a calcium ionophore (e.g. 2.5 μM ionomycin or 4Br-A23187) to the cells. This enables Ca^{2+} entry into the cells, to achieve maximal saturation of the intracellular fura-2 with Ca^{2+} . Then, excess EGTA (20 mM) is added to bind all Ca^{2+} , and the fluorescence of Ca^{2+} -free fura-2 is measured, giving the minimal obtainable ratio R_{min} and $F380_{max}$. From $F380_{min}$ and $F380_{max}$, β is calculated. As to the K_D needed to calculate $[Ca^{2+}]_i$, the value originally reported by Grynkiewicz *et al.*¹ is most commonly used. However, a number of researchers have reported that the K_D of fura-2, and also its absorption and emission spectra may vary in response to differences in polarity, ionic strength, viscosity, pH and temperature of the

solutions used.⁸⁻¹⁰ The experimenter should be aware that the value chosen for K_D has a profound effect on the calculated $[Ca^{2+}]_i$.

Problems associated with the use of fura-2

Although the application of fura-2 and the recording of its fluorescence signals are within reach of many researchers, the interpretation of the data obtained is not without difficulty. Many theoretical and practical problems may interfere with the accurate determination of $[Ca^{2+}]_i$ (for review, see ref. 11). This section describes various problems and some solutions to them, which may be encountered when working with fura-2.

1. Incomplete hydrolysis. After a successful loading procedure using fura-2/AM, less than 5% of fura-2 in the cells is still present in the ester form.⁷ Complete hydrolysis is a prerequisite for quantitative $[Ca^{2+}]_i$ measurement. The presence of unhydrolysed ester which is Ca^{2+} -insensitive but does contribute to the total fura-2 fluorescence signal, will result in an underestimation of $[Ca^{2+}]_i$, and a reduced dynamic response to Ca^{2+} -transients. To facilitate the hydrolysis of fura-2/AM, it is recommended to incubate the fura-2/AM loaded cells for 15-30 min at 37°C in fura-2/AM-free medium. This allows the intracellular esterases to hydrolyse the AM ester bonds. If a considerable quantity of unhydrolysed ester is suspected, it must be quantified to allow either correction of the fluorescence signals or adaptation of the loading protocol. Two approaches for quantification of unhydrolysed dye exist:^{12,13}

1) After lysis of the cell by Triton X-100 or digitonin, fura-2 fluorescence is determined at the isosbestic wavelength (360 nm) in the absence and the presence of 1-2 mM Mn^{2+} . Manganese ions react with hydrolysed dye, but not with the ester form. As binding of Mn^{2+} to fura-2 results in quenching of the fura-2 fluorescence, the residual fluorescence after Mn^{2+} addition represents unhydrolysed fura-2/AM; or
2) After lysis of the cells, unhydrolysed ester can be cleaved by exogenously added KOH. By determining the fura-2 fluorescence at saturating Ca^{2+} concentrations before and after KOH hydrolysis the quantity of unhydrolysed ester originally present can be calculated.

2. Calibration. The calibration of fura-2 fluorescence signals constitutes a great challenge. For $[Ca^{2+}]_i$ values to be calculated from the fluorescence intensities, the factors K_D , β , R_{min} and R_{max} , (see equation [1]) should be determined. Several authors have reported shortcomings in calibration procedures and have proposed improvements.¹¹ Other researchers have given up on the calibration issue and merely

report the raw fluorescence data instead of calculated $[Ca^{2+}]_i$ values, as they feel that the latter may not be accurate.¹⁴

In the *in vitro* calibration method, the fluorescence of the free salt of fura-2 is measured in solutions mimicking the intracellular environment with various known concentrations of Ca^{2+} , to produce a calibration curve.

The difficulties with this method are:

1) The exact computation of the $[Ca^{2+}]_i$ in the calibration solution. In the calibration solutions, EGTA is normally used as the Ca^{2+} buffer. Apart from the impurities that are often present in EGTA,¹⁵ the various values for the apparent K_D of EGTA which have been reported for any given pH, ionic strength, temperature, viscosity and degree of dye-protein binding,⁷ can make the accurate preparation of Ca^{2+} calibration solutions difficult. In addition, the glassware used should be cleaned exhaustively, as glass may be contaminated with trace amounts of Ca^{2+} , which can spoil an otherwise meticulously prepared Ca^{2+} solution.¹⁶ For the calculation of the parameters needed for the Ca^{2+} solutions, computer programs such as Eqcal[®] (Biosoft) can be of help. In our hands, the calibration curve obtained with this method was a sigmoid curve as would be expected (Fig. 3), but which yielded a K_D value for fura-2 which was unrealistically low.

2) The exact mimicking of the intracellular environment. The spectral characteristics of fura-2 are influenced by the polarity, viscosity and presence of other metal ions in the calibration solution.⁹ In order to rightfully extrapolate *in vitro* calibration data to fluorescence data obtained in cells, the calibration solutions should mimic the intracellular environment as closely as possible. If not corrected, the values obtained for R_{min} and R_{max} will be too high for fura-2 and too low for indo-1. Various solutions to this problem have been proposed.⁷

In the *in vivo* approach to calibrate fura-2 fluorescence signals in cells, the above mentioned problem with respect to the intracellular environment is eliminated. However, other problems arise. In this method, fura-2 is first forced to maximal Ca^{2+} saturation to yield R_{max} , and then maximally depleted of Ca^{2+} to give R_{min} . Calcium ionophores, such as ionomycin and 4Br-A23187 ($> 1 \mu M$) are used to equilibrate the intracellular and extracellular $[Ca^{2+}]$. Sometimes, also monensin and nigericin are added to dissipate Na^+ and K^+ gradients, respectively, thereby blocking Na^+ -dependent Ca^{2+} transport.¹⁷ When the ratio of fura-2 fluorescence no longer increases, the R_{max} value is obtained.

However, as mentioned previously, cells may contain a variable quantity of unhydrolysed Ca^{2+} -insensitive fura-2 ester. This quantity, which even may increase relatively as fura-2 leaks from the cells during the course of the experiment, can cause serious underestimation of R_{max} . For determination of the quantity of unhydrolysed ester see 1. *incomplete hydrolysis*.

The value of R_{\min} is determined by adding excess EGTA (20 mM) to remove all intracellular Ca^{2+} . However, Bond *et al.* showed that EGTA did not remove all Ca^{2+} from the cells,¹⁸ which leads to an overestimation of R_{\min} .

3. *Photobleaching.* Photobleaching is the loss or alteration of the fluorescent compound as a result of excessive illumination of the dye. This can lead to either a loss of fluorescence or to the formation of a different configuration of the fluorophore which remains fluorescent but has different spectral and ion-binding characteristics. Fura-2 is relatively resistant to photobleaching. However, excessive illumination leads to the formation of a Ca^{2+} -insensitive form, which shows greater fluorescence intensities at higher wavelengths including 380 nm.¹⁹ Accumulation of this compound will thus lead to an underestimation of $[\text{Ca}^{2+}]_i$. Precautions one can take to minimise photobleaching include minimizing the exposure to light by a) using a shutter to illuminate the sample only when acquiring data, b) attenuating the intensity of the excitation light and c) keeping samples from light (working in a darkened room). In addition, the collection of emitted fluorescence should be optimised by using good quality optical components and wide bandpass emission filters. Also, the signal-to-noise ratio can be improved by using sufficient dye, while preventing stray light.

4. *Compartmentalization and leakage.* Ideally, the fura-2/AM which has entered the cytoplasm during the dye loading procedure, is immediately de-esterified by the cytoplasmic esterases to yield the membrane impermeable fura-2. However, high concentrations of fura-2/AM may saturate cytoplasmic esterases and cause penetration of fura-2/AM into intracellular organelles. Alternatively, fully hydrolysed fura-2 may be actively transported from the cytosol into cellular organelles. Both pathways will lead to accumulation of fura-2 in intracellular organelles such as the sarcoplasmic reticulum and mitochondria. This process of compartmentalization interferes with the accurate determination of cytoplasmic $[\text{Ca}^{2+}]_i$. If the fura-2 in the organelles is in the AM form, this will lead to an underestimation of total cellular $[\text{Ca}^{2+}]_i$, whereas if it is in the free acid form e.g. in the sarcoplasmic reticulum, it would yield artifactually high $[\text{Ca}^{2+}]_i$ values.

The extent of compartmentalization can be assessed by selective lysis of the plasma membrane using digitonin, leaving the intracellular membranes intact.⁷ After lysis and release of cytosolic fura-2, the remaining fura-2 fluorescence represents compartmentalized fura-2.

In addition to transport of fura-2 within a cell, fura-2 may also be transported out of the cell, leading to dye leakage. This causes a decrease in cellular fura-2 fluorescence and an increase in fura-2 fluorescence in the Ca^{2+} -rich extracellular

medium. These events complicate measurement of $[Ca^{2+}]_i$ as they will lead to a reduction in sensitivity and an increase in background fluorescence, respectively.

Compartmentalization and dye leakage can be prevented by the anion-transport inhibiting compounds probenecid and sulfinpyrazone,²⁰ which suggests that compartmentalization of fura-2 is probably due to an active, enzyme-mediated transport process. Addition of 2.5 mM probenecid to the incubation medium decreases fura-2 loss by 81% after 90 min (M. Persoon, personal communication). A lower temperature during the experiment also decreases fura-2 leakage.

5. *Buffering of intracellular Ca^{2+} by fura-2.* A potential problem with the measurement of $[Ca^{2+}]_i$ using fura-2 is the Ca^{2+} buffering capacity of fura-2. This could have an effect on $[Ca^{2+}]_i$ itself and on Ca^{2+} -dependent processes in the cells. The Ca^{2+} buffering capacity of cells has been estimated to be almost 1 mM.²¹ Typically, fura-2 loaded cells contain 50-100 μ M of the indicator. Given a K_D of 224 nM⁻¹, a $[Ca^{2+}]_i$ of 100 nM, and $[fura-2]_i$ of 50 μ M, approximately 15 μ M of fura-2 would bind Ca^{2+} , expanding the quantity of cellular Ca^{2+} that is bound to Ca^{2+} buffers by about 10%. The remaining 35 μ M fura-2 represents approximately 5-10% of the totally available cytosolic Ca^{2+} binding sites.⁷ Therefore, the calcium buffering effect of fura-2 is relatively small, provided that excessive loading of the cells with fura-2 is avoided.

Part II. Fluorescence imaging video microscopy

Imaging of individual cells has advantages over the study of cell populations when one is interested in 1) the variability between single cells with respect to biological responses, or 2) changes that occur within single cells.

The following section describes the various components for a system designed to image and to measure quantitatively fluorescence intensities on a microscopic scale.

Hardware

1. *Light source.* The use of fura-2 dictates the use of a UV light source. The most commonly used UV light sources are mercury or xenon arcs lamps.

Mercury arc lamps in general have a less optimal spectrum for fluorescence applications since their UV spectrum contains several high intensity lines. In contrast, xenon lamps have a relatively smooth spectrum in the range of 300 to 450 nm.

In our microscope set-up the excitation UV light came from a 100 W mercury lamp, the Osram HB 100W. This lamp has a high intensity spectral line around 365 nm,

and the two excitation wavelengths for fura-2, 340 nm and 380 nm, fall in the shoulders of this line. The resulting uneven light intensity at 340 nm and 380 nm requires the adjustment of the light intensity at these wavelengths with neutral density filters at the level of the filterwheel (see below).

2. *Heat filter.* A heat filter after the light source is obligatory, since a fairly large part of the spectrum of the light sources, especially xenon, falls in the IR-region, and may damage the equipment and/or the biological specimen.

3. *Filter changer.* The measurement of $[Ca^{2+}]_i$ using fura-2 requires two excitation wavelengths, so provisions should be present to place the appropriate excitation filters into the light path. In our set-up, we used a filterwheel with 10 filter positions (Lambda 10, Sutter, USA). This filterwheel has ample space for excitation filters and has a maximum filter change speed of 50 ms. However, the presence of filters in the filterwheel increases its mass, and its momentum upon rotation. This makes it more difficult to prevent overshoot from the correct filter position. Lowering the rotation speed of the filterwheel restored the correct positioning of the filters, at the expense of high-speed filter changing. Although the filterwheel is suitable for recording the $[Ca^{2+}]_i$ on a time scale of 1 second, the study of rapid Ca^{2+} transients (duration 10-20 ms) with fura-2 requires a different filter changing mechanism, such as a chopper.²² For the excitation filters we used bandpass filters (Melles Griott) with a bandwidth of 10 nm between 50% transmission points, as they represent a good compromise between selectivity and transmission efficiency. The availability of nine different excitation filters in the filterwheel allowed multiple probes to be used in the same experiment. The tenth position contained a blank disc, and served as a light shutter. Serial communication (RS-232) between the image acquisition computer and the microprocessor controlled interface unit of the filterwheel allowed the synchronisation of filter changing with image acquisition.

4. *Neutral density filters.* It may be necessary to attenuate the intensity of the light source either at all wavelengths to prevent photodamage or bleaching of the fluorescent chromophore (see Part I), or at selected wavelengths to correct disproportionate illumination intensity at two or more wavelengths. For fura-2, it is recommended that the neutral density filters are chosen such that under normal conditions, the fura-2 signals from cells are roughly equal at 340 nm and 380 nm excitation. We had to use a neutral density filter with a transmittance of 25% (Melles Griott) in the 380 nm light path to meet this condition.

5. *Microscope body.* A standard upright or inverted epifluorescence microscope body is suitable for imaging of single cells. The inverted microscope has several advantages over the upright microscope, as with the inverted microscope one can study cells attached to glass coverslips mounted at the bottom of a culture dish. Also, it is easier to use high numerical-aperture oil- or glycerin-immersion objectives if desired. The experimenter has better access to the culture dish from above, facilitating addition of compounds, changing of media, insertion of patch pipettes or sensors for temperature or pO_2 , and other manipulations.

In our set-up, an inverted Leitz Diavert microscope body was used.

6. *Dichroic mirror.* Excitation light must be reflected from the source through the objective, and the fluorescence returning from the cells must be passed straight on to the emission filter. This task can be best performed by a dichroic mirror, which is an interference filter designed to optimally reflect short excitation wavelengths (efficiency >90%) and to transmit longer emission wavelengths. For fura-2 a transition wavelength of 400 nm is suitable.

7. *Objective.* The use of UV illumination dictates that all components in the light path be transmittant to these wavelengths. Normal microscope objectives do not transmit UV light. Quartz objectives provide the optimal light transmission, although their high price often prevents their application. A good alternative is the use of Fluor-objectives. These objectives, also employed by us, combine an adequate UV transmission with a reasonable price. We used the Olympus DPlanApo 10 UV 10x with a numerical aperture (NA) of 0.40, the Nikon Fluor 20 x with a NA of 0.75, and the Nikon Fluor 40x with a NA of 0.85. The resulting fields of view were: $1033 \times 677 \mu m^2$, $511 \times 338 \mu m^2$ and $257 \times 169 \mu m^2$, respectively. Resolution of the digitized image was $4.0 \mu m/pixel$, $2.0 \mu m/pixel$ and $1.0 \mu m/pixel$, respectively.

8. *Emission filter.* An emission filter, which can either be a band pass filter or a long pass filter, blocks non-specific fluorescence and stray light. For fura-2 a long pass filter transmitting wavelengths > 490 nm is suitable.

9. *Video camera.* The basic choices for a camera which is capable to image the faint fluorescence image are either a Silicon Intensified Target (SIT) camera or an Intensified Charge Coupled Device (ICCD) camera.

Advantages of SIT cameras are their good sensitivity, high spatial resolution and low noise, whereas their disadvantages are their non-linearity at low light levels and, most importantly, their slow response to changes in light intensity. Typically, they have a lagtime of about 70 ms, making this type of camera suitable only for the

recording of relatively slow $[Ca^{2+}]_i$ dynamics. Advantages of the ICCD cameras are their fast response time (lagtime about 3 ms), good sensitivity and small geometric distortion, whereas their major disadvantage is noise, often making digital filtering, time-averaging or cooling of the CCD-chip necessary. ICCDs are extremely suitable for the imaging of fast Ca^{2+} transients.

The video camera we employed was a SIT camera (Hamamatsu C2400-08). This camera has a resolution of 625 TV lines, with a signal to noise ratio of 40 dB.

10. Framegrabber. The video image recorded by the camera must be digitized before the images can be manipulated and analyzed. The developments in video frame grabbers are very rapid, with high-performance grabbers becoming available at progressively lower prices. In addition to converting the analog video signal to a digital format, some frame grabbers are also capable of performing real-time calculations, such as subtraction of dark current images, averaging, filtering, etc. Often a framegrabber contains several megabytes of memory, allowing the recording of a number of images in real-time (video rate: 25 images/s in Europe). In our set-up we used the PCVision-plus frame grabber (Imaging Technologies Inc.). This computer expansion card digitizes the incoming video signal with a resolution of eight bits (256 grey values) at 25 Hz. Its one megabyte video memory can store either one 640 x 512, two 512 x 512, or eight 256 x 256 pixel images. The frame grabber also displays the digitized images on a RGB monitor, after converting the digital signal back to an analog video signal. It has look-up tables (LUTs) for both the video input and the display output. A LUT contains 256 values, each of which can be addressed by a specific input value. The input value is then replaced by its corresponding value from the LUT. This scheme allows the rapid (real-time) transformation of either input signal or display signal. In this way, different fluorescence intensities in the incoming video images can be transformed to various pseudo colours on the RGB monitor, allowing rapid interpretation of the image.

11. Host computer. The filterwheel control, the image acquisition and processing, and storage of the images are performed in an industry-standard MS-DOS 33 MHz 80486 personal computer, equipped with 8 Mb internal memory and a 200 Mb harddisk. The host computer runs the image processing software TIM (see *Software*), which in addition to processing of the fluorescence images takes care of the filterwheel control and storage of the images.

12. Video monitor. To observe the video signal from the SIT camera, a video monitor is connected to the output of the camera amplifier. In this way one can select suitable fields of view, even when fluorescence is too low to be observed with the

dark adapted naked eye. This monitor also facilitates the focusing of the microscope, especially after changes in the field of view.

13. RGB monitor. The digitized image is displayed by the frame grabber board on a RGB monitor (Sony PVM-1442QM). On this display the raw digitized images are shown, as well as the images that are produced after off-line manipulation of these images by the image processing software. The display of raw images helps the experimenter when setting up the experiment in the optimal positioning of the cell culture and in the setting of the sensitivity of the SIT camera. In addition, this monitor displays the calculated ratio image of the fura-2 loaded cells in false colours. This gives the experimenter a near real-time feedback on the changes in $[Ca^{2+}]_i$ during an experiment, and allows him to adapt the experimental protocol to the observed cellular responses.

14. Mass storage. The vast amount of images produced by fluorescence video microscopy systems most often has to be stored for later (re)analysis. One ratio image is produced from one F340 and one F380 image, each occupying 64 Kb of disk space (when an eight bits 256x256 pixels image is used). In our experimental practice, a typical day of experiments easily produces 250 ratio images. With the corresponding F340 and F380 images this amounts to 48 Mbytes. Compression of this data by the shareware program PKARC reduces this to roughly 20 Mbytes. For long term storage of the acquired images, an optical WORM (Write Once Read Many) system (Reflection Systems Ltd., Melbourn, UK) is used. In this way, 940 Mb of graphic information can be stored on one single disc.

15. Video printer. We used a Sony UP-850 video printer to make black and white hard copies of the video images. These are used for documentation purposes by the experimenter, or used for display on posters for scientific meetings.

16. Incubation chamber. During the experiments, the cells were incubated on the microscope stage in a two-compartment culture dish, described in more detail in chapter 3. The culture dish was placed in a micro-incubator, previously described by Ince *et al.*²³ In some experiments the cardiomyocytes were exposed to hypoxia ($pO_2 < 5$ Torr) by incubating the cells with N_2 saturated buffer and by blowing argon gas over the culture dish through a slit in the micro-incubator during the experiment. During hypoxic experiments pO_2 was constantly monitored using a Clark-type micro oxygen probe (YSI 5357). A thermistor which was suspended into the incubation medium measured buffer temperature, which was kept constant by a custom made closed-loop temperature controller.

17. XY-table. The culture dish and its micro-incubation chamber were mounted on a microscope xy-table, which was fitted with precision position sensors and actuation motors. This way, the experimenter can define microscopic field-of-view positions in the culture with sub-micrometer resolution, panning the xy-table using a joystick. Selected positions can be stored in a personal computer, and can be refound automatically and rapidly. This set-up allows the experimenter to shuttle between the two compartments of the culture dish (see chapter 3) during the experiment, to compare selected cells in one compartment with those in the other compartment, even when using objective magnifications of 100 x. In addition, in each compartment more than one field-of-view can be studied during the experiment, thereby increasing the number of cells which can be studied in the same experiment.

Software

The control of the filterwheel, the acquisition, processing and storage of the images was performed by dedicated software on the host computer. This software, called TIM™ (version 3.36), is a commercially available image processing and pattern recognition software package (Difa, Breda, The Netherlands), which has originally been developed at the Technical University, Delft, The Netherlands. It is a command driven program, with a command file interpreter, which allows the development of command files that are tailored to perform specific tasks.

1. Image format. Although the PC-Vision-plus frame grabber used by us is capable of producing images of 512 x 512 pixels with 8 bits intensity resolution, we have chosen to restrict ourselves to images of 256 x 256 pixels, with 8 bits intensity resolution. This choice was influenced mainly by the fourfold reduction in image storage requirements, combined with the relatively little added information in the larger 512 x 512 pixels images. Also, manipulation of the smaller images is faster and requires less overhead.

2. Acquisition of images. Images at each wavelength were averaged to improve the signal to noise ratio. For fura-2, after positioning of the 340 nm filter into the light path and a 1 s delay needed to stabilize the camera image, 16 consecutive video frames were acquired in a 16 bit image buffer. After division by 16, this yielded the 340 nm averaged image with a four-fold improved signal-to-noise ratio. Then, the 380 nm filter was inserted into the lightpath, and after a 1 s delay, an averaged 380 nm imaged was produced similarly. Finally, an averaged darkcurrent image was produced after acquiring 16 images in the absence of excitation light. This image

reflects the dark current of the camera and its amplifier. The darkcurrent image was then subtracted from the 340 nm and 380 nm image. The raw 340 nm and 380 nm images were then saved on harddisk to be processed off-line.

3. *Off-line analysis of the images.* After the experiment, the images were loaded from harddisk into memory. As the images contain information concerning both the cells and the background, the cellular pixels needed to be separated from the non-cellular pixels by the use of a template. To this end, the 340 nm and 380 nm images were added to yield a summation image showing total fluorescence. Then, a threshold value was entered by the operator to suppress the (lower) background fluorescence, producing a template which represents only cellular pixels. By using the summation image rather than either wavelength image alone, the accuracy of generating a reliable template at fluctuating fluorescence values was improved, as the fluorescence at either wavelength changes inversely with changing $[Ca^{2+}]_i$, but the sum of their fluorescence values remains relatively constant.

After the interactive definition of the template by the experimenter, the template was applied to the 340 nm and 380 nm images, resulting in the suppression of the background values. After changing the values 0 to 1 in the 380 nm image to avoid divide-by-zero errors, the 340 nm image was divided by the 380 nm image on a pixel-by-pixel basis. This yielded a ratio image, which is then multiplied by a preset factor (16 or 32) to scale the ratio image into a suitable range (0-255). Then, a histogram of the greyscale in the images was made, and several statistical parameters were determined, including the mean, median, standard deviation, minimum and maximum values. These values were stored in a separate data file, which could be used for further calculation and graphing purposes. The processed image files were stored under their original names on the harddisk, overwriting their unprocessed versions.

In addition to the processing of complete images, single cells were analysed separately. In that case, the experimenter draws either a polygon or a free curve around the individual cells or group of cells. The cell(s) of interest were then isolated from the total image and analyzed separately as described above. The results were stored in a datafile.

The acquired fluorescence images and the calculated ratio images were displayed either in greyvalues ranging from 0 to 255, or in pseudocolors for easier visual interpretation.

4. *Miscellaneous command files.* In addition to the above mentioned functions, several other command files have been written, which are dedicated to a variety of tasks, including image acquisition at other wavelengths, image manipulation,

parameter handling, memory management, filterwheel control, I/O tasks, and statistical procedures.

References

1. Grynkiewicz G, Poenie M, Tsien RY. A new generation of Ca^{2+} indicators with greatly improved fluorescence properties. *J Biol Chem.* 1985;260:3440-3450.
2. Tsien RY. New calcium indicators and buffers with high selectivity against magnesium and protons: Design, synthesis and properties of prototype structures. *Biochemistry.* 1980;19:2396-2404.
3. Lev-Ram V, Grinvald A. Activity-dependent calcium transients in central nervous system myelinated axons revealed by the calcium indicator fura-2. *Biophys J.* 1987;52:571-576.
4. Hollingworth S, Baylor SM. Fura-2 signals from intact frog skeletal muscle fibers. *Biophys J.* 1987;51:549A.
5. Klein MG, Simon BJ, Szucs G, Schneider MF. Simultaneous recording of calcium transients in skeletal muscle using high and low affinity calcium indicators. *Biophys J.* 1988;53:971-978.
6. Tsien RY, Pozzan T. Measurement of cytosolic free Ca^{2+} with quin-2. *Methods Enzymol.* 1989;172:230-262.
7. Poenie M. Measurement of intracellular calcium with fluorescent calcium indicators. In: Boulton A, Baker G, Taylor C, eds. *Neuromethods.* The Humana Press, Inc. New York. 1992:129-175.
8. Roe MW, Lemasters JJ, Herman B. Assessment of Fura-2 for measurement of cytosolic free calcium. *Cell Calcium.* 1991;11:63-73.
9. Poenie M. Alteration of intracellular Fura-2 fluorescence by viscosity: a simple correction. *Cell Calcium.* 1990;11:85-91.
10. Popov EG, Garrilov IY, Pozin EY, Gabassov ZA. Multi-wavelength method for measuring concentration of free cytosolic calcium using the fluorescent probe indo-1. *Arch Biochem Biophys.* 1988;261:91-96.
11. Moore E, Becker PL, Fogarty KE, Williams DA, Fay FS. Ca^{2+} imaging in single living cells: theoretical and practical issues. *Cell Calcium.* 1990;11:157-179.
12. Scanlon M, Williams DW, Fay FS. A calcium-insensitive form of fura-2 associated with polymorphonuclear leukocytes. *J Biol Chem.* 1987;262:6308-6312.
13. Highsmith S. Sarcoplasmic reticulum interacts with the Ca^{2+} indicator precursor Fura-2-AM. *Biochem Biophys Res Comm.* 1986;138:1153-1162.
14. Moreton RB. Single-cell imaging technology. In: Boulton A, Baker G and Taylor C, eds. *Neuromethods.* The Humana Press, Inc. New York. 1992;175-230.
15. Miller DJ, Smith GL. EGTA purity and the buffering of calcium ions in physiological solutions. *Am J Physiol.* 1984;246:C160-C166.
16. McGuigan JAS, Luthi D, Buri A. Calcium buffer solutions and how to make them: a do it yourself guide. *Can J Physiol Pharmacol.* 1990;69:1733-1749.
17. Williams DA, Fay FS. Intracellular calibration of the fluorescent calcium indicator Fura-2. *Cell Calcium.* 1990;11:75-83.
18. Bond M, Shuman H, Somlyo AP, Somlyo AV. Total cytoplasmic calcium in relaxed and maximally contracted rabbit portal vein smooth muscle. *J Physiol (Lond).* 1984;357:185-201.
19. Becker PL, Fay FS. Photobleaching of fura-2 and its effect on the determination of calcium concentrations. *Am J Physiol.* 1988;11:C613-C618.

20. Di Virgilio F, Steinberg TH, Silverstein SC. Inhibition of Fura-2 sequestration and secretion with organic anion transport blockers. *Cell Calcium*. 1990;11:57-62.
21. Johansson JS, Haynes D. Deliberate Quin2 overload as a method for in situ characterization of active calcium extrusion systems and cytoplasmic calcium binding. Application to the human platelet. *J Membr Biol*. 1988;104:147-163.
22. Tsien RY, Harootunian AT. Practical design criteria for a dynamic ratio imaging system. *Cell Calcium*. 1990;11:93-109.
23. Ince C, Ypey DL, Diesselhoff-Den Dulk MMC, Visser JAM, De Vos A, Van Furth R. Micro-CO₂-Incubator for use on a microscope. *J Immunol Meth*. 1983;60:269-275.

Chapter 3

A novel two-compartment culture dish allows microscopic evaluation of two different treatments in one cell culture simultaneously

Influence of external pH on Na⁺/Ca²⁺ exchanger activity in cultured rat cardiomyocytes

Douwe E. Atsma,¹ E.M.Lars Bastiaanse,¹ Can Ince,² Arnoud Van der Laarse¹

¹Department of Cardiology, University Hospital, Leiden, The Netherlands,

²Department of Physiology and Anaesthesiology, University of Amsterdam, The
Netherlands

Pflügers Arch. 1994;428:296-299

Abstract

A new type of culture dish containing two separate compartments is described, that can be used in high-magnification microscopy. Using the dish, two halves of a single cell culture grown on a standard coverslip can be exposed to different treatments simultaneously, allowing the effect of one treatment to be compared with that of the other treatment in the same culture. This way, the natural variability that might exist between different individual cultures is circumvented. In addition, by simultaneously conducting two experiments per dish, the number of experiments needed can be decreased. This both reduces the time to complete a series of experiments, and allows the optimal use of specimens that are difficult to obtain, such as human material. We found there is an excellent barrier between the two compartments for lipophilic and hydrophilic compounds, and for low molecular weight cations. To illustrate the use of the dish we describe the influence of external pH on the activity of the $\text{Na}^+/\text{Ca}^{2+}$ exchanger in intact cultured neonatal rat ventricular cardiomyocytes. The intracellular free calcium concentration ($[\text{Ca}^{2+}]_i$) in the cardiomyocytes, measured using fura-2 and imaging fluorescence microscopy, was studied during sodium-free incubation. The resulting rise in $[\text{Ca}^{2+}]_i$ at pH 7.4 in one compartment was compared with that in the other compartment in which the pH was either 6.0, 7.0, 7.4 or 8.0. It was found that at pH below 7.4, $\text{Na}^+/\text{Ca}^{2+}$ exchanger activity was diminished, whereas at pH higher than 7.4 the $\text{Na}^+/\text{Ca}^{2+}$ exchanger activity was increased.

We conclude that the two-compartment culture dish offers researchers a valuable new tool in the manipulation and the observation of single cells in culture.

Introduction

Ince *et al.* previously reported on a Teflon culture dish and an accompanying micro-incubator to be used in a variety of biomedical research applications, including high-magnification microscopy and electrophysiology.^{1,2} These scientific tools have found wide acceptance.³⁻¹¹ We developed a new variation of this culture dish that contains two compartments. In the modified dish, two halves of a cell culture grown on a single coverslip, can be exposed to different treatments simultaneously, allowing the effect of one treatment to be compared with that of the other in the same culture. Using this dish, the natural variability that might exist between different individual cultures is circumvented. This encertains that the observed differences between the two compartments can be attributed solely to the difference in treatments. Furthermore, by simultaneously conducting two experiments per dish, the number of experiments needed can be decreased. This both reduces the time to complete a

series of experiments, and allows the optimal use of specimens that are difficult to obtain, such as human material.

Previously, Philipson *et al.* studied the effect of pH on the activity of the Na⁺/Ca²⁺ exchanger in sarcolemmal vesicles isolated from canine cardiac tissue using ⁴⁵Ca²⁺.¹² To illustrate the use of the novel two-compartment culture dish, we studied the influence of external pH on the activity of the Na⁺/Ca²⁺ exchanger in intact cultured neonatal rat ventricular cardiomyocytes, using the fluorescent calcium indicator fura-2 and imaging fluorescence microscopy. To this end, we exposed the cardiomyocytes to sodium-free buffer solutions with varying pH in one compartment, and compared this with sodium-free buffer with pH 7.4 in the other compartment. The lack of extracellular sodium induces a reversal of the action of the Na⁺/Ca²⁺ exchanger, resulting in transport of Na⁺ ions out of the cells in return for Ca²⁺ ions. This then leads to an increase of the intracellular free calcium concentration ([Ca²⁺]_i) in the myocytes.¹³ The rate of rise and the amplitude of the rise in [Ca²⁺]_i reflect the influence of external pH on Na⁺/Ca²⁺ exchanger activity. We found that at pH below 7.4, Na⁺/Ca²⁺ exchanger activity was diminished, whereas at pH higher than 7.4 the Na⁺/Ca²⁺ exchanger activity was increased.

Materials and Methods

Culture dish. The two-compartment culture dish is shown schematically in figure 1. The unit, with an overall diameter of 36 mm, consists of five parts: 1. an open-centred dish made of a hard and durable Teflon derivative, Eriflon (Eriks, Alkmaar, The Netherlands), 2. an Eriflon insert containing the two compartments, 3. a silicon rubber patch, 4. a conventional glass coverslip with a diameter of 24 mm and a thickness of 0.17 mm, and 5. a stainless steel ring to secure the coverslip to the Eriflon dish. The dish is assembled upside-down as follows: the Eriflon insert (2) is positioned in the Eriflon dish (1), and the silicon rubber patch (3) is placed in the groove of the dish. Then, the glass coverslip with the adherent cell culture (4) is placed over the silicon rubber patch, and the stainless steel securing ring (5) is fitted on the assembly by a snap-type sealing mechanism, shown in detail in figure 2. This way, a good contact between the coverslip and the silicon rubber patch is established and leakage is prevented. After assembly, each half of the culture is covered with 500 µl medium, the bottom of the cover slip is cleaned with ethanol, and the entire unit is placed on the microscope stage in the thermostated micro-incubator, previously described by Ince *et al.*²

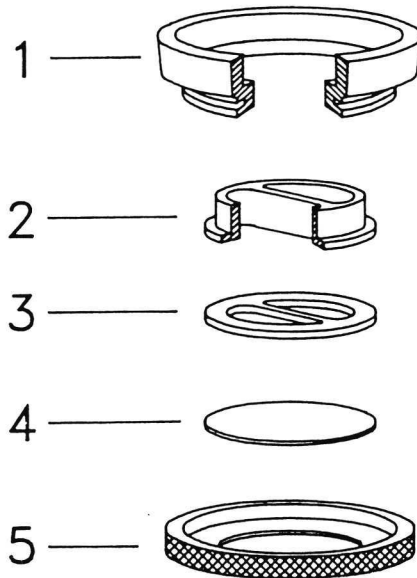


Figure 1. Exploded view of the culture dish containing two compartments. The Eriflon insert [2](\varnothing 21 mm, depth 5.8 mm, compartment volume $\pm 750 \mu\text{l}$) is inserted in the Eriflon ring [1](\varnothing 36 mm). Then, the glass coverslip [4] is secured to the dish by a stainless steel ring [5](\varnothing 36 mm), with a silicon rubber patch [3] (thickness 1 mm) providing a good seal.

Culture dish testing. To test the quality of the barrier between the two compartments, we measured whether high concentrations of various compounds exchanged from one compartment to the other. Both bare glass coverslips and coverslips covered with a confluent monolayer of beating cultured cardiomyocytes (see: *Cell culture*) were used. The following compounds were added to one of the two compartments: the lipophilic fluorochrome 1,6-diphenyl-1,3,5-hexatriene (DPH, 25 μM , Molecular Probes, Eugene, OR, USA), the hydrophilic fluorochrome fura-2 pentapotassium salt (10 μM , Molecular Probes) and the cations H^+ (pH 7.0 vs. pH 4.0 in water) and Ca^{2+} (10 mM). After incubation for 6 h at 37°C, we measured whether the compounds were detectable in the other compartment. Using fluorescence spectroscopy with an imaging fluorescence microscope (see: *Fura-2 fluorescence video microscopy*), we measured DPH (λ_{ex} : 360 nm, λ_{em} : 430 nm), fura-2 pentapotassium salt (λ_{ex} : 360 nm, λ_{em} : 490 nm) and Ca^{2+} (using fura-2: λ_{ex} : 340 and 380 nm, λ_{em} : 490 nm). Permeation of H^+ was measured using a miniature pH electrode (LoT 440 M4, Ingold, Urdorf, Switzerland).

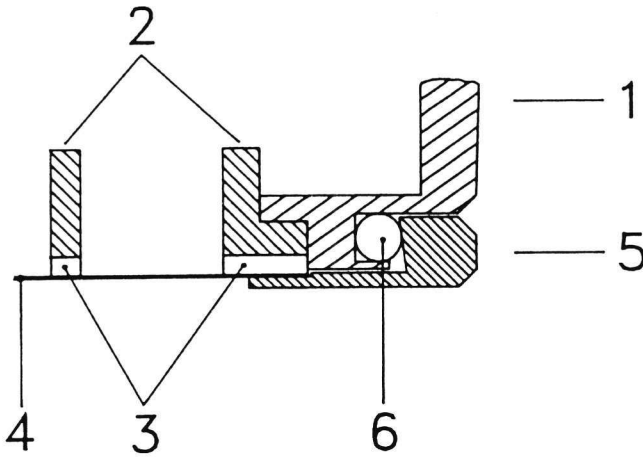


Figure 2. Close-up of the snap-type sealing mechanism. In the assembled culture dish, the glass coverslip [4] is secured to the EriFlon insert [2] by the stainless steel ring [5], while the silicon patch [3] provides a reliable seal. In addition, sealing is achieved by the pressure exerted by a silicon O ring [6] on the conically drilled stainless steel ring [5].

XY-table. In our experiments the culture dish and its micro-incubation chamber are mounted on the table of an inverted imaging fluorescence microscope. The microscope XY-table is fitted with two digital precision sliding gauges (Mitutoyo, Veenendaal, The Netherlands) with a resolution of 10 μm , to allow the precise positioning of the culture dish over the microscope objective. This set-up allows the experimenter to shuttle between the two compartments during the experiment to compare selected cells in one compartment with those in the other compartment, even when using objective magnifications of 100 times.

Cell culture. The myocyte cultures were prepared using the method described by Van der Laarse *et al.*¹⁴ Briefly, hearts of 2 days old anaesthetised Wistar rats were dissected, the ventricles were minced into small fragments and dissociated using collagenase CLS type I (Worthington, Freehold, NJ, USA). The cells were suspended in a culture medium consisting of Ham's F-10 medium (Flow Laboratories, Irvine, UK) supplemented with 10% foetal bovine serum and 10% horse serum (Flow Laboratories). The cells were plated in culture dishes (35 x 10 mm Falcon, Becton Dickinson, Etten-Leur, The Netherlands) containing a round glass coverslip, in a density of 0.5×10^6 cells per dish. The myocyte cultures were kept in a humidified incubator (37°C) with an atmosphere of 95% air and 5% CO_2 . Culture medium was changed after 3 h and after 48 h. Three days after plating the spontaneously beating myocytes, attached to the coverslips, were used.

Fura-2. $[Ca^{2+}]_i$ was measured using the fluorescent calcium indicator fura-2.¹⁵ The cardiomyocytes were loaded with fura-2 by incubation with 2 μ M fura-2/AM (Molecular Probes) in 1 ml of a N-2-hydroxyethyl piperazine-N'-2-ethanesulfonic acid (HEPES) balanced salt solution (HBSS), containing in mM: NaCl 125, KCl 5, MgSO₄ 1, KH₂PO₄ 1, CaCl₂ 2.5, NaHCO₃ 10, HEPES 20, pyruvate 5, pH 7.4, for 30 min at 37°C. After rinsing three times, the glass coverslip was mounted in the two-compartment culture dish. Each compartment of the dish was filled with 500 μ l HBSS at 37°C.

Fura-2 fluorescence video microscopy. The cells were studied in an imaging dual-wavelength fluorescence microscope, consisting of an inverted microscope (Leitz Diavert, Wetzlar, Germany) equipped with a 20x fluorite objective (Nikon, Badhoevedorp, The Netherlands) and a mercury light source (HBO-100, Osram, Montgomery, NY, USA). A filter wheel (Sutter, Novato, CA, USA) allows the selection of excitation filters of 340 nm or 380 nm. Emission fluorescence is led through a 490 nm high-pass filter and is imaged by a high-sensitivity SIT camera (C2400-08 Hamamatsu, Herrsching, Germany). The resulting video signal is digitised by a frame-grabber board (PCVISIONplus™, Imaging Technologies Inc., Woburn, MA, USA) in a PC-AT 486 computer. Spatial resolution of the images is 256*256 pixels, with an 8 bits intensity resolution. Sixteen images of each wavelength were averaged to improve the S/N ratio. This was achieved within 3 s, minimising photo bleaching of the fura-2. The images were processed and analysed using dedicated image processing software (TIM, Difa, Breda, The Netherlands). After the subtraction of the background fluorescence, the 340 nm image was divided by the 380 nm image on a pixel by pixel basis to yield a ratio image. Statistical parameters (mean, median, standard deviation) were calculated by the software and used to calculate $[Ca^{2+}]_i$.

Calibration of fura-2 fluorescence. At the end of the experiment, 10 μ M of the Ca²⁺ ionophore ionomycin (Boehringer, Mannheim, Germany) was added to obtain the highest obtainable ratio value, R_{max}. Then, 20 mM ethylene glycol-bis(β -aminoethyl ether) N,N,N',N'-tetra acetic acid (EGTA) was added to obtain the lowest obtainable ratio value, R_{min}. Calculation of $[Ca^{2+}]_i$ was then performed using the formula described by Grynkiewicz *et al.*¹⁵

Experimental protocol. After inserting the culture dish with the fura-2 loaded myocyte culture in the micro-incubator on the stage of the fluorescence microscope, the culture was equilibrated with HBSS for 30 min at 37°C. Then, the media in the two compartments were changed to Na⁺-free HBSS, in which Na⁺ was substituted on a molar basis by choline.¹³ In one compartment the pH of the Na⁺-free HBSS was 7.4 (control), whereas the pH in the other compartment was either 6.0, 7.0, 7.4 or 8.0. Every minute, a 340 nm and 380 nm image pair was taken per compartment, for

nearly 70 minutes. Off-line, the ratio images were calculated and statistical procedures performed. At each pH, 3-6 cultures were used. A paired t-test was used to test for differences between the two culture halves ($P < 0.05$ was considered significant).

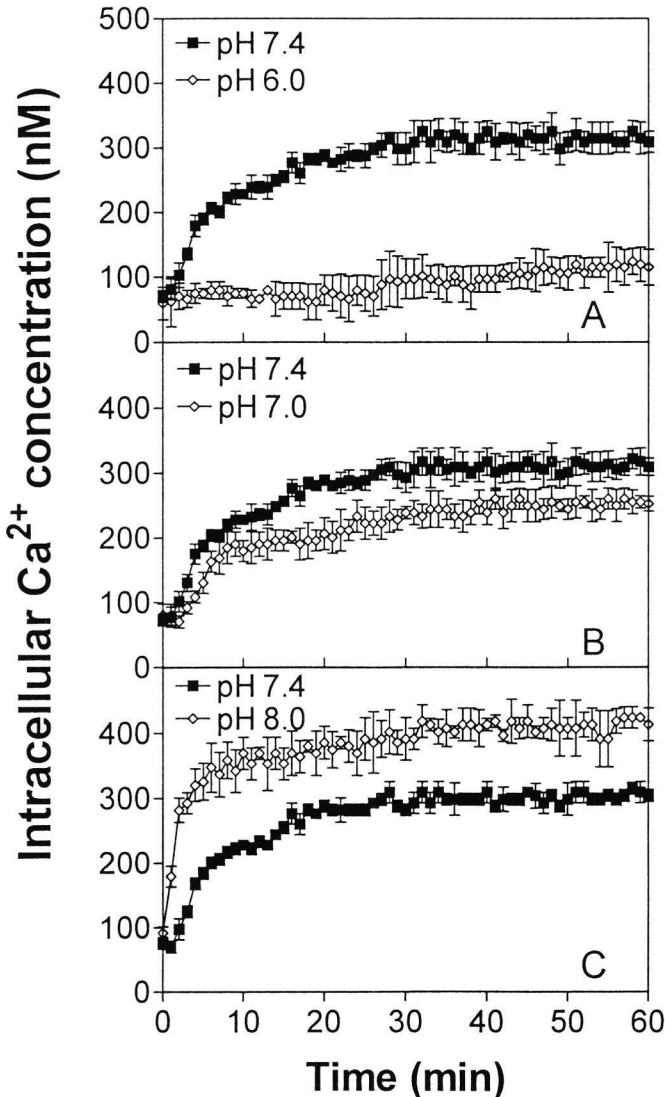


Figure 3. Time course of the intracellular Ca^{2+} concentration (in nM) in cardiomyocyte cultures measured with fura-2, upon incubation with Na^{+} -free buffer with various pH, starting at $t=0$. Panel A: pH 6.0 vs. pH 7.4, Panel B: 7.0 vs. pH 7.4, Panel C: pH 8.0 vs. pH 7.4. (mean \pm SD, $n=3-6$ cultures). Differences were significant in panel A at $t \geq 4$ min, in panel B at $t \geq 13$ min and in panel C at $t \geq 1$ min ($P < 0.05$).

Results

Culture dish testing. None of the compounds tested, either lipophilic (DPH), hydrophilic (fura-2 pentapotassium salt), or low molecular weight cations (Ca^{2+} and H^+) permeated from one compartment to the other compartment during the 6 hours experiment. This lack of permeation ($<0.1\%$) was measured when both bare coverslips and coverslips covered with a monolayer of beating cardiomyocytes were used. The results indicate that the culture dish provides an excellent barrier between the two compartments.

Sodium-free incubation experiments. Upon incubation of the fura-2 loaded cardiomyocytes with sodium-free buffer at pH 7.4, an increase in $[\text{Ca}^{2+}]_i$ was observed from a basal value of 72 ± 12 nM (mean \pm SD) to a steady-state value of 320 ± 30 nM (Fig. 3A). In contrast, during incubation with Na^+ -free buffer at pH 6.0, $[\text{Ca}^{2+}]_i$ rose to only 110 ± 30 nM (Fig. 3A). At pH 7.0, Na^+ -free incubation induced a rise in $[\text{Ca}^{2+}]_i$ which was slower than that observed at pH 7.4 (Fig. 3B), but faster than at pH 6.0. In addition, the $[\text{Ca}^{2+}]_i$ rose to a steady-state value intermediate between that of pH 7.4 and pH 6.0, namely 250 ± 30 nM. Upon incubation with Na^+ -free buffer at pH 8.0, a rapid increase of $[\text{Ca}^{2+}]_i$ was measured to a steady-state value of 410 ± 35 nM. (Fig. 3C). As a decreased rise in $[\text{Ca}^{2+}]_i$ during Na^+ -free incubation reflects a diminished activity of the $\text{Na}^+/\text{Ca}^{2+}$ exchanger, it is apparent from these experiments that at pH 6.0 and 7.0 the activity of the $\text{Na}^+/\text{Ca}^{2+}$ exchanger is decreased as compared with pH 7.4. Conversely, the increased rise in $[\text{Ca}^{2+}]_i$ during Na^+ -free incubation at pH 8.0 indicates an increased $\text{Na}^+/\text{Ca}^{2+}$ exchanger activity.

Discussion

The two-compartment culture dish is a further modification of the original culture dish described earlier.^{1,2} It therefore retains the advantages of the original design such as the possibility to use oil immersion optics (x100), the re-usability of the culture dish, the ability to endure standard sterilisation procedures, the fabrication from non-toxic material, the accessibility of the culture during the experiment and the maintenance of a constant temperature and atmosphere. In addition, the presently described modification allows the exposure of the two halves of the same culture to different treatments. This way, the effects of a drug in one half can be compared to the control situation in the other half of the same culture. Similarly, the effects of a different composition of the incubation buffer can be studied. To facilitate positioning of the two-compartment culture dish, the XY-table of the microscope was fitted with digital sliding gauges for positioning purposes. Since the gauges have

a data output, positioning of the culture dish could be automated with a control unit and a motorised XY-table.

The application of the two-compartment dish is of benefit particularly if a wide variability between different cultures exists, or if the supply of cultures is limited, as with human specimens. A further advantage is the shorter time needed to complete a series of experiments, as two different experiments are conducted simultaneously. Of statistical importance is the fact that the modified dish now allows the use of paired comparison of the two culture halves, since the two treatments are conducted in the same culture.

In the experiment we used to illustrate the application of the two-compartment culture dish, we found that incubation of intact rat cardiomyocytes with sodium-free buffer at pH 7.4 resulted in the increase of $[Ca^{2+}]_i$ consistent with a reversal of the action of the Na⁺/Ca²⁺ exchanger.¹³ When the pH of the Na⁺-free buffer was varied, it was found that below physiological pH, the $[Ca^{2+}]_i$ rose slower and to a lesser extent as compared to pH 7.4. This effect was more pronounced at pH 6.0 than at pH 7.0. In contrast, elevation of the pH of the Na⁺-free buffer to pH 8.0 resulted in an accelerated increase in $[Ca^{2+}]_i$, as compared to pH 7.4, to a steady-state level above that at pH 7.4.

These results suggest that the action of the Na⁺/Ca²⁺ exchanger in cultured neonatal rat ventricular myocytes is diminished at a low extracellular pH, whereas at pH higher than 7.4 the activity of the Na⁺/Ca²⁺ exchanger was accelerated. These findings are in agreement with the results of Philipson *et al.*, who studied the Na⁺/Ca²⁺ exchanger in isolated cardiac sarcolemmal vesicles from the dog.¹²

It is concluded that 1) the two-compartment culture dish is a valuable new tool in the study of individual cells that may have many applications, and 2) the activity of the Na⁺/Ca²⁺ exchanger in cultured neonatal rat ventricular myocytes is diminished at an extracellular pH below 7.4, whereas at higher than physiological pH the action of the Na⁺/Ca²⁺ exchanger is accelerated.

Acknowledgement: The skilful help of G.J. Verschragen of the Department of Physiology of the University of Leiden in the manufacturing of the two-compartment culture dish is gratefully acknowledged. The Department of Physiology of the University of Leiden, where this device is manufactured, has licensed Medical Systems Corporation, 1 Plaza Rd., Greenvale, NY 11548, USA, to market the present chamber under the name 'Two-Compartment Culture Dish'. This research was supported by a grant from the Netherlands Heart Foundation no. 90.089.

References

1. Ince C, van Dissel JT, Diesselhoff-Den Dulk MMC. A teflon culture dish for high magnification observations and measurements from single cells. *Pflügers Arch.* 1985;403:240-244.
2. Ince C, Ypey DL, Diesselhoff-Den Dulk MMC, Visser JAM, De Vos A, Van Furth R. Micro-CO₂-incubator for use on a microscope. *J Immunol Meth.* 1983;60:269-275.
3. Braga PC. Versatile perfusion chamber for high-magnification microscopy. *J Pharmacol Meth.* 1989;22:195-205.
4. Crowe WE, Wills NK. A simple method for monitoring changes in cell height using fluorescent microbeads and an Ussing-type chamber for the inverted microscope. *Pflügers Arch.* 1991;419:349-357.
5. Debey P, Renard JP, Coppey-Moisan M, Monnot I, Geze M. Dynamics of chromatin changes in live one-cell mouse embryos: a continuous follow-up by fluorescence microscopy. *Exp Cell Res.* 1989;183:413-433.
6. Van Duijn B, Inoué K. Regulation of movement speed by intracellular pH during *dictyostelium discoideum* chemotaxis. *Proc Natl Acad Sci USA.* 1991;88:4951-4955.
7. De Erausquin GA, Manev H, Guidotti A, Costa E, Brooker G. Gangliosides normalize distorted single-cell intracellular free Ca²⁺ dynamics after toxic doses of glutamate in cerebellar granule cells. *Proc Natl Acad Sci USA.* 1990;87:8017-8021.
8. Forsythe ID. Micro incubator for regulating temperature and superfusion of tissue-cultured neurons during electrophysiological or optical studies. *Meth Neurosc.* 1991;4:301-318.
9. McKenna NM, Wang YL. Culturing cells on the microscope stage. *Meth Cell Biol.* 1989;29:195-205.
10. Peres A, Bertolini L, Racca C. Characterization of Ca²⁺ transients induced by intracellular photo release of InsP₃ in mouse ovarian oocytes. *Cell Calcium.* 1991;12:457-465.
11. Walsh IB, Van der Berg RJ, Marani E, Rietveld WJ. Spontaneous and stimulated firing in cultured rat suprachiasmatic neurons. *Brain Res.* 1992;588:120-131.
12. Philipson KD, Bersohn MM, Nishimoto AY. Effects of pH on Na⁺-Ca²⁺ exchange in canine cardiac sarcolemmal vesicles. *Circ Res.* 1982;50:287-293.
13. Ziegelstein RC, Zweier JL, Mellits ED, Younes A, Lakatta EG, Stern MD, Silverman HS. Dimethylurea, an oxygen radical scavenger, protects isolated cardiac myocytes from hypoxic injury by inhibition of Na⁺-Ca²⁺ exchange and not by its antioxidant effects. *Circ Res.* 1992;70: 804-811.
14. Van der Laarse A, Hollaar L, Van der Valk EJM. Release of alpha-hydroxybutyrate dehydrogenase from neonatal rat heart cell cultures exposed to anoxia and reoxygenation: comparison with impairment of structure and function of damaged cardiac cells. *Cardiovasc Res.* 1979;13:345-353.
15. Grynkiewicz G, Poenie M, Tsien RY. A new generation of Ca²⁺ indicators with greatly improved fluorescence properties. *J Biol Chem.* 1985;260:3440-3450.

Chapter 4

Role of calcium activated neutral protease (Calpain) in cell death in cultured neonatal rat cardiomyocytes during metabolic inhibition

Douwe E. Atsma, E. M. Lars Bastiaanse, Anastazia Jerzewski, Lizet J.M. Van der Valk, Arnoud Van der Laarse

Department of Cardiology, University Hospital, Leiden, The Netherlands

Circ Res. 1995; 76:1071-1078

Part of this study was presented at the 66th Scientific Meeting of the American Heart Association in Atlanta, USA, November 1993.

Abstract

Calcium Activated Neutral Protease (CANP), also known as calpain, has been implicated in the development of cell death in ischemic hearts. CANP is thought to be activated by the calcium overload that develops during ischemia. We studied the involvement of CANP in cell death in cultured neonatal rat cardiomyocytes during metabolic inhibition (5 mM NaCN + 10 mM 2-deoxyglucose). First, CANP was isolated using ion-exchange and affinity chromatography. Then, the efficacy of the CANP inhibitors calpain I inhibitor, leupeptin and E64 to inhibit isolated CANP activity was tested using fluorescently labeled β -casein as a substrate. IC_{50} for the inhibitors was between 2.1 μ M and 56 μ M. Uptake of the inhibitors by intact cells was assessed employing ^{99m}Tc -radiolabeled inhibitors. The calculated intracellular inhibitor concentrations were sufficiently high to yield substantial inhibition of intracellular CANP activity. Intracellular CANP activity was measured directly using the cell permeant fluorogenic CANP-specific substrate N-succinyl-Leu-Leu-Val-Tyr-7-amido-4-methyl-coumarin. During metabolic inhibition, intracellular CANP activity was increased as compared to control incubation. The time course of CANP activation was compatible with that of the rise in the intracellular Ca^{2+} concentration, as measured using fura-2 and digital imaging fluorescence microscopy. Calpain I inhibitor and leupeptin inhibited intracellular CANP activity both during metabolic inhibition and control incubation, whereas E64 did not. Despite their substantial inhibition of intracellular CANP activity, calpain I inhibitor and leupeptin did not attenuate cell death during metabolic inhibition. We therefore conclude that intracellular CANP in cardiomyocytes is activated during metabolic inhibition, but that it does not play a major role in the development of cell death.

Introduction

The mechanism of myocardial cell death during ischemia, anoxia and metabolic inhibition is still unclear. The rise in the intracellular free calcium concentration in cardiomyocytes observed under these conditions is considered to be a pivotal event in the process of cell death.^{1,2} The resulting calcium overload is thought to massively activate dormant intracellular calcium-activated enzymes, such as Calcium Activated Neutral Protease (CANP), leading to structural damage of the sarcolemmal membrane and, eventually, cell death.^{3,4}

The ubiquitously distributed thiol protease CANP (EC 3.4.22.17) exists in two forms, CANP I and CANP II, which are activated at micromolar and millimolar concentrations of Ca^{2+} , respectively. The physiological significance of the two isoforms of CANP is not clear.

CANP is thought to play a harmful role in a variety of pathologic states, such as in Duchenne muscular dystrophy,⁵ in neurodegenerative conditions including Alzheimer disease,⁶ ischemia,⁷ and multiple sclerosis,⁸ in toxic⁹ and anoxic^{10,11} injury in hepatocytes, oxidative stress in endothelial cells¹² and the development of cataract.¹³

Several studies have addressed the involvement of CANP in anoxic or ischemic cell death in heart cells. In these studies conflicting results have been reported as to the activation of CANP during anoxia or ischemia, and the effects of inhibitors of CANP on cell injury. An increased CANP activity was found in regionally ischemic rat hearts *in vivo*,¹⁴ in Langendorff-perfused rat hearts after ischemia/reperfusion¹⁵ and in anoxic cultured rat cardiomyocytes.¹⁶ In contrast, a *decreased* CANP activity was found in ischemic dog heart.¹⁷ In addition, a CANP inhibitor temporarily protected the ischemic heart in one study,¹⁷ whereas in another study no effect of inhibitors of CANP on infarct size in ischemic rat hearts was found.¹⁸

In these studies the activity of myocardial CANP was measured *post hoc* after the isolation of the enzyme, which procedure could potentially influence the measured enzyme activity¹⁹ and therefore may not accurately reflect the intracellular CANP activity.

Therefore, in our study we used the membrane-permeant fluorogenic CANP-specific substrate N-succinyl-Leu-Leu-Val-Tyr-7-amido-4-methyl-coumarin²⁰ to investigate the role of CANP in the development of cell injury in intact cardiomyocytes during metabolic inhibition. This approach allows the serial monitoring of CANP activity during the course of the experiment. In addition, we assessed the efficacy of inhibitors of CANP, namely calpain I inhibitor, leupeptin and E64, to inhibit CANP activity both *in vitro* and in intact cells, and determined their ability to reduce cell death in cardiomyocytes during metabolic inhibition. It was found that CANP activity is increased during metabolic inhibition, and that it can be inhibited in intact cells by calpain I inhibitor and leupeptin. Since this inhibition of CANP does not lead to improved viability of the cardiomyocytes during metabolic inhibition, we conclude that CANP does not play a major role in the development of cell death in cardiomyocytes during metabolic inhibition.

Materials and Methods

Calpain I inhibitor, leupeptin and E64 were purchased from Boehringer (Mannheim, Germany). DEAE-cellulose and phenyl-sepharose were obtained from Whatman, (Maidstone, UK). β -Casein, fluorescamine, N-(7-dimethylamino-4-methylcoumarinyl) -maleimide (DACM) and fluorescein isothiocyanate (FITC), N-succinyl-Leu-Leu-Val-Tyr-7-amido-4-methyl-coumarin (Suc-Leu-Leu-Val-Tyr-

AMC) and 7-amido-4-methyl-coumarin (AMC) were obtained from Sigma (St. Louis, MO, USA). Fura-2/AM was purchased from Molecular Probes (Eugene, OR, USA). All other reagents used were of analytical grade.

Cell culture. The myocyte cultures were prepared using the method described by Van der Laarse *et al.*²¹ Briefly, hearts of 2 days old Wistar rats were dissected and transferred to a solution containing in mM: NaCl 137, KCl 5, Na₂HPO₄ 0.4, KH₂PO₄ 0.4, glucose 5.5, HEPES 20, phenol red 0.5 mg/l, pH 7.4. The ventricles were minced into small fragments and dissociated using collagenase (type I CLS, Worthington, Freeho7ld, NJ, USA) during two periods of 20 min in a shaking water bath at 37°C. After centrifugation at 50 x g for 15 min, the cells were suspended in a culture medium consisting of Ham's F-10 medium (Flow Laboratories, Irvine, UK) supplemented with 10% fetal bovine serum (Flow Laboratories) and 10% horse serum (Flow Laboratories). The cells were plated in 60 mm culture dishes (Becton-Dickinson, Etten-Leur, The Netherlands) in a density of 4.2×10^6 cells per dish. Myocytes were separated from non-muscle cells using a selective adhesion technique.²² After 45 min the medium, enriched in myocytes, was transferred to either 24-well plates or 35 mm culture dishes, some of which contained 25 mm round glass coverslips. The myocyte cultures were kept in a humidified incubator (37°C) with an atmosphere of 95% air and 5% CO₂. Culture medium was changed after 3 h and after 48 h. After three days the monolayers of spontaneously beating myocytes were used for the experiment.

CANP isolation. To test whether CANP was present in our model, we isolated the enzyme using the method described by Spalla *et al.*²³ Briefly, ventricular myocytes obtained from 5 days old Wistar rats were homogenised in a basic buffer containing in mM: 3-(N-morpholino)propanesulfonic acid (MOPS) 20, ethylene glycol-bis(β-aminoethyl ether)N,N,N',N'-tetraacetic acid (EGTA) 1, ethylenediaminetetraacetic acid (EDTA) 1, and 2-mercaptoethanol 3 (pH 7.2), supplemented with 10 mM NaCl. After centrifugation of the homogenate at 12000 x g for 30 min, the supernatant was collected, the pellet resuspended and centrifuged as before. After pooling of the supernatants, the mixture was loaded on a 2.5 x 10 cm DEAE-cellulose column. After elution with a NaCl gradient from 0.01 to 0.5 M in basic buffer, the fractions containing CANP I and CANP II were identified on the basis of 280 nm absorbance.²³ To separate CANP I from its endogenous inhibitor calpastatin, the CANP I pool was adjusted to 0.25 M NaCl and loaded on a 1 x 10 cm phenyl-Sepharose column. After washing of the column with a gradient of basic buffer supplemented with 0.25 M NaCl and basic buffer supplemented with 20% ethylene glycol, CANP I was eluted from the column with basic buffer containing 20%

ethylene glycol alone. The CANP I and CANP II fractions were then concentrated using membrane filters (Amicon, Stonehouse, UK), and protein concentration in the fractions was determined using the method of Lowry *et al.*²⁴

In vitro CANP activity. The proteolytic activity of the isolated CANP was studied employing a sensitive kinetic *in vitro* protease assay described by Farmer *et al.*, using β -casein as a substrate.²⁵ The β -casein was double labeled with N-(7-dimethylamino-4-methylcoumarinyl)-maleimide (DACM) and fluorescein isothiocyanate (FITC), yielding a fluorescence donor and acceptor pair. In the intact molecule, the DACM fluorescence at 470 nm, upon excitation at 385 nm, is quenched by the adjacent FITC and is therefore very low. However, degradation of the FITC-DACM- β -casein complex by CANP separates the two moieties and releases the quenching of DACM fluorescence by FITC. This results in an increase of DACM fluorescence in proportion with CANP proteolytic activity.

To a mixture of 980 μ l of a 20 mM TRIS-HCl buffer, pH 7.0, and 20 μ l casein-substrate solution (1.34 mg protein/ml), either 400 μ l CANP I solution (0.87 mg protein/ml) or 400 μ l CANP II solution (0.79 mg protein/ml) was added. The increase in DACM fluorescence was measured in a spectrofluorometer (Perkin-Elmer LS-3, Beaconsfield, UK) for at least 5 min under constant stirring at a temperature of 37°C. CANP proteolytic activity was expressed as the increase of fluorescence in arbitrary units per min. The calcium dependency of the CANP proteolytic activity was demonstrated by using the TRIS-HCl buffer supplemented with either 5 mM CaCl₂ to measure calcium-dependent proteolysis, or with 1 mM EGTA to measure calcium-independent proteolysis.

Inhibition of CANP in vitro. The effect of the protease inhibitors calpain I inhibitor, leupeptin and E64 on the proteolytic activity of CANP was tested *in vitro* using the assay described above. To this end, the inhibitors were added to the reaction mixture of the proteolytic assay in a final concentration between 0.1 and 200 μ M, and the reduction in proteolytic activity was expressed as the percentual inhibition compared with the proteolytic activity in the absence of the inhibitors. Calpain I inhibitor was dissolved in ethanol, E64 in 50% ethanol, and leupeptin in water. Control experiments showed that the final concentrations ethanol used (<0.25%) did not influence the assay.

Cellular protease-inhibitor uptake. To study whether the protease-inhibitors calpain I inhibitor, leupeptin and E64 were taken up by cultured myocytes in sufficiently high quantities to yield inhibitory effects, the inhibitors were labeled with ^{99m}Tc, using the method previously described by Pauwels *et al.*²⁶ Purity of the labeled

compounds was verified by HPLC before further use, which procedure also allowed the calculation of the specific radioactivity of the radiolabeled inhibitors. The myocardial cells were incubated in a cell incubation solution containing in mM: NaCl 140, KCl 4, CaCl₂ 2.5, MgSO₄ 1.2, KH₂PO₄ 0.44, Na₂HPO₄ 0.34, NaHCO₃ 21 and sodium pyruvate 5, pH 7.4 in an atmosphere of 95% air and 5% CO₂ at 37°C. Then, 10 μM ^{99m}Tc-leupeptin, 10 μM ^{99m}Tc-calpain I inhibitor or 10 μM ^{99m}Tc-E64 were added and the cultures were incubated for 2 h at 37°C. After this period the medium was separated from the cells, and the radioactivity in the cells and in the incubation medium was counted in a well-type counter (Scalar Ratemeter R4, Delft, The Netherlands). After determination of the uptake of radioactivity by the cells, the intracellular protease-inhibitor concentration was calculated using the specific radioactivity values determined after HPLC.

Metabolic inhibition of cardiomyocytes. Metabolic inhibition of the cardiomyocyte cultures was imposed by incubating the cells with 5 mM NaCN and 10 mM 2-deoxyglucose in a N-2-hydroxyethyl piperazine-N'-2-ethanesulfonic acid (HEPES) balanced salt solution (HBSS), containing in mM: NaCl 125, KCl 5, MgSO₄ 1, KH₂PO₄ 1, CaCl₂ 2.5, NaHCO₃ 10, HEPES 20, sodium pyruvate 5, pH 7.4, for 5 h at 37°C. Before the start of metabolic inhibition each culture was allowed to equilibrate in HBSS for 1 h at 37°C.

Intracellular Ca²⁺ concentration. To record the changes in the intracellular Ca²⁺ concentration ([Ca²⁺]_i) in the myocytes during metabolic inhibition and control incubation, [Ca²⁺]_i was measured using the fluorescent calcium indicator fura-2.²⁷ The cardiomyocytes, cultured on round glass coverslips, were loaded with Fura-2 by incubation with 2 μM Fura-2/AM in 1 ml HBSS for 30 min at 37°C. After rinsing three times, the glass coverslip was mounted in a culture dish containing two compartments, previously described by us.²⁸ Using the two-compartment culture dish, the two halves of a single cell culture grown on a standard coverslip can be exposed to different treatments simultaneously, allowing the effect of one treatment to be compared with that of the other treatment in the same culture. This arrangement circumvents the natural variability that might exist between different individual cultures. In addition, by simultaneously conducting two experiments per dish, the time and the number of cultures needed for the experiment is essentially halved. After mounting the coverslip with the culture in the two-compartment culture dish, each compartment of the dish was incubated with 500 μl HBSS at 37°C. The cells were studied using digital imaging fluorescence microscopy, as described in detail previously.²⁸ The fluorescence microscope consists of an inverted microscope body (Leitz Diavert, Wetzlar, Germany) equipped with a 20x fluorite

objective (Nikon, Tokyo, Japan) and a mercury light source (HBO-100, Osram, Montgomery, NY, USA). A filter wheel (Sutter Instruments, Novato, CA, USA) allows the selection of excitation filters of 340 nm or 380 nm. Emission fluorescence is led through a 490 nm high-pass filter and is imaged by a high-sensitivity SIT camera (Hamamatsu C2400-08, Herrsching, Germany). The resulting video signal is digitized by a frame-grabber board (PCVISIONplus™, Imaging Technologies Inc, Woburn, MA, USA) in a PC-AT 486 computer. Spatial resolution of the images is 256 x 256 pixels, with an 8 bits intensity resolution. Every 5 min, sixteen images of each wavelength were averaged to improve the signal to noise ratio. This was achieved within 3 s, minimising photo bleaching of the fura-2. The images were processed and analysed using dedicated image processing software (TIM, Difa, Breda, The Netherlands). After the subtraction of the background fluorescence, the 340 nm image was divided by the 380 nm image on a pixel by pixel basis to yield a ratio image. The software allows the analysis of individual cells. Statistical parameters (mean, median, standard deviation) were calculated by the software and used to calculate $[Ca^{2+}]_i$.

Calibration of fura-2 fluorescence. At the end of the experiment, 10 μ M of the Ca^{2+} ionophore ionomycin (Boehringer, Mannheim, Germany) was added to obtain the highest obtainable ratio value, R_{max} . Then, 20 mM ethylene glycol-bis(β -aminoethyl ether) N,N,N'-tetra acetic acid (EGTA) was added to obtain the lowest obtainable ratio value, R_{min} . Calculation of $[Ca^{2+}]_i$ was then performed using the formula described by Grynkiewicz *et al.*²⁷

LDH release. In all experiments, cell death was quantified by measuring the LDH activity released from the cardiomyocytes into the medium. To this end, 15 μ l samples of the medium were taken at the indicated time points, and the LDH activity in the samples was measured using a photometric assay (1442597, Boehringer, Mannheim, Germany). At the end of the experiment the cells were lysed using 0.1% Triton X-100 and total LDH activity in the cell culture, i.e. in cells + medium, was determined. After correction for the changes in medium volume during the course of the experiment, LDH activity in the medium samples was expressed as percentage of total LDH activity.

Effect of CANP inhibitors on cell death during metabolic inhibition. To study the effect of calpain I inhibitor, leupeptin and E64 on cell death during metabolic inhibition, cardiomyocyte cultures in 24-well plates were preincubated with HBSS containing either 0 μ M (control), 2.5 μ M, 5 μ M and 10 μ M of the inhibitors for 2 hours at 37°C. Then, the medium was changed and metabolic inhibition was

initiated. The CANP inhibitors were present during the entire experiment. In separate control experiments, the effect of the inhibitors on cell viability during incubation without metabolic inhibition was determined. In the absence of metabolic inhibition, none of the inhibitors induced LDH release in concentrations $\leq 10 \mu\text{M}$. However, E64 caused LDH release at concentrations $> 15 \mu\text{M}$, whereas calpain I inhibitor and leupeptin failed to induce LDH release in concentrations up to $80 \mu\text{M}$ (data not shown).

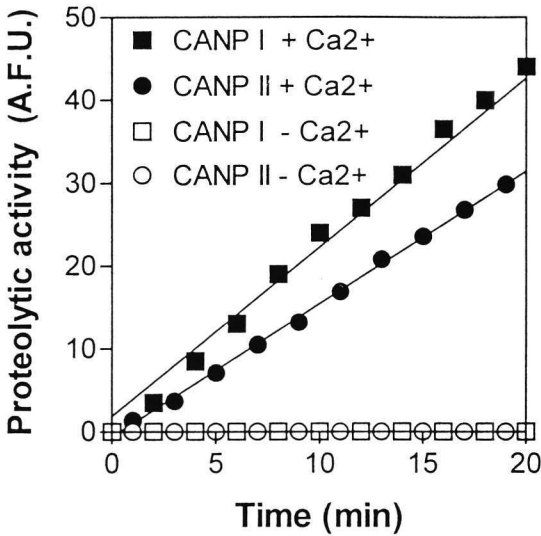
Intracellular CANP activity. To study the involvement of CANP in cell death in more detail, the activity of CANP in intact cells was assessed using the cell permeable synthetic fluorogenic substrate for CANP, Suc-Leu-Leu-Val-Tyr-AMC,²⁰ previously used to measure CANP activity in intact liver cells.^{10,11} The intact substrate exhibits little fluorescence at 430 nm upon excitation at 360 nm. However, specific proteolysis of the substrate by CANP liberates the fluorescent AMC group, leading to an increase of its fluorescence which is proportional to the proteolytic activity of CANP.

Cardiomyocyte cultures in 35 mm culture dishes were incubated with 3 ml HBSS, containing either 5 mM NaCN and 10 mM 2-deoxyglucose (metabolic inhibition) or no addition (control). Immediately after start of the metabolic inhibition or control incubation, Suc-Leu-Leu-Val-Tyr-AMC ($20 \mu\text{M}$) was added to each culture dish and after an equilibration period of 3 min, a sample of 400 μl was taken ($t=0$). Subsequent samples were taken after 30, 60, 90, and 120 min, and AMC fluorescence was measured in a spectrofluorometer (Hitachi F4500, Wokingham, UK). Control experiments showed that the concentration Suc-Leu-Leu-Val-Tyr-AMC used was adequate, and was not a limiting factor in the determination of CANP activity. Also, autofluorescence of the medium was negligible during the entire experiment.

It would be expected that CANP, if it plays a causal role in cell death during metabolic inhibition, is activated before the actual onset of cell death.

In order to draw firm conclusion concerning the time course of CANP activation during metabolic inhibition, we found it was unavoidable to select a subpopulation from the cultures used. Preliminary experiments showed that after the onset of cell death a further steep increase in CANP activity takes place, possibly due to the interaction of cellular CANP with the Ca^{2+} -rich medium. This phenomenon would make it difficult to discern increased CANP activity in still intact cells from the increased CANP activity in already irreversibly injured cells, hampering the correct identification of the time course of CANP activation. To resolve this problem, we also measured cell death in each culture by lactate dehydrogenase (LDH) release

Figure 1. Proteolytic activity of Calcium Activated Neutral Protease I (CANP I, squares) and Calcium Activated Neutral Protease II (CANP II, circles), isolated from neonatal rat myocardium,



in the presence (filled symbols) or absence (open symbols) of 5 mM Ca²⁺, measured *in vitro* using fluorescently labeled β -casein as a substrate. Proteolytic degradation of the substrate leads to an increase in fluorescence, expressed in arbitrary fluorescence units (A.F.U.).

(see below) in addition to CANP activity, to ensure that the CANP activity was from viable cardiomyocytes. When LDH release in a culture

during metabolic inhibition exceeded the LDH release in control cultures at the corresponding time point by more than two standard deviations, the CANP activity data were discarded. At $t \geq 120$ min all cultures in the metabolic inhibition group exceeded this limit. After correction for the changes in medium volume during the course of the experiment, the AMC concentration in the sample was calculated by comparing the measured fluorescence with a calibration curve made with various known concentrations of AMC.

Effect of CANP inhibitors on intracellular CANP activity. To test whether calpain I inhibitor, leupeptin and E64 are able to inhibit CANP proteolytic activity in intact heart cells during control incubation and during metabolic inhibition, the cultures were preincubated in HBSS with 10 μ M of each inhibitor for 2 h at 37°C. Then, medium was changed to HBSS with (metabolic inhibition), or without (control) 5 mM NaCN and 10 mM 2-deoxyglucose, and again 10 μ M of each inhibitor was added. After addition of 20 μ M Suc-Leu-Leu-Val-Tyr-AMC, CANP activity was measured for 2 h as described above.

Statistical analysis. All results are expressed as mean \pm SD. Statistical analysis was performed using ANOVA, followed by the Bonferroni t-test when appropriate. Differences were considered significant if $P < 0.05$.

Results

In vitro protease assay. Proteolytic activity of CANP I and CANP II isolated from neonatal rat heart, as measured using the protease assay with FITC-DACM-casein as a substrate, is shown in figure 1. In the presence of 5 mM Ca^{2+} , a rapid and linear increase in DACM fluorescence was recorded for both isoforms for at least 20 min, whereas in the absence of Ca^{2+} no degradation of the casein substrate occurred. These results show that calcium activated proteolytic activity is present in neonatal rat heart.

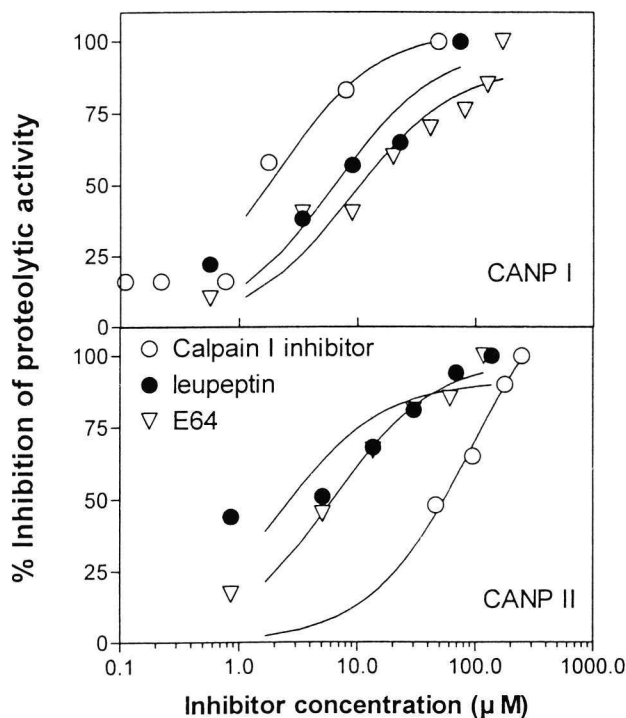


Figure 2. Inhibition *in vitro* of the proteolytic activity of isolated Calcium Activated Neutral Protease I (CANP I, upper panel) and Calcium Activated Neutral Protease II (CANP II, lower panel) by various concentrations of the protease inhibitors calpain I inhibitor (open circles), leupeptin (closed circles) and E64 (open triangles).

In vitro efficacy of CANP inhibitors. The potency of calpain I inhibitor, leupeptin and E64 to inhibit CANP proteolytic activity *in vitro* was tested also using the FITC-DACM-casein substrate. All three inhibitors were able to inhibit CANP I and CANP II (Fig. 2). CANP I activity was half-maximally inhibited at 2.1 μM , 5.9 μM and 8.8 μM of calpain I inhibitor, leupeptin and E64, respectively. Complete inhibition of CANP I was achieved with 45 μM , 65 μM and 168 μM , respectively. For CANP II proteolytic activity, half-maximal inhibition was observed at 56 μM calpain I inhibitor, 4.6 μM leupeptin and 6.2 μM E64, whereas complete inhibition was obtained at 240 μM , 103 μM and 101 μM of the inhibitors, respectively.

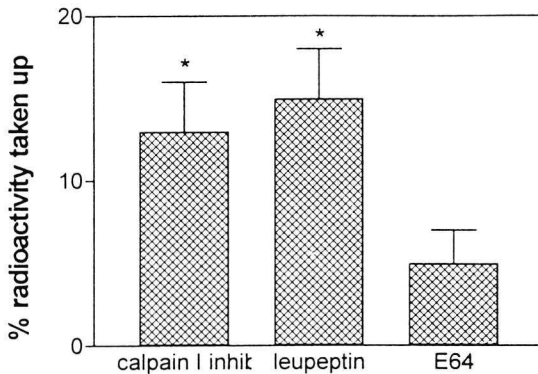


Figure 3. Uptake of ^{99m}Tc -labeled calpain I inhibitor, leupeptin or E64 by cultured neonatal rat cardiomyocytes after incubation with $10\ \mu\text{M}$ of each inhibitor for 2 h at 37°C . (mean \pm SD, * $P < 0.05$ as compared to E64, $n = 6-8$).

Cellular uptake of radiolabeled protease-inhibitors. In order to test the ability of calpain I inhibitor, leupeptin and E64 to enter the cells, we measured the uptake of the radiolabeled inhibitors. After incubation with $10\ \mu\text{M}$ inhibitor in $500\ \mu\text{l}$ medium for 2 hours, $13 \pm 3\%$ of calpain I inhibitor, $15 \pm 3\%$ of leupeptin, and $5 \pm 2\%$ of E64 was incorporated in the cells (Fig. 3). Given a cell volume of $3.3\ \text{pl}$,²⁹ and a cell number of 410,000 cells per well,³⁰ the calculated intracellular concentrations of calpain I inhibitor, leupeptin and E64 were $470\ \mu\text{M}$, $520\ \mu\text{M}$, and $150\ \mu\text{M}$, respectively. Based on the results shown in figure 2, these concentrations are expected to result in near complete inhibition of intracellular CANP activity.

Intracellular Ca^{2+} concentration. The intracellular Ca^{2+} concentration in the cardiomyocytes during metabolic inhibition and control incubation is shown in figure 4. The number of cells analysed was 53 cells in the control incubation group and 42 cells in the metabolic inhibition group. Cells were from at least 5 different cultures. During control incubation, $[\text{Ca}^{2+}]_i$ did not change significantly from the basal value of $82 \pm 30\ \text{nM}$ during the 120 min incubation. In contrast, upon metabolic inhibition $[\text{Ca}^{2+}]_i$ started to rise after 25 min, from a basal value of $86 \pm 24\ \text{nM}$ ($n = 42$ cells), and reached the micromolar range after 45 min. At 120 min, $[\text{Ca}^{2+}]_i$ had risen to a value of $3278 \pm 636\ \text{nM}$.

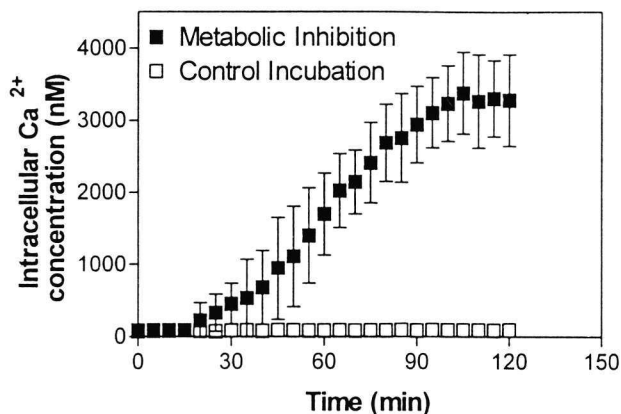


Figure 4. Intracellular Ca^{2+} concentration ($[\text{Ca}^{2+}]_i$) in cardiomyocytes during control incubation (\square $n=53$ cells) and during metabolic inhibition (\blacksquare , $n=42$ cells), measured using fura-2 and digital imaging fluorescence microscopy. Values represent mean \pm SD. The increase in $[\text{Ca}^{2+}]_i$ during metabolic inhibition is significantly higher than during control incubation from $t=25$ min onward ($P<0.05$).

Effect of CANP inhibitors on cell death during metabolic inhibition. The effects of calpain I inhibitor, leupeptin and E64 on cell death during metabolic inhibition are shown in figure 5. After preloading the cardiomyocytes with 0 μM (Control), 2.5 μM , 5 μM , or 10 μM of each inhibitor and in the presence of the inhibitors in these concentrations during the experiment, the time course of cell death during metabolic inhibition in the treated groups is not different from the untreated group for all three CANP inhibitors. Extension of the preloading period of the inhibitors from 2h to 18 h did not lead to protection of the cardiomyocytes during metabolic inhibition. Higher concentrations of calpain I inhibitor (up to 40 μM) or leupeptin (up to 80 μM) did not protect the cells from cell death during metabolic inhibition, whereas higher concentrations of E64 (≥ 15 μM) accelerated, rather than delayed, cell death during metabolic inhibition (data not shown).

Intracellular CANP activity. Invariably, when CANP activity data from all cultures exposed to metabolic inhibition were combined, an increased CANP activity as compared to control incubation was observed at all time points from $t=30$ min onward (data not shown). However, as explained in the *Materials and Methods* section, part of this increase in CANP activity was caused by CANP activity from cardiomyocytes that were already grossly damaged. As this phenomenon would make it impossible to establish the exact time course of CANP activation in intact cells, we measured in each culture LDH release in addition to CANP activity and selected the still viable cardiomyocyte cultures (see also *Materials and Methods*). During control incubation, a gradual increase in AMC fluorescence was observed, reflecting basal CANP proteolytic activity (Fig. 6A). In contrast, upon metabolic inhibition CANP activity is significantly increased at 60 and 90 minutes after onset of metabolic inhibition, as indicated by a higher rate of fluorescence increase

($P < 0.05$) (figure 6A). As in the cultures exposed to metabolic inhibition no significant cell death takes place at $t \leq 90$ min (figure 6B), the values measured in these cultures at these timepoints reflect CANP activity in still intact cells. However, at $t = 120$ min, cell death in all metabolically inhibited cultures was higher than in control cultures, and therefore the values measured at $t = 120$ min also represent CANP activity in fatally damaged cells.

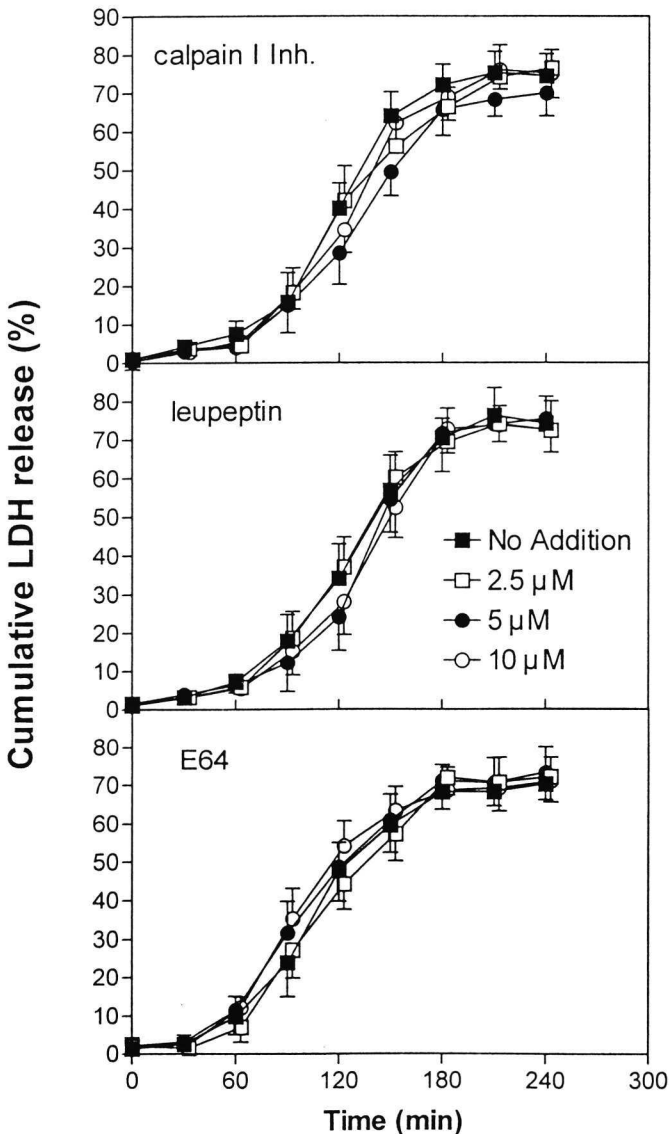


Figure 5. Cumulative release of lactate dehydrogenase (LDH) activity from cultured neonatal rat cardiomyocytes during metabolic inhibition, in the absence (no addition ■), or presence of 2.5 μM (□), 5 μM (●), or 10 μM (○) of the CANP inhibitors calpain I inhibitor (upper panel), leupeptin (middle panel) or E64 (lower panel). No statistical differences were observed between treated and untreated groups for all three inhibitors (n=4-6 triplicate experiments).

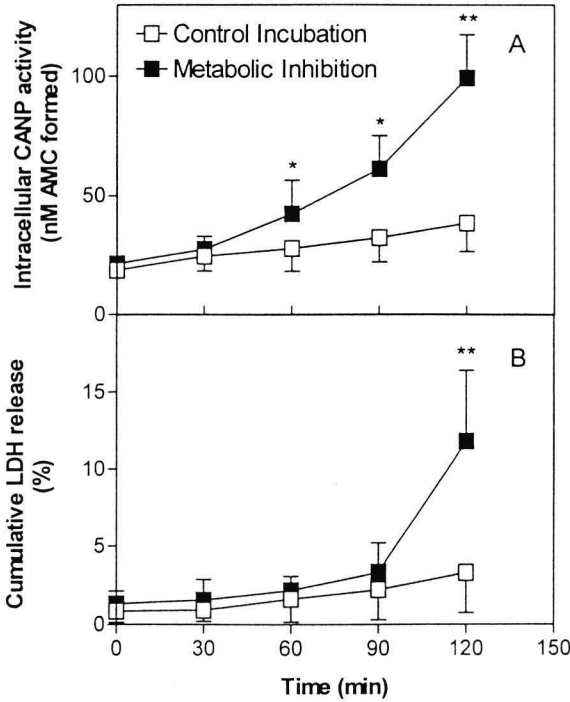


Figure 6.A. Intracellular proteolytic activity of Calcium Activated Neutral Protease (CANP) in viable neonatal rat cardiomyocytes during control incubation (□) and during metabolic inhibition (■), assessed using the membrane-permeant fluorogenic CANP-specific substrate Suc-Leu-Leu-Val-Tyr-AMC). Proteolysis of the substrate by CANP leads to the liberation of the fluorescent AMC moiety, leading to an increase of its fluorescence in proportion to the proteolytic activity of CANP.

B. Cumulative release of lactate dehydrogenase (LDH) activity from neonatal rat cardiomyocytes in the same cultures shown in panel A, during control incubation (□) and during metabolic inhibition (■). (Values are mean±SD. * P<0.05, ** P<0.01, n ≥ 13 cultures).

Effect of CANP inhibitors on intracellular CANP activity. Calpain I inhibitor (10 μM) and leupeptin (10 μM) inhibited intracellular CANP activity almost completely during control incubation (Fig. 7A). Also during metabolic inhibition did calpain I inhibitor and leupeptin inhibit intracellular CANP activity, to values comparable to basal CANP activity (Fig. 7B). The inhibition of the intracellular CANP activity by calpain I inhibitor or leupeptin was significant at all time points as compared to control incubation or metabolic inhibition without inhibitors (P<0.05). In contrast, E64 (10 μM) did not inhibit intracellular CANP activity during control incubation nor during metabolic inhibition (Fig. 7A and B). Also at higher concentrations of E64 (≤ 40 μM) no inhibition of CANP activity was observed. The increase of the concentrations of calpain I inhibitor and leupeptin up to 40 μM did not cause a further inhibition of the intracellular CANP activity.

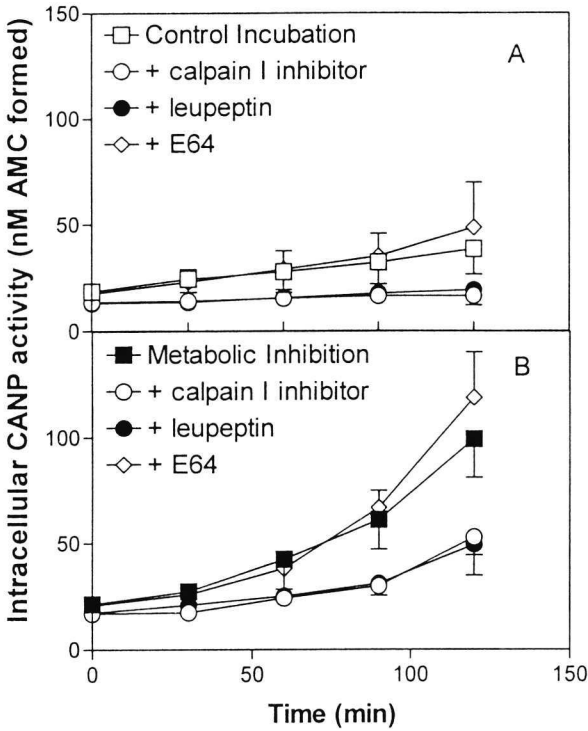


Figure 7. Intracellular proteolytic activity of Calcium Activated Neutral Protease (CANP) in intact cultured neonatal rat cardiomyocytes, measured using the membrane-permeant fluorogenic CANP-specific substrate Suc-Leu-Leu-Val-Tyr-AMC (see *Materials and Methods*). **A.** Intracellular CANP activity during control incubation in the absence (control incubation, □) or the presence of 10 μ M of the CANP inhibitors calpain I inhibitor (○), leupeptin (●) or E64 (◇). The lower CANP activity in the presence of calpain I inhibitor and leupeptin as compared to CANP activity during control incubation was significant at all time points (n=9-11 cultures).

B. Intracellular CANP activity during metabolic inhibition in the absence (metabolic inhibition, ■) or the presence of 10 μ M of the CANP inhibitors calpain I inhibitor

(○), leupeptin (●) or E64 (◇). The lower CANP activity in the presence of calpain I inhibitor and leupeptin as compared to CANP activity during metabolic inhibition was significant at all time points (n=7-9 cultures).

Discussion

The role of CANP in ischemic cell death in cardiomyocytes remains unclear. The involvement of CANP in cell death as an effector of irreversible cell injury constitutes an attractive hypothesis, as the proteolytic action of CANP is Ca^{2+} -dependent and among its purported substrates are several key cytoskeletal proteins.¹⁹ Thus, massive supra-physiological activation of CANP during ischemia would link the developing calcium overload with the subsequent degradation of the sarcolemmal membrane, thereby causing myocardial cell death.

In our study, we used cultured neonatal rat cardiomyocytes as a model. Although developmental differences may exist compared to adult heart cells, the neonatal cardiomyocytes constitute an attractive model as several key events during metabolic

inhibition or ischemia mimic the events occurring in adult heart cells. For example, during energy depletion neonatal and adult cells have comparable time courses of a) the rise in the intracellular free calcium concentration,^{31,32} b) the development of sarcolemmal blebs^{33,34} and, c) the cumulative enzyme release.^{33,35} These findings indicate that the differences in development between neonatal and adult cells only have a slight influence with respect to the above mentioned cellular dysfunction and cell death.

We isolated the two isoforms of CANP, namely CANP I and CANP II from neonatal rat heart and demonstrated the Ca^{2+} -dependency of the proteolytic activity of both isoforms, using a sensitive kinetic proteolytic assay with a double-labeled fluorescent β -casein substrate. Using this assay, it was established that the CANP inhibitors calpain I inhibitor, leupeptin and E64 were able to effectively inhibit the proteolytic activity of both CANP isoforms *in vitro*. Until now, CANP activity has not been directly assessed in intact myocardial cells, but instead was measured *post hoc* after isolation of the enzyme from ischemic or anoxic tissue. As the isolation procedure itself may induce artefacts leading to a less accurate estimation of intracellular CANP activity,¹⁹ we used the cell permeant fluorogenic CANP-specific substrate Suc-Leu-Leu-Val-Tyr-AMC to serially measure CANP activity in intact cells during the course of the experiment.

Although it was found, using this method, that CANP activity was significantly increased already 30 min after addition of the metabolic inhibitors when compared with the CANP activity in control cultures, this result proved deceptive. Control experiments showed that after onset of cell death, CANP activity in cardiomyocyte cultures was greatly increased, most likely due to massive activation of the intracellular CANP by the millimolar concentration Ca^{2+} present in the incubation medium. As cardiomyocyte cultures contain a heterogeneous population of heart cells, it is to be expected that already fairly soon after start of the metabolic inhibition, cell death occurs in a number of cells which leads to an early rise in measured CANP activity.

As these values of CANP activity do not provide insight into the role of CANP in the development of sarcolemmal damage, but rather reflect sarcolemmal damage that has already been inflicted, cell death was assessed concurrently with the determination of CANP activity. This way, a distinction could be made between CANP activity data obtained from viable cells, and that obtained from cells with already gross irreversible sarcolemmal damage. Data from the latter group was discarded. Only through this correction method, a firm conclusion could be drawn concerning the time course of CANP activation during metabolic inhibition.

Using this correction method, it was found that during metabolic inhibition the intracellular CANP activity was significantly increased 60 min and 90 min after

addition of the metabolic inhibitors when compared with the intracellular CANP activity during control incubation.

This time course of CANP activation during metabolic inhibition is consistent with that of the rise in the intracellular free calcium concentration ($[Ca^{2+}]_i$) under these conditions. Measurement of $[Ca^{2+}]_i$ using fura-2 and digital imaging fluorescence microscopy showed that $[Ca^{2+}]_i$ starts to rise 25 min after onset of metabolic inhibition from the basal value of approximately 80 nM, and reaches the micromolar range after 45 min. This finding is in agreement with results obtained in other models of metabolic inhibition.^{36,37} Thus, the time course of the rise in $[Ca^{2+}]_i$ in our model is compatible with the finding of an increased CANP activity at $t = 60$ min and $t = 90$ min. The increased CANP activity during metabolic inhibition reported in the present study is in agreement with the rise in CANP activity found by Tolnai and Korecky,¹⁴ and Yoshida *et al.*¹⁵ in ischemic rat hearts, and Iizuka *et al.*¹⁶ in hypoxic cultured rat cardiomyocytes. The reason Toyo-oka *et al.*¹⁷ found a decreased CANP activity in ischemic dog heart is not clear. It is possible that in this study the previously activated CANP had already been inactivated, and therefore its increased proteolytic activity could not be measured any more.

In addition to an increased CANP activity in the ischemic hearts, Tolnai and Korecky also found a concomitant decrease in the activity of the endogenous CANP inhibitor calpastatin, which may well contribute to the observed rise in CANP activity.¹⁴

In our experiments, the protease inhibitors calpain I inhibitor and leupeptin were able to decrease intracellular CANP activity in the cardiomyocytes both during control conditions, and during metabolic inhibition. Treatment with E64 did not lead to inhibition of CANP activity in control cells, nor in metabolically inhibited cells. Since E64 does inhibit CANP *in vitro*, lack of CANP inhibition in intact cells could - at least in part - be due to the inability of the charged E64 molecule to readily cross the sarcolemmal membrane.³⁸ This explanation is corroborated by our finding that radiolabeled calpain I inhibitor and leupeptin were taken up by the cells in quantities 3-4 times higher than E64. However, even this lower uptake of E64 is expected to result in an intracellular concentration sufficiently high (150 μ M) to inhibit CANP activity considerably. An explanation for the failure of E64 to exert its inhibitory action despite its substantial intracellular concentration could be that upon entering the cells, E64 is bound by intracellular components preventing the charged molecule to reach the CANP molecule.

Having established that CANP activity could be inhibited intracellularly by calpain I inhibitor and leupeptin, we studied the effect of these CANP inhibitors and of E64 on cell death during metabolic inhibition. We found that none of the three inhibitors protected the cardiomyocytes from cell death under these conditions. Even with

concentrations of calpain I inhibitor up to 40 μM or of leupeptin up to 80 μM , still no protective effect was observed. Higher concentrations of E64 ($\geq 15 \mu\text{M}$) caused an accelerated, rather than a delayed, cell death. Also, prolongation of the period of loading the cells with the inhibitors up to 18 h did not alter the outcome of the experiment. These results are in agreement with the observations of Bolli *et al.* who also did not find a protective effect of the protease inhibitors leupeptin, antipain or pepstatin on infarct size in ischemic rat hearts.¹⁸ In contrast, Toyooka *et al.* did find a beneficial effect of the protease inhibitor NCO-700, previously shown to inhibit CANP,³⁹ on infarct size in ischemic dog heart.¹⁷ The protection provided by NCO-700 in this model (a decrease in infarct size from 14.4 % to 10.2 %), was only observed at 3 hours after onset of ischemia, and was no longer present at 6 hours after onset of ischemia. A possible explanation for the protective effect of NCO-700 could lie in its ability to attenuate myocardial acidosis during ischemia rather than in its CANP inhibiting properties.⁴⁰

Iizuka *et al.*¹⁶ found a protective effect of the CANP inhibitors calpain I inhibitor and E64-c, a more membrane-permeant derivative of E64, on cell death in hypoxic cultured rat cardiomyocytes. The reason for the discrepancy with our results is not clear, although it could be due to differences in model used, i.e. metabolic inhibition vs. hypoxia.

In summary, we have isolated CANP from neonatal rat heart and we have demonstrated the efficacy of the protease inhibitors calpain I inhibitor, leupeptin and E64 to inhibit isolated CANP activity *in vitro*. It was then shown that CANP in intact cardiomyocytes is activated during metabolic inhibition as measured using the fluorogenic CANP-specific substrate Suc-Leu-Leu-Val-Tyr-AMC. Using fura-2 and digital imaging fluorescence microscopy, it was shown that the time course of the rise in $[\text{Ca}^{2+}]_i$ in the cardiomyocytes during metabolic inhibition is compatible with the observed intracellular CANP activation. We showed that calpain I inhibitor and leupeptin were taken up by the cardiomyocytes, as assessed by the accumulation of radiolabeled inhibitors and by the inhibition of CANP activity in intact cardiomyocytes. Finally, despite substantial inhibition of intracellular CANP activity during metabolic inhibition by calpain I inhibitor and leupeptin, no effect of these inhibitors was observed on cell death during metabolic inhibition. Therefore, we conclude that CANP in cardiomyocytes is activated during metabolic inhibition, but that it does not play a major role in the development of cell death.

References

1. Nayler WG. The role of calcium in the ischemic myocardium. *Am J Pathol.* 1981;102:262-270.
2. Steenbergen C, Murphy E, Watts JA, London RE. Correlation between cytosolic free calcium, contracture, ATP, and irreversible ischemic injury in perfused rat hearts. *Circ Res.* 1990;66:135-146.
3. Toyooka T, Ross JR. Ca^{2+} sensitivity change and troponin loss in cardiac natural actomyosin after coronary occlusion. *Am J Physiol.* 1981;240:H704-H708.
4. Steenbergen C, Murphy E, Levy L, London RE. Elevation of cytosolic free calcium concentration early in myocardial ischemia in perfused rat heart. *Circ Res.* 1987;60:700-707.
5. Reddy PA, Anandavalli TE, Anandaraj MPJS. Calcium activated neutral protease (milli- and microCANP) and endogenous CANP inhibitor of muscle in Duchenne muscular dystrophy (DMD). *Clin Chim Acta.* 1986;160:281-288.
6. Saito KI, Elce JS, Hamos JE, Nixon RA. Widespread activation of calcium-activated neutral proteinase (Calpain) in the brain in Alzheimer disease - A potential molecular basis for neuronal degeneration. *Proc Natl Acad Sci USA.* 1993;90:2628-2632.
7. Hong SC, Goto Y, Lanzino G, Soleau S, Kassell NF, Lee KS. Neuroprotection with a calpain inhibitor in a model of focal cerebral ischemia. *Stroke.* 1994;25:663-669.
8. Zimmerman U-JP, Schlaepfer A. Calcium-activated neutral protease (CANP) in brain and other tissues. *Prog Neurobiol.* 1984;23:63-78.
9. Nicotera P, Hartzell P, Davis G, Orrenius S. The formation of plasma membrane blebs in hepatocytes exposed to agents that increase cytosolic Ca^{2+} is mediated by the activation of a non-lysosomal proteolytic system. *FEBS Lett.* 1986;209:139-144.
10. Bronk SF, Gores GJ. pH-Dependent nonlysosomal proteolysis contributes to lethal anoxic injury of rat hepatocytes. *Am J Physiol.* 1993;264:G744-G751.
11. Nichols JC, Bronk SF, Mellgren RL, Gores GJ. Inhibition of nonlysosomal calcium-dependent proteolysis by glycine during anoxic injury of rat hepatocytes. *Gastroenterology.* 1994;106:168-176.
12. Geeraerts MD, Ronveauw-Dupal MF, Lemasters JJ, Herman B. Cytosolic free Ca^{2+} and proteolysis in lethal oxidative injury in endothelial cells. *Am J Physiol.* 1991;261:C889-C896.
13. Lampi KJ, Kadoya K, Azuma M, David LL, Shearer TR. Comparison of cell-permeable calpain inhibitors and E64 in reduction of cataract in cultured rat lenses. *Toxicol Appl Pharmacol.* 1992;117:53-57.
14. Tolnai S, Korecky B. Calcium-dependent proteolysis and its inhibition in the ischemic rat myocardium. *Can J Cardiol.* 1986;2:42-47.
15. Yoshida K, Yamasaki Y, Kawashima S. Calpain activity alters in rat myocardial subfractions after ischemia or reperfusion. *Biochim Biophys Acta.* 1993;1182:215-220.
16. Iizuka K, Kawaguchi H, Kitabatake A. Effects of thiol protease inhibitors on fodrin degradation during hypoxia in cultured myocytes. *J Mol Cell Cardiol.* 1993;25:1101-1109.
17. Toyooka T, Kamishiro T, Gotoh Y, Fumino H, Masaki T, Hosoda S. Temporary salvage of ischemic myocardium by the protease inhibitor bis[ethyl(2R,3R)-3-[(S)-methyl-1-[4-(2,3,4-trimethoxy-phenyl-methyl)piperazin-1-ylcarbonyl]butyl-carbonyl]oxiran-2-carboxylate]sulfate. *Arzneimittelforschung.* 1986;36:671-675.
18. Bolli R, Cannon RO, Speir E, Goldstein RE, Epstein SE. Role of cellular proteinases in acute myocardial infarction. II. Influence of in vivo suppression of myocardial proteolysis by

- antipain, leupeptin and pepstatin on myocardial infarct size in the rat. *J Am Coll Cardiol.* 1983;2:681-686.
19. Croall DE, Demartino GN. Calcium-activated neutral protease (calpain) system: structure, function and regulation. *Physiol Rev.* 1991;71:813-847.
 20. Sasaki T, Kikuchi T, Yumoto N, Yoshimura N, Murachi T. Comparative specificity and kinetic studies on porcine calpain I and calpain II with naturally occurring peptides and synthetic substrates. *J Biol Chem.* 1984;259:12489-12494.
 21. Van der Laarse A, Hollaar L, Van der Valk EJM. Release of alpha-hydroxybutyrate dehydrogenase from neonatal rat heart cell cultures exposed to anoxia and reoxygenation: Comparison with impairment of structure and function of damaged cardiac cells. *Cardiovasc Res.* 1979;13:345-353.
 22. Blondel B, Royen J, Cheneval JP. Heart cells in culture: a simple method for increasing the proportion of myoblasts. *Experimenta.* 1971;27:356-358.
 23. Spalla M, Tsang W, Kuo TH, Giacomelli F, Wiener J. Purification and characterization of two distinct Ca^{2+} -activated proteinases from hearts of hypertensive rats. *Biochim Biophys Acta.* 1985;830:258-266.
 24. Lowry OH, Rosebrough NJ, Farr AL, Randall RJ. Protein measurement with the Folin phenol reagent. *J Biol Chem.* 1951;193:265-275.
 25. Farmer W, Yuan Z. A continuous fluorescent assay for measuring protease activity using natural protein substrate. *Anal Biochem.* 1991;197:347-352.
 26. Pauwels EKJ, Welling MM, Feitsma RIJ, Atsma DE, Nieuwenhuizen W. The labeling of proteins and LDL with ^{99m}Tc : a new direct method employing KBH₄ and stannous chloride. *Nucl Med Biol.* 1993;20:825-833.
 27. Grynkiewicz G, Poenie M, Tsien RY. A new generation of Ca^{2+} indicators with greatly improved fluorescence properties. *J Biol Chem.* 1985;260:3440-3450.
 28. Atsma DE, Bastiaanse EML, Ince C, Van der Laarse A. A novel two-compartment culture dish allows microscopic evaluation of two different treatments in one cell culture simultaneously - Influence of external pH on Na^+/Ca^{2+} exchanger activity in cultured rat cardiomyocytes. *Pflügers Arch.* 1994;428:296-299.
 29. Atkins DL, Rosenthal JK, Krumm PA, Marvin WJ. Application of stereological analysis of cell volume to isolated myocytes in culture with and without adrenergic innervation. *Anat Rec.* 1991;231:209-217.
 30. Van der Laarse A, Hollaar L, Van der Valk EJM, Hamers S. A method to quantitate cell numbers of muscle cells and non-muscle cells in homogenised heart cell cultures. *Cardiovasc Res.* 1989;23:928-933.
 31. Noda N, Hayashi H, Miyata S, Kobayashi A, Yamazaki N. Cytosolic Ca^{2+} concentration and pH of diabetic rat myocytes during metabolic inhibition. *J Mol Cell Cardiol.* 1992;24:435-446.
 32. Siegmund B, Zude R and Piper HM. Recovery of anoxic-reoxygenated cardiomyocytes from severe Ca^{2+} overload. *Am J Physiol.* 1992;263:H1262-H1269.
 33. Bhatti S, Zimmer G, Bereiter HJ. Enzyme release from chick myocytes during hypoxia and reoxygenation: dependence on pH. *J Mol Cell Cardiol.* 1989;21:995-1008.
 34. Schwartz P, Piper HM, Spahr R, Spieckermann PG. Ultrastructure of cultured adult myocardial cells during anoxia and reoxygenation. *Am J Pathol.* 1984;115:349-361.
 35. Murphy MP, Hohl C, Brierly GP, Altschuld RA. Release of enzymes from adult heart myocytes. *Circ Res.* 1982;51:560-568.
 36. Chacon E, Reece JM, Nieminen AL, Zahrebelski G, Herman B, Lemasters JJ. Distribution of electrical potential, pH, free Ca^{2+} , and volume inside cultured adult rabbit cardiac myocytes

- during chemical hypoxia - A multiparameter digitized confocal microscopic study. *Biophys J.* 1994;66:942-952.
37. Li Q, Altschuld RA, Stokes BT. Myocyte deenergization and intracellular free calcium dynamics. *Am J Physiol.* 1988;255:C162-C168.
 38. Mehdi S. Cell-penetrating inhibitors of calpain. *Trends Biochem Sci.* 1991;16:150-153.
 39. Toyo-oka T, Kamishiro T, Masaki M, Masaki T. Reduction of experimentally produced acute myocardial infarction by a new synthetic inhibitor, NCO700, against calcium activated neutral protease. *Jpn Heart J.* 1982;23:829-834.
 40. Haga N, Ishibashi T, Abiko Y. Effect of NCO-700, an inhibitor of protease, on myocardial pH decreased by coronary occlusion in dogs. *Pharmacology.* 1985;31:208-217.

Chapter 5

I. Role of phospholipid degradation in death of anoxic cardiomyocytes

Effect of purported PLA₂ inhibitors on calcium overload and phospholipid degradation

Douwe E. Atsma, E. M. Lars Bastiaanse, Lizet J.M. Van der Valk, Arnoud Van der Laarse

Department of Cardiology, University Hospital, Leiden, The Netherlands

Submitted

Parts of this study were presented at the 14th European Section Meeting of the International Society for Heart Research, Jerusalem, Israel, 1993 and the 43rd Scientific Meeting of the American College of Cardiology, Atlanta, USA, 1994.

Abstract

We studied the roles of calcium overload and phospholipid degradation in cell death in cardiomyocytes during chemical anoxia (*CA*) (5 mM NaCN + 10 mM 2-deoxyglucose), using imaging fluorescence microscopy and PLA₂ inhibitors chlorpromazine (CPZ) and trifluoperazine (TFP). Upon *CA*, calcium overload developed, followed by cell death. CPZ and TFP dose-dependently attenuated calcium overload and cell death. CPZ and TFP delayed onset of contracture, but did not affect cellular ATP content during *CA*. Phospholipid degradation, assessed by ³H-arachidonic acid release, increased 3-fold during *CA*, which increase was limited by CPZ and TFP by approx. 35 %. Phospholipid degradation was predictive for ensuing cell death. CPZ and TFP also dose-dependently inhibited the sarcolemmal Na⁺/Ca²⁺ exchanger, considered to mediate calcium overload in anoxia. We used Ni²⁺ ions to selectively inhibit Na⁺/Ca²⁺ exchange without inhibiting PLA₂. Ni²⁺ ions dose-dependently attenuated calcium overload and cell death during *CA*. The relation between Ca²⁺ exposure and cell death was dissimilar for untreated and Ni²⁺-treated cells as compared to CPZ and TFP treated cells. We conclude: 1) CPZ and TFP protect cardiomyocytes during *CA* by limiting phospholipid degradation and Na⁺/Ca²⁺ exchanger activity, 2) calcium overload is an important but no single determinant in anoxic cell death.

Introduction

The basic mechanism responsible for cell death of ischemic cardiomyocytes is still unknown. Calcium overload is considered to play a pivotal role in the development of irreversible cell death.^{1,2} The rise in intracellular free calcium concentration ([Ca²⁺]_i) has been proposed to massively activate intracellular enzymes, including Calcium Activated Neutral Protease (CANP) and calcium-dependent phospholipase A₂ (PLA₂).^{3,4} Activation of these enzymes would then lead to sarcolemmal damage and, eventually, cell death. We recently showed that upon severe ATP depletion, activation of CANP did occur in cardiomyocytes, but that activated CANP did not play a major role in the development of cell death.⁵ The involvement of PLA₂ in the development of cell death during ischemia, anoxia and energy depletion is inferred from the accumulation of lysophospholipids and arachidonic acid (AA), a fatty acid almost exclusively esterified to the sn-2 position in myocardial phospholipids.⁶⁻⁹ However, although in these studies a close correlation has been observed between phospholipid degradation and cell death, it is not clear whether activation of PLA₂ is a causal factor in cell death, or rather the consequence of cell death, reflecting the autolysis of necrotic cells.¹⁰ Several authors have reported that PLA₂ activity was

decreased rather than *increased* during anoxia,^{11,12} further complicating the understanding of the involvement of PLA₂ in myocardial cell death.

Experiments in which purported inhibitors of PLA₂ produced protective effects on heart cells during ischemia, anoxia or metabolic inhibition suggest that PLA₂ is involved in the process of cell death.^{7,13,14,16} However, lack of specificity of the PLA₂ inhibitors used severely complicates the interpretation of the results, as many of the inhibitors may have effects other than inhibition of PLA₂, such as inhibition of calmodulin,¹⁶ Ca²⁺ channels¹⁷ and Ca²⁺-ATPase,¹⁸ or act as membrane stabilizing agents.^{19,20}

Quinacrine, a purported PLA₂ inhibitor, was shown to influence the activity of the sarcolemmal Na⁺/Ca²⁺ exchanger, which is considered to mediate the development of Ca²⁺ overload during ischemia.²¹ As Ca²⁺ overload in itself may cause physico-chemical perturbations in the cardiac sarcolemma during ischemia which could lead to cell death,^{22,23} inhibition of Ca²⁺ overload might be an important protective property of PLA₂ inhibitors.

Therefore, we studied the effect of purported PLA₂ inhibitors on the development of Ca²⁺ overload as well as on phospholipid degradation in energy-depleted cardiomyocytes, in an effort to establish the relative contribution of each factor to the pathogenesis of cell injury. To this end, we measured [Ca²⁺]_i, AA release and cell death in cultured neonatal rat cardiomyocytes during chemical anoxia (5 mM NaCN and 10 mM 2-deoxyglucose). We used purported inhibitors of PLA₂ (chlorpromazine and trifluoperazine), an inhibitor of calmodulin (calmidazolium) and an inhibitor of the sarcolemmal Na⁺/Ca²⁺ exchanger (Ni²⁺), and studied their effect on 1) [Ca²⁺]_i, 2) phospholipid degradation, and 3) cell death.

Materials and Methods

Cell culture. Myocyte cultures were prepared using the method described by Van der Laarse *et al.*²⁴ Briefly, hearts of 2 days old Wistar rats were dissected and transferred to a solution containing in mM: NaCl 137, KCl 5, Na₂HPO₄ 0.4, KH₂PO₄ 0.4, glucose 5.5, N-2-hydroxyethyl piperazine-N'-2-ethanesulfonic acid (HEPES) 20, phenol red 0.5 mg/l, pH 7.4. The ventricles were minced into small fragments and dissociated using collagenase (type I CLS, Worthington, Freehold, NJ, USA) during two periods of 20 min in a shaking water bath at 37°C. After centrifugation at 50 x g for 15 min, the cells were suspended in a culture medium consisting of Ham's F-10 medium (Flow Laboratories, Irvine, UK) supplemented with 10% fetal bovine serum (Flow Laboratories) and 10% horse serum (Flow Laboratories). The cells were plated in 60 mm culture dishes (Becton-Dickinson, Oxnard, CA, USA) in a density of 4.2 x 10⁶ cells per dish. Myocytes were separated from nonmuscle cells using a

selective adhesion technique.²⁵ After 45 min the medium, enriched in myocytes, was transferred to either 24-well plates or 35 mm culture dishes, some of which contained 25 mm diameter round glass coverslips. The myocyte cultures were kept in a humidified incubator (37°C) with an atmosphere of 95% air and 5%CO₂. Culture medium was changed after 3 h and after 48 h. After three days the monolayers of spontaneously beating myocytes were used for the experiment. The experiments had the approval of the Animal Experiments Committee of our institution.

Chemical anoxia. Chemical anoxia of the cardiomyocyte cultures was imposed by incubating the cells with 5 mM NaCN and 10 mM 2-deoxyglucose in HEPES buffered salt solution (HBSS), containing in mM: NaCl 125, KCl 5, MgSO₄ 1, KH₂PO₄ 1, CaCl₂ 2.5, NaHCO₃ 10, HEPES 20, sodium pyruvate 5, pH 7.4, at 37°C. Before the start of chemical anoxia each culture was allowed to equilibrate in HBSS for 1 h at 37°C.

Inhibitors: Chlorpromazine and trifluoperazine. Chlorpromazine (CPZ) (Sigma, St. Louis, MO, USA) and trifluoperazine (TFP) (Sigma) were dissolved as 10 mM stock solution in dimethylsulfoxide (DMSO). Thirty min before start of the experiment, CPZ or TFP were added to the cardiomyocyte cultures in concentrations of 2.5 μM or 5 μM, while the final concentration of DMSO remained < 0.1%. The compounds were present during the entire experiment. Control experiments revealed that at concentrations > 20 μM, both CPZ and TFP caused accelerated cell death in cultures during control incubation, i.e. in the absence of chemical anoxia.

Calmidazolium. Calmidazolium (Sigma) was dissolved as 4 mM stock solution in ethanol, and was added to the cardiomyocyte cultures 30 min before start of the experiment in concentrations from 0.5 μM to 8 μM, while final ethanol concentration remained <0.2 %. Calmidazolium was present during the entire experiment.

Ni²⁺. NiCl₂ (Sigma) was dissolved as 250 mM stock solution in HBSS. Ni²⁺ was added to the cultures 20-30 min before start of the experiment, and remained present during the course of the experiment.

In vitro PLA₂ assay. We investigated the effect of CPZ, TFP, calmidazolium and Ni²⁺ ions on the activity of isolated PLA₂ *in vitro*. To this end, a mixture of low molecular weight PLA₂ isolated from *Naja Naja*, bee venom and pancreas (1:1:1) (Sigma) was added to the fluorescent phospholipid BODIPY-phosphatidylcholine²⁶ (Molecular Probes, Eugene, OR, USA). This substrate contains two fluorescent acyl-moieties at the sn-1 and sn-2 position, yielding a fluorescence acceptor-donor pair. The inherent low fluorescence intensity from the intact substrate is enhanced upon

liberation of the acyl moiety at the sn-2 position due to PLA₂ activity. The rate by which fluorescence increases reflects the level of lipolytic activity of PLA₂. In the assay, 1 μM BODIPY-PC (in micelles) was added to 2 ml HBSS in a thermostated cuvette (37°C) in a spectrofluorometer (LS-3B, Perkin-Elmer, Beaconsfield, UK). BODIPY-PC fluorescence was recorded at 530 nm during excitation at 480 nm. To start the reaction, 10 μl (3 U) of the PLA₂ mixture was added. After establishing baseline PLA₂ activity, CPZ or TFP (0-40 μM), calmidazolium (0-10 μM) or Ni²⁺ (0-3 mM) was added to the reaction mixture and the resulting alteration in PLA₂ activity was expressed as a percentage of PLA₂ activity before addition of the inhibitor.

Digital imaging fluorescence microscopy. Intracellular free calcium concentration ($[Ca^{2+}]_i$) and cell death were measured with digital imaging fluorescence microscopy, employing the fluorescent calcium indicator fura-2²⁷ and the fluorescent DNA probe propidium iodide,²⁸ respectively.

Fura-2 : The cardiomyocytes were loaded with fura-2 by incubation with 2 μM fura-2/AM (Molecular Probes) in 1 ml HBSS, for 30 min at 37°C. Then, the glass coverslip was rinsed three times with HBSS and was mounted in a novel culture dish containing two compartments which was recently described by us.²⁹ Using the two-compartment culture dish, the two halves of a single cell culture grown on a standard coverslip can be exposed to two treatments simultaneously, allowing the effect of one treatment to be compared with that of the other treatment in the same culture. This way, the natural variability that might exist between different individual cultures is circumvented. In addition, by simultaneously conducting two experiments per dish, the time and the number of cultures needed for the experiments is essentially halved.

After mounting the coverslip with the culture in the two-compartment culture dish, each compartment of the dish was incubated with 200 μl HBSS at 37°C. Then, propidium iodide (Sigma) was added to each compartment in a final concentration of 100 nM.

The two-compartment culture dish was mounted in a thermostated micro-incubator³⁰ on the microscope stage equipped with a computer-controlled XY-table. This set-up allows the experimenter to shuttle between the two compartments of the culture dish during the experiment in order to compare selected cells in one compartment with those in the other compartment. The cells were studied in an imaging fluorescence microscope, previously described.^{29,31} The set-up consists of an inverted microscope (Leitz Diavert, Wetzlar, Germany) equipped with a 20x fluorite objective (Nikon, Tokyo, Japan) and a mercury light source (HBO-100, Osram, Montgomery, NY, USA). A filterwheel (Sutter Instruments, Novato, CA, USA) allows the selection of

excitation filters (340 nm and 380 nm for fura-2, 535 nm for propidium iodide). Emission fluorescence is led through a high-pass filter (>490 nm for fura-2, >590 nm for propidium iodide), and is imaged by a high-sensitivity silicon intensified target camera (Hamamatsu C2400-08, Herrsching, Germany). The video image is digitised by a frame-grabber board (Imaging Technologies Inc., Woburn, MA, USA) in a PC-AT 486 computer. Spatial resolution of the images is 256 x 256 pixels, with an 8 bits intensity resolution. At each wavelength, sixteen consecutive video frames were averaged to improve the signal to noise ratio. The images were processed using dedicated image processing software (TIM, Difa, Breda, The Netherlands). After subtraction of the background fluorescence, the 340 nm image was divided by the 380 nm image on a pixel by pixel basis to yield a ratio image. The software allows the analysis of individual cells. Statistical parameters (mean, median, standard deviation) were calculated by the software and used to calculate $[Ca^{2+}]_i$.

Propidium iodide: In propidium iodide imaging, dead cells were identified by the propidium iodide fluorescence of their nuclei, whereas living cells showed no such fluorescence. At the end of the experiment, total number of cells in the culture was determined after addition of 20 μ M digitonin to perforate the surviving cells. The number of dead cells during the experiment was expressed as a percentage of the total number of cells. In addition to $[Ca^{2+}]_i$ and cell death, the imaging technique allows the identification of the time of onset of contracture of the cardiomyocytes. For each group, the time point at which 50% of the cardiomyocytes showed contracture was determined.

Calibration of fura-2 fluorescence. At the end of the experiment, 10 μ M of the Ca^{2+} ionophore ionomycin (Boehringer, Mannheim, Germany) was added to obtain the highest obtainable ratio value, R_{max} . Then, 20 mM ethylene glycol-bis(β -aminoethyl ether) N,N,N',N'-tetraacetic acid (EGTA) was added to obtain the lowest obtainable ratio value, R_{min} . Subsequently, $[Ca^{2+}]_i$ was calculated using the formula described by Grynkiewicz *et al.*²⁷

Imaging protocol: After inserting the two-compartment incubation dish with the fura-2 loaded myocyte culture in the micro-incubator on the stage of the fluorescence microscope, the culture was equilibrated with HBSS for approximately 30 min at 37°C. During this time, one half of the culture was incubated with one of the inhibitors, while the other half received vehicle only and served as control. CPZ or TFP did not influence the measurement of $[Ca^{2+}]_i$ or cell death at concentrations \leq 5 μ M. Suitable fields of view were selected and their positions stored in the computer which controls the XY-table. Next, chemical anoxia was imposed by addition of 200 μ l HBSS buffer with NaCN and 2-deoxyglucose to each compartment, to achieve a final concentration of 5 mM NaCN and 10 mM 2-deoxyglucose. At indicated time

I. Role of phospholipid degradation in cell death

points, images at 340 nm, 380 nm and 535 nm were taken at each side. Off-line, the fura-2 ratio images were calculated, individual cardiomyocytes were analysed and statistics performed. After evaluation of the propidium iodide images, cell viability at each time point was calculated.

LDH release. When using the 24-wells plates, cell death was quantified by measuring lactate dehydrogenase (LDH) activity released from the cardiomyocytes into the medium. To this end, 15 μ l samples of the medium were taken at indicated time points, and the LDH activity in the samples was measured using a photometric assay (1442597, Boehringer, Mannheim, Germany). At the end of the experiment the cells were lysed using 0.1% Triton X-100, and total LDH activity in the cell culture, i.e. in cells + medium, was determined. After correction for the changes in medium volume during the course of the experiment, LDH activity in the medium was expressed as percentage of total LDH activity. No effect of any of the inhibitors was observed on the LDH activity assay itself.

ATP. Intracellular ATP content was measured in cardiomyocytes cultured in 24-well plates, after 60 min of control incubation or after exposure for 0-60 min to chemical anoxia in the absence or presence of 5 μ M CPZ or TFP. At indicated time points, the cells were lysed in 0.1% Triton X-100, scraped from the dish, collected, and put on ice. Within 10 min, ATP was measured using a luciferin-luciferase method (LUMAC, Perstorp Analytical Comp., Oud-Beijerland, The Netherlands) as previously described.³² Protein in the samples was measured as described by Lowry *et al.*³³ Cellular ATP concentration (in nmol/mg protein) at each time point was expressed as the percentage of the ATP concentration at t=0 min.

Phospholipid degradation. Phospholipid degradation was assessed by measuring the liberation of ³H-labelled arachidonic acid (³H-AA) from previously labelled cardiomyocytes. To this end, cardiomyocyte cultures in 35 mm culture dishes were loaded with [5,6,8,9,11,12,14,15-³H]-AA (specific activity 171 Ci/mmol) (Amersham, Buckinghamshire, UK) by incubating the cell cultures with 1 μ Ci of ³H-AA for 18-24 h in culture medium. After labelling, the cultures were washed three times with HBSS containing 10 mg/ml fatty acid-free albumin (Sigma) and pre-incubated with 1 ml HBSS for 1 h at 37°C. Then, the cultures were exposed to either control incubation or chemical anoxia, in the absence or presence of 2.5 μ M and 5 μ M CPZ or TFP. At indicated time points, the medium was removed, and cells and medium were scraped in 2 ml ice-cold methanol:14 N HCl (100:1, v/v). After addition of 2 ml chloroform and 1 ml 2.5 N HCl, the mixture was centrifuged at 4°C,

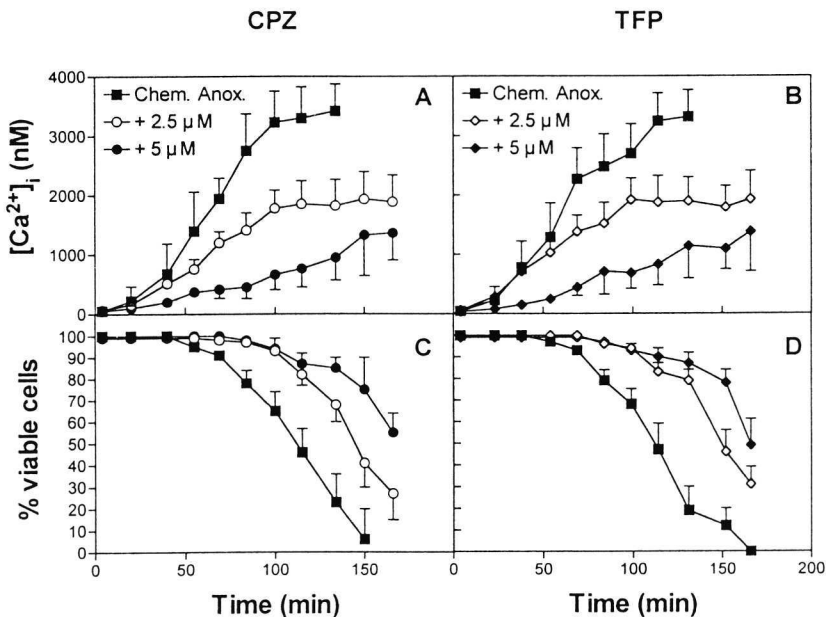


Figure 1. Intracellular Ca^{2+} ion concentration ($[Ca^{2+}]_i$) (panels A and B) and cell viability (panels C and D) in cardiomyocytes exposed to chemical anoxia (5 mM NaCN + 10 mM 2-deoxyglucose), in the absence (No addition) or presence of 2.5 μ M or 5 μ M chlorpromazine (CPZ) or trifluoperazine (TFP). Values represent mean \pm SD for at least 60 cells in each group. Panel A: $[Ca^{2+}]_i$ in cultures without CPZ (closed squares) is significantly higher than in cultures treated with 5 μ M CPZ (closed circles) at $t \geq 20$ min ($P=0.02$), and in cultures treated with 2.5 μ M CPZ (open circles), at $t \geq 40$ min ($P<0.001$). Panel B: $[Ca^{2+}]_i$ in cultures without TFP (closed squares) is significantly higher than in cultures treated with 5 μ M TFP (closed diamonds) at $t \geq 23$ min ($P=0.001$), and in cultures treated with 2.5 μ M TFP (open diamonds), at $t \geq 38$ min ($P=0.03$). Panel C: Percentage viable cells in cultures without CPZ (closed squares) is significantly lower than in cultures treated with 2.5 μ M CPZ (open circles) and 5 μ M CPZ (closed circles) at $t \geq 69$ min ($P<0.05$). From $t=115$ min onward, the percentage viable cells in cultures treated with 2.5 μ M CPZ is lower than in cultures treated with 5 μ M CPZ ($P<0.05$). Panel D: Percentage viable cells in cultures without TFP (closed squares) is significantly lower than in cultures treated with 2.5 μ M TFP (open diamonds) and 5 μ M CPZ (closed diamonds) at $t \geq 70$ min ($P<0.05$). From $t=114$ min onward, percentage viable cells in cultures treated with 2.5 μ M TFP is lower than in cultures treated with 5 μ M TFP ($P<0.05$).

after which the organic phase was collected. After re-extraction of this phase with 2 ml ice-cold chloroform:ethanol:0.6 N HCl (3:48:47,v/v), the organic phase was collected and dried under a stream of nitrogen. After dissolving in 20 μ l chloroform, the lipids were spotted on Kieselgel 60 plates (Merck, Amsterdam, the Netherlands), which had been activated at 120°C for 1 h after impregnation in 1% boric acid in methanol. Then, the plates were developed in ethyl acetate:isooctane:acetic

acid:water (90:50:20:100, v/v) for 60 min and the lipid constituents were localised in iodine vapour. After identification of the spots with the help of co-developed phospholipid and arachidonic acid standards, the various lipid spots were scraped off and radioactivity was measured by liquid scintillation counting. For each culture, the radioactivity of the free $^3\text{H-AA}$ spot was expressed as a percentage of the total $^3\text{H-AA}$ radioactivity in the culture. In each experiment, the $^3\text{H-AA}$ release in cultures exposed to chemical anoxia (with or without inhibitor) was compared to that in a control group which was not exposed to chemical anoxia, at the corresponding time point (0 min, 30 min, 60 min and 90 min).

Sarcolemmal $\text{Na}^+/\text{Ca}^{2+}$ exchanger activity. The activity of the sarcolemmal $\text{Na}^+/\text{Ca}^{2+}$ exchanger was assessed by exposing the cardiomyocytes in the two-compartment culture dish to Na^+ -free buffer, in which Na^+ ions had been replaced with choline on a molar basis. The lack of extracellular Na^+ ions induces a reversed action of the $\text{Na}^+/\text{Ca}^{2+}$ exchanger, resulting in outward transport of Na^+ ions coupled to inward transport of Ca^{2+} ions. This leads to an increase of the intracellular free calcium concentration ($[\text{Ca}^{2+}]_i$), which is measured with fura-2.³⁴

The effects the inhibitors have on the rate of rise and the amplitude of the rise of $[\text{Ca}^{2+}]_i$ reflect the influence of the inhibitors on $\text{Na}^+/\text{Ca}^{2+}$ exchanger activity. The effect of the inhibitors on the $\text{Na}^+/\text{Ca}^{2+}$ exchanger was tested after preincubation of one half of a culture with either CPZ, TFP, calmidazolium or Ni^{2+} in Na^+ -containing HBSS, for 30 min at 37°C. Then, the medium of the treated and the untreated culture-half was replaced with Na^+ -free HBSS (with the inhibitor remaining present in the treated culture half) and $[\text{Ca}^{2+}]_i$ was measured in each compartment every 10 seconds. The extent of inhibition of $\text{Na}^+/\text{Ca}^{2+}$ exchanger activity by the inhibitors was expressed by calculating $\text{Na}^+/\text{Ca}^{2+}$ exchanger activity in the treated cells as a percentage of the activity of the $\text{Na}^+/\text{Ca}^{2+}$ exchanger in the untreated cells of the same culture.

Statistical analysis. Results are expressed as mean \pm SD, unless indicated otherwise. Statistical analysis was performed using two-way ANOVA, followed by Bonferroni t-test when appropriate. Differences were considered significant if $P < 0.05$. Graphpad Prism (Graphpad Software Inc., San Diego, CA, USA) was used to perform curve fitting of the data obtained from the $^3\text{H-AA}$ release experiments.

Results

Intracellular Ca^{2+} concentration, cell death and contracture. The time courses of calcium overload and cell death in cardiomyocytes during chemical anoxia without

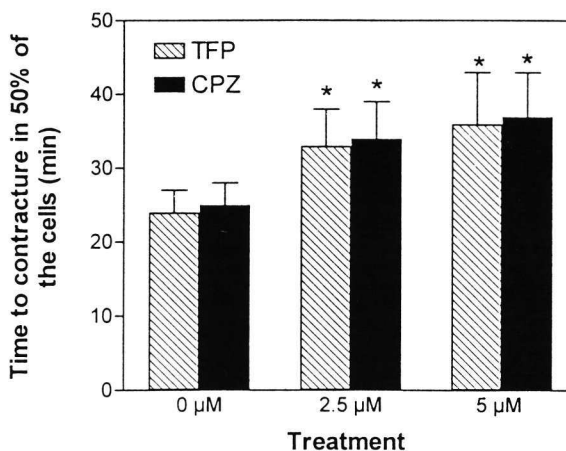


Figure 2. Time of onset of contracture in 50% of cardiomyocytes exposed to chemical anoxia in the absence (0 μM) or presence of 2.5 μM and 5 μM of chlorpromazine (CPZ) or trifluoperazine (TFP). Values are mean \pm SD, $n \geq 60$ cells, * $P < 0.001$ compared to chemical anoxia (0 μM) alone. For both CPZ and TFP treated cells, no significant difference was observed between cells treated with either 2.5 μM or 5 μM of the inhibitors.

or with 2.5 μM or 5 μM CPZ or TFP are shown in figure 1. At least 60 cells from at least five different cultures were analysed in each group. During chemical anoxia, $[\text{Ca}^{2+}]_i$ in untreated cells increased from a basal value of 86 ± 38 nM to >3 μM after approximately 100 min (Fig. 1, panels A and B). In the presence of CPZ, the increase in $[\text{Ca}^{2+}]_i$ during chemical anoxia was slower and reached lower values of approximately 2 μM and 1.3 μM for 2.5 μM and 5 μM CPZ, respectively, after 150 min (Fig. 1, panel A).

A similar pattern was observed in the presence of TFP; the increase in $[\text{Ca}^{2+}]_i$ during chemical anoxia was limited to 2.1 μM (2.5 μM TFP) and 1.3 μM (5 μM TFP) after 170 min (Fig. 1, panel B). Cell death, as assessed by propidium iodide fluorescence, began 55-60 min after the onset of chemical anoxia, and 50% of the cells were still viable after 113 min in untreated cultures (Fig. 1, panels C and D). Addition of CPZ delayed the time at which 50 % of the cardiomyocytes were still viable to 146 min (2.5 μM) and 189 min (5 μM) (Fig. 1, panel C), while for TFP the time to 50% cell death was delayed to 150 min (2.5 μM) and 171 min (5 μM), respectively (Fig. 1, panel D). An increase of the concentration of CPZ or TFP to 10 μM did not yield additional protection (data not shown).

The imaging technique allowed the determination of the time of onset of contracture in individual cells during chemical anoxia. Contracture was delayed by 2.5 μM CPZ and TFP from the control value of 24 min by at least 10 min ($P < 0.01$) (Fig. 2). In the presence of 5 μM CPZ or TFP, a small additional delay in onset of contracture was measured, although the values obtained with 5 μM CPZ or TFP did not differ significantly from those obtained with 2.5 μM CPZ or TFP.

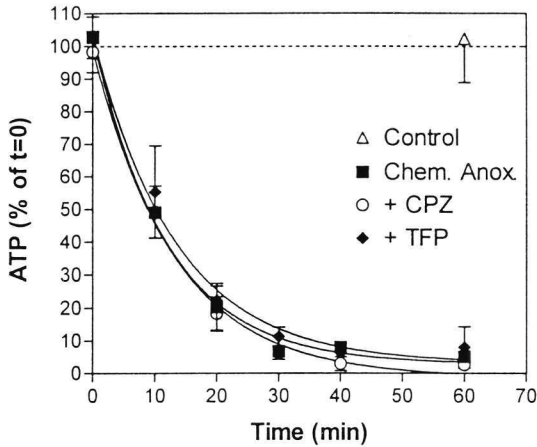


Figure 3. Intracellular ATP concentration in cardiomyocytes during control incubation (Control), and during chemical anoxia (5 mM NaCN + 10 mM 2-deoxyglucose) in the absence (Chem. Anox.) or presence of 5 μ M chlorpromazine (CPZ) or trifluoperazine (TFP). Compared to control incubation, ATP was significantly reduced in all three groups subjected to chemical anoxia at $t \geq 10$ min (values are mean \pm SEM, $n=3$, $P<0.01$), with no difference between the three treatment groups exposed to chemical anoxia.

ATP. We measured the ATP concentration in the cardiomyocytes to establish the time course of ATP depletion during chemical anoxia, and to study any effects of TFP and CPZ on the rate or extent of ATP depletion. During incubation with 5 mM NaCN and 10 mM 2-deoxyglucose, the level of ATP decreased exponentially (rate constant: $0.084 \pm 0.009 \text{ min}^{-1}$) with only 10% of ATP remaining after 40 min of chemical anoxia (Fig. 3). In the absence of chemical anoxia ATP levels remained constant for at least 60 min. The presence of either 5 μ M CPZ or 5 μ M TFP during chemical anoxia had no influence on the time course or extent of ATP depletion during chemical anoxia (rate constant: $0.077 \pm 0.008 \text{ min}^{-1}$ for CPZ and $0.075 \pm 0.010 \text{ min}^{-1}$ for TFP) (Fig. 3).

Phospholipid degradation. In the absence of chemical anoxia, the liberation of ^3H -arachidonic acid (^3H -AA) from cultures prelabelled with ^3H -AA for 18-24 h equalled approximately 1% of incorporated ^3H -AA per hour. This indicates a phospholipid degradation rate of about 2.3 nmole phospholipid/mg protein per hour, given a value of $226 \pm 30.6 \text{ nmol/mg protein}$ for total phospholipids in the cultures.³⁵ Liberation of ^3H -AA during chemical anoxia, either in the absence or presence of 5 μ M CPZ or 5 μ M TFP, was expressed as percentage of ^3H -AA release from cultures not exposed to chemical anoxia, at the corresponding time point. A curve $Y=100+(B*X-0.02X^2)$ was fitted through the data obtained for each of the three groups ($R^2 > 0.95$, $P<0.01$) (Fig. 4). Compared to control cultures not exposed to chemical anoxia, chemical anoxia was associated with higher ^3H -AA release by a factor of three at 60 and 90 min (Fig. 4), indicating a phospholipid degradation rate of approximately 6.9 nmol/mg protein per hour.

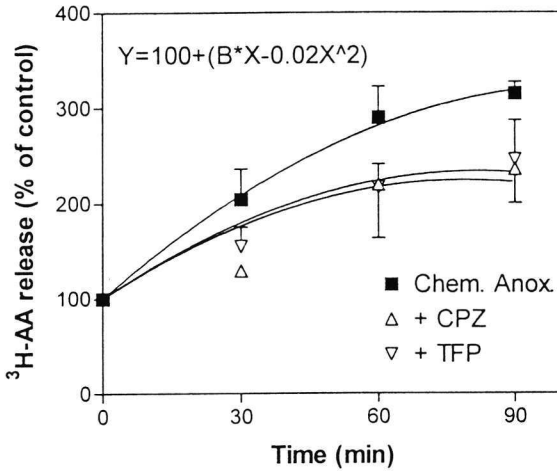


Figure 4. Release of ^3H -arachidonic acid ($^3\text{H-AA}$) during chemical anoxia (5 mM NaCN + 10 mM 2-deoxyglucose) in the absence (Chem. Anox.) or presence of 5 μM chlorpromazine (CPZ) or trifluoperazine (TFP). At each time point, the $^3\text{H-AA}$ release in the three groups are expressed as a percentage of the $^3\text{H-AA}$ release in control cells not exposed to chemical anoxia for an identical period of time. A curve ($Y=100 + B \cdot X - 0.02 \cdot X^2$) was fitted through the data with $R^2 > 0.954$, $P < 0.01$.

The release of $^3\text{H-AA}$ during

chemical anoxia ($B=4.23$, 95% confidence interval (CI): 4.07-4.40) was significantly reduced by both CPZ ($B=3.16$, CI: 2.38-3.93) and TFP ($B=3.27$, CI: 2.79-3.76) ($P=0.002$), with no differences between CPZ and TFP ($n = 3-6$ cultures). Values are mean \pm SD.

The increased liberation of $^3\text{H-AA}$ during chemical anoxia ($B=4.23$, 95% confidence interval (CI): 4.07-4.40) was significantly reduced by treatment with 5 μM CPZ by approximately 32% ($B=3.16$, CI: 2.38-3.93) or TFP by approximately 29% ($B=3.27$, CI: 2.79-3.76) ($P < 0.002$), with no differences between cultures treated with CPZ and with TFP.

In the *in vitro* PLA₂ activity assay, CPZ and TFP inhibited PLA₂ activity dose-dependently, with an IC₅₀ value of 10 μM for TFP, and 22 μM for CPZ. PLA₂ was completely inhibited at 18 μM TFP and 44 μM CPZ (data not shown).

Calmidazolium. As CPZ and TFP are also known to be calmodulin inhibitors,^{36,37} we tested whether CPZ and TFP exerted their protective effects during chemical anoxia by inhibition of calmodulin. To this end, we studied the effect of the specific calmodulin inhibitor calmidazolium on cell death during chemical anoxia. The time course of LDH release from cardiomyocytes during chemical anoxia was not influenced by 0.5 μM calmidazolium (Fig. 5). At 1 μM , 2 μM and 4 μM calmidazolium, however, cell death during chemical anoxia was accelerated rather than attenuated. In control cultures not exposed to chemical anoxia, calmidazolium also caused an accelerated cell death at concentrations higher than 4 μM (22% vs 8% LDH release after 240 min at 8 μM calmidazolium and control, respectively).

I. Role of phospholipid degradation in cell death

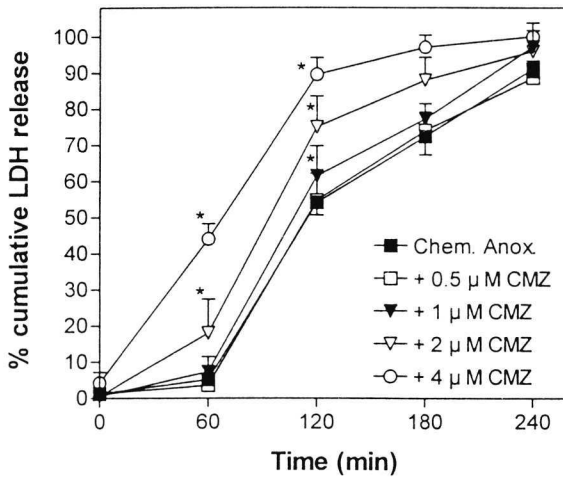


Figure 5. Effect of the calmodulin inhibitor calmidazolium (CMZ) on cell death, expressed as percentage cumulative LDH release, in cardiomyocytes exposed to chemical anoxia (5 mM NaCN + 10 mM 2-deoxyglucose). (* $P < 0.05$ vs. chemical anoxia without inhibition of calmodulin). Values are mean \pm SEM, $n = 12$ cultures.

Effect of inhibitors on the $\text{Na}^+/\text{Ca}^{2+}$ exchanger activity. Inspired by the finding that CPZ and TFP were capable to attenuate calcium overload in cells exposed to chemical anoxia, and given the supposition that calcium overload is due to the reversed action of the sarcolemmal $\text{Na}^+/\text{Ca}^{2+}$ exchanger, we examined whether CPZ and TFP affected transsarcolemmal Ca^{2+} -fluxes via the $\text{Na}^+/\text{Ca}^{2+}$ exchanger during chemical anoxia. We studied the activity of the sarcolemmal $\text{Na}^+/\text{Ca}^{2+}$ exchanger in the absence or presence of 0-10 μM CPZ or TFP during Na^+ -free incubation, which reverses the action of the $\text{Na}^+/\text{Ca}^{2+}$ exchanger (see the Methods section). CPZ and TFP inhibited the $\text{Na}^+/\text{Ca}^{2+}$ exchanger dose-dependently, with half-maximal inhibition at 5.5 μM and 5.3 μM for CPZ and TFP, respectively (Fig. 6). There was no difference in inhibitory effect between CPZ and TFP.

We confirmed the inhibitory action of Ni^{2+} ions on the $\text{Na}^+/\text{Ca}^{2+}$ exchanger. We found a dose-dependent inhibition of the exchanger by Ni^{2+} ions (Fig. 6), in agreement with earlier reports.^{38,39} Calmidazolium did not have modulatory effects on the $\text{Na}^+/\text{Ca}^{2+}$ exchanger (data not shown).

Effect of Ni^{2+} ions on calcium overload and cell death. The role of calcium overload in the development of cell death during chemical anoxia was studied further by selectively modulating calcium overload during chemical anoxia via inhibition of the $\text{Na}^+/\text{Ca}^{2+}$ exchanger activity with Ni^{2+} ions. These ions were shown to inhibit the exchanger (Fig. 6),^{38,39} whereas they were found not to inhibit the PLA_2 used in the *in vitro* PLA_2 activity assay. Actually, Ni^{2+} caused a dose-dependent increase in this PLA_2 activity, with a 250% increase in PLA_2 activity at Ni^{2+} concentrations ≥ 1 mM.

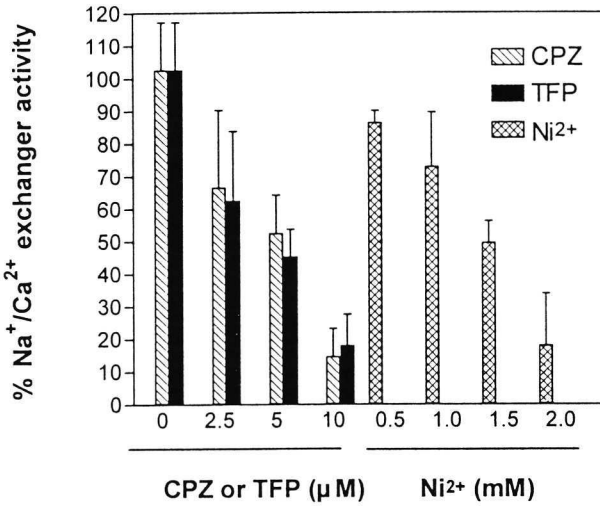


Figure 6. Effect of chlorpromazine (CPZ), trifluoperazine (TFP) and nickel ions (Ni²⁺) on the activity of the sarcolemmal Na⁺/Ca²⁺ exchanger activity upon incubation in Na⁺-free medium. All three protocols inhibit the sarcolemmal Na⁺/Ca²⁺ exchanger dose-dependently, with IC₅₀ values of 5.5 μM for CPZ, 5.3 μM for TFP and 1.76 mM for Ni²⁺ (n=3-6 experiments for each data point). Values are mean ± SD.

Using digital imaging fluorescence microscopy, we measured [Ca²⁺]_i in cardiomyocytes exposed to chemical anoxia, in the presence of 1 mM, 1.5 mM or 2 mM Ni²⁺. We found that 1 mM Ni²⁺ caused a significant attenuation of [Ca²⁺]_i overload during chemical anoxia as compared to untreated anoxic cells (Fig. 7A). At 1.5 mM Ni²⁺, a further attenuation of Ca²⁺ overload was observed, whereas at 2 mM Ni²⁺, [Ca²⁺]_i rose only to 170 nM after 190 min (Fig. 7A). The dose-dependent attenuation of Ca²⁺ overload during chemical anoxia by Ni²⁺ ions was associated with a dose-dependent decrease in cell death as assessed by propidium iodide fluorescence (Fig. 7B).

Discussion

In this study we investigated the interrelationship between calcium overload, phospholipid degradation and cell death in energy depleted neonatal rat cardiomyocytes. Upon chemical anoxia calcium overload developed, followed by cell death (Fig. 1). The purported PLA₂ inhibitors CPZ and TFP dose-dependently attenuated calcium overload during anoxia and limited cell death (Fig. 1). As ATP depletion is a prominent feature in ischemia and is considered to be a key determinant in the development of cell injury,⁴⁰ we measured cellular ATP levels to investigate whether the protective effects of CPZ and TFP during chemical anoxia were due to a sparing effect on high-energy phosphate stores. However, during chemical anoxia ATP content decreased rapidly with no conservation of ATP as a result of treatment with CPZ or TFP (Fig. 3), ruling out a protective effect of the inhibitors by preservation of ATP.

I. Role of phospholipid degradation in cell death

Using digital imaging fluorescence microscopy we observed that anoxic cardiomyocytes treated with either CPZ or TFP went into contracture later than untreated cells (Fig. 2). As contracture is considered to reflect depletion of cellular ATP stores in the presence of elevated $[Ca^{2+}]_i$,⁴¹ the delay in onset of contracture in treated cells is caused most likely by the delayed and attenuated Ca^{2+} overload in the treated cells (Fig. 1A and 1B), as compared to untreated cells.

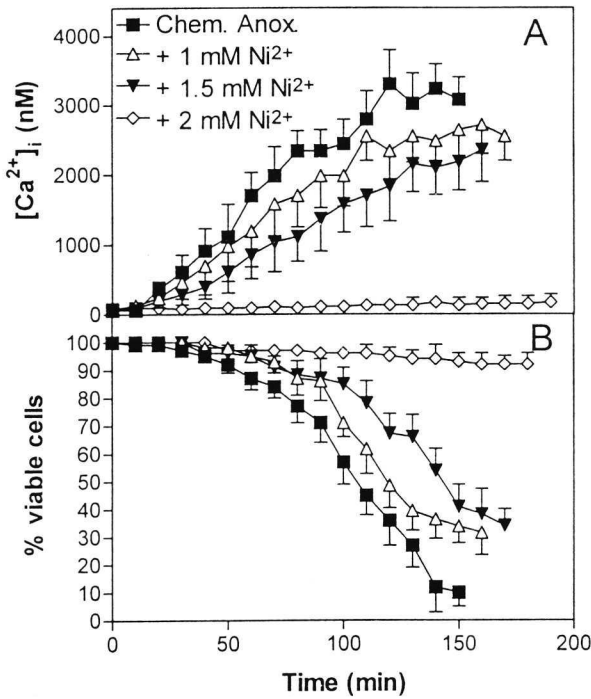


Figure 7. Effect of Ni^{2+} -ion concentration on $[Ca^{2+}]_i$ (panel A) and the percentage of viable cells (panel B) in cardiomyocytes exposed to chemical anoxia. $[Ca^{2+}]_i$ in cells treated with 2 mM Ni^{2+} was significantly lower than in untreated cells at $t \geq 30$ min ($P < 0.05$), whereas at $t \geq 40$ min, $[Ca^{2+}]_i$ in all Ni^{2+} -treated cells was dose-dependently lower than in untreated cells ($P < 0.01$). Percentage viable cells in all Ni^{2+} -treated cultures was higher than in untreated cells ($P < 0.05$) at $t \geq 60$ min, whereas at $t \geq 100$ min cell viability was statistically different between the three Ni^{2+} -treated groups ($P < 0.05$). Values represent mean \pm SD for at least 32 cells in each group.

As CPZ and TFP are also known to be inhibitors of calmodulin,^{36,37} we tested the effects of the specific calmodulin inhibitor calmidazolium on cell death in anoxic cardiomyocytes. We found that calmidazolium accelerated, rather than delayed, cell death in cardiomyocytes exposed to chemical anoxia (Fig. 5).

Thus, the protective effects of CPZ and TFP are not likely to be mediated by their effect on calmodulin.

Phospholipid degradation, as measured by the liberation of incorporated ^3H -arachidonic acid, was increased approximately three-fold during the first 90 min after start of chemical anoxia as compared to myocyte cultures not exposed to chemical anoxia (Fig. 4). This corresponds to a phospholipid degradation rate of approximately 6.9 nmol/mg protein per hour, which value is comparable to those reported by Van der Vusse *et al.* in anoxic myocardium (10 nmol/mg protein/hour⁴² and by Otani *et al.* in ischemic myocardial tissue (15 nmol/mg protein/hour).⁴³

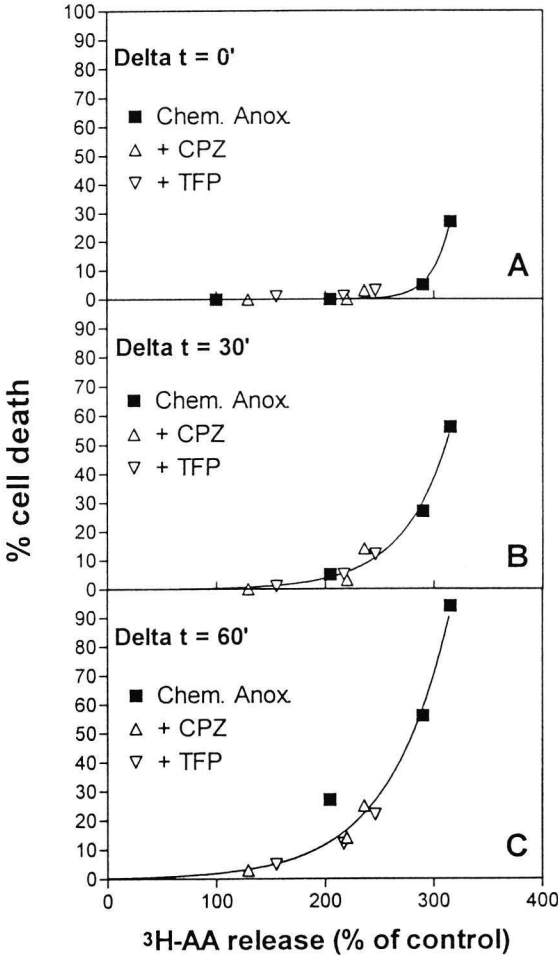


Figure 8. The relation between the relative number of dead cells and PLA₂ activity at t=30, 60 and 90 min after start of chemical anoxia (5 mM NaCN + 10 mM 2-deoxyglucose), assessed by liberation of ^3H -arachidonic acid ($^3\text{H-AA}$), in the absence (Chem. Anox) or presence of chlorpromazine (CPZ) or trifluoperazine (TFP). The plotted values of cell death were obtained a) at the same moment of PLA₂ activity measurement (panel A, delta t=0 min), b) at 30 min after PLA₂ activity measurement (panel B, delta t=30 min) or c) at 60 min after PLA₂ activity measurement (panel C, delta t=60 min).

We used the PLA₂ inhibitors chlorpromazine (CPZ) and trifluoperazine (TFP) to test the hypothesis that an increased PLA₂ activity is responsible for the occurrence of cell death during energy depletion. We found that CPZ or TFP had a dose-dependent protective effect on cell death during chemical anoxia (Fig. 1C and 1D), which was associated with a decreased phospholipid degradation, as assessed by the liberation of ³H-arachidonic acid from the cultures (Fig. 4). These findings are in agreement with the results reported by other authors.^{7,44} However, the observation that decreased phospholipid degradation was associated with attenuated cell death provides no answer to the question whether the decreased phospholipid degradation had led to the decrease in cell death, or *vice versa*, that as a result of less cell death (autolytic) phospholipid degradation was diminished.

To answer this question, we studied PLA₂ activity (reflected by ³H-AA release) in relation to cell death determined at a) the same time point of PLA₂ activity measurement (Fig. 8A), b) 30 min after PLA₂ activity measurement (Fig. 8B), and c) 60 min after the PLA₂ activity measurement (Fig. 8C). In all three analyses a unique relation between PLA₂ activity and (ensuing) cell death was observed. These findings indicate that PLA₂ activity is a good predictor of ensuing cell death. Thus a causal role for PLA₂ activation in the development of cell death cannot be ruled out. Treatment of anoxic cardiomyocytes with the PLA₂ inhibitors CPZ or TFP resulted in decreased PLA₂ activity, associated with attenuated cell death, without alteration of the relation between PLA₂ activity and cell death. This suggests that the protective effects of CPZ and TFP are at least partly mediated by their inhibitory effect on PLA₂ activity.

In addition to attenuating cell death, CPZ and TFP limit calcium overload during chemical anoxia (Fig. 1A and 1B). Calcium overload is considered to result from the reversed action of the sarcolemmal Na⁺/Ca²⁺ exchanger.^{45,46} This exchanger permits influx of extracellular Ca²⁺ ions into the cell via reversed action, driven by an increase in the intracellular Na⁺ concentration during ischemia and energy depletion.^{47,48} Calcium overload in itself may cause physico-chemical perturbations in the cardiac sarcolemma during ischemia, potentially leading to cell death.^{22,23} During chemical anoxia, calcium overload and ensuing cell death can be limited or prevented by inhibition of the Na⁺/Ca²⁺ exchanger, as we showed earlier using extracellular acidosis⁴⁹ or simvastatin,⁵⁰ and was shown with the oxygen radical scavenger dimethylthiourea by Ziegelstein *et al.*³⁴ We investigated whether the attenuation of Ca²⁺ overload during chemical anoxia by CPZ and TFP could be attributed to their action on the activity of the sarcolemmal Na⁺/Ca²⁺ exchanger. As CPZ and TFP inhibited the activity of the Na⁺/Ca²⁺ exchanger dose-dependently (Fig. 6), we argue that the attenuation of calcium overload in anoxic cardiomyocytes by CPZ and TFP is most likely due to their inhibitory effect on the sarcolemmal

Na⁺/Ca²⁺ exchanger. Faced with a dual role of CPZ and TFP during chemical anoxia, i.e. attenuation of calcium overload and inhibition of phospholipid degradation, it remained unclear which effect of CPZ and TFP was primarily responsible for their protection against cell death.

To delineate the relative importance of the two roles, we sought to attenuate Ca²⁺ overload without inhibition of PLA₂ activity. Ni²⁺ ions, known to inhibit the sarcolemmal Na⁺/Ca²⁺ exchanger (Fig. 6),^{38,39,51} had no inhibitory effect on low molecular weight PLA₂ activity *in vitro*, but rather a stimulatory effect on this enzyme activity. It should be emphasized that although low molecular weight PLA₂ is present in cardiomyocytes,^{52,53} these *in vitro* data should be extrapolated to intact heart cells with care, as myocardium also contains other PLA₂ species.⁵⁴

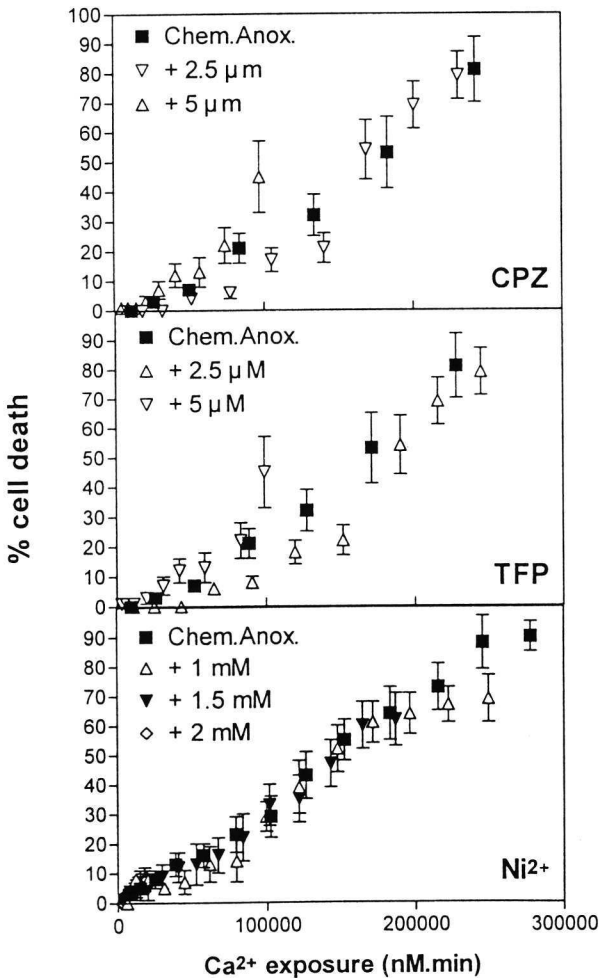


Figure 9. Relation between the relative number of dead cardiomyocytes and Ca²⁺ exposure, determined by calculation of the area-under-curve of figures 1A, 1B and 7 and expressed as nM*min, during chemical anoxia (5 mM NaCN + 10 mM 2-deoxyglucose), in the absence (Chem. Anox.) or presence of chlorpromazine (CPZ, upper panel), trifluoperazine (TFP, middle panel) or Ni²⁺ ions (Ni²⁺, lower panel).

Ni^{2+} ions dose-dependently limited calcium overload in anoxic cardiomyocytes, associated with a dose-dependent decrease in cell death (Fig. 7). Control experiments verified that the observed decrease in calcium overload was not due to quenching of the fura-2 fluorophore, as fura-2 fluorescence at its isosbestic wavelength of 360 nm remained constant. Also other authors have reported that extracellular Ni^{2+} does not quench intracellular fura-2.⁵⁵ In addition, the range of Ni^{2+} concentrations which inhibited $\text{Na}^+/\text{Ca}^{2+}$ exchanger activity in our experiments is in agreement with the Ni^{2+} concentrations which were reported to inhibit the sarcolemmal $\text{Na}^+/\text{Ca}^{2+}$ exchanger of guinea-pig myocytes in patch clamp experiments.³⁹

To analyse whether calcium overload is a determinant in the process of cell death, we plotted the total exposure of the cell to intracellular Ca^{2+} , determined by calculating the area-under-curve in figures 1A and 1B, against cell death, determined from figures 1C and 1D (Fig. 9). For untreated cells we found a unique, almost linear, relation between Ca^{2+} exposure and cell death (Fig. 9). Treatment of the cells with Ni^{2+} ions, which proved to attenuate Ca^{2+} overload but not to inhibit PLA_2 activity, did not change the relation between Ca^{2+} exposure and cell death as compared to untreated cells, i.e. a lower Ca^{2+} exposure was associated with a decreased cell death and *vice versa* (Fig. 9C). When the PLA_2 inhibitors CPZ or TFP were used, however, the relation between Ca^{2+} exposure and cell death at certain time points was somewhat different from that observed in untreated cells or cells treated with Ni^{2+} ions (Fig. 9A and 9B). At 2.5 μM CPZ or TFP, an attenuated cell death was observed for a given Ca^{2+} exposure as compared to untreated and Ni^{2+} -treated cells, indicating that the cells were able to withstand a higher Ca^{2+} exposure. With 5 μM CPZ or TFP the Ca^{2+} exposure vs. cell death relation is similar to untreated or Ni^{2+} -treated cells except for the data points obtained at the end of the experiment, which show that cell death occurred at a relatively low Ca^{2+} exposure (Fig. 9A and 9B). These findings indicate that although CPZ and TFP limit Ca^{2+} overload during chemical anoxia (Fig. 1), the protective effect of CPZ and TFP cannot be explained solely by limitation of Ca^{2+} overload, but that an additional mechanism is involved in cell death, most likely inhibition of activated PLA_2 , as was already suggested by figure 8.

A potential mechanism explaining the observed relation between the magnitude of intracellular Ca^{2+} exposure and the occurrence of cell death in anoxic cardiomyocytes is the phenomenon of lateral-phase separation.^{22,23} This phenomenon implies an increased tendency of the sarcolemmal membrane of energy-depleted cells to transform into a non-bilayer configuration, as a result of loss of transsarcolemmal phospholipid asymmetry.⁵⁶ This membrane reconfiguration, which is associated with weakening and loss of function of membranous proteins, is

promoted by elevated Ca^{2+} concentrations,²³ which may imply that attenuation of Ca^{2+} overload limits anoxic cell death by decreasing the extent of physical membrane perturbations.

It is conceivable that Ca^{2+} -induced lateral-phase transition and enzymatic phospholipid degradation occur in concert, and even may enhance each other.

In summary, we have found that in cardiomyocytes exposed to chemical anoxia the PLA_2 inhibitors CPZ and TFP delay the occurrence of cell death, limit Ca^{2+} overload, delay the onset of contracture and attenuate the degradation of cellular phospholipids. The salutary effects of CPZ and TFP were not caused by conservation of ATP, nor by their inhibitory effect on calmodulin. In addition to their inhibitory action on PLA_2 , CPZ and TFP were shown to be inhibitors of the sarcolemmal $\text{Na}^+/\text{Ca}^{2+}$ exchanger. Treatment of cardiomyocytes exposed to chemical anoxia with Ni^{2+} ions, which inhibit the sarcolemmal $\text{Na}^+/\text{Ca}^{2+}$ exchanger, limited Ca^{2+} overload and cell death dose-dependently. CPZ and TFP attenuated Ca^{2+} overload during chemical anoxia, although this effect could not completely explain the protective property of the inhibitors. A unique relation was found between PLA_2 activity and ensuing cell death, both in the presence and absence of CPZ and TFP.

We conclude that CPZ and TFP protects cardiomyocytes during chemical anoxia by inhibition of phospholipid degradation and of the $\text{Na}^+/\text{Ca}^{2+}$ exchanger activity. Calcium overload is a major determinant in the process leading to cell death, but additional mechanisms, including PLA_2 activity, seem to be involved in the development of anoxic cell death.

Acknowledgement

This study was supported by a grant from the Netherlands Heart Foundation, no. 90.089. The authors thank Prof. dr. G.J. Van der Vusse for critically reading the manuscript.

References

1. Cheung JY, Bonventre JV, Malis CD, Leaf A. Calcium and ischemic injury. *N Engl J Med.* 1986;314:1670-1676.
2. Nayler WG. The role of calcium in the ischemic myocardium. *Am J Pathol.* 1981;102:262-270.
3. Steenbergen C, Fralix TA, Murphy E. Role of increased cytosolic free calcium concentration in myocardial ischemic injury. *Basic Res Cardiol.* 1993;88:456-470.
4. Toyooka T, Ross JR. Ca^{2+} sensitivity change and troponin loss in cardiac natural actomyosin after coronary occlusion. *Am J Physiol.* 1981;40:H704-H708.
5. Atsma DE, Bastiaanse EML, Jerzewski A, Van der Valk EJM, Van der Laarse A. Role of calcium-activated neutral protease (calpain) in cell death in cultured neonatal rat cardiomyocytes during metabolic inhibition. *Circ Res.* 1995;76:1071-1078.

I. Role of phospholipid degradation in cell death

6. Chien KR, Han A, Sen A, Buja LM, Willerson JT. Accumulation of unesterified arachidonic acid in ischemic canine myocardium. *Circ Res.* 1984;54:313-322.
7. Jones RL, Miller JC, Hagler HK, Chien KR, Willerson JT, Buja LM. Association between inhibition of arachidonic acid release and prevention of calcium loading during ATP depletion in cultured rat cardiac myocytes. *Am J Pathol.* 1989;135:541-556.
8. Otani H, Engelman RM, Rousou JA, Bryer RH, Das DK. Enhanced prostaglandin synthesis due to phospholipid breakdown in ischemic-reperfused myocardium. *J Mol Cell Cardiol.* 1986;18:953-961.
9. Van der Vusse GJ, Roemen THM, Prinzen FW, Coumans WA, Reneman RS. Uptake and tissue content of fatty acids content in dog myocardium under normoxic and ischemic conditions. *Circ Res.* 1982;50:538-546.
10. Van der Vusse GJ, Van Bilsen M, Reneman RS. Is phospholipid degradation a critical event in ischemia and reperfusion-induced damage? *NIPS.* 1989;4:49-53.
11. Bentham JM, Higgins AJ, Woodward B. The effects of ischemia, lysophosphatidylcholine and palmitoylcarnitine on rat heart phospholipase A₂ activity. *Basic Res Cardiol.* 1987;82 (Suppl II): 127-137.
12. Grynberg A, Nalbone G, Leonardi J, Lafont H, Athias P. Eicosapentanoic and docosahexanoic acids in cultured rat ventricular myocytes and hypoxia-induced alterations in phospholipase-A activity. *Mol Cell Biochem.* 1992;116: 75-78.
13. Chien KR, Sen A, Reynolds R, Chang A, Kim Y, Gunn MD, Buja LM, Willerson JT. Release of arachidonate from membrane phospholipids in cultured neonatal rat myocardial cells during adenosine triphosphate depletion. *J Clin Invest.* 1985;75:1770-1780.
14. Das DK, Engelman RM, Rousou JA, Breyer RH, Otani H, Lemeshow S. Role of membrane phospholipids in myocardial injury induced by ischemia and reperfusion. *Am J Physiol.* 1986;251:H71-H79.
15. Prasad MR, Popescu LM, Moraru II, Liu X, Maity S, Engelman RM, Das DK. Role of phospholipases A₂ and C in myocardial ischemic reperfusion injury. *Am J Physiol.* 1991;260:H877-H883.
16. Gonzalezdaros F, Carrascoluna J, Calatayud A, Salguero J, Delvalletascon S. Effects of calmodulin antagonists on auxin-stimulated proton extrusion in *avena sativa* coleoptile segments. *Physiol Plant.* 1993;87:68-76.
17. Nakazawa K, Higo K, Abe K, Tanaka Y, Saito H, Matsuki N. Blockade by calmodulin inhibitors of Ca²⁺ channels in smooth muscle from rat vas deferens. *Br J Pharmacol.* 1993;109:137-141.
18. Carafoli E. Intracellular calcium homeostasis. *Annu Rev Biochem.* 1987;56:395-433.
19. Cullis PR, De Kruijff B. Hope MJ, Verkleij AJ, Nayar R, Farren SB, Tilcock S, Madden ST, Bally MB. Membrane fluidity in biology. R. C. Aloia. Academic Press, New York. 1983, 39-81.
20. Kanaho Y, Sato T, Fuji T. The affinity of various phenothiazine drugs for membranes of intact erythrocytes and their membrane-transforming activity. *Mol Pharmacol.* 1981;20:704-708.
21. De la Pena P, Reeves JP. Inhibition and activation of Na⁺/Ca²⁺ exchange activity by quinacrine. *Am J Physiol.* 1987;252:C24-C29.
22. Post JA, Leunissen-Bijvelt J, Ruigrok TJC, Verkleij AJ. Ultrastructural changes in sarcolemma and mitochondria in the isolated rabbit heart during ischemia and reperfusion. *Biochim Biophys Acta.* 1985;845:119-123.
23. Verkleij AJ, Post JA. Physico-chemical properties and organization of lipids in membranes: their possible role in myocardial injury. *Basic Res Cardiol.* 1987;82 (Suppl. I):85-91.

Chapter 5

24. Van der Laarse A, Hollaar L, Van der Valk EJM. Release of alpha-hydroxybutyrate dehydrogenase from neonatal rat heart cell cultures exposed to anoxia and reoxygenation: Comparison with impairment of structure and function of damaged cardiac cells. *Cardiovasc Res.* 1979;13:345-353.
25. Blondel B, Royen J, Cheneval JP. Heart cells in culture: a simple method for increasing the proportion of myoblasts. *Experientia.* 1971;27:356-358.
26. Schmidt N, Guenther G. Synthesis of a fluorescent analog of phosphatidylcholine. *Chem Phys Lipids.* 1985;38:309-311.
27. Gryniewicz G, Poenie M, Tsien RY. A new generation of Ca^{2+} indicators with greatly improved fluorescence properties. *J Biol Chem.* 1985;260:3440-3450.
28. Crissman HA, Stevenson AP, Kissane RJ, Tobey RA. Techniques for quantitating staining of cellular DNA for flow cytometric analysis. M. Y. Melanned, P. F. Mullaney and M. L. Mendelsohn. New York. Wiley. 1979, 243-261.
29. Atsma DE, Bastiaanse EML, Ince C, Van der Laarse A. A novel two-compartment culture dish allows microscopic evaluation of two different treatments in one cell culture simultaneously - Influence of external pH on $\text{Na}^+/\text{Ca}^{2+}$ exchanger activity in cultured rat cardiomyocytes. *Pflügers Arch.* 1994;428:296-299.
30. Ince C, Ypey DL, Diesselhoff-Den Dulk MMC, Visser JAM, De Vos A, Van Furth R. Micro- CO_2 -incubator for use on a microscope. *J Immunol Meth.* 1983;60:269-275.
31. Draijer R, Atsma DE, Van der Laarse A, Van Hinsbergh VWM. cGMP and nitric oxide modulate thrombin-induced endothelial permeability. Regulation via different pathways in human aortic and umbilical vein endothelial cells. *Circ Res.* 1995;76:199-208.
32. Wettermark G, Stymne H. Substrate analysis in single cells. I. Determination of ATP. *Anal Biochem.* 1975;63:293-307.
33. Lowry OH, Rosebrough NJ, Farr AL, Randall RJ. Protein measurement with the Folin phenol reagent. *J Biol Chem.* 1951;193:265-275.
34. Ziegelstein RC, Zweier JL, Mellits ED, Younes A, Lakatta EG, Stern MD, Silverman HS. Dimethylthiourea, an oxygen radical scavenger protects isolated cardiac myocytes from hypoxic injury by inhibition of $\text{Na}^+/\text{Ca}^{2+}$ exchange and not by its antioxidant effects. *Circ Res.* 1992;70: 804-811.
35. Bastiaanse EML, Van der Valk-Kokshoorn EJM, Egas-Kenniphaas JM, Atsma DE, Van der Laarse A. The effect of sarcolemmal cholesterol content on the tolerance to anoxia in cardiomyocyte cultures. *J Mol Cell Cardiol.* 1994;26:639-648.
36. Marshak DR, Lukas TJ, Watterson DM. Drug-protein interactions: Binding of chlorpromazine to calmodulin, calmodulin fragments, and related calcium binding proteins. *Biochemistry.* 1985;24:144-150.
37. Massom L, Lee H, Jarrett HW. Trifluoperazine binding to brain calmodulin and skeletal troponin C. *Biochemistry.* 1990;29:671-681.
38. Kaczorowski GJ, Garcia ML, King VF, Slaughter RS. Development and use of inhibitors to study sodium-calcium exchange. Allen TJA, Noble D and Reuter H. Oxford New York Tokyo. Oxford University Press. 1989, 127-158.
39. Kimura J, Miyamae S, Noma A. Identification of sodium-calcium exchange current in single ventricular cells of guinea-pig. *J Physiol (Lond).* 1987;384:199-222.
40. Jennings RB, Hawkins HK, Lowe JE, Hill ML, Klotman S, Reimer KA. Relation between high energy phosphate and lethal injury in myocardial ischemia in the dog. *Am J Pathol.* 1978;92:187-215.

I. Role of phospholipid degradation in cell death

41. Kingsley PB, Sako EY, Yang MQ, Zimmer SD, Ugurbil K, Foker JE, From AL. Ischemic contracture begins when anaerobic glycolysis stops: a 31 P-NMR study of isolated rat hearts. *Am J Physiol.* 1991;H469-H478.
42. Van der Vusse GJ, De Groot MJM, Willemsen PHM, Van Bilsen M, Schrijvers AHGJ, Reneman RS. Degradation of phospholipids and triacylglycerol, and accumulation of fatty acids in anoxic myocardial tissue, disrupted by freeze-thawing. *Mol Cell Biochem.* 1989;88: 83-90.
43. Otani H, Prasad MR, Jones RM, Das DK. Mechanism of membrane phospholipid degradation in ischemic-reperfusion rat hearts. *Am J Physiol.* 1989;257:H252-H258.
44. Sen A, Miller JC, Reynolds R, Willerson JT, Buja LM, Chien KR. Inhibition of the release of arachidonic acid prevents the development of sarcolemmal membrane defects in cultured rat myocardial cells during adenosine triphosphate depletion. *J Clin Invest.* 1988;82:1333-1338.
45. Haigney MCP, Miyata H, Lakatta EG, Stern MD, Silverman HS. Dependence of hypoxic cellular calcium loading on $\text{Na}^+/\text{Ca}^{2+}$ exchange. *Circ Res.* 1992;71:547-557.
46. Silverman HS, Stern MD. Ionic basis of ischaemic cardiac injury: Insights from cellular studies. *Cardiovasc Res.* 1994;28: 581-597.
47. Butwell NB, Ramasamy R, Lazar I, Sherry AD, Malloy CR. Effect of lidocaine on contracture, intracellular sodium, and pH in ischemic rat hearts. *Am J Physiol.* 1993;264:H1884-H1889.
48. Van Echteld CJA, Kirkels JH, Eijgelshoven MHJ, Van der Meer P, Ruigrok TJC. Intracellular sodium during ischemia and calcium-free perfusion: A ^{23}Na NMR study. *J Mol Cell Cardiol.* 1991;23:297-307.
49. Atsma DE, Bastiaanse EML, Van der Valk EJM, Van der Laarse A. Low external pH limits cell death in energy depleted cardiomyocytes by decreasing Ca^{2+} overload via $\text{Na}^+/\text{Ca}^{2+}$ exchange inhibition. *Am J Physiol.* In press.
50. Bastiaanse EML, Atsma DE, Kuijpers MMC, Van der Laarse A. Simvastatin-sodium delays cell death of anoxic cardiomyocytes by inhibition of the $\text{Na}^+/\text{Ca}^{2+}$ exchanger. *FEBS Lett.* 1994;343: 151-154.
51. Sheu YA, Kricka LJ, Pritchett DB. Measurement of intracellular calcium using bioluminescent aequorin expressed in human cells. *Anal Biochem.* 1993;209:343-347.
52. Chen J, Engle SJ, Seilhamer JJ, Tischfield JA. Cloning and recombinant expression of a novel human low molecular weight Ca^{2+} dependent phospholipase A_2 . *J Biol Chem.* 1994;269:2365-2368.
53. Kriegsmann J, Muller WD, Richter W, Wunderlich W, Wallukat G. Demonstration of membrane-associated phospholipase A_2 in cultivated heart muscle cells by immunogold-technique in surface replicas. *Acta Histochem.* 1993;95:61-66.
54. Van Bilsen M, Van der Vusse GJ. Phospholipase- A_2 -dependent signalling in the heart. *Cardiovasc Res.* 1995;30:518-529.
55. Satoh H, Hayashi H, Noda N, Terada H, Kobayashi A, Hirano M, Yamashita Y, Yamazaki N. Regulation of $[\text{Na}^+]_i$ and $[\text{Ca}^{2+}]_i$ in guinea pig myocytes - Dual loading of fluorescent indicators SBFI and Fluo 3. *Am J Physiol.* 1994;266:H568-H576.
56. Musters RJP, Otten E, Biegelmann E, Bijvelt J, Keijzer JHH, Post JA, Op Den Kamp JAF, Verkleij AJ. Loss of asymmetric distribution of sarcolemmal phosphatidylethanolamine during simulated ischemia in the isolated neonatal rat cardiomyocyte. *Circ Res.* 1993;73:514-523.

Chapter 6

II. Role of phospholipid degradation in death of anoxic cardiomyocytes

Effect of halo-enol lactone, a synthetic inhibitor of plasmalogen-selective phospholipase A₂ on cell death

Douwe E. Atsma¹, E. M. Lars Bastiaanse¹, Steven van Leeuwen², Lizet J.M. Van der Valk¹, Jaap H. van Boom² Arnoud Van der Laarse¹

¹Department of Cardiology, University Hospital, Leiden, The Netherlands,

²Department of Organic Chemistry, University of Leiden, Leiden, The Netherlands

Submitted

Part of this study was presented at the 17th Congress of the European Society of Cardiology, Amsterdam, The Netherlands, August 1995.

Abstract

The involvement of plasmalogen-selective PLA₂ (PS-PLA₂) in the development of cell death in cardiomyocytes during chemical anoxia (5 mM NaCN + 10 mM 2-deoxyglucose) was studied using the specific PS-PLA₂ inhibitor halo-enol lactone suicide substrate (HELSS) (*E*)-6-(bromomethylene)-tetrahydro-3-(1-naphthalenyl)-2*H*-pyran-2-one. During chemical anoxia, HELSS delayed half-maximal cell death from 146 min in untreated cells to 175 min (2.5 μM) and 191 min (5 μM). HELSS did not affect the development of Ca²⁺ overload, as assessed with fura-2, nor did it influence the time course of cellular ATP depletion. Phospholipid degradation, assessed by the liberation of ³H-arachidonic acid from labelled cardiomyocytes was increased three-fold during chemical anoxia. HELSS in concentrations between 1 and 5 μM strongly reduced this increased phospholipid breakdown by 70-80%. As this strong reduction of accelerated phospholipid degradation was accompanied by either no (1 μM HELSS) or only a temporary effect on cell death (2.5 μM and 5 μM HELSS), we conclude that accelerated phospholipid degradation is not the only factor responsible for cell death. The mechanism of the protective effect of HELSS on cell death during chemical anoxia remains to be established.

Introduction

The basic mechanism responsible for cell death of cardiomyocytes during ischemia, anoxia and chemical anoxia is still unknown. Phospholipase A₂ (PLA₂) has been implicated in myocardial injury during ischemia, anoxia and chemical anoxia.¹⁻⁴ This involvement of PLA₂ is inferred from the accumulation of degradation products of phospholipids, including arachidonic acid and lysophospholipids. Generally, PLA₂ activation is thought to be the result of the calcium overload that develops during ischemia.^{5,6}

Recently, a new type of PLA₂ has been described which is calcium-independent and selective for plasmalogen phospholipids.⁷⁻⁹ In these phospholipids, the acyl moiety at the sn-1 position is linked to the glycerol backbone by a vinyl ether rather than an ester bond. Plasmalogen phospholipids appear to be exclusively confined to electroresponsive tissues such as heart, brain and nerves,¹⁰ and their structure likely reflect the specialized nature of these tissues. In cardiac tissue of various species, plasmalogen phospholipids were found to constitute a sizeable fraction (12-45%) of the total amount of cellular phospholipids.¹¹⁻¹³

The newly discovered plasmalogen-selective PLA₂ (PS-PLA₂) is an attractive candidate for the role of effector of ischemic injury, as it is reported to be activated in the first few minutes of ischemia in canine myocardium and its activation involves

translocation to the sarcolemmal membrane,¹⁴ the injury of which is considered to be a pivotal event in the development of cell death.

In this study we tested the involvement of PS-PLA₂ in the development of cell injury in cultured neonatal rat cardiomyocytes during chemical anoxia (5 mM NaCN + 10 mM 2-deoxyglucose), using the specific PS-PLA₂ inhibitor halo-enol-lactone suicide substrate (HELSS).^{15,16} We studied the effect of the inhibitor on the intracellular free calcium concentration ($[Ca^{2+}]_i$) and subsequent cell death during chemical anoxia, and measured the release of ³H-arachidonic acid to quantitate PS-PLA₂ activity.

Materials and Methods

Cell culture. The myocyte cultures were prepared using the method described by Van der Laarse *et al.*¹⁷ Briefly, hearts of 2 days old Wistar rats were dissected and transferred to a solution containing in mM: NaCl 137, KCl 5, Na₂HPO₄ 0.4, KH₂PO₄ 0.4, glucose 5.5, N-2-hydroxyethyl piperazine-N'-2-ethanesulfonic acid (HEPES) 20, phenol red 0.5 mg/l, pH 7.4. The ventricles were minced into small fragments and dissociated using collagenase (type I CLS, Worthington, Freehold, NJ, USA) during two periods of 20 min in a shaking water bath at 37°C. After centrifugation at 50 x g for 15 min, the cells were suspended in a culture medium consisting of Ham's F-10 medium (Flow Laboratories, Irvine, UK) supplemented with 10% fetal bovine serum (Flow Laboratories) and 10% horse serum (Flow Laboratories). The cells were plated in 60 mm culture dishes (Becton-Dickinson, Oxnard, USA) in a density of 4.2 x 10⁶ cells per dish. Myocytes were separated from non-muscle cells using a selective adhesion technique.¹⁸ After 45 min the medium, enriched in myocytes, was transferred to either 24-well plates or 35 mm culture dishes, some of which contained 25 mm round glass coverslips. The myocyte cultures were kept in a humidified incubator (37°C) with an atmosphere of 95% air and 5% CO₂. Culture medium was changed after 3 h and after 48 h. After three days the monolayers of spontaneously beating myocytes were used for the experiment.

Plasmalogen-specific PLA₂ inhibitor. The halo-enol lactone suicide substrate (HELSS) (*E*)-6-(bromomethylene)-tetrahydro-3-(1-naphtalenyl)-2*H*-pyran-2-one was synthesized as previously described.¹⁹ After synthesis, purity of the compound was established by NMR spectroscopy. The inhibitor exhibits a specificity for calcium-independent plasmalogen-specific PLA₂ which is >1000 fold greater than for calcium-dependent PLA₂.¹⁵ HELSS, dissolved in ethanol, was added to the cardiomyocyte cultures 30 min before the start of the chemical anoxia, in concentrations of 1 μM, 2.5 μM, 5 μM, 10 μM or 20 μM. The compound was present during the entire experiment. In separate control experiments the effect of

HELSS on cell viability during control incubation without chemical anoxia was determined. If HELSS concentration was below 10 μM , no cell death was observed in control cultures. However, at 20 μM the inhibitor induced cell death in cardiomyocytes during control incubation.

Chemical anoxia of the cardiomyocytes. Chemical anoxia of the cardiomyocyte cultures was imposed by incubating the cells with 5 mM NaCN and 10 mM 2-deoxyglucose in a HEPES balanced salt solution (HBSS), containing in mM: NaCl 125, KCl 5, MgSO_4 1, KH_2PO_4 1, CaCl_2 2.5, NaHCO_3 10, HEPES 20, sodium pyruvate 5, pH 7.4, at 37°C. Before the start of chemical anoxia each culture was allowed to equilibrate in HBSS for 1 h at 37°C.

LDH release. In the experiments using the 24-wells plates, cell death was quantified by measuring the LDH activity released from the cardiomyocytes into the medium. To this end, 15 μl samples of the medium were taken at the indicated time points, and the LDH activity in the samples was measured using a photometric assay (1442597, Boehringer, Mannheim, Germany). At the end of the experiment the cells were lysed using 0.1% Triton X-100, and total LDH activity in the cell culture, i.e. in cells + medium, was determined. After correction for the changes in medium volume during the course of the experiment, LDH activity in the medium samples was expressed as percentage of total LDH activity. HELSS did not have any effect on the photometric LDH activity assay itself.

Digital imaging fluorescence microscopy. Intracellular free calcium concentration ($[\text{Ca}^{2+}]_i$) and cell death were measured by digital imaging fluorescence microscopy, employing the fluorescent calcium indicator fura-2,²⁰ and the fluorescent DNA probe propidium iodide,²¹ respectively.

Fura-2 : The cardiomyocytes were loaded with fura-2 by incubation with 2 μM fura-2/AM (Molecular Probes, Eugene, OR, USA) in 1 ml HBSS, for 30 min at 37°C. Then, the glass coverslip was rinsed three times with HBSS and was mounted in a culture dish containing two compartments which was recently described by us.²² Using the two-compartment culture dish, the two halves of a single cell culture grown on a standard coverslip can be exposed to two treatments simultaneously, allowing the effect of one treatment to be compared with that of the other treatment in the same culture. This way, the natural variability that might exist between different individual cultures is circumvented. In addition, by simultaneously conducting two experiments per dish, the time and the number of cultures needed for the experiments is essentially halved.

II. Role of phospholipid degradation in cell death

The two-compartment culture dish was mounted in a thermostated micro-incubator²³ on the microscope stage equipped with a computer-controlled XY-table. This set-up allows the experimenter to shuttle between the two compartments of the culture dish during the experiment in order to compare selected cells in one compartment with those in the other compartment.

The cells were studied in an imaging fluorescence microscope, previously described.^{22,24} The set-up consists of an inverted microscope (Leitz Diavert, Wetzlar, Germany) equipped with a 20x fluorite objective (Nikon, Tokyo, Japan) and a mercury light source (HBO-100, Osram, Montgomery, NY, USA). A filterwheel (Sutter Instruments, Novato, CA, USA) allows the selection of excitation filters (340 nm and 380 nm for fura-2, 535 nm for propidium iodide). Emission fluorescence is led through a high-pass filter (>490 nm for fura-2, > 590 nm for propidium iodide), and is imaged by a high-sensitivity silicon intensified target camera (Hamamatsu C2400-08, Herrsching, Germany). The resulting video image is digitized by a frame-grabber board (Imaging Technologies Inc., Woburn, MA, USA) in a PC-AT 486 computer. Spatial resolution of the images is 256 x 256 pixels, with an 8 bits intensity resolution. Every 10 min, sixteen video frames of each wavelength were averaged to improve the signal to noise ratio. The images were processed using dedicated image processing software (TIM, Difa, Breda, The Netherlands). After the subtraction of the background fluorescence, the 340 nm image was divided by the 380 nm image on a pixel by pixel basis to yield a ratio image. The software allows the analysis of individual cells. Statistical parameters (mean, median, standard deviation) were calculated by the software and used to calculate $[Ca^{2+}]_i$.

Propidium iodide: In propidium iodide imaging, dead cells were identified by the propidium iodide fluorescence of their nuclei. Living cells showed no such fluorescence. If appropriate, cells were made permeable at the end of the experiment by addition of 20 μ M digitonin. The number of dead cells during the experiment was expressed as a percentage of the total number of cells, as counted after digitonin addition.

Calibration of fura-2 fluorescence. At the end of the experiment, 10 μ M of the Ca^{2+} ionophore ionomycin (Boehringer, Mannheim, Germany) was added to obtain the highest obtainable ratio value, R_{max} . Then, 20 mM ethylene glycol-bis(β -aminoethyl ether) N,N,N',N'-tetraacetic acid (EGTA) was added to obtain the lowest obtainable ratio value, R_{min} . Calculation of $[Ca^{2+}]_i$ was then performed using the formula described by Grynkiewicz *et al.*²⁰

Imaging protocol: After inserting the two-compartment incubation dish with the fura-2 loaded myocyte culture in the micro-incubator on the stage of the fluorescence microscope, the culture was equilibrated with 200 μ l HBSS for 30 min at 37°C. Also, propidium iodide (Sigma, St. Louis, MO, USA) was added to each

compartment in a final concentration of 100 nM. During this time, the cultures were incubated with either 0 μ M or 5 μ M HELSS. After this, to each compartment 200 μ l HBSS buffer with NaCN and 2-deoxyglucose was added to achieve a final concentration of 5 mM NaCN and 10 mM 2-deoxyglucose, respectively. Every 10 min a 340 nm, 380 nm and 535 nm image was taken at each side. Off-line, the fura-2 ratio images were calculated, statistics performed and the propidium iodide images evaluated.

ATP depletion. We measured intracellular ATP levels in the cardiomyocytes to establish the time course of ATP depletion during chemical anoxia, and to study the influence of HELSS on the depletion of ATP. Cardiomyocytes cultured in 24-well plates were exposed to control incubation or chemical anoxia, in the absence or presence of 5 μ M HELSS. At indicated time points, the cells were lysed in 0.1% Triton X-100, scraped from the dish, collected and put on ice. Within 10 min, ATP was measured using a luciferin-luciferase method (LUMAC, Perstorp Analytical Comp., Oud-Beijerland, The Netherlands) as previously described.²⁵ Protein in the samples was measured as described by Lowry *et al.*²⁶ Cellular ATP concentration (in nmoles/mg protein) at each time point was expressed as the percentage of the ATP concentration at t=0 min.

³H-arachidonic acid release. Phospholipid degradation was assessed by measuring the liberation of ³H-labelled arachidonic acid (³H-AA) from previously labelled cardiomyocytes. To this end, cardiomyocyte cultures in 35 mm culture dishes were loaded with [5,6,8,9,11,12,14,15-³H]-AA (specific activity 171 Ci/mmol) (Amersham, Amersham, Buckinghamshire, UK) by incubating the cell cultures with approx. 1 μ Ci of ³H-AA for 18-24 h in culture medium. After labelling, the cultures were washed three times with HBSS containing 10 mg/ml fatty acid-free albumin and pre-incubated with 1 ml HBSS for 1 hour at 37°C. Then, the cultures were exposed to either control incubation or chemical anoxia, in the absence or presence of 1 μ M, 2.5 μ M and 5 μ M HELSS. At indicated time points, the cells and medium were collected in 2 ml ice-cold methanol:14 N HCl (100:1). After addition of 2 ml chloroform and 1 ml 2.5 N HCl, the mixture was centrifuged at 4°C, after which the organic phase was collected. After re-extraction of this phase with 2 ml ice-cold CHCl₃:CH₃OH:0.6 N HCl (3:48:47), the organic phase was collected and dried under a stream of nitrogen. After dissolving in 20 μ l chloroform, the lipids were spotted on Kieselgel 60 plates (Merck, Amsterdam, The Netherlands), which had been activated at 120°C for 1 h, after impregnation in 1% H₃BO₃ in methanol. Then, the plates were developed in ethyl acetate:isooctane:acetic acid:water (90:50:20:100 v/v) for 60 min and the lipid constituents were localized in iodine vapour. After

II. Role of phospholipid degradation in cell death

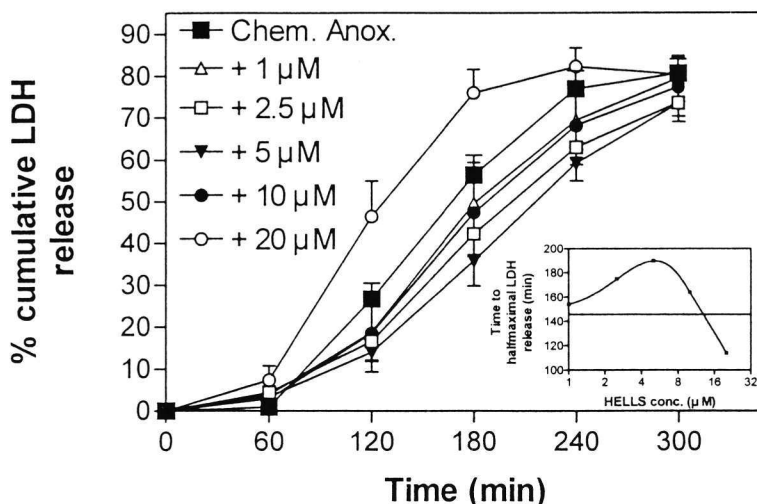


Figure 1. Cell death, expressed as percentage cumulative LDH release, in cardiomyocytes exposed to chemical anoxia (5 mM NaCN + 10 mM 2-deoxyglucose) in the absence (Chem. Anox.) or presence of various concentrations of halo-enol lactone suicide substrate (HELSS), an inhibitor of plasmalogen-selective phospholipase A₂. At $t \geq 60$ min, cell death in cultures treated with 20 μM HELSS is accelerated as compared to untreated cultures. At $t \geq 120$ min, cell death in cultures treated with 2.5-10 μM HELSS is delayed as compared to untreated cultures. Values are mean \pm SEM, $n=12$ cultures. The insert shows the time to half-maximal LDH release as a function of HELSS concentration. The horizontal straight line represents time to half-maximal LDH release in the absence of HELSS (146 min).

identification of the spots with the help of co-developed phospholipid and arachidonic acid standards, the various lipid spots were scraped off and radioactivity was measured by liquid scintillation counting. For each culture, the radioactivity of the free ³H-AA spot was expressed as a percentage of the total ³H-AA radioactivity in the culture. In each experiment, the ³H-AA release in cultures exposed to chemical anoxia (with or without HELSS) was compared to that in a control group not exposed to chemical anoxia, at the corresponding time point (0 min, 30 min, 60 min and 90 min).

Statistical analysis. All results are expressed as mean \pm SD or mean \pm SEM if so indicated. Statistical analysis was performed using ANOVA, followed by the Bonferroni t-test when appropriate. Differences were considered significant if $P < 0.05$.

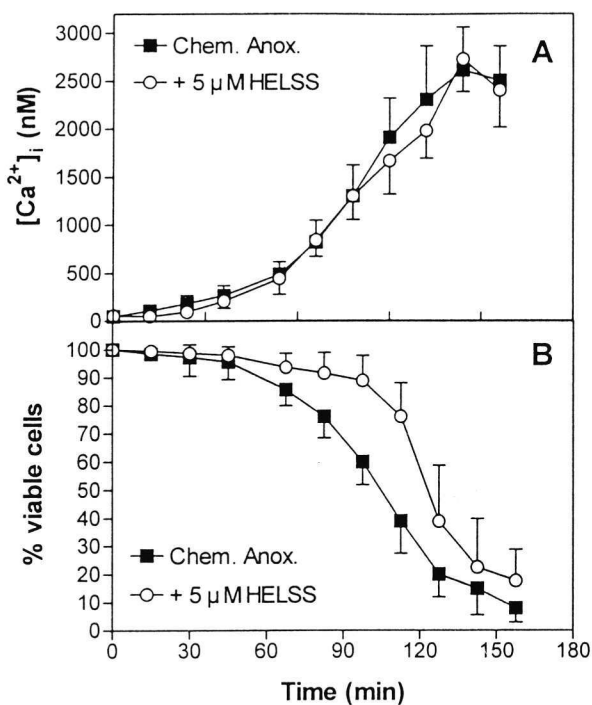


Figure 2. Intracellular Ca^{2+} ion concentration ($[Ca^{2+}]_i$) (panel A) and cell viability (panel B) in cardiomyocytes exposed to chemical anoxia (5 mM NaCN + 10 mM 2-deoxyglucose), in the absence (Chem. Anox.) or presence of 5 μ M halo-enol lactone suicide substrate (HELSS), an inhibitor of plasmalogen-selective phospholipase A_2 .

Panel A: Values of $[Ca^{2+}]_i$ in treated and untreated cells do not differ significantly.

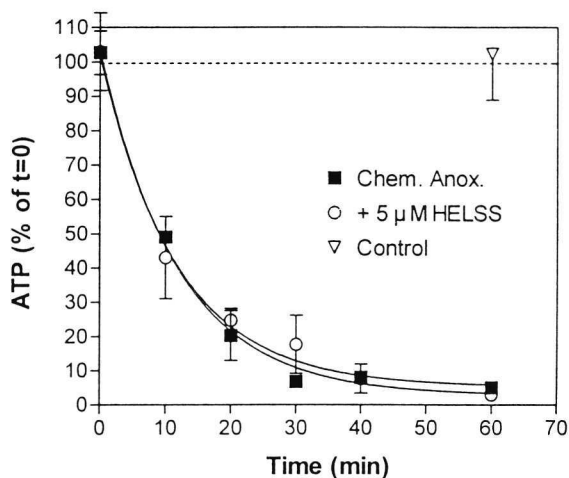
Panel B: Percentage viable cells in cultures without HELSS (closed squares) is significantly lower than in cultures treated with 5 μ M HELSS (open circles) at $t \geq 65$ min ($P < 0.05$). Values represent mean \pm SD for at least 80 cells in each group.

Results

LDH release during chemical anoxia. The release of cellular LDH into the medium, an indicator of the occurrence of cell death, in cultures exposed to chemical anoxia in the absence or presence of various concentrations of HELSS is shown in Figure 1. In untreated cells, half maximal LDH release occurred 146 min after start of chemical anoxia, with 80% of LDH released after 240 min. In the presence of 2.5 μ M HELSS, cell death was significantly delayed with half-maximal LDH release at 175 min. With 5 μ M HELSS, half-maximal LDH release was further delayed to 191 min. However, at higher concentrations of HELSS the protective effect diminished, with half-maximal LDH release for 10 μ M and 20 μ M HELSS at only 164 min and 112 min, respectively (see insert Fig. 1).

Fluorescence videomicroscopy. The time course of development of calcium overload and cell death in cardiomyocytes during chemical anoxia in the presence or absence of 5 μ M HELSS is shown in Figure 2. At least 80 cells from at least 6 different cultures were analysed in each group. During chemical anoxia, $[Ca^{2+}]_i$ in untreated cells increased from a basal value of 88 ± 29 nM to > 2.5 μ M after 130 min (Fig. 2A). In the presence of 5 μ M HELSS, the rise in $[Ca^{2+}]_i$ was similar to that Figure 3.

II. Role of phospholipid degradation in cell death



Intracellular ATP concentration in cardio-myocytes during control incubation (Control), and during chemical anoxia in the absence (Chem. Anox.) or presence of 5 μ M halo-enol lactone suicide substrate (HELSS), an inhibitor of plasmalogen-selective PLA₂. As compared to control incubation, ATP was significantly reduced in the groups subjected to chemical anoxia at $t \geq 10$ min (mean \pm SEM, $n = 3$, $P < 0.01$), with no difference between the groups exposed to chemical anoxia with or without HELSS.

observed in the untreated cells (Fig. 2A). Cell death, as assessed by propidium iodide fluorescence, began 65 min after onset of chemical anoxia and 50% of the cells were still viable after 105 min in untreated cultures (Fig. 2B). Treatment of the cardiomyocytes with 5 μ M HELSS delayed the time at which 50% of the cells were still viable to 128 min ($P < 0.05$). An increase of the concentration of HELSS did not yield any additional protection (data not shown).

ATP depletion. During incubation with 5 mM NaCN and 10 mM 2-deoxyglucose, the level of ATP decreased exponentially (rate constant: $0.084 \pm 0.009 \text{ min}^{-1}$) with only 10% of ATP remaining after 40 min of chemical anoxia (Fig. 3). The presence of 5 μ M HELSS during chemical anoxia had no influence on the time course or extent of ATP depletion during chemical anoxia (rate constant: $0.085 \pm 0.011 \text{ min}^{-1}$) (Fig. 4). In the absence of chemical anoxia ATP levels remained constant for at least 60 min.

Phospholipid degradation during chemical anoxia. During control incubation, the liberation of ³H-arachidonic acid (³H-AA) equalled approximately 1% of incorporated ³H-AA per hour. This value implies a phospholipid degradation rate of about 2.3 nmole phospholipid/mg protein per hour, given a value of 226 ± 30.6 nmol/mg protein for total phospholipids in the cultures.²⁷

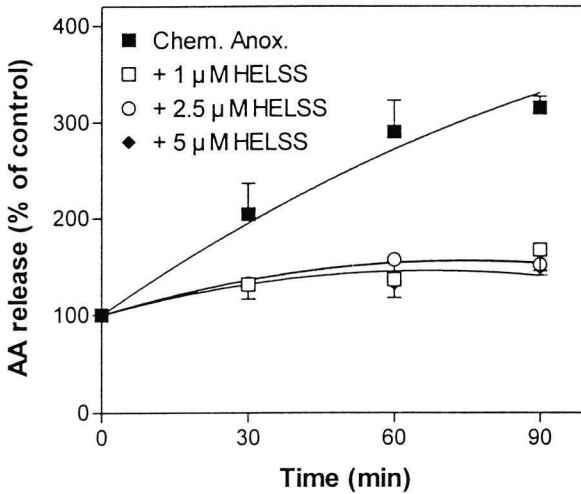


Figure 4. Release of ^3H -arachidonic acid (^3H -AA) during chemical anoxia in the absence (Chem. Anox.) or presence of 1 μM , 2.5 μM and 5 μM halo-enol lactone suicide substrate (HELSS), an inhibitor of plasmalogen-selective PLA_2 . At each time point, the ^3H -AA release in the four groups is expressed as a percentage of the ^3H -AA release in control cells not exposed to chemical anoxia for an identical period of time. A curve ($Y=100 + B \cdot X - 0.01 \cdot X^2$) was fitted through the data per group

($R^2 > 0.914$, $P < 0.02$). The release of ^3H -AA during chemical anoxia ($B=3.46$, 95% confidence interval (CI): 3.04-3.88) was significantly reduced by 1 μM HELSS ($B=1.50$, CI: 1.13-1.87), 2.5 μM HELSS ($B=1.49$, CI: 1.40-1.57) and 5 μM HELSS ($B=1.35$, CI: 1.10-1.60) ($P < 0.001$), with no differences between the various HELSS concentrations ($n=3-6$ cultures).

Liberation of ^3H -AA during chemical anoxia, either in the absence or presence of 5 μM HELSS, was expressed as percentage of ^3H -AA release from cultures not exposed to chemical anoxia, at the corresponding time point.

A curve $Y=100+(B \cdot X - 0.01X^2)$ was fitted through the data for each groups ($R^2 > 0.914$, $P < 0.02$). During chemical anoxia the rate of ^3H -AA release determined at 60 and 90 min had increased threefold (Fig. 4). This increased liberation of ^3H -AA during chemical anoxia (Chemical anoxia: $B=3.46 \pm 0.13$, CI: 3.04-3.88) was significantly reduced by 70-80% as a result of treatment with 1 μM HELSS ($B=1.50 \pm 0.12$, CI: 1.13-1.87), 2.5 μM HELSS ($B=1.49 \pm 0.03$, CI: 1.40-1.57) and 5 μM HELSS ($B=1.35 \pm 0.08$, CI: 1.10-1.60) ($P < 0.001$), with no differences between the different concentrations of HELSS (Fig. 4).

Discussion

The role of PLA_2 in the development of ischemic myocardial cell injury is not clear. The present study shows that halo-enol-lactone suicide substrate (HELSS), a specific inhibitor of plasmalogen-specific PLA_2 activity reduces cell death in cardiomyocytes exposed to chemical anoxia. Optimal protection was provided at a concentration of 5 μM HELSS, with less protection observed at both lower and higher concentrations HELSS. At concentrations below 5 μM HELSS, this could be due to dose-

II. Role of phospholipid degradation in cell death

dependency, whereas at concentrations higher than 5 μM HELLS the protective effects of the inhibitor may have been exceeded by deleterious effects of HELLS, as evidenced by the cell damage in control cells not exposed to chemical anoxia at higher concentrations of HELLS.

Although the fall in the cellular ATP level is a prominent feature in ischemia and is considered to be a key phenomenon in the process of ischemic cell injury,²⁸ 5 μM HELSS did not modify the rate or extent of ATP depletion during chemical anoxia as compared to untreated cells. This indicates that the protective effect of HELSS was not mediated by conservation of ATP stores.

The rise in intracellular Ca^{2+} ion concentration ($[\text{Ca}^{2+}]_i$) during ischemia, anoxia and energy depletion, leading to calcium overload, is considered to constitute an intermediate step in the development of irreversible cell injury.^{29,30} Upon chemical anoxia, we did not find any effect of 5 μM HELSS on the development of calcium overload as compared to untreated cells. However, in accordance to the delay in half-maximal LDH release, cell death as assessed by propidium iodide fluorescence was significantly delayed in the cultures treated with 5 μM HELSS.

Phospholipid degradation, as measured by the liberation of incorporated ^3H -arachidonic acid, was increased three-fold during chemical anoxia as compared to myocyte cultures not exposed to chemical anoxia, leading to a phospholipid degradation rate of approximately 6.9 nmol/mg protein per hour. This value is in agreement with the phospholipid degradation rates reported by Van de Vusse *et al.* in anoxic myocardium (10 nmol/mg protein/hour)³¹ and by Otani *et al.* in ischemic myocardial tissue (15 nmol/mg protein/hour).³²

In the cultures treated with either 1 μM , 2.5 μM or 5 μM HELSS, the accelerated phospholipid degradation during chemical anoxia was almost completely prevented, compatible with an inhibition of PLA_2 activity by HELSS.

However, this finding was associated with an only slight and temporary attenuation of cell death (Fig. 1 and Fig. 2B). The apparent dissociation between phospholipid degradation and cell death suggests that cell death may occur despite an almost complete prevention of phospholipid degradation. This would indicate that phospholipid degradation is not the single decisive factor for cell death to occur, and that the phospholipid degradation observed during ischemia and energy depletion may be considered an epiphenomenon, most likely reflecting autolysis of cells already severely damaged. In support with this conclusion, Steenbergen and Jennings reported that in isolated ischemic myocardium irreversible cell damage precedes the accumulation of phospholipid degradation products.³³ Also, Van der Vusse *et al.* failed to identify convincing evidence in favour of or against the involvement of PLA_2 -mediated phospholipid degradation in the development of cell death.³⁴ Alternative mechanisms proposed to play a pivotal role in ischemic myocardial cell

death include a) destabilization and disruption of myocardial sarcolemma due to phase transition of membrane phospholipids,³⁵ b) aggregation of membrane-linked proteins^{36,37} and c) damage to the cytoskeleton.³⁸

The mechanism by which HELSS delays cell death in anoxic cardiomyocytes remains unclear and requires additional research.

In summary, the synthetic plasmalogen-selective PLA₂ inhibitor HELSS attenuates cell death in cultured neonatal rat cardiomyocytes during chemical anoxia, as assessed by LDH release and by propidium iodide fluorescence. This protective effect is not mediated by conservation of cellular ATP stores nor by influencing the development of calcium overload. During chemical anoxia, HELSS strongly inhibited the degradation of phospholipids at concentrations as low as 1 μM. However, cell death during chemical anoxia was not (1 μM) or only temporary (2.5 μM and 5 μM) attenuated by HELSS.

We conclude that HELSS attenuates cell death in cardiomyocytes during chemical anoxia through a yet unknown mechanism. The finding of an almost complete prevention of phospholipid degradation with no or a marginal attenuation of cell death, suggests that phospholipid degradation is not the single decisive factor for cell death during chemical anoxia, but rather may reflect autolysis of cell already severely damaged. The plasmalogen-specific PLA₂ is likely responsible for the accelerated phospholipid degradation in anoxic cardiomyocytes.

Acknowledgement

This study was supported by grants from the Netherlands Heart Foundation, no. 90.089 and 93.092.

The authors thank Prof. dr. G.J. Van der Vusse for critically reading the manuscript.

Legend

1. Van der Vusse GJ, Roemen THM, Prinzen FW, Coumans WA, Reneman RS. Uptake and tissue content of fatty acids content in dog myocardium under normoxic and ischemic conditions. *Circ Res.* 1982;50:538-546.
2. Chien KR, Han A, Sen A, Buja LM, Willerson JT. Accumulation of unesterified arachidonic acid in ischemic canine myocardium. *Circ Res.* 1984;54:313-322.
3. Jones RL, Miller JC, Hagler HK, Chien KR, Willerson JT, Buja LM. Association between inhibition of arachidonic acid release and prevention of calcium loading during ATP depletion in cultured rat cardiac myocytes. *Am J Pathol.* 1989;135:541-556.
4. Otani H, Engelman RM, Rousou JA, Bryer RH, Das DK. Enhanced prostaglandin synthesis due to phospholipid breakdown in ischemic-reperfused myocardium. *J Mol Cell Cardiol.* 1986;18:953-961.
5. Steenbergen C, Fralix TA, Murphy E. Role of increased cytosolic free calcium concentration in myocardial ischemic injury. *Basic Res Cardiol.* 1993;88:456-470.

II. Role of phospholipid degradation in cell death

6. Toyo-oka T, Ross JR. Ca^{2+} sensitivity change and troponin loss in cardiac natural actomyosin after coronary occlusion. *Am J Physiol*. 1981;240:H704-H708.
7. Hazen SL, Stuppy RJ, Gross RW. Purification and characterization of canine myocardial cytosolic phospholipase A_2 . *J Biol Chem*. 1990;265:10622-10630.
8. Gross RW. Myocardial phospholipases A_2 and their membrane substrates. *Trends Cardiovasc Med*. 1992;2:115-121.
9. Hazen SL, Gross RW. Identification and characterization of myocardial phospholipase A_2 from transplant recipients suffering from end-stage ischemic heart disease. *Circ Res*. 1992;70:486-495.
10. Han X, Gross RW. Plasmenylcholine and phosphatidylcholine membrane bilayers possess distinct conformational motifs. *Biochemistry*. 1990;29:4992-4996.
11. Post JA, Verkleij AJ, Roelofsen B, Op den Kamp JAF. Plasmalogen content and distribution in the sarcolemma of cultured neonatal rat cardiomyocytes. *FEBS Lett*. 1988;240:78-82.
12. Schulz R, Strynadka KD, Panas DL, Olley PM, Lopaschuk GD. Analysis of myocardial plasmalogen and diacyl phospholipids and their arachidonic acid content using high-performance liquid chromatography. *Anal Biochem*. 1993;213:140-146.
13. Hazen SL, Gross RW. Principles of membrane biochemistry and their application to the pathophysiology of cardiovascular disease. In: Fozzard ea, eds. *The heart and cardiovascular system*. New York. Raven Press. 1992:839-860.
14. Ford DA, Hazen SL, Saffitz JE, Gross RW. The rapid and reversible activation of a calcium-independent plasmalogen-selective phospholipase A_2 during myocardial ischemia. *J Biol Chem*. 1991;260:7295-7303.
15. Hazen SL, Zupan LA, Weiss RH, Getman DP, Gross RW. Suicide inhibition of canine myocardial cytosolic calcium-independent phospholipase A_2 . *J Biol Chem*. 1991;266:7227-7232.
16. Zupan LA, Weiss RH, Hazen SL, Parnas BL, Aston KW, Lennon PJ, Getman DP, Gross RW. Structural determinants of haloenol lactone-mediated suicide inhibition of canine myocardial calcium-independent phospholipase- A_2 . *J Med Chem*. 1993;36:95-100.
17. Van der Laarse A, Hollaar L, Van der Valk EJM. Release of alpha-hydroxybutyrate dehydrogenase from neonatal rat heart cell cultures exposed to anoxia and reoxygenation: Comparison with impairment of structure and function of damaged cardiac cells. *Cardiovasc Res*. 1979;13:345-353.
18. Blondel B, Royen J, Cheneval JP. Heart cells in culture: a simple method for increasing the proportion of myoblasts. *Experientia*. 1971;27:356-358.
19. Durley RC, Parnas BL, Weiss RH. Synthesis of high specific activity Tritium labelled (E)-6-(bromomethylene)-tetrahydro-3-(1-naphtalenyl)-2H-pyran-2-one as a selective probe for calcium-independent phospholipase A_2 . *J Labelled Comp Radiopharmac*. 1992;31:685-691.
20. Grynkiewicz G, Poenie M, Tsien RY. A new generation of Ca^{2+} indicators with greatly improved fluorescence properties. *J Biol Chem*. 1985;260:3440-3450.
21. Crissman HA, Stevenson AP, Kissane RJ, Tobey RA. Techniques for quantitating staining of cellular DNA for flow cytometric analysis. In: Melanned MY, Mullaney PF and Mendelsohn ML, eds. *Flow cytometry and sorting*. New York. Wiley. 1979:243-261.
22. Atsma DE, Bastiaanse EML, Ince C, Van der Laarse A. A novel two-compartment culture dish allows microscopic evaluation of two different treatments in one cell culture simultaneously - Influence of external pH on $\text{Na}^+/\text{Ca}^{2+}$ exchanger activity in cultured rat cardiomyocytes. *Pflugers Arch*. 1994;428:296-299.

23. Ince C, Ypey DL, Diesselhoff-Den Dulk MMC, Visser JAM, De Vos A, Van Furth R. Micro-CO₂-Incubator for use on a microscope. *J Immunol Meth.* 1983;60:269-275.
24. Atsma DE, Bastiaanse EML, Jerzewski A, Van der Valk EJM, Van der Laarse A. Role of calcium-activated neutral protease (calpain) in cell death in cultured neonatal rat cardiomyocytes during metabolic inhibition. *Circ Res.* 1995;76:1071-1078.
25. Wettermark G, Stymne H. Substrate analysis in single cells. I. Determination of ATP. *Anal Biochem.* 1975;63:293-307.
26. Lowry OH, Rosebrough NJ, Farr AL, Randall RJ. Protein measurement with the Folin phenol reagent. *J Biol Chem.* 1951;193:265-275.
27. Bastiaanse EML, Van der Valk-Kokshoorn LJM, Egas-Kenniphaas JM, Atsma DE, Van der Laarse A. The effect of sarcolemmal cholesterol content on the tolerance to anoxia in cardiomyocyte cultures. *J Mol Cell Cardiol.* 1994;26:639-648.
28. Jennings RB, Hawkins HK, Lowe JE, Hill ML, Klotman S, Reimer KA. Relation between high energy phosphate and lethal injury in myocardial ischemia in the dog. *Am J Pathol.* 1978;92:187-215.
29. Steenbergen C, Murphy E, Levy L, London RE. Elevation of cytosolic free calcium concentration early in myocardial ischemia in perfused rat heart. *Circ Res.* 1987;60:700-707.
30. Silverman HS and Stern MD. Ionic basis of ischaemic cardiac injury: Insights from cellular studies. *Cardiovasc Res.* 1994;28:581-597.
31. Van der Vusse GJ, De Groot MJM, Willemsen PHM, Van Bilsen M, Schrijvers AHGJ, Reneman RS. Degradation of phospholipids and triacylglycerol, and accumulation of fatty acids in anoxic myocardial tissue, disrupted by freeze-thawing. *Mol Cell Biochem.* 1989;88:83-90.
32. Otani H, Prasad MR, Jones RM, Das DK. Mechanism of membrane phospholipid degradation in ischemic-reperfusion rat hearts. *Am J Physiol.* 1989;257:H252-H258.
33. Steenbergen C, Jennings RB. Relationship between lysophospholipid accumulation and plasma membrane injury during total in vitro ischemia in dog heart. *J Mol Cell Cardiol.* 1984;16:605-621.
34. Van der Vusse GJ, Van Bilsen M, Reneman RS. Is phospholipid degradation a critical event in ischemia and reperfusion-induced damage? *NIPS.* 1989;4:49-53.
35. Musters RJP, Otten E, Biegelmann E, Bijvelt J, Keijzer JJH, Post JA, Op Den Kamp JAF, Verkleij AJ. Loss of asymmetric distribution of sarcolemmal phosphatidylethanolamine during simulated ischemia in the isolated neonatal rat cardiomyocyte. *Circ Res.* 1993;73:514-523.
36. Verkleij AJ, Post JA. Physico-chemical properties and organization of lipids in membranes: their possible role in myocardial injury. *Basic Res Cardiol.* 1987;82 (Suppl. I):85-91.
37. Post JA, Leunissen-Bijvelt J, Ruigrok TJC, Verkleij AJ. Ultrastructural changes in sarcolemma and mitochondria in the isolated rabbit heart during ischemia and reperfusion. *Biochim Biophys Acta.* 1985;845:119-123.
38. Steenbergen C, Hill ML, Jennings RB. Cytoskeletal damage during myocardial ischemia: changes in vinculin immunofluorescence during total in vitro ischemia in canine heart. *Circ Res.* 1987;60:478-486.

Chapter 7

Low external pH limits cell death in energy depleted cardiomyocytes by decreasing Ca^{2+} overload via $\text{Na}^+/\text{Ca}^{2+}$ exchange inhibition

Douwe E. Atsma, E.M. Lars Bastiaanse, Lizet van der Valk, Arnoud Van der Laarse,

Department of Cardiology, University Hospital, Leiden, The Netherlands

Am J Physiol. 1996; 270: H2149-H2156

Parts of this study were presented at the 15th European Section Meeting of the International Society for Heart Research, Copenhagen, Denmark, 1994, and on the 17th Meeting of the European Society of Cardiology, Amsterdam, The Netherlands, August 1995.

Abstract.

We studied the effect of external pH (pH_e) on cell injury, ATP content, intracellular concentration of Ca^{2+} ($[\text{Ca}^{2+}]_i$), Na^+ ($[\text{Na}^+]_i$) and H^+ (pH_i) during metabolic inhibition (*Mi*) ($\text{NaCN} + 2\text{-deoxyglucose}$) in neonatal rat cardiomyocytes. Cell death during *Mi* decreased at pH_e below 7.4, with practically no cell death at pH_e 6.0. Lowering pH_e resulted in only temporary ATP conservation. During *Mi* at pH_e 7.4, $[\text{Ca}^{2+}]_i$ rose from 86 ± 44 nM to 2.5 ± 0.4 μM , but at pH_e 6.0 to only 510 ± 215 nM. Upon *Mi* at pH_e 7.4, pH_i decreased from 7.25 ± 0.06 to 6.82 ± 0.16 , but at pH_e 6.0 to 6.34 ± 0.17 . During *Mi* at pH_e 7.4, $[\text{Na}^+]_i$ increased from 9.1 ± 0.86 mM to 26.1 ± 4.1 mM. At pH_e 6.0, $[\text{Na}^+]_i$ rose more rapidly, to 27.3 ± 3.5 mM. At $\text{pH}_e < 7.4$, sarcolemmal $\text{Na}^+/\text{Ca}^{2+}$ exchanger activity, involved in the development of Ca^{2+} overload, was decreased, as assessed during Na^+ -free incubation. We conclude that low pH_e protects cardiomyocytes during *Mi* by limiting Ca^{2+} overload via $\text{Na}^+/\text{Ca}^{2+}$ exchanger inhibition.

Introduction

Recent reports have indicated that during ischemia, anoxia and metabolic inhibition, a low external pH (pH_e) protects various organs, including kidney,¹ liver² and neonatal³ and adult heart⁴ against lethal injury. Also during reperfusion or reoxygenation a low pH_e has a protective effect, whereas restoration of pH_e during reperfusion or reoxygenation to physiological values is associated with significant additional cell damage. This latter phenomenon is known as the pH-paradox.⁵

In ischemic tissue, intracellular acidosis develops as a result of lactate production, net hydrolysis of ATP and CO_2 retention.⁶ The resulting H^+ -gradient over the sarcolemma is considered to increase the intracellular Na^+ concentration ($[\text{Na}^+]_i$) via sarcolemmal Na^+/H^+ exchange.⁷ This is thought to induce Ca^{2+} overload through reversed action of the sarcolemmal $\text{Na}^+/\text{Ca}^{2+}$ exchanger.⁷ The calcium overload is considered a pivotal event in the development of cell death, as it may lead to irreversible cell injury via activation of intracellular enzymes including phospholipases and proteases.^{8,9}

The protective effect of low pH_e during ischemia may be due to a decrease in cellular Na^+ loading via Na^+/H^+ exchange as a result from a reduction in the transsarcolemmal H^+ -gradient, which would attenuate Ca^{2+} loading via $\text{Na}^+/\text{Ca}^{2+}$ exchange.^{10,11} This notion is further corroborated by the protective effects observed from purported specific inhibitors of the sarcolemmal Na^+/H^+ exchanger during ischemia/reperfusion.^{12,13}

However, this assumption may not completely explain the observed protection by low pH_e during ischemia or energy depletion, as it has been reported that Na^+ influx under these conditions may also occur through fast sodium channels,¹⁴ thereby contributing to the development of cellular Na^+ overload and, subsequently, Ca^{2+} overload. In addition, in rat hearts exposed to lactate to mimic ischemic conditions, lowering of pH_e from 7.4 to 6.4 resulted in an increase in $[Na^+]_i$ rather than in a decreased $[Na^+]_i$,¹⁵ further illustrating that the mechanism responsible for the protective effects of low pH_e during ischemia or energy depletion is still unclear.

Previously we showed that the activity of the Na^+/Ca^{2+} exchanger in cultured neonatal rat cardiomyocytes is influenced by pH_e , as measured with fluorescent techniques.¹⁶ We observed a decreased activity of the Na^+/Ca^{2+} exchanger at low pH_e , which effect may also contribute to the protective effects of low pH_e during ischemia, anoxia or metabolic inhibition.

To study the mechanism responsible for the protective effect of low pH_e in more detail, we exposed cultured neonatal rat cardiomyocytes to metabolic inhibition (5 mM NaCN + 10 mM 2-deoxyglucose), and we measured pH_i , $[Na^+]_i$, intracellular Ca^{2+} concentration ($[Ca^{2+}]_i$) and cell death employing digital imaging fluorescence microscopy and fluorescent probes. In addition, we studied the effect of pH_e on the activity of the sarcolemmal Na^+/Ca^{2+} exchanger. It was found that during metabolic inhibition at low pH_e , Na^+ overload still developed, whereas Ca^{2+} overload did not. The activity of the Na^+/Ca^{2+} exchanger was substantially decreased at low pH_e , implying that the protective effect of low external pH on cell death is not due to decreased Na^+/H^+ exchanger activity, but results - at least in part - from a diminished Ca^{2+} overload via inhibition of the sarcolemmal Na^+/Ca^{2+} exchanger.

Methods

Cell culture. Cardiomyocyte cultures were prepared using the method described by Van der Laarse *et al.*¹⁷ Briefly, hearts of 2-day old Wistar rats were dissected and transferred to a solution containing in mM: NaCl 137, KCl 5, Na_2HPO_4 0.4, KH_2PO_4 0.4, glucose 5.5, HEPES 20, phenol red 0.5 mg/l, pH 7.4. The ventricles were minced into small fragments and dissociated using collagenase (type I CLS, Worthington, Freehold, NJ, USA) during two periods of 20 min in a shaking water bath at 37°C. After centrifugation at 50 x g for 15 min, the cells were suspended in a culture medium consisting of Ham's F-10 medium (Flow Laboratories, Irvine, UK) supplemented with 10% foetal bovine serum (Flow Laboratories) and 10% horse serum (Flow Laboratories, Irvine, UK). The cells were plated in 60 mm culture dishes (Becton-Dickinson, Oxnard, CA, USA) in a density of 4.2×10^6 cells per dish. Myocytes were separated from nonmuscle cells using a selective adhesion

technique.¹⁸ After 45 min the medium, enriched in myocytes, was transferred to either 24-well plates or 35 mm culture dishes, which contained 25 mm round glass coverslips. The myocyte cultures were kept in a humidified incubator (37°C) with an atmosphere of 95% air and 5% CO₂. Culture medium was changed after 3 h and 48 h. After three days the monolayers of spontaneously beating myocytes were used for the experiment. The experiments had the approval of the Animal Experiments Committee of our institution.

Metabolic inhibition of the cardiomyocytes. Metabolic inhibition of the cardiomyocyte cultures was imposed by interruption of the respiratory chain by incubating the cells with 5 mM NaCN and 10 mM 2-deoxyglucose in a N-2-hydroxyethyl piperazine-N'-2-ethanesulfonic acid (HEPES) balanced salt solution (HBSS), containing in mM: NaCl 125, KCl 5, MgSO₄ 1, KH₂PO₄ 1, CaCl₂ 2.5, NaHCO₃ 10, HEPES 20 (pH 7.0-8.0) or piperazine-N,N'-bis[2-ethanesulfonic acid] (PIPES) 20 (pH 5.5-6.5), sodium pyruvate 5, pH 7.4, at 37°C. Before the start of metabolic inhibition each culture was allowed to equilibrate in HBSS for 1 h at 37°C.

LDH release. In the experiments using 24-well plates, cell death was quantified by measuring the LDH activity released from the cardiomyocytes into the medium. To this end, 15 µl samples of the medium were taken at the indicated time points, and the LDH activity in each sample was measured using a photometric assay (1442597, Boehringer, Mannheim, Germany). At the end of the experiment the cells were lysed using 0.1% Triton X-100, and total LDH activity in the cell culture, i.e. in cells + medium, was determined. After correction for the changes in medium volume during the course of the experiment, LDH activity in the medium samples was expressed as percentage of total LDH activity. Control experiments showed that the pH of the samples did not influence the LDH assay itself.

ATP. We measured cellular ATP levels in the cardiomyocytes to establish the time course of ATP depletion during metabolic inhibition at various pHe. Cardiomyocytes cultured in 24-well plates were exposed to control incubation at pHe 7.4, or metabolic inhibition at pHe 6.0, 6.5, 7.0, or 8.0. At indicated time points, the cells were lysed in 0.1% Triton X-100, scraped from the dish, collected and put on ice. Within 10 min, ATP was measured using a luciferin-luciferase method (LUMAC, Perstorp Analytical Comp., Oud-Beijerland, The Netherlands). Protein in the samples was measured as described by Lowry *et al.*¹⁹ Cellular ATP concentration (in nmoles/mg protein) at each time point was expressed as the percentage of the ATP concentration at t=0 min.

Digital imaging fluorescence microscopy. Intracellular Ca^{2+} concentration ($[Ca^{2+}]_i$), intracellular Na^+ concentration ($[Na^+]_i$) and intracellular pH (pH_i) were measured by digital imaging fluorescence microscopy, employing the fluorescent ion indicators fura-2,²⁰ sodium-binding benzofuran isophthalate (SBFI) and 2',7'-bis(carboxyethyl)-5',6'-carboxyfluorescein (BCECF), respectively. Cell death was measured using the fluorescent DNA probe propidium iodide.

Fura-2 : The cardiomyocytes were loaded with fura-2 by incubation with 2 μ M fura-2/AM (Molecular Probes, Eugene, OR, USA) in 1 ml HBSS, for 30 min at 37°C. Then, the glass coverslip was rinsed three times with HBSS and was mounted in a culture dish containing two compartments which was recently described by us.¹⁶ Using the two-compartment culture dish, the two halves of a single cell culture grown on a standard coverslip can be exposed to two treatments simultaneously, allowing the effect of one treatment to be compared with that of the other treatment in the same culture. This way, the natural variability that might exist between different individual cultures is circumvented. In addition, by simultaneously conducting two experiments per dish, the time and the number of cultures needed for the experiments are essentially halved.

After mounting the coverslip with the culture in the two-compartment culture dish, each compartment of the dish was incubated with 200 μ l HBSS at 37°C.

BCECF: The cardiomyocytes were loaded with BCECF by incubation with 1 μ M BCECF/AM (Molecular Probes) in 1 ml HBSS for 20 min at room temperature. Then, the glass coverslip was rinsed three times with HBSS, and was mounted in the two-compartment culture dish.

SBFI: The cells were loaded with SBFI by incubation with 5 μ M SBFI/AM (Molecular Probes) in 1.25 % Pluronic F-127 for 30 min at 37°C. Then, the glass coverslip was rinsed three times with HBSS, and was mounted in the two-compartment culture dish.

Propidium iodide: Propidium iodide (Sigma, St. Louis, MO, USA) was added to each compartment in a final concentration of 100 nM.

Instrumentation: The two-compartment culture dish was mounted in a thermostated micro-incubator²¹ on the microscope stage equipped with a computer controlled XY-table. This set-up allows the experimenter to shuttle between the two compartments of the culture dish during the experiment in order to compare selected cells in one compartment with those in the other compartment. The cells were studied in an imaging fluorescence microscope, previously described.^{16,22} The set-up consists of an inverted microscope (Leitz Diavert, Wetzlar, Germany) equipped with a 20x fluorite objective (Nikon, Tokyo, Japan) and a mercury light source (HBO-100, Osram, Montgomery, NY, USA).

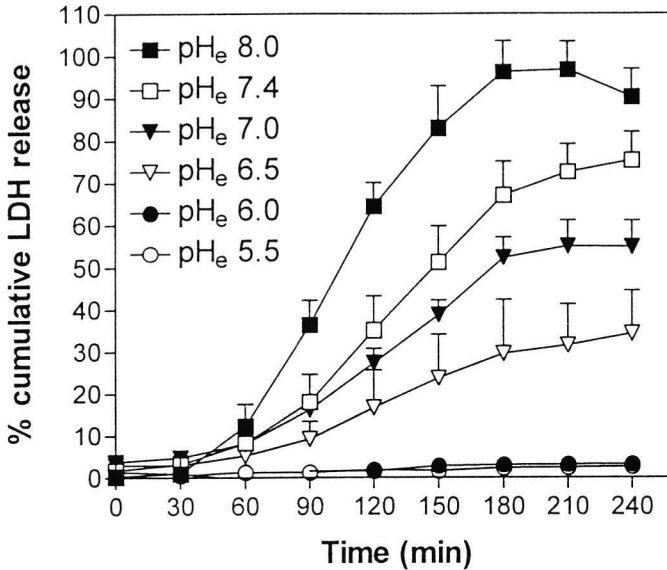


Figure 1. Release of cellular lactate dehydrogenase (LDH) activity from cardiomyocytes upon metabolic inhibition (5 mM NaCN + 10 mM 2-deoxyglucose) with external pH (pH_e) ranging from 5.5 to 8.0. Values are mean \pm SD, $n=8$ cultures in each group.

A filterwheel (Sutter Instruments, Novato, CA, USA) allows the selection of excitation filters (340 nm and 380 nm for fura-2 or SBFI, 535 nm for propidium iodide, 438 nm and 486 nm for BCECF). Emission fluorescence is led through a high-pass filter (>490 nm for fura-2 and SBFI, >590 nm for propidium iodide, >530 nm for BCECF), and is imaged by a high-sensitivity silicon intensified target camera (Hamamatsu C2400-08, Herrsching, Germany). The resulting video image is digitised by a frame-grabber board (Imaging Technologies Inc., Woburn, MA, USA) in a PC-AT 486 computer. Spatial resolution of the images is 256x256 pixels, with an 8 bits intensity resolution. Every 10 min, at each wavelength sixteen consecutive video frames were averaged to improve the signal to noise ratio. The images were processed using dedicated image processing software (TIM, Difa, Breda, The Netherlands). After the subtraction of the background fluorescence, the 340 nm image was divided by the 380 nm image on a pixel by pixel basis to yield a ratio image. The software allows the analysis of individual cells. Statistical parameters (mean, median, standard deviation) were calculated by the software and used to calculate $[Ca^{2+}]_i$.

In propidium iodide imaging, dead cells were identified by the propidium iodide fluorescence of their nuclei, whereas living cells showed no such fluorescence. If appropriate, cells were permeabilised at the end of the experiment by addition of 20 μ M digitonin. The number of dead cells during the experiment was expressed as a percentage of the total number of cells, as counted after digitonin addition.

Calibration of fura-2. At the end of the experiment, 10 μ M of the Ca^{2+} ionophore ionomycin (Boehringer, Mannheim, Germany) was added to obtain the highest

obtainable ratio value, R_{max} . Then, 20 mM ethylene glycol-bis(β -aminoethyl ether) N,N,N',N'-tetraacetic acid (EGTA) was added to obtain the lowest obtainable ratio value, R_{min} . Calculation of $[Ca^{2+}]_i$ was then performed using the formula described by Grynkiewicz *et al.*²⁰

Calibration of BCECF. The fluorescence of BCECF was calibrated *in situ* as described previously.⁴ BCECF-loaded cardiomyocytes were incubated with a calibration buffer containing (mM): KCl 140, NaCl 3.8, MgSO₄ 1.2, HEPES 20 (for pH_e 6.8-7.8) or MOPS 20 (for pH_e 6.1-6.8) adjusted to various pH, and 10 μ M of the K⁺-H⁺ ionophore nigericin (Sigma). The resulting calibration curve was used to calculate pH_i .

Calibration of SBFI. Calibration of SBFI fluorescence was performed *in situ* as described earlier.²³ Cardiomyocytes loaded with SBFI were incubated in a calibration buffer, containing 10 mM HEPES, 1 mM EGTA, and 0.3 μ g/ml of the monovalent cation ionophore gramicidin D (Sigma) (pH 7.2), with 0-50 mM of NaCl. KCl was added to maintain a final concentration of $[Na^+]_e + [K^+]_e = 140$ mM. The omission of divalent cations in the calibration solutions renders the L-type Ca²⁺ channels highly permeable for Na⁺, facilitating the equilibration of intracellular and extracellular Na⁺ concentrations.²⁴ We ensured that the calibration data were obtained from still elongated cardiomyocytes, as contracture of the cells during the calibration procedure renders the results useless.²⁵ The calibration curve obtained was used to calculate $[Na^+]_i$.

Experimental protocol: After the loading protocol, the incubation dish with the loaded myocyte culture was inserted in the micro-incubator on the stage of the fluorescence microscope and both culture halves were equilibrated with HBSS for 30 min at 37°C. During this period, suitable fields of view were selected and their positions stored in the computer which controls the XY-table. Then, medium was changed to HBSS containing 5 mM NaCN + 10 mM 2-deoxyglucose with a pH of 7.4 in one compartment, and a pH of 6.0 in the other compartment. Every 10 min, images were recorded at each side. Off-line, the ratio images of either fura-2, SBFI and BCECF were calculated, individual cardiomyocytes were analysed, and statistics were performed. Also, the propidium iodide images were evaluated this way. At each pH, between 43 and 116 individual cells from at least 4 different cultures were evaluated.

Sarcolemmal Na⁺/Ca²⁺ exchanger activity. The effect of pH_e on the activity of the sarcolemmal Na⁺/Ca²⁺ exchanger was studied by exposing the cardiomyocytes to Na⁺-free buffer with varying pH, in which Na⁺ ions had been replaced by choline on a molar basis. The lack of extracellular Na⁺ ions induces a reversed action of the Na⁺/Ca²⁺ exchanger, resulting in outward transport of Na⁺ ions combined with

inward transport of Ca^{2+} ions. This leads to an increase in $[\text{Ca}^{2+}]_i$, which is measured with fura-2.²⁶ The rate of rise and the amplitude of the rise in $[\text{Ca}^{2+}]_i$ reflect the activity of the $\text{Na}^+/\text{Ca}^{2+}$ exchanger activity. Cardiomyocytes in one compartment were exposed to Na^+ -free HBSS with pH 7.4 (control), whereas in the other compartment the cells were exposed to Na^+ -free HBSS with pH of either 6.0, 7.0, 7.4 or 8.0. Every 10 s, $[\text{Ca}^{2+}]_i$ was measured in each compartment. Off-line, ratio images were calculated and statistical procedures performed. The extent of inhibition or stimulation of $\text{Na}^+/\text{Ca}^{2+}$ exchanger activity by pH_e was expressed by calculating the activity of the $\text{Na}^+/\text{Ca}^{2+}$ exchanger in the treated cells (pH_e is 6.0, 7.0, 7.5 or 8.0) as a percentage of the activity of the $\text{Na}^+/\text{Ca}^{2+}$ exchanger in the cells which received reference treatment (pH_e 7.4).

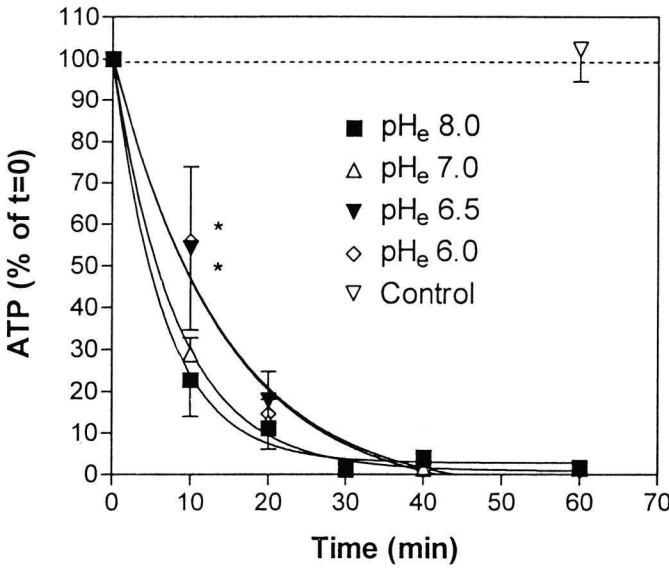


Figure 2. Cellular ATP content in cultured cardiomyocytes upon metabolic inhibition (5 mM NaCN + 10 mM 2-deoxyglucose) with an external pH (pH_e) ranging from 8.0 to 6.0. In control cultures not subjected to metabolic inhibition ATP content was measured at $t = 60$ min. Values are mean \pm SD, $n = 2-4$ cultures per group, * $P < 0.05$ vs. pH 7.0.

Statistics. Values are expressed as mean \pm standard deviation unless stated otherwise. Statistical analysis was performed with the use of ANOVA, followed by the Bonferroni t-test when appropriate. Results obtained with the two-compartment culture dish were analysed with the use of paired t-test. Differences were considered significant at $P < 0.05$.

Results

LDH release. The release of cellular LDH into the medium, which indicates the occurrence of cell death, is shown in figure 1 in cultures exposed to metabolic inhibition with various pH_e . At pH_e 7.4, half-maximal LDH release occurred 130 min after start of metabolic inhibition, with 75 % of LDH released after 240 min. At pH_e 8.0, LDH release was accelerated and reached higher levels. In contrast, reduction of pH_e below 7.4 resulted in a delayed LDH release which reached lower levels after 240 min. During metabolic inhibition at pH_e 6.0 and 5.5, hardly any LDH release was measured in 240 min.

ATP. The ATP concentration in cardiomyocytes at $t=0$ min was 110.7 ± 17.9 nmol/mg protein. This value was unaltered after 60 min of control incubation without metabolic inhibition (Fig. 2). However, during metabolic inhibition at pH_e 7.0, cellular ATP decreased exponentially (rate constant: $0.122 \pm 0.009 \text{ min}^{-1}$) (Fig. 3). In comparison, 10 min after start of metabolic inhibition at pH_e 6.5 and 6.0, ATP depletion was less severe than at pH_e 7.0 ($P < 0.05$), but at later time points no difference was observed with pH_e 7.0. At pH_e 8.0, ATP depletion during metabolic inhibition was not different from that at pH_e 7.0 at any time point.

$[Ca^{2+}]_i$ and cell death. We investigated the relation between pH_e , $[Ca^{2+}]_i$ and cell death during metabolic inhibition at varying pH_e using digital imaging fluorescence microscopy, fura-2, and propidium iodide. Fura-2 loaded cardiomyocytes were exposed to metabolic inhibition at either the reference value of pH_e 7.4, or at the value of 6.0, which had proven to be protective (see Fig.1). Upon metabolic inhibition at pH_e 7.4, $[Ca^{2+}]_i$ started to rise 20 min after start of metabolic inhibition from a control value of 86 ± 44 nM to a peak value of 2.5 ± 0.4 μM after 120 min ($n=47$ cells, Fig. 3A). Cell blebbing was present after 40 min, and increased in severity in time. In contrast, during metabolic inhibition at pH_e 6.0, $[Ca^{2+}]_i$ rose gradually to a peak value of 510 ± 215 nM after 170 min ($n=43$ cells). Cell blebbing was also present in these cells, but this process started later (60 min) and was less severe as compared to cells during metabolic inhibition at pH_e 7.4. Cell death at pH_e 7.4, as assessed by the influx of the DNA probe propidium iodide into irreversibly damaged cells, was half-maximal 100 min after start of metabolic inhibition, with only 10 % viable cell remaining after 175 min (Fig. 3B). However, during metabolic inhibition at pH_e 6.0, 86% of the cells were still viable after 210 min of metabolic inhibition.

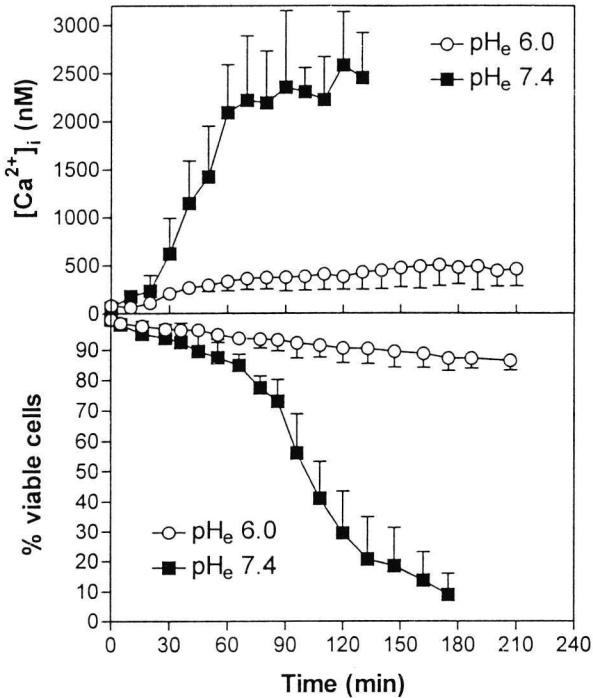


Figure 3. A. Intracellular Ca^{2+} ion concentration ($[Ca^{2+}]_i$) in cultured cardiomyocytes upon metabolic inhibition (5 mM NaCN + 10 mM 2-deoxyglucose) with external pH (pH_e) 7.4 (■) or pH_e 6.0 (○), measured with the fluorescent Ca^{2+} indicator fura-2. Values are mean \pm SD, $n = 47$ cells (pH_e 7.4) and 42 cells (pH_e 6.0). Differences between the groups are significant from 28 min onward.

B. Relative number of viable cardiomyocytes upon metabolic inhibition at an external pH (pH_e) 7.4 (■), or pH_e 6.0 (○), measured with the fluorescent DNA probe propidium iodide. Values are mean \pm SD from 4 cultures in each group. Differences between the groups are significant from 55 min onward.

pH_i . The intracellular pH (pH_i), as measured using BCECF, in control cardiomyocytes was 7.25 ± 0.06 . During metabolic inhibition at pH_e 7.4, pH_i decreased to 6.82 ± 0.16 after 25 min and remained constant ($n = 116$ cells) (Fig. 4). We observed that shortly before cell death, pH_i in the myocytes rose again slightly. During metabolic inhibition at pH_e 6.0, pH_i rapidly decreased to 6.58 ± 0.28 within 2.5 min, ($P < 0.001$), and further decreased more slowly to 6.34 ± 0.17 after 20 min ($n = 67$ cells). During the remainder of the experiment, pH_i stayed at this level.

$[Na^+]_i$. The intracellular Na^+ concentration ($[Na^+]_i$) in control cardiomyocytes, as measured using SBFI, was 9.10 ± 0.86 mM. Upon metabolic inhibition at pH_e 7.4, $[Na^+]_i$ increased steadily to 26.1 ± 4.1 mM after 120 min ($n = 64$ cells) (Fig. 5). Upon metabolic inhibition at pH_e 6.0, the rise in $[Na^+]_i$ was initially more rapid as compared to metabolic inhibition at pH_e 7.4, with a significantly higher $[Na^+]_i$ after 15 min of metabolic inhibition ($n = 59$ cells, $P < 0.001$). After 65 min, a maximal value of 27.3 ± 3.5 mM was reached. From 85 min after start of metabolic inhibition onward, the difference in $[Na^+]_i$ between the two pH-groups was no longer present (Fig. 5).

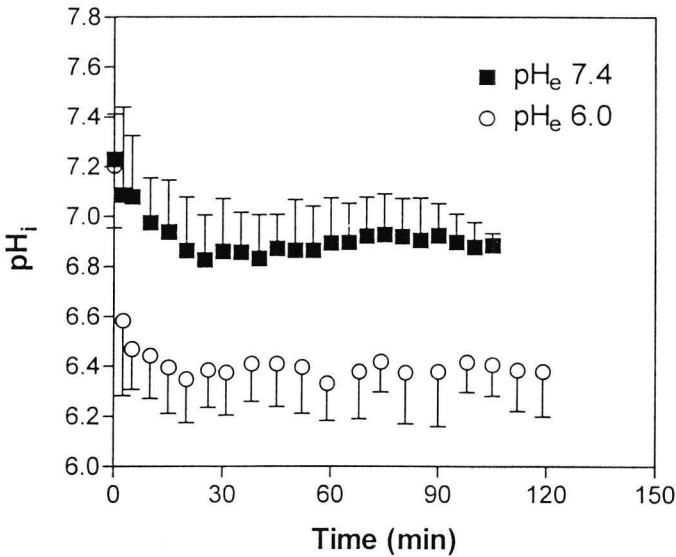


Figure 4. Intracellular pH (pH_i) in cultured cardiomyocytes upon metabolic inhibition (5 mM NaCN + 10 mM 2-deoxyglucose) with external pH (pH_e) 7.4 (■) or pH_e 6.0 (○), measured with the fluorescent pH indicator BCECF. Values are mean \pm SD, $n = 116$ cells (pH_e 7.4) and 67 cells (pH_e 6.0). Differences between the groups are significant from 2.5 min onward.

Effect pH_e on the sarcolemmal Na^+ / Ca^{2+} exchanger. As calcium overload during ischemia and energy depletion is considered to play a key role in the transition from reversible to irreversible cell injury, and calcium overload is considered to be the result of reversed action of the Na^+ / Ca^{2+} exchanger,⁷ we tested the influence of pH_e on the activity of the Na^+ / Ca^{2+} exchanger. Incubation of fura-2 loaded rat cardiomyocytes with Na^+ -free buffer at pH 7.4 resulted in an increase of $[Ca^{2+}]_i$ (Fig. 6 inset: pH 7.4), consistent with a reversal of the action of the Na^+ / Ca^{2+} exchanger.²⁶ When the pH of the Na^+ -free buffer was varied, it was found that at pH_e 7.0 and 6.0, the $[Ca^{2+}]_i$ rose slower and to lower peak values as compared to pH_e 7.4 (Fig. 6 inset: pH 6.0), indicating a decreased activity of the sarcolemmal Na^+ / Ca^{2+} exchanger at pH_e below 7.4. This effect was more pronounced at pH 6.0 than at pH 7.0 (Fig. 6). In contrast, elevation of the pH of the Na^+ -free buffer to pH 8.0 resulted in an accelerated increase in $[Ca^{2+}]_i$ as compared to pH 7.4, to a steady-state level above that at pH 7.4, indicating an increased activity of the Na^+ / Ca^{2+} exchanger (Fig. 6).

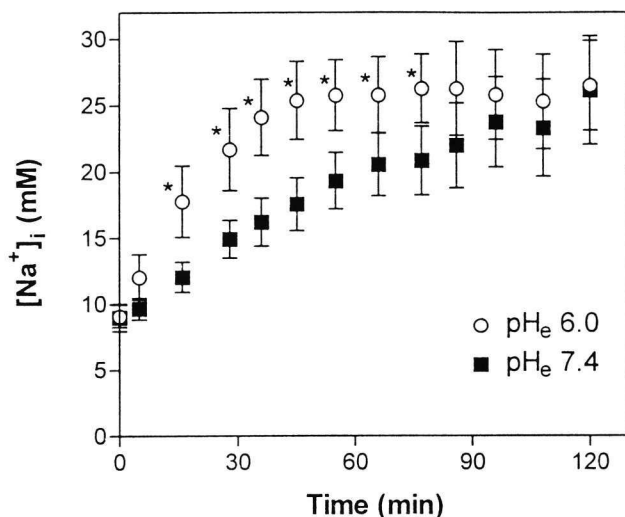


Figure 5. Intracellular Na^+ ion concentration ($[\text{Na}^+]_i$) in cultured cardiomyocytes upon metabolic inhibition (5 mM NaCN + 10 mM 2-deoxyglucose) with external pH (pH_e) 7.4 (■) or pH_e 6.0 (○), measured with the fluorescent Na^+ indicator SBFI. Values are mean \pm SD, $n = 64$ cells (pH_e 7.4) and 59 cells (pH_e 6.0). $[\text{Na}^+]_i$ during metabolic inhibition at pH_e 6.0 was higher than at pH_e 7.4 between $t = 15$ min and $t = 85$ min (* $P < 0.01$).

Discussion

In the present study we found that a low external pH (pH_e) limits cell injury in cultured neonatal cardiomyocytes during energy depletion due to exposure to 5 mM NaCN + 10 mM 2-deoxyglucose (metabolic inhibition). Cell death during metabolic inhibition at pH_e 7.4 was 75% after 240 min. A decrease in pH_e below pH_e 7.4 during metabolic inhibition resulted in an attenuated cell death, with hardly any LDH release at a pH_e of 6.0 and 5.5. In contrast, metabolic inhibition at pH_e 8.0 resulted in an accelerated LDH release.

The depletion of cellular ATP is a prominent feature of ischemia and metabolic inhibition, and is considered one of the pivotal events in cell death. As it has been reported that ATP depletion is attenuated by the presence of low pH_e ,⁴ we measured cellular ATP levels to determine whether the attenuation of cell death during metabolic inhibition at low pH_e was due to a less severe ATP depletion. We found that in the first 10 min of metabolic inhibition, a low pH_e value (6.0 and 6.5) was associated with a slower rate of ATP depletion. However, this sparing effect was only temporary, as no differences in cellular ATP could be measured from 20 min onwards.

In view of these results, it is unlikely that the salutary effect of low pH_e during metabolic inhibition is a result of the preservation of cellular ATP stores.

Using digital imaging fluorescence microscopy and fluorescent ion indicators, we studied the disturbances in cellular ion homeostasis which precede cell death. Intracellular Ca^{2+} ($[\text{Ca}^{2+}]_i$), Na^+ ($[\text{Na}^+]_i$) and H^+ (pH_i) concentrations were measured in cardiomyocytes exposed to metabolic inhibition at pH_e of 7.4, and were compared

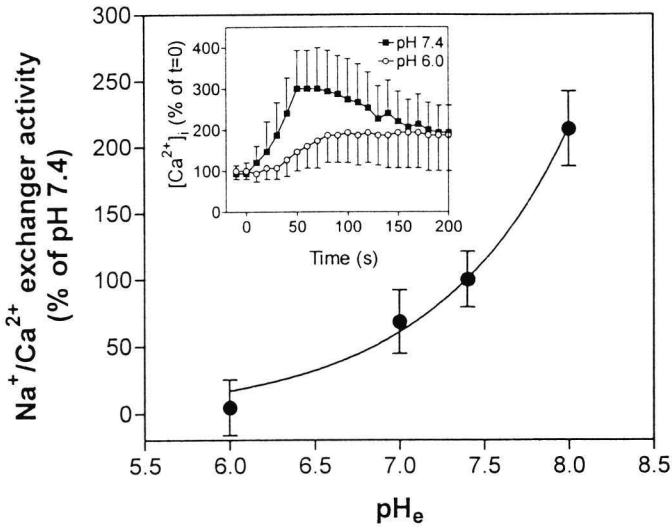


Figure 6. Sarcolemmal Na^+/Ca^{2+} exchanger activity in intact cultured cardiomyocytes at various external pH (pH_e). The activity of the Na^+/Ca^{2+} exchanger was assessed by the amplitude of the rise in the $[Ca^{2+}]_i$ upon Na^+ -free incubation. Values are mean \pm SD, $n = 3-6$ experiments at each pH_e . Inset shows $[Ca^{2+}]_i$ during Na^+ -free incubation, started at $t=0$, at pH_e 7.4 (\blacksquare) and pH_e 6.0 (\circ) in a representative experiment.

to those in cardiomyocytes exposed to metabolic inhibition at pH_e 6.0. This latter pH_e value was chosen as it protected cardiomyocytes completely during metabolic inhibition as measured by LDH release (Fig. 1). The development of Ca^{2+} overload is considered crucial to the development of cell death, as a massive increase in $[Ca^{2+}]_i$ may lead to activation of cellular degradative enzymes including proteases and phospholipases.^{8,9}

During metabolic inhibition at pH_e 7.4, $[Ca^{2+}]_i$ rose from its control value of 86 nM to a peak value of 2.5 μ M after 120 min. This finding is in agreement with earlier reports.^{27,28} In contrast, metabolic inhibition at pH_e 6.0 resulted in only a modest and slow rise to 510 nM after 170 min. The development of Ca^{2+} overload during ischemia, anoxia and metabolic inhibition is thought to result from the combined action of the sarcolemmal Na^+/H^+ exchanger and Na^+/Ca^{2+} exchanger. It has been proposed that the drop in pH_i during ischemia leads to cellular Na^+ loading via Na^+/H^+ exchange, which in turn elicits the reversed action of the Na^+/Ca^{2+} exchanger, resulting in Na^+ extrusion combined with cellular Ca^{2+} loading.⁷ In this hypothesis, the attenuated rise in $[Ca^{2+}]_i$ during metabolic inhibition at pH_e 6.0 observed by us might be explained by a decreased Na^+ overload, as the reduced pH_e may have reduced the transsarcolemmal H^+ gradient, thereby preventing cellular Na^+ uptake via Na^+/H^+ exchange activity.

Upon exposure to metabolic inhibition at pH_e 7.4, the pH_i decreased rapidly from the control value of 7.25 ± 0.06 to 6.82 ± 0.16 . If the pH_e during metabolic inhibition was reduced to 6.0, pH_i decreased to 6.34 ± 0.17 . These results indicate that during metabolic inhibition at pH_e 7.4, a transsarcolemmal H^+ gradient exists of 0.58 pH

unit, with $\text{pH}_i < \text{pH}_e$. In contrast, during metabolic inhibition at pH_e 6.0, the transsarcolemmal H^+ gradient (ΔpH 0.34 pH unit) is reversed, with $\text{pH}_i > \text{pH}_e$. This reversal of transsarcolemmal H^+ gradient was also observed in anoxic cardiomyocytes by Koop and Piper⁴ who reported that at pH_e 7.04, pH_i and pH_e were identical while at higher pH_e , pH_i was more acid and at lower pH_e , pH_i was more alkaline. Also in hepatocytes the transsarcolemmal H^+ gradient was reversed upon metabolic inhibition at low pH_e .²⁹ This situation is likely to attenuate cellular Na^+ loading via Na^+/H^+ exchange and, consequently, to limit Ca^{2+} loading.

We found that under control conditions, $[\text{Na}^+]_i$ in rat cardiomyocytes was 9.10 ± 0.86 mM. Although widely varying values for $[\text{Na}^+]_i$ in rats have been measured, with upper values as high as 16.8 mM,³⁰ the $[\text{Na}^+]_i$ found by us falls within the range of 6.4–10.9, usually reported.^{15,23,31} Upon metabolic inhibition at pH_e 7.4, $[\text{Na}^+]_i$ increased steadily to 26.1 ± 4.1 mM after 120 min (Fig. 5). However, upon metabolic inhibition at pH_e 6.0, $[\text{Na}^+]_i$ increased more rapidly, to a similar value of 27.3 ± 3.5 mM, which was reached after 65 min. This result was unexpected, as the transsarcolemmal H^+ gradient during metabolic inhibition at pH_e 6.0 is expected to result in a *diminished* Na^+ loading via Na^+/H^+ exchange, rather than in an *accelerated* Na^+ loading. A similar result was reported by Turvey and Allen, who found that lowering pH_e from 7.4 to 6.4 in isolated rat heart during exposure to lactate resulted in an increase in $[\text{Na}^+]_i$, as measured using SBF1.¹⁵ The possibility of an artifactually low $[\text{Na}^+]_i$ due to the effect of low pH on SBF1 was ruled out by these authors. In addition, other researchers have reported that at low pH, $[\text{Na}^+]_i$ measured with SBF1 may be underestimated, rather than overestimated.³²

A possible explanation for the more rapid development of Na^+ overload during metabolic inhibition at pH_e 6.0 as compared to pH_e 7.4 could be a more rapid and a more complete inhibition of the sarcolemmal Na^+/K^+ -ATPase during the first period of metabolic inhibition, due to the faster and more extensive decline of pH_i (Fig.4).³³ This would increase the retention of intracellular Na^+ , thereby increasing $[\text{Na}^+]_i$. This hypothesis is corroborated by the finding by Katoh *et al.*,³¹ that inhibition of the sarcolemmal Na^+/K^+ -ATPase by K^+ -free perfusion during metabolic inhibition resulted in an accelerated rise in $[\text{Na}^+]_i$ as compared to metabolic inhibition alone.

Another potential mechanism leading to the higher rise in $[\text{Na}^+]_i$ during metabolic inhibition at pH_e 6.0 could be an increased Na^+ influx via the Na^+/H^+ exchanger. Kaila and Vaughan-Jones found in sheep Purkinje fibres that, although the activity of the sarcolemmal Na^+/H^+ exchanger was decreased five-fold after lowering of pH_e from 7.4 to 6.4,³⁴ the Na^+/H^+ exchanger activity was *increased* 5–10 fold by lowering of pH_i from 7.15 to 6.68,³⁵ giving the possibility that the combined effect of lowering pH_e as well as pH_i (as is the case in this study) could yield a net increased

Na^+/H^+ exchanger activity, which might be responsible for the accelerated rise in $[Na^+]_i$.

The contribution of Na^+ influx through ion channels to the development of Na^+ overload during metabolic inhibition at various pH_e remains unclear. In rat cardiomyocytes, various Na^+ -channel blocking agents including R56865, lidocaine and tetrodotoxin inhibited the rise in $[Na^+]_i$ during hypoxia.¹⁴ In contrast, patch-clamp experiments revealed that Na^+ influx via voltage-sensitive Na^+ channels was not responsible for the increase in $[Na^+]_i$ during metabolic inhibition in guinea-pig myocytes.³⁶

When $[Ca^{2+}]_i$ was measured during metabolic inhibition using fura-2, we found that the calcium overload was substantially less severe during metabolic inhibition at pH_e 6.0 as compared to metabolic inhibition at pH_e 7.4. As this attenuation of Ca^{2+} overload took place in the presence of an increased $[Na^+]_i$, it is plausible that the lower $[Ca^{2+}]_i$ was the result of a decreased activity of the sarcolemmal Na^+/Ca^{2+} exchanger. We therefore tested the effect of pH_e on the activity of the Na^+/Ca^{2+} exchanger in the intact cardiomyocytes by incubation of fura-2 loaded cells with Na^+ -free medium. This condition induces the reversed action of the Na^+/Ca^{2+} exchanger, leading to a rapid rise in $[Ca^{2+}]_i$.²⁶ The amplitude and rate of the rise of $[Ca^{2+}]_i$ are in proportion with Na^+/Ca^{2+} exchanger activity. If the cardiomyocytes were exposed to Na^+ -free medium at pH_e 7.0, sarcolemmal Na^+/Ca^{2+} exchanger activity was 68 % of the activity measured at pH_e 7.4 (Fig. 6). At pH_e 6.0, Na^+/Ca^{2+} exchanger activity was reduced to only 5%. In contrast, at pH_e 8.0 the activity of the exchanger was increased to 213%. Our findings in intact rat cardiomyocytes correspond well with the results reported by Philipson *et al.*³⁷ and by Khananshvilii and Weil-Maslansky³⁸ who studied the pH-dependence of Na^+/Ca^{2+} exchanger activity in isolated sarcolemmal membrane vesicles prepared from canine heart and bovine heart, respectively.

Although it is likely that during metabolic inhibition part of the protective effect of low pH_e is mediated by an attenuated Ca^{2+} overload, it is also conceivable that low pH_e acts via other mechanisms. For example, the intracellular acidosis that results from low pH_e may prevent mechanical sarcolemmal damage due to contracture by desensitisation of the myofibrillar system.³⁹ Also, the action of degradative non-lysosomal enzymes involved in the process of cell injury may be reduced as a result of intracellular acidosis.²⁹ The beneficial effect of extracellular acidosis during reperfusion remains to be further investigated. However, Harada *et al.* reports that acidosis during reperfusion attenuates the development of Ca^{2+} overload, and improves post-ischemic mechanical function in adult dog heart.⁴⁰ Also Kitakaze *et al.* found that acidic reperfusion prevents stunning in the perfused adult ferret hearts.⁴¹

In summary, a low pH_e during metabolic inhibition protects cardiomyocytes from cell death, as assessed by LDH release and propidium iodide fluorescence. As compared to pH_e 7.4, metabolic inhibition at pH_e 6.0 leads to a further acidification of the myocytes, an accelerated development of Na^+ overload, and an attenuated development of Ca^{2+} overload. In addition, low pH_e reduces the activity of the sarcolemmal Na^+/Ca^{2+} exchanger upon Na^+ -free incubation.

We therefore conclude that low external pH during metabolic inhibition protects cultured neonatal rat cardiomyocytes during metabolic inhibition by reducing Ca^{2+} overload. This reduction of Ca^{2+} overload is most likely not due to decreased Na^+/H^+ exchange activity, but to inhibition of the sarcolemmal Na^+/Ca^{2+} exchanger.

Acknowledgement. This study was supported by a grant from the Netherlands Heart Foundation no. 90.089.

References

1. Zager RA, Schimpf BA, Gmur DJ. Physiological pH - Effects on posthypoxic proximal tubular injury. *Circ Res.* 1993;72: 837-846.
2. Gasbarrini A, Caraceni P, Farghali H, Van Thiel DH, Borle AB. Effects of high and low pH on Ca-I(2+) and on cell injury evoked by anoxia in perfused rat hepatocytes. *Biochim. Biophys. Acta.* 1994;1220:277-285.
3. Bond JM, Herman B, Lemasters JJ. Protection by acidotic pH against anoxia/reoxygenation injury to rat neonatal cardiac myocytes. *Biochem. Biophys. Res. Comm.* 1991;179:798-803.
4. Koop A, Piper HM. Protection of energy status in hypoxic cardiomyocytes by mild acidosis. *J Mol Cell Cardiol.* 1992;24: 55-65.
5. Bond J M, Chacon E, Herman B, Lemasters JJ. Intracellular pH and Ca^{2+} homeostasis in the pH paradox of reperfusion injury to neonatal rat cardiac myocytes. *Am J Physiol.* 1993;265:C129-C137.
6. Dennis SC, Gevers W, Opie LH. Protons in ischemia: where do they come from; where do they go? *J Mol Cell Cardiol.* 1991;23:1077-1086.
7. Silverman HS, Stern MD. Ionic basis of ischaemic cardiac injury: Insights from cellular studies. *Cardiovasc Res.* 1994;28: 581-597.
8. Steenbergen C, Fralix TA, Murphy E. Role of increased cytosolic free calcium concentration in myocardial ischemic injury. *Basic Res Cardiol.* 1993;88: 456-470.
9. Toyo-oka T, Ross JR. Ca^{2+} sensitivity change and troponin loss in cardiac natural actomyosin after coronary occlusion. *Am J Physiol.* 1981;240: H704-H708.
10. Harrison SM, Frampton JE, McCall E, Boyett MR, Orchard CH. Contraction and intracellular Ca^{2+} , Na^+ , and H^+ during acidosis in rat ventricular myocytes. *Am J Physiol.* 1992;262: C348-C357.
11. Kim D, Cragoe EJ, Smith TW. Relations among sodium pump inhibition, Na-Ca and Na-H exchange activities and Ca-H interaction in cultured chick heart cells. *Circ Res.* 1987;60: 185-193.

12. Harper IS, Bond JM, Chacon E, Reece JM, Herman B, Lemasters JJ. Inhibition of Na^+/H^+ exchange preserves viability, restores mechanical function, and prevents the pH paradox in reperfusion injury to rat neonatal myocytes. *Basic Res Cardiol.* 1993;88: 430-442.
13. Sack S, Mohri M, Schwarz ER, Arras M, Schaper J, Ballagipordany G, Scholz W, Lang HJ, Scholkens BA, Schaper W. Effects of a new Na^+/H^+ antiporter inhibitor on postischemic reperfusion in pig heart. *J Cardiovasc Pharmacol.* 1994;23: 72-78.
14. Haigney MCP, Lakatta EG, Stern MD, Silverman HS. Sodium channel blockade reduces hypoxic sodium loading and sodium-dependent calcium loading. *Circulation.* 1994;90:391-399.
15. Turvey SE, Allen DG. Changes in myoplasmic sodium concentration during exposure to lactate in perfused rat heart. *Cardiovasc Res.* 1994;28: 987-993.
16. Atsma DE, Bastiaanse EML, Ince C, Van der Laarse A. A novel two-compartment culture dish allows microscopic evaluation of two different treatments in one cell culture simultaneously - Influence of external pH on Na^+/Ca^{2+} exchanger activity in cultured rat cardiomyocytes. *Pflügers Arch.* 1994;428: 296-299.
17. Van der Laarse A, Hollaar L, Van der Valk EJM. Release of alpha-hydroxybutyrate dehydrogenase from neonatal rat heart cell cultures exposed to anoxia and reoxygenation: Comparison with impairment of structure and function of damaged cardiac cells. *Cardiovasc Res.* 1979;13: 345-353.
18. Blondel B, Royen J, Cheneval JP. Heart cells in culture: a simple method for increasing the proportion of myoblasts. *Experimenta.* 1971;27: 356-358.
19. Lowry OH, Rosebrough NJ, Farr AL, Randall RJ. Protein measurement with the Folin phenol reagent. *J Biol Chem.* 1951;193: 265-275.
20. Gryniewicz G, Poenie M, Tsien RY. A new generation of Ca^{2+} indicators with greatly improved fluorescence properties. *J. Biol. Chem.* 1985;260:3440-3450.
21. Ince C, Ypey DL, Diesellhoff-Den Dulk MMC, Visser JAM, De Vos A, Van Furth R. Micro- CO_2 -Incubator for use on a microscope. *J Immun Meth.* 1983;60: 269-275.
22. Atsma DE, Bastiaanse EML, Jerzewski A, Van der Valk EJM, Van der Laarse A. Role of calcium-activated neutral protease (calpain) in cell death in cultured neonatal rat cardiomyocytes during metabolic inhibition. *Circ. Res.* 1995;76:1071-1078.
23. Donoso P, Mills JG, O'Neill SC, Eisner DA. Fluorescence measurements of cytoplasmic and mitochondrial sodium concentration in rat ventricular myocytes. *J. Physiol. (Lond).* 1992;488:493-509.
24. Chapman RA, Fozzard HA, Friedlander IR. Effects of Ca/Mg removal on $aiNa$, aiK and tension in cardiac Purkinje fibres. *Am. J. Physiol.* 1986;251:C920-C927.
25. Levi AJ, Lee CO, Brooksby P. Properties of the fluorescent sodium indicator SBFI in rat and rabbit cardiac myocytes. *J Cardiovasc Electrophysiol.* 1994;5: 241-257.
26. Ziegelstein RC, Zweier JL, Mellits ED, Younes A, Lakatta EG, Stern MD, Silverman HS. Dimethylthiourea, an oxygen radical scavenger protects isolated cardiac myocytes from hypoxic injury by inhibition of $Na^+ -Ca^{2+}$ exchange and not by its antioxidant effects. *Circ Res.* 1992;70: 804-811.
27. Chacon E, Reece JM, Nieminen AL, Zahrebelski G, Herman B, Lemasters JJ. Distribution of electrical potential, pH, free $Ca(2)^+$, and volume inside cultured adult rabbit cardiac myocytes during chemical hypoxia - A multiparameter digitized confocal microscopic study. *Biophys J.* 1994;66:942-952.
28. Li Q, Altschuld RA, Stokes BT. Myocyte deenergization and intracellular free calcium dynamics. *Am J Physiol.* 1988;255: C162-C168.

29. Gores GJ, Nieminen A-L, Wray BE, Herman B, Lemasters JJ. Intracellular pH during 'chemical hypoxia' in cultured rat hepatocytes. *J. Clin. Invest.* 1989;83:386-396.
30. Haworth RA., Goknur AB, Hunter DR, Hegge JO, Berkhoff HA. Inhibition of calcium influx in isolated rat heart cells by ATP depletion. *Circ Res.* 1987;60: 586-594.
31. Katoh H, Satoh H, Nakamura T, Terada H, Hayashi H. The role of Na^+/H^+ exchange and the Na^+/K^+ pump in the regulation of $[\text{Na}^+]_i$ during metabolic inhibition in guinea pig myocytes. *Biochem Biophys Res Comm.* 1994;203: 93-98.
32. Negulescu PA, Machen TE. Intracellular ion activities and membrane transport in parietal cells measured with fluorescent dyes. *Method Enzymol.* 1990;192: 38-81.
33. Sperlakis N, Lee EC. Characterization of $(\text{Na}^+, \text{K}^+)\text{-ATPase}$ isolated from embryonic chick hearts and cultured chick heart cells. *Biochim Biophys Acta.* 1971;233: 562-579.
34. Vaughan-Jones RD, Mei-Lin W. Extracellular H^+ inactivation of the Na^+/H^+ exchange in the sheep cardiac Purkinje fibre. *J Physiol (Lond).* 1990;428: 441-466.
35. Kaila K, Vaughan-Jones RD. Influence of sodium-hydrogen exchange on intracellular pH, sodium and tension in sheep cardiac Purkinje fibres. *J Physiol (Lond).* 1987;390: 93-118.
36. Mejia-Alvarez R, Marban E. Mechanism of the increase in intracellular sodium during metabolic inhibition - Direct evidence against mediation by voltage-dependent sodium channels. *J Mol Cell Cardiol.* 1992;24: 1307-1320.
37. Philipson KD, Bersohn MM, Nishimoto AY. Effects of pH on $\text{Na}^+/\text{Ca}^{2+}$ exchange in canine cardiac sarcolemmal vesicles. *Circ Res.* 1982;50: 287-293.
38. Khananshvil D, Weil-Maslansky E. The cardiac $\text{Na}^+/\text{Ca}^{2+}$ Exchanger - Relative rates of calcium and sodium movements and their modulation by protonation-deprotonation of the carrier. *Biochemistry.* 1994;33: 312-319.
39. Fabiato A, Fabiato F. Effects of pH on the myofilaments and the sarcoplasmic reticulum of skinned cells from cardiac and skeletal muscles. *J. Physiol. (Lond).* 1978;276:1015-1032.
40. Harada K, Franklin A , Johnson RG, Grossman W, Morgan JP. Acidemia and hypernatremia enhance postischemic recovery of excitation-contraction coupling. *Circ Res.* 1994;74:1197-1209.
41. Kitakaze M, Weisfeldt ML, Marban E. Acidosis during early reperfusion prevents myocardial stunning in perfused ferret hearts. *J Clin Invest.* 1988;82: 920-927.

Chapter 8

Summary and general discussion

Summary and general discussion

The ultimate mechanism responsible for the development of cell death during ischemia, anoxia and metabolic inhibition is still unknown. A variety of hypotheses has been proposed, and the research described in this thesis has investigated the involvement of 1) calcium overload, 2) increased calcium activated neutral protease (CANP) activity and 3) phospholipid degradation in the process of cell death. The pathophysiological background of these three phenomena is presented in Chapter 1. Chapter 2 describes the theoretical and practical considerations involved in the set-up and use of a digital imaging fluorescence microscopy system designed to measure intracellular concentrations of ions such as Ca^{2+} , Na^+ , and H^+ using fluorescent probes.

In our experiments, we used cultures of neonatal rat cardiomyocytes as a model. The advantages of the use of cultured neonatal rat cardiomyocytes include: 1) over 15 years of experience with these cell cultures in biochemical studies, 2) the model is convenient to study intracellular processes using fluorescent probes and digital imaging fluorescence microscopy, and 3) the opportunity to derive many results from one batch of cell cultures, seeded in, for example, 24-well plates. The problem of natural variability that might exist between different individual cultures was circumvented by the development of a new type of culture dish containing two separate compartments (Chapter 3). Using this dish, two halves of a single cell culture grown on a standard coverslip can be exposed to different treatments simultaneously, allowing the effect of one treatment in one compartment to be compared with that of the other treatment in the other compartment in the same culture. In addition, by simultaneously conducting two experiments per dish, the number of experiments needed can be decreased. This reduces the time to complete a series of experiments, and allows the optimal use of specimens which are difficult to obtain, such as human material.

Anoxia was simulated by exposure of the cardiomyocytes to NaCN and 2-deoxyglucose, in order to inhibit ATP production by mitochondrial oxidative phosphorylation and glycolysis, respectively. This treatment, known as 'chemical anoxia' or 'metabolic inhibition' results in a rapid energy depletion and, eventually, cell death (Chapters 5, 6 and 7).

After the onset of chemical anoxia, cardiomyocytes start accumulating Na^+ and Ca^{2+} ions, later followed by cell death (Chapter 7). To investigate whether the increase in intracellular Ca^{2+} ion concentration during energy depletion (referred to as calcium overload) is a causal factor in the development of cell death, we studied the role of the sarcolemmal $\text{Na}^+/\text{Ca}^{2+}$ exchanger in the development of calcium overload. The

$\text{Na}^+/\text{Ca}^{2+}$ exchanger normally extrudes 3 Na^+ ions from the myocyte while transporting 1 Ca^{2+} -ion into the cell. Upon chemical anoxia, the development of a high intracellular Na^+ concentration induces the exchanger to reverse its mode of action, leading to Ca^{2+} influx in exchange for Na^+ efflux. This mechanism is considered to be responsible for the development of calcium overload in the anoxic cardiomyocyte. Earlier it was established that several compounds (simvastatin, dimethylthiourea) have an inhibitory action on the $\text{Na}^+/\text{Ca}^{2+}$ exchanger activity. We used Ni^{2+} ions, well-known to inhibit the $\text{Na}^+/\text{Ca}^{2+}$ exchanger and indeed found a dose-dependent reduction of calcium overload, associated with a dose-dependent attenuation of cell death (Chapter 5). Furthermore, a lowered external pH also inhibited the sarcolemmal $\text{Na}^+/\text{Ca}^{2+}$ exchanger, with an attenuation of both calcium overload and cell death in cardiomyocytes during anoxia (Chapters 3 and 7). The finding that interventions of a widely different nature attenuate calcium overload as well as cell death via inhibition of the sarcolemmal $\text{Na}^+/\text{Ca}^{2+}$ exchanger, strongly implies that the development of calcium overload via reversed action of the sarcolemmal $\text{Na}^+/\text{Ca}^{2+}$ exchanger is a causal factor in cell death in energy-depleted cardiomyocytes.

We studied whether phospholipases and proteases are determinants in the development of cell death of cardiomyocytes during chemical anoxia.

Phospholipase A_2 (PLA_2) is thought to be involved in cell death, as it was found earlier that arachidonic acid, a fatty acid almost exclusively located at the sn-2 position in phospholipids, is present in increased concentrations in ischemic myocardium. Using two PLA_2 inhibitors, chlorpromazine (CPZ) and trifluoperazine (TFP), cell death of anoxic myocytes was attenuated, associated with less calcium overload. Although CPZ and TFP inhibited PLA_2 activity *in vitro* and limited phospholipid degradation *in situ*, the salutary effects of the two compounds on anoxic cardiomyocytes could not be ascribed solely to their inhibitory effect on phospholipid degradation. It was found that CPZ and TFP are potent inhibitors of the $\text{Na}^+/\text{Ca}^{2+}$ exchanger as well, which action is likely to be responsible for the observed limitation of calcium overload. The finding of a dual salutary action of CPZ and TFP during chemical anoxia, i.e. attenuation of calcium overload and inhibition of phospholipid degradation, makes it difficult to establish the definite role of phospholipid degradation in the development of cell death. It was found that phospholipid degradation was a predicting factor for ensuing cell death. Also, TFP and CPZ did not alter the relation between phospholipid degradation and ensuing cell death. These findings are in favor of a role of phospholipid degradation in anoxic cell death. However, using a specific inhibitor of plasmalogen-specific PLA_2 activity, halo-enol lactone suicide substrate (HELSS), it was found that this compound prevented phospholipid degradation in anoxic cardiomyocytes almost

completely, with no or only a moderate reduction of cell death (Chapter 6). So it appears that phospholipid degradation is not the single decisive factor responsible for anoxic cell death.

Taken together, these findings indicate that 1) the liberation of arachidonic acid from cardiomyocytes during metabolic inhibition is almost exclusively due to plasmalogen-specific PLA₂ activity, 2) CPZ and TFP thus have an inhibitory effect on plasmalogen-specific PLA₂ activity as well, in addition to an inhibitory action on diacyl-specific PLA₂ activity, 3) cell death can occur despite an almost complete inhibition of anoxic phospholipid degradation, arguing against a causal role of phospholipid degradation in cell death, and 4) HELSS has (an) other activit(y)ies in addition to inhibition of plasmalogen-specific PLA₂ activity, which account(s) for its temporary and modest protective effect on cell death during metabolic inhibition.

As to cellular proteases, the involvement of calcium activated neutral protease (CANP) constitutes an attractive hypothesis, as the proteolytic action of CANP is Ca²⁺-dependent, and among its purported substrates are several key cytoskeletal proteins. Thus, massive supraphysiological activation CANP would link calcium overload to the subsequent degradation of the sarcolemma, leading to cell death.

Using a fluorogenic substrate, we found that CANP activity in the cardiomyocytes was increased during chemical anoxia (Chapter 4). Two inhibitors of CANP, leupeptin and calpain I inhibitor, inhibited CANP activity in intact cells, during control incubation as well as during chemical anoxia. However, despite their substantial inhibition of intracellular CANP activity, these inhibitors did not attenuate cell death during chemical anoxia. We therefore conclude that increased CANP activity does not play a major role in the development of cell death in anoxic cardiomyocytes.

A potential explanation for the observed relation between the magnitude of calcium overload and the ensuing cell death, could lie in the phenomenon of lateral-phase separation of the sarcolemmal membrane. This theory implies an increased tendency of the sarcolemma of energy-depleted cells to transform into a non-bilayer configuration, as a result of loss of membrane asymmetry. This membrane reconfiguration, which is associated with aggregation and loss of function of membranous proteins, is promoted by elevated Ca²⁺ ion concentrations. This implies that attenuation of calcium overload limits anoxic cell death by decreasing the extent of physical membrane perturbations. However, it is conceivable that the processes of Ca²⁺-induced lateral-phase transition and biochemical phospholipid degradation occur in concert, and may even enhance each other.

Future directions

In order to test the lateral phase transition hypothesis, future research should be aimed at investigating the perturbations that occur at the level of the cellular membranes during ischemia, anoxia and metabolic inhibition.

Ideally, this should be investigated in single individual myocytes with the use of optical methods (fluorescence, phosphorescence, life-time imaging, fluidity imaging), to study the integrity and distribution of phospholipids over inner and outer leaflets of the sarcolemmal in order to define the relation between intracellular Ca^{2+} concentration, phospholipid asymmetry and lateral phase transition.

Although we found that CANP was not involved in anoxic cell death, CANP has also been implicated in the development of myocardial stunning. Further research should be aimed to measure CANP activity in stunned myocardium, and to assess the effects of its inhibition on post-ischemic function.

It is conceivable that calcium overload may lead to derangements in the nucleus, such as the activation of nuclear endonucleases, which event may lead to DNA strand breaks. In addition, the elevated intracellular Ca^{2+} ion concentration may be interpreted erroneously by the nucleus as a transduced signal, and may result in the expression of genes that may have adverse effects (*c-fos*, *c-jun*, suicide genes). Additional research in this area should be aimed at elucidating the nuclear response to calcium overload.

The role of PLA_2 in the development of ischemic cell death remains unclear. Its contribution to anoxic cell damage may only be demonstrated using highly specific inhibitors, such as monoclonal antibodies. Also, transgenic animals with a variable expression of PLA_2 may aid to delineate the contribution of PLA_2 in ischemic cell death.

The research in which we found that attenuation of calcium overload in cultured cardiomyocytes during energy depletion limits cell death should be expanded to more complicated models. The effect of inhibitors of the sarcolemmal $\text{Na}^+/\text{Ca}^{2+}$ exchanger on myocardial cell death, hemodynamic function and arrhythmogenesis should be investigated.

Chapter 9

Samenvatting en algemene discussie

Samenvatting en algemene discussie

Het mechanisme dat verantwoordelijk is voor het ontstaan van celdood in de hartspier gedurende ischemie, anoxie en metabole inhibitie is nog steeds niet bekend. Een aantal hypothesen zijn geponeerd en het onderzoek dat wordt beschreven in dit proefschrift onderzoekt de betrokkenheid van 1) calcium overload, 2) verhoogde activiteit van het enzym 'calcium-activated neutral protease' (CANP) en 3) fosfolipiden afbraak bij het ontstaan van celdood.

De pathofysiologische achtergronden van deze drie verschijnselen worden besproken in hoofdstuk 1. Hoofdstuk 2 bespreekt de theoretische en praktische overwegingen bij het samenstellen en gebruiken van een digitaal beeldvormend fluorescentie microscoop systeem, dat gebruikt kan worden om intracellulaire concentraties van ionen, zoals Ca^{2+} , Na^+ , en H^+ ionen, te meten.

Voor de experimenten die in dit proefschrift zijn beschreven werd gebruikt gemaakt van gekweekte neonatale rattehart cellen. Dit model heeft een aantal voordelen: 1) er is meer dan 15 jaar ervaring met deze celkweken in biochemisch onderzoek, 2) het is een geschikt model om intracellulaire processen te bestuderen met behulp van fluorescerende probes en digitale beeldvormende fluorescentie microscopie en 3) het is mogelijk om uit één batch cellen veel gegevens te verkrijgen, na uitzaaien van de cellen in bijvoorbeeld 24-wells platen. Het probleem van de natuurlijke variabiliteit die kan bestaan tussen de verschillende celkweken werd omzeild door een nieuw weefselbakje te ontwerpen, waarin twee verschillende compartimenten aanwezig zijn (Hoofdstuk 3). De natuurlijke variabiliteit maakt het moeilijk om uit te maken of verschillen in respons tussen verschillende celkweken het gevolg zijn van een bepaalde behandeling van een celkweek door de onderzoeker, of simpelweg een uiting zijn van de natuurlijk optredende biologische variabiliteit. Met het nieuwe bakje kunnen de twee helften van een celkweek gelijktijdig worden blootgesteld aan verschillende behandelingen, zodat het effect van een behandeling direct vergeleken kan worden met het effect van een andere behandeling in dezelfde celkweek. Tevens wordt het totaal aantal benodigde experimenten verminderd, omdat nu twee experimenten gelijktijdig worden uitgevoerd. Dit levert een besparing in de benodigde tijd en het aantal proefdieren voor een experiment op en staat daarnaast het optimale gebruik toe van moeilijk verkrijgbaar cel materiaal, bijvoorbeeld cellen van menselijke oorsprong.

Anoxie werd nagebootst door blootstelling van de cardiomyocyten aan NaCN and 2-deoxyglucose, met als doel de productie van ATP via respectievelijk mitochondriale oxidatieve fosforylering en glycolyse te verhinderen. Deze behandeling, bekend als

'metabole inhibitie' of 'chemische anoxie', resulteerde in een snelle uitputting van cellulaire energie, en uiteindelijk, celdood (Hoofdstuk 5,6 en 7)

Na blootstelling aan chemische anoxie, accumuleerden de cardiomyocyten Na^+ en Ca^{2+} ionen, enige tijd later gevolgd door afsterven van de cellen (Hoofdstuk 7).

We onderzochten of de stijging van de intracellulair Ca^{2+} ion concentratie gedurende chemische anoxie een oorzakelijke factor is in het ontstaan van hartceldood, en bestudeerden hiervoor de rol van de $\text{Na}^+/\text{Ca}^{2+}$ uitwisselaar in het sarcolemma bij het ontstaan van calcium overload. In de normale situatie transporteert de $\text{Na}^+/\text{Ca}^{2+}$ uitwisselaar drie Na^+ ionen van binnen naar buiten de cel en neemt gelijktijdig één Ca^{2+} ion in de cel op. Gedurende chemische anoxie veroorzaakt de stijging van de intracellulaire Na^+ concentratie een omkering van de werkingsrichting van de $\text{Na}^+/\text{Ca}^{2+}$ uitwisselaar, zodat nu Na^+ efflux gekoppeld is aan Ca^{2+} influx. Dit mechanisme wordt geacht verantwoordelijk te zijn voor het ontstaan van calcium overload gedurende energie uitputting van de hartcel. Het was reeds eerder vastgesteld dat een aantal farmacologische stoffen (simvastatine, dimethylthiourem) de $\text{Na}^+/\text{Ca}^{2+}$ uitwisselaar remmen. Wij gebruikten Ni^{2+} ionen, een bekende $\text{Na}^+/\text{Ca}^{2+}$ uitwisselaar remmende stof, en vonden inderdaad een dosisafhankelijke vermindering van de calcium overload tijdens chemische anoxie, in combinatie met een dosisafhankelijke vermindering van hartceldood (Hoofdstuk 5).

Tevens vonden wij dat een verlaging van de extracellulaire pH tijdens chemische anoxie zowel de activiteit van de $\text{Na}^+/\text{Ca}^{2+}$ uitwisselaar in het sarcolemma remde, alsook de celdood verminderde (Hoofdstuk 3 en 7).

De observatie dat interventies van verschillende aard de $\text{Na}^+/\text{Ca}^{2+}$ uitwisselaar in het sarcolemma remmen met als resultaat een vermindering van calcium overload en celdood, suggereert sterk dat het ontstaan van calcium overload via een omgekeerde werking van de $\text{Na}^+/\text{Ca}^{2+}$ exchanger een oorzakelijke factor is in het ontstaan van celdood in energie-gedepleteerde cellen.

We onderzochten of fosfolipases en proteases betrokken zijn bij het ontstaan van hartceldood tijdens chemische anoxie. Van fosfolipase A_2 wordt vermoed dat het betrokken is bij hartceldood omdat bij eerder onderzoek het vetzuur arachidonzuur, dat nagenoeg exclusief gebonden is aan de sn-2 positie in fosfolipiden, in verhoogde concentraties werd aangetroffen in ischemisch hartspierweefsel. Na toediening van remmers van fosfolipase A_2 , chlorpromazine (CPZ) of trifluoperazine (TFP), aan anoxische cardiomyocyten was celdood verminderd, evenals de calcium overload (Hoofdstuk 5). Hoewel CPZ en TFP de activiteit van fosfolipase A_2 *in vitro* remden en de afbraak van fosfolipiden in de celkweken verminderden, kon de gunstige werking van de twee remmers niet alleen aan hun remmende effect op fosfolipiden afbraak worden toegeschreven. We vonden namelijk dat CPZ en TFP ook krachtige

remmers zijn van de $\text{Na}^+/\text{Ca}^{2+}$ uitwisselaar in het sarcolemma. Deze remming is zeer waarschijnlijk verantwoordelijk voor de verminderde calcium overload, hetgeen op zich al een gunstig effect heeft op de overleving van anoxische hartcellen, zoals hierboven reeds is uitgelegd.

Het vinden van een dubbele gunstige werking van CPZ en TFP, namelijk vermindering van calcium overload en remming van fosfolipidenafbraak, maakt een definitieve rol van fosfolipidenafbraak in het ontstaan van celdood moeilijk.

Wel bleek fosfolipidenafbraak een goede voorspellende factor te zijn voor de later optredende celdood (Hoofdstuk 5). Tevens bleek dat CPZ en TFP de relatie tussen fosfolipidenafbraak en celdood niet veranderden. Deze bevindingen pleiten voor een rol van fosfolipidenafbraak in het ontstaan van celdood tijdens anoxie.

Echter, we vonden ook dat een remmer van plasmalogen-specifiek fosfolipase A_2 , halo-enol lacton suicide substrate (HELLS) genaamd, de fosfolipidenafbraak in anoxische hartcellen bijna geheel remde. Desondanks was er maar een gering gunstig effect op de overleving van de hartcellen (Hoofdstuk 6). Het lijkt daarom waarschijnlijk dat fosfolipidenafbraak niet dé beslissende factor in het ontstaan van hartceldood tijdens anoxie is.

Samengevat wijzen onze bevindingen erop dat 1) het vrijkomen van arachidonzuur in hartcellen tijdens anoxie vrijwel geheel door activiteit van het plasmalogen-selectief fosfolipase A_2 veroorzaakt wordt, 2) CPZ en TFP een remmend effect hebben op plasmalogen-selectieve fosfolipase A_2 , naast hun remmend effect op diacyl-specifieke fosfolipase A_2 , 3) celdood kan optreden ondanks een bijna complete remming van fosfolipidenafbraak, hetgeen pleit tegen een rol voor fosfolipidenafbraak bij het ontstaan van celdood en 4) HELLS (een) andere beschermende werking(en) heeft naast remming van het plasmalogen-specifieke fosfolipase A_2 .

De betrokkenheid van calcium-activated neutral protease (CANP) in het ontstaan van anoxische hartceldood is een aantrekkelijke hypothese, omdat de proteolytische activiteit van CANP Ca^{2+} -afhankelijk is, en omdat zich onder de vermeende substraten van het enzym een aantal belangrijke membraaneiwitten bevinden. Een massale supra-fysiologische activatie van CANP zou een verband kunnen leggen tussen calcium overload en de erop volgende afbraak van het sarcolemma, waarna celdood volgt.

We vonden, gebruik makend van een fluorogeen substraat, dat de activiteit van CANP in hartcellen tijdens chemische anoxie verhoogd was (Hoofdstuk 4). Twee remmers van CANP, leupeptine en calpain I inhibitor, bleken in staat de CANP activiteit te remmen in zowel controle cellen als in anoxische hartcellen. Ondanks een effectieve remming van CANP in anoxische cellen was er geen effect op de overleving van deze cellen. Daarom concluderen wij dat CANP activiteit welliswaar

verhoogd is tijdens chemische anoxie, maar niet bijdraagt aan het ontstaan van hartceldood.

Een mogelijke verklaring voor het eerder beschreven verband tussen de hoogte van calcium overload en de erop volgende celdood, is het fenomeen van “lateral-phase transition” van het sarcolemma. Deze theorie suggereert een verhoogde neiging van het sarcolemma van energie-gedepleteerde cellen om een niet-dubbellaag configuratie aan te nemen. Deze herconfiguratie van de celmembraan, welke gepaard gaat met een aggregatie en functieverlies van membraaneiwwitten, wordt bevorderd door de aanwezigheid van verhoogde Ca^{2+} concentraties. Dit impliceert dat vermindering van calcium overload, celdood remt vanwege een vermindering van de fysische verstoringen van de celmembraan. Het is echter mogelijk dat de Ca^{2+} -geïnduceerde membraanverstoringen optreden in combinatie met de eerder besproken biochemische fosfolipidenafbraak, en dat deze twee processen elkaar zelfs versterken.

Suggesties voor toekomstig onderzoek

Om de “lateral-phase transition” theorie te testen, zou toekomstig onderzoek zich moeten richten op het verder bestuderen van de biochemische en fysische veranderingen in de cellulaire membranen tijdens ischemie, anoxie en metabole inhibitie. Idealiter zou dit moeten gebeuren in individuele cardiomyocyten met behulp van optische methoden (fluorescentie, fosforescentie, life-time imaging, fluiditeit imaging), om aldus de integriteit en distributie van fosfolipiden over de binnen- en buitenlaag van het sarcolemma te bestuderen. Op deze wijze kan inzicht worden verkregen in de relatie tussen de intracellulaire Ca^{2+} concentratie, fosfolipiden asymmetrie en lateral-phase transition.

Hoewel wij vonden dat CANP geen rol speelt bij het ontstaan van anoxische hartceldood, wordt verondersteld dat CANP betrokken is bij stunning van het myocard. Toekomstig onderzoek kan gericht zijn op het meten van CANP activiteit in stunned myocard, en op het evalueren van het effect van remming van CANP op post-ischemische functie.

Het is mogelijk dat calcium overload tot verstoringen in de celkern leidt, zoals activatie van endonucleases hetgeen mogelijk leidt tot DNA schade. Tevens zou de verhoogde intracellulaire Ca^{2+} ion concentratie ten onrechte door de celkern kunnen worden opgevat als een second messenger signaal, met als mogelijk gevolg het tot expressie brengen van genen met een ongunstige effect (*c-fos*, *c-jun*, suicide genen). Toekomstig onderzoek op dit gebied zou de nucleaire respons op calcium overload kunnen bestuderen.

De rol van fosfolipase A₂ bij het ontstaan van ischemische hartceldood is nog steeds onduidelijk. De betrokkenheid van dit enzym bij celdood kan slechts worden aangetoond met behulp van uiterst specifieke remmers, zoals bijvoorbeeld monoclonale antilichamen. Tevens kan het gebruik van transgene muizen met een variabele expressie van fosfolipase A₂ bijdragen aan het beantwoorden van deze vraagstelling.

Het onderzoek waarin wij vonden dat vermindering van calcium overload in hartcellen tijdens anoxie de overleving van de cellen verbetert dient te worden uitgebreid met andere, meer complexe modellen. Het effect van remmers van de Na⁺/Ca²⁺ uitwisselaar in het sarcolemma op hartceldood, hemodynamische functie en aritmogenese dient te worden onderzocht.

Nawoord

Het in dit proefschrift beschreven onderzoek werd uitgevoerd op het laboratorium Cardiobiochemie (Prof. dr. A. van der Laarse) van de vakgroep Cardiologie (hoofd: Prof. dr. A.V.G Brusckhe) van het Academisch Ziekenhuis Leiden. Graag wil ik de medewerkers van dit laboratorium bedanken: Lizet van der Valk-Kokshoorn voor het vervaardigen van de talloze celkweken die in dit onderzoek zijn gebruikt en de hulp bij verschillende incubatie-experimenten, Janneke Egas-Kenniphaas, Leny Hollaar, Ton Vroom, Cham Le Thi, Herman Schaefer en Marion Persoon voor de prettige samenwerking, Lars Bastiaanse en Robert Verbunt voor de discussies en de adviezen, en de studenten Karin Höld en Anastazia Jerzewski voor hun hulp bij de verschillende proeven.

De steun van de computergroep, instrumentatiegroep, en secretariaat van de afdeling Cardiologie was onmisbaar en wordt zeer op prijs gesteld. De vakkundigheid van de werknemers op de fijnmechanica werkplaats van de vakgroep Fysiologie o.l.v. Gerard Verschragen was essentieel voor het tot stand komen van de "two-compartment culture dish" beschreven in hoofdstuk 3.

Het doorzettingsvermogen van drs. S. van Leeuwen van de vakgroep Organische Chemie tijdens de synthese van het fluorscerende PLA₂ substraat heb ik zeer gewaardeerd. Alle medewerkers van het laboratoria Maag-, darm- en leverziekten en Endocrinologie worden bedankt voor hun hulp en gezelligheid!

Publications

Abstracts

1. D.E. Atsma, E.K.J. Pauwels, F.M. van 't Hooft, R.I.J. Feitsma and H.J.M. Kempen. Labeling of LDL with ^{99m}Tc for imaging of atherosclerosis. Comparison of different methods. *Arteriosclerosis* 1989;9:724a.
2. D.E. Atsma, L.J.M. van der Valk-Kokshoorn, A. van der Laarse. Effect of the phospholipase A₂ inhibitor trifluoperazine on intracellular calcium concentration and cell death in cultured cardiomyocytes during metabolic inhibition. *J Mol Cell Cardiol* 1993;25 (Supplement I); S59.
3. D.E. Atsma, A. van der Laarse. Single cell imaging of the intracellular free calcium concentration in isolated intact cardiomyocytes during anoxia and reoxygenation. *Eur Heart J.* ;14 (Abstract supplement): 137.
4. D.E. Atsma, L.E. Bastiaanse, L. van der Valk-Kokshoorn, A. van der Laarse. Effect of protease inhibitors E64 and Calpain I inhibitor on cell death during anoxia and metabolic inhibition in cultured neonatal rat ventricular myocytes. *Circulation.* 1993; 88: I-4, (Supplement).
5. Lars E. Bastiaanse, D.E. Atsma, L.J. van der Valk, A. van der Laarse. The increase in sarcolemmal fluidity in cardiomyocytes during metabolic inhibition is caused by a loss of cellular cholesterol. *Circulation* 1993;88: I-442, (Supplement).
6. E.M.L. Bastiaanse, D.E. Atsma, M.M.C. Kuijpers, L.J.M. van der Valk, A. van der Laarse. Cellular cholesterol modulation affects the intracellular calcium ion concentration in cardiomyocytes independent of membrane fluidity. *J Am Coll Cardiol.* 1994;463A: 825-1.
7. D.E. Atsma, E.M.L. Bastiaanse, L. van der Valk, A. van der Laarse. Attenuation of calcium overload and delay of cell death by chlorpromazine and trifluoperazine in cardiomyocytes during chemical anoxia. *J Am Coll Cardiol.* 1994;31A: 845-109.
8. E.M.Lars Bastiaanse, Douwe E. Atsma, Arnoud van der Laarse. Intracellular calcium ion concentration in cardiomyocytes is affected by cellular cholesterol content independent of membrane fluidity. *Eur Heart J.* 1994;15: 351.
9. D.E. Atsma, E.M.L Bastiaanse, A. van der Laarse. Low medium pH limits injury in heart cells upon metabolic inhibition by limiting Ca^{2+} overload via $\text{Na}^{+}\text{-Ca}^{2+}$ exchanger inhibition. *J Moll Cell Cardiol.* 1994;26: 219.

10. D.E. Atsma, E.M.L Bastiaanse, S. van Leeuwen, A. van der Laarse. Protective effect of a plasmalogen-selective phospholipase A₂ inhibitor on cardiomyocytes subjected to chemical anoxia. *Eur Heart J.* 1995;16: 26.

11. D.E. Atsma, E.M.L Bastiaanse, L.J.M. van der Valk, A. van der Laarse. Low external pH limits cardiomyocyte injury upon chemical anoxia by limiting Ca²⁺ overload via Na⁺/Ca²⁺ exchanger inhibition. *Eur Heart J.* 1995;16: 363.

Articles

1. D.E. Atsma, W. Nieuwenhuizen, H.J.M. Kempen, F. M. van 't Hooft and E.K.J. Pauwels. Partial characterisation of Low Density Lipoprotein preparations isolated from fresh and frozen plasma after radiolabeling by seven different methods. *J Lipid Res.* 1991;32: 173-181.

2. D.E. Atsma, R.I.J. Feitsma, J. Camps, F.M. van 't Hooft, E.E. van der Wall, W. Nieuwenhuizen and E.K.J. Pauwels. Potential of ^{99m}Tc-Low Density Lipoproteins labeled by two different methods for the scintigraphic detection of experimental atherosclerosis in rabbits. *Arteriosclerosis Thromb.* 1993;13: 78-83.

3. D.E. Atsma. Scintigraphic detection of atherosclerosis with radiolabeled low density lipoprotein. Chapter in: "What's new in cardiac imaging?" 1993. Editors: E.E. van der Wall, H. Sochor, A. Righitti, M.G. Niemeyer, Kluwer academic publishers, Dordrecht, Holland.

4. E.K.J. Pauwels, M.M. Welling, R.I.J. Feitsma, D.E. Atsma and W. Nieuwenhuizen. The labeling of proteins and LDL with ^{99m}Tc: a new direct method employing KBH₄ and stannous chloride. *Nucl Med Biol.* 1993;20: 825-833.

5. E.M.L Bastiaanse, D.E. Atsma, M.M.C. Kuijpers, L.J.M. van der Valk, A. van der Laarse. Simvastatin-sodium delays cell death of anoxic cardiomyocytes by inhibition of the Na⁺-Ca²⁺ exchanger. *FEBS Lett.* 1994;443:151-154.

6. E.M.L. Bastiaanse, L.J.M. van der Valk-Kokshoorn, J.M. Egas-Kenniphaas, D.E. Atsma, and A. van der Laarse. The effect of sarcolemmal cholesterol content on the tolerance to anoxia in cardiomyocyte cultures. *J Mol Cell Cardiol.* 1994;26: 639-648.

7. E.M.Lars Bastiaanse, Douwe E. Atsma, Marinette M.C. Kuijpers, Arnoud van der Laarse. The effect of sarcolemmal cholesterol content on intracellular calcium ion concentration in cultured cardiomyocytes. *Arch Biochem Biophys.* 1994;313: 58-63.

8. D.E. Atsma, E.M.L. Bastiaanse, C. Ince, A. van der Laarse. A novel two-compartment culture dish allows microscopic evaluation of two different treatments in

one cell culture simultaneously: Influence of external pH on $\text{Na}^+/\text{Ca}^{2+}$ exchanger activity in cultured rat cardiomyocytes. *Pflügers Archiv*. 1994;428:296-299.

9. Richard Draijer, Douwe E. Atsma, Arnoud van der Laarse, Victor W.M. van Hinsbergh. cGMP and nitric oxide modulate thrombin-induced endothelial permeability. Regulation via different pathways in human aortic and umbilical vein endothelial cells. *Circ Res*. 1995;76: 199-208.

10. Douwe E. Atsma, E.M.Lars Bastiaanse, Anastazia Jerzewski, Lizet J.M.van der Valk, Arnoud Van der Laarse. The Role of Calcium Activated Neutral Protease (Calpain) in Cell Death in Cultured Neonatal Rat Cardiomyocytes During Metabolic Inhibition. *Circ Res*. 1995;76:1071-1078.

11. H.W. de Jonge, D.E. Atsma, E.J.M. Van der Valk-Kokshoorn, H.A.A. Van Heugten, A. Van der Laarse, J.M.J. Lamers. Alpha-adrenergic agonist and endothelin-1 induced intracellular Ca^{2+} response in the presence of a Ca^{2+} entry blocker in cultured rat ventricular myocytes. *Cell Calcium*. 1995;18: 515-525.

12. Y. van den Eijnden-Schrauwen, D.E. Atsma, R.E.M. de Vries, T. Kooistra, J.J. Emeis. Intracellular signalling pathways involved in the differential release of von Willebrand factor (vWF) and tissue-type plasminogen activator (tPA) from human endothelial cells. *Submitted*.

13. E.M. Lars Bastiaanse, Douwe E. Atsma, Lizet van der Valk, Arnoud van der Laarse. Metabolic inhibition of cardiomytes causes an increased sarcolemmal fluidity which may be due to loss of cellular cholesterol. *Arch Biochem Biophys*. 1995;319: 350-354.

14. Douwe E. Atsma, E.M.Lars Bastiaanse, Lizet van der Valk, Arnoud van der Laarse. Low external pH limits cell death in energy depleted cardiomyocytes by decreasing Ca^{2+} overload via $\text{Na}^+/\text{Ca}^{2+}$ exchanger inhibition. *Am J Physiol*. 1996;270: H2149-H2156).

15. Douwe E. Atsma, E.M.Lars Bastiaanse Lizet, van der Valk, Arnoud van der Laarse. I. Role of phospholipid degradation in death of anoxic cardiomyocytes. Effect of purported PLA_2 inhibitors on calcium overload and phospholipid degradation. *Submitted*.

16. Douwe E. Atsma, E.M.Lars Bastiaanse, Steven van Leeuwen, Lizet van der Valk, Jaap H. van Boom, Arnoud van der Laarse. II. Role of phospholipid degradation in death of anoxic cardiomyocytes. Effect of halo-enol lacton, an inhibitor of plasmalogen-specific phospholipid A_2 . *Submitted*.

Curriculum vitae

De schrijver van dit proefschrift werd op 17 november 1961 te Rijswijk geboren. Het diploma Gymnasium B werd in 1981 behaald aan het Stedelijk Gymnasium te Leiden. In ditzelfde jaar werd een aanvang gemaakt met de studie Geneeskunde aan de Rijksuniversiteit te Leiden. Van september 1983 tot september 1985 was hij werkzaam als student-assistent ten behoeve van het snijzaal-practicum op de afdeling Anatomie van de Rijksuniversiteit Leiden. Van september 1985 tot september 1987 werkte hij als student-assistent op het Laboratorium Cardiobiochemie van de vakgroep Cardiologie van het Academisch Ziekenhuis Leiden (hoofd: Prof. dr. A. van der Laarse). In 1986 werd een wetenschappelijke stage gedaan op de afdeling chirurgie van het Hillel Jaffe Memorial Hospital, in Hadera, Israel. In 1987 werd het doctoraal examen Geneeskunde behaald en werd met de co-assistentschappen begonnen. Van maart 1988 tot oktober 1990 werden deze co-assistentschappen onderbroken voor een onderzoeksproject van de Nederlandse Hartstichting, no. 87.042. Dit onderzoek werd uitgevoerd op het Gaubius Instituut TNO onder leiding van Dr. H.J.M. Kempen en Dr. W. Nieuwenhuizen, en op de afdeling Nucleaire Geneeskunde van het Academisch Ziekenhuis Leiden (hoofd: Prof. dr. E.K.J Pauwels). Na voltooiing van de co-assistentschappen werd in 1991 het artsexamen behaald (cum laude). Vanaf juli 1991 tot mei 1995 is het in dit proefschrift beschreven onderzoek verricht op het Laboratorium Cardiobiochemie van de vakgroep Cardiologie van het Academisch Ziekenhuis Leiden (hoofd: Prof. dr. A. van der Laarse), in het kader van het Nederlandse Hartstichtingsprojecten no. 90.089 en no. 92.093. Sinds 1 mei 1995 is de schrijver, in het kader van de opleiding tot cardioloog (Academisch Ziekenhuis Leiden, opleider: Prof. dr. A.V.G. Brusckke), werkzaam als arts-assistent interne geneeskunde in het Leyenburg Ziekenhuis te 's-Gravenhage (opleider: Dr. J.C.M. van der Vijver, internist).

Appendix

Cyclic GMP and nitric oxide modulate thrombin-induced endothelial permeability. Regulation via different pathways in human aorta and umbilical vein endothelial cells

Richard Draijer¹, Douwe E. Atsma², Arnoud Van der Laarse²
and Victor W.M. Van Hinsbergh¹

¹Gaubius Laboratory TNO-PG, Leiden, The Netherlands

²Department of Cardiology, University Hospital, Leiden, The Netherlands

Circulation Research 1995; 76: 199-208

Abstract

Previous studies have demonstrated that guanosine-3',5'-cyclic monophosphate (cGMP) and adenosine-3',5'-cyclic monophosphate (cAMP) reduce the endothelial permeability for fluids and macromolecules when the endothelial permeability is increased by thrombin. In this study we have investigated the mechanism by which cGMP improves the endothelial barrier function and examined whether nitric oxide (NO) can serve as an endogenous modulator of endothelial barrier function. Thrombin increased the passage of macromolecules through human umbilical vein and human aorta endothelial cell monolayers and concomitantly increased the cytoplasmic calcium ion concentration *in vitro*. Inhibition of these increases by the intracellular calcium chelator BAPTA indicated that cytoplasmic calcium ion elevation contributes to the thrombin-induced increase in endothelial permeability. The cGMP-dependent protein kinase activators 8-bromo-cGMP (8-Br-cGMP) and 8-(4-chlorophenylthio)-cGMP (8-PCPT-cGMP) decreased thrombin-induced passage of macromolecules. Two pathways accounted for this observation. Activation of cGMP-dependent protein kinase by 8-PCPT-cGMP decreased the accumulation of cytoplasmic calcium ions in aorta endothelial cells, and hence reduced the thrombin-induced increase in permeability. On the other hand, in umbilical vein endothelial cells, cGMP-inhibited-phosphodiesterase (PDE III) activity was mainly responsible for the cGMP-dependent reduction of endothelial permeability. The PDE III-inhibitors Indolidan (LY195115) and SKF94120 decreased the thrombin-induced increase in permeability by 50% in these cells. Thrombin treatment increased cGMP formation in the majority, but not all cell cultures. Inhibition of NO production by N^G-nitro-L-arginine methyl ester (L-NAME) enhanced the thrombin-induced increase in permeability, which was restricted to those cell cultures which displayed an increased cGMP formation after addition of thrombin. Simultaneous elevation of the endothelial cGMP concentration by atrial natriuretic peptide, sodium nitroprusside or 8-Br-cGMP prevented the additional increase in permeability induced by L-NAME.

These data indicate that cGMP reduces thrombin-induced endothelial permeability by inhibition of the thrombin-induced calcium accumulation and/or by inhibition of cAMP degradation by PDE III. The relative contribution of these mechanisms differs in aortic and umbilical vein endothelial cells. NO can act *in vitro* as an endogenous permeability-counteracting agent by raising cGMP in endothelial cells of large vessels.

Introduction

The endothelium, the inner lining of blood vessels, regulates the extravasation of fluid and macromolecules. Impairment of the barrier function of the endothelium results in

vascular leakage and edema. This can occur by exposure to toxic agents, after stimulation of the endothelium by vasoactive substances, or during inflammation, in particular in postcapillary venules. It is generally believed that the increase in endothelial permeability induced by vasoactive substances is caused by contraction of endothelial cells.¹⁻⁷ Endothelial contraction involves interaction of actin and non-muscle myosin, which is activated by a calcium/calmodulin ($\text{Ca}^{2+}/\text{CaM}$) and ATP-dependent phosphorylation of the myosin light chain (MLC) by MLC-kinase.^{5,8,9} The barrier function of endothelial cells is improved both *in vivo* and *in vitro* by agents that increase the intracellular cAMP concentration.¹⁰⁻¹⁵ An increase in cellular cAMP was found to be accompanied by a reduced degree of phosphorylation of the myosin light chain in cultured endothelial cells.⁹ Several *in vitro* studies have shown that elevation of the cGMP concentration also reduces endothelial permeability in large vessel endothelial cells.¹⁶⁻¹⁸ The modulating effect of cGMP is most prominent when the endothelial permeability has been increased, for instance by thrombin or oxidants, whereas it is minor or absent under basal conditions.^{16,18,19} In perfused rat lungs, stimulation of cGMP production by atrial natriuretic peptide also reduced oxidant-induced vascular leakage.²⁰ However, the mechanism by which cGMP reduces oxidant- and thrombin-enhanced permeability is not known.

The process of endothelial cell contraction resembles the regulation of actin-myosin interaction in smooth muscle cells and platelets. The effects of cGMP on smooth muscle relaxation are thought to be mediated via cGMP-dependent protein kinase, which affects the intracellular calcium metabolism.²¹⁻²³ In smooth muscle and several other cell types cGMP also contributes indirectly by inhibiting phosphodiesterase type III (PDE III), which results in a decreased breakdown of cAMP.^{24,25} In the present study we have investigated, in human umbilical vein and aortic endothelial cells, whether cGMP regulates endothelial permeability by affecting the regulation of the cytoplasmic calcium ion accumulation or by inhibiting PDE III activity.

Stimulation of the influx of calcium ions in endothelial cells not only causes endothelial cell contraction, but also results in the release of several endothelial products, including prostacyclin and nitric oxide (NO). Production of NO is due to the calcium/calmodulin-dependent activation of the constitutive nitric oxide synthase, which is predominantly present in muscular vessel endothelial cells.^{26,27} The production of NO not only reduces the contraction of smooth muscle cells and counteracts platelet activation, but it also stimulates guanylate cyclase in the endothelial cell itself. Because the cGMP thereby generated may counteract the stimulus-induced increase in permeability, we wondered whether the production of NO attenuates the contraction of endothelial cells. Our data point to a possible counter-regulatory role of nitric oxide on the regulation of endothelial permeability.

Materials and Methods

Materials. Medium 199 supplemented with 20 mmol/L HEPES was obtained from Flow Laboratories (Irvine, UK); tissue culture plastics from Corning (Corning, NY, USA) or Costar (Cambridge, MA, USA); and Transwells (diameter 0.65 cm, pore size 3 μm) from Costar. A crude preparation of endothelial cell growth factor was prepared from bovine brain as described by Maciag *et al.*²⁸ Human serum was obtained from the local blood bank and was prepared from fresh blood taken from healthy donors; the sera were pooled, and stored at 4°C. Newborn calf serum was obtained from GIBCO (Grand Island, NY, USA) and heat-inactivated before use (30 min, 56°C). Pyrogen-free human serum albumin was purchased from the Central Laboratory of Blood Transfusion Service (Amsterdam, The Netherlands). Horseradish peroxidase EC 1.11.1.7 type I (HRP), sodium nitroprusside, 8-bromo-cGMP (8-Br-cGMP), N^G-nitro-L-arginine methyl ester (L-NAME) and fluorescein isothiocyanate (FITC)-dextrans with a molecular masses of 35,600, 38,900 and 487,000 D were obtained from Sigma Chemical Company (St. Louis, MO, USA); bovine α -thrombin from LEO Pharmaceutical Products (Ballerup, Denmark); forskolin from Hoechst (La Jolla, CA, USA); isobutylmethylxanthine (IBMX) from Janssen Chimica (Beerse, Belgium); SKF96365 from Biomol Research Laboratories (Plymouth Meeting, PA, USA); BAPTA-AM and fura-2-AM from Molecular Probes (Eugene, OR, USA); 8-(4-chlorophenylthio)-cGMP (8-PCPT-cGMP) from Biolog Life Science Institute (Bremen, Germany); ionomycin from Calbiochem Corporation (La Jolla, CA, USA); [¹⁴C]sucrose from Dupont NEN (Bad Hamburg, Germany); and human atrial natriuretic factor-(99-128) from Bissendorf Peptide GmbH (Wedermark, Germany). SKF94120 was a gift from Smith Kline & French Laboratories Ltd. (Welwyn Garden, UK); Rolipram (ZK62711), a gift from Schering Aktiengesellschaft (Berlin, Germany); and Indolidan (LY195115), a gift from Lilly Research Laboratories (Indianapolis, IN, USA).

Isolation and culture of endothelial cells. Human umbilical vein endothelial cells were isolated by the method of Jaffe *et al.*²⁹ and characterized as described previously.³⁰ Isolation and characterization of human endothelial cells from the pulmonary artery and aorta were performed as earlier described.³¹ The blood vessels of human origin were obtained according to the guidelines of the Institutional Review Board of the University Hospital Leiden. Cells were cultured on fibronectin-coated dishes in Medium 199 supplemented with 10% human serum, 10% newborn calf serum, 150 $\mu\text{g}/\text{ml}$ crude endothelial cell growth factor, 5 U/ml heparin, 100 U/ml penicillin and 0.1 mg/ml streptomycin. Cells were kept at 37°C under 5% CO₂/95% air. For the evaluation of the barrier function, confluent monolayers of endothelial cells from

umbilical vein (primary), pulmonary artery (first, second or third passage) or aorta (fourth or fifth passage) were released with trypsin-EDTA and seeded in high density on fibronectin-coated polycarbonate filters of the Transwell system and cultured as described by Langelier *et al.*^{32,33} Medium was renewed every other day.

Evaluation of the barrier function. Endothelial cells cultured on filters were used between 4 and 6 days after seeding. Exchange of macromolecules through the endothelial monolayers was investigated by assay of the transfer of HRP and FITC-dextran. Passage of HRP through human endothelial cell monolayers was performed as described previously.³² Briefly, endothelial cell monolayers were cultured on porous membranes (0.33 cm²; 3 μm pore size) to form a tight monolayer. Before the start of the experiment, cells were incubated for one hour in Medium 199 with 1% albumin. In pretreatment, the cells were incubated for 15 minutes with 8-Br-cGMP (1-1000 μM), 8-PCPT-cGMP (1-1000 μM), SNP (0.1 mM), ANP (10⁻⁷ M), SKF94120 (100 μM), Indolidan (100 μM) or Rolipram (100 μM) in the upper and lower compartment. BAPTA/AM (10 μM) and L-NAME (100 μM) were preincubated for one hour to achieve sufficient loading. At the start of the experiment, 5 μg/ml horseradish peroxidase in Medium 199 with 1% albumin was added to the upper compartment of the Transwell system in the presence or absence of thrombin (1 U/ml). Samples were taken from the lower compartment (at the other side of the endothelial monolayer) at various time intervals, and an equal volume of Medium 199 containing 1% albumin was readded to this lower compartment. Cells were kept at 37°C under 5% CO₂/95% air. All passage experiments were performed in triplicate. The concentration of HRP was derived from the HRP activity in each sample with peroxide and tetramethyl benzidine, as substrate and expressed as ng passed per cm² in a certain time interval. The permeability coefficient (PC) was derived from Fick's law of diffusion and was determined by:

$$PC = \text{mass flux peroxidase} / ([\text{peroxidase}]_{UC} - [\text{peroxidase}]_{LC})$$

where UC is the upper compartment and LC is the lower compartment. The mass flux of HRP is expressed in ng.cm⁻².h⁻¹. Because the initial passage of molecules proceeds linearly in time, the mass flux of peroxidase was calculated from the initial hour of passage, and the mean concentrations of the upper and lower compartments during this period were used to calculate the concentration difference.

The PC was corrected for the contribution of the filter membrane (<0.5%):

$$1/PC_{EC} = 1/PC_{EC-F} - 1/PC_F$$

where PC_{EC} represents the PC of the endothelial cell monolayer, PC_F the PC of the empty filter, and PC_{EC-F} the PC determined for the filter and the endothelial cells together. The PC_F was determined at 37°C under identical conditions with separate fibronectin-coated filters that had been preincubated in culture medium for 24 hours. The passage of FITC-dextran (input upper compartment 1 mg/ml) was determined similarly with the use of an inverted fluorescence microscope equipped with a photometer and a scanning stage, and operated by a microprocessor.³⁴

Extraction and assays of cyclic nucleotides. Cultured human endothelial cells were grown to confluence in 5 cm² wells. Medium of the monolayers was renewed with Medium 199 supplemented with 1% albumin, with or without 100 μM L-NAME, one hour before the incubation period. Cells were preincubated for 15 min with IBMX (1 mM) to prevent degradation of cyclic nucleotides by phosphodiesterases. At the start of the experiment, thrombin was added to the medium and incubated for 15 min. Immediately upon removal of the medium, 3.5% perchloric acid (0.5 ml) and a small known amount of [³H]-cGMP or [³H]-cAMP were added to each well for the determination of the intracellular cyclic nucleotide concentration. The cell lysates were transferred to Eppendorf reaction tubes and neutralized by using potassium hydrogen carbonate (50% saturated). After centrifugation, the supernatants were collected and dried under a stream of nitrogen gas. The concentration of the intracellular cyclic nucleotides was determined using radioimmunoassays (Amersham, Amersham, UK), according to Steiner *et al.*³⁵ and corrected for the recoveries in the various samples.

Measurement of [Ca²⁺]_i. Endothelial cells were cultured on 5 cm² glass coverslips and loaded with fura-2 by incubation with 2 μM fura-2/AM for 45 to 60 min at 37°C in Medium 199 supplemented with 1% human serum albumin. Then, the cells were washed three times with Tyrode buffer. The coverslips were mounted in a teflon two compartment incubation dish, incubated in 1 ml Tyrode buffer, and placed in a temperature controlled micro-incubator.^{36,37} The two compartment dish allows the exposure of the two halves of the same culture to different treatment. In this way, the effect of thrombin on [Ca²⁺]_i in one half can be compared to the effect of thrombin, in the presence of 8-PCPT-cGMP, 8-Br-cGMP, BAPTA or SKF96365 in the other half of the same culture. Fura-2 fluorescence was measured with an imaging dual-wavelength fluorescence microscope, which consisted of an inverted microscope body (Leitz Diavert, Wetzlar, Germany) equipped with a 20x fluorite objective (Nikon,

Badhoevedorp, The Netherlands) and a mercury light source (HBO-100, Osram, Montgomery, NY, USA). A filterwheel (Sutter, Novato, CA, USA) allowed the selection of excitation filters of 340 nm and 380 nm. Emission fluorescence was led through a 490 nm high-pass filter and imaged by a high-sensitivity SIT camera (Hamamatsu C2400-08, Herrsching, Germany). The resulting video signal was digitized by a frame-grabber board (PCVISIONplus™, Imaging Technologies, Woburn, MA, USA) in a PC-AT 486 computer. Spatial resolution of the images was 256 x 256 pixels, with an eight bits intensity resolution. Every 3.6 s, a pair of images at 340 nm and 380 nm excitation wavelength was made. Off-line, background fluorescence was subtracted and the 340 nm image was divided by the 380 nm image on a pixel-by-pixel basis, yielding a ratio image. Statistical analysis was performed using dedicated image processing software (TIM, Difa, Breda, The Netherlands). The mean $[Ca^{2+}]_i$ was determined from a field of fifty cells and was calculated by the equation:

$$[Ca^{2+}]_i = K_d * \beta * [(R-R_{min})/(R_{max}-R)] \quad (\text{in nM})$$

in which R represents the ratio of the fluorescence values at 340 nm and 380 nm; R_{max} and R_{min} are the maximal and minimal ratio values, respectively, being determined after each experiment by addition of 1 μ M ionomycin and 10 mM EGTA, respectively; β represents the ratio of the fluorescence at 380 nm of free fura-2 and fura-2 completely saturated with Ca^{2+} (3.6). The K_d , the dissociation constant of the fura-2- Ca^{2+} complex, was assumed to be 224 nM at 37°C, according to Grynkiewicz *et al.*³⁸

Statistical analysis. Data are presented as mean \pm SEM. Statistical analysis as indicated in the text was performed with the Mann-Whitney and Wilcoxon rank sum tests. Statistical significance was assumed at $p < 0.05$.

Results

Elevation of $[Ca^{2+}]_i$ during thrombin-induced increase in endothelial permeability. FITC-dextran and HRP, which has a Stokes radius similar to that of albumin, were used as marker molecules to assay the permeability of human endothelial cell monolayers for macromolecules. Upon addition of 1 U/ml thrombin the permeability of human umbilical vein endothelial cell monolayers for ^{14}C -sucrose (360 D), FITC-dextran (38,900 D), HRP and FITC-dextran (487,000 D) increased two-, five-, seven- and fifteenfold, respectively (average values of ten different cultures; not shown). The increase in permeability was detectable rapidly after addition of thrombin (Fig. 1A) and lasted for at least one hour. It was accompanied by an immediate decrease in the

Appendix

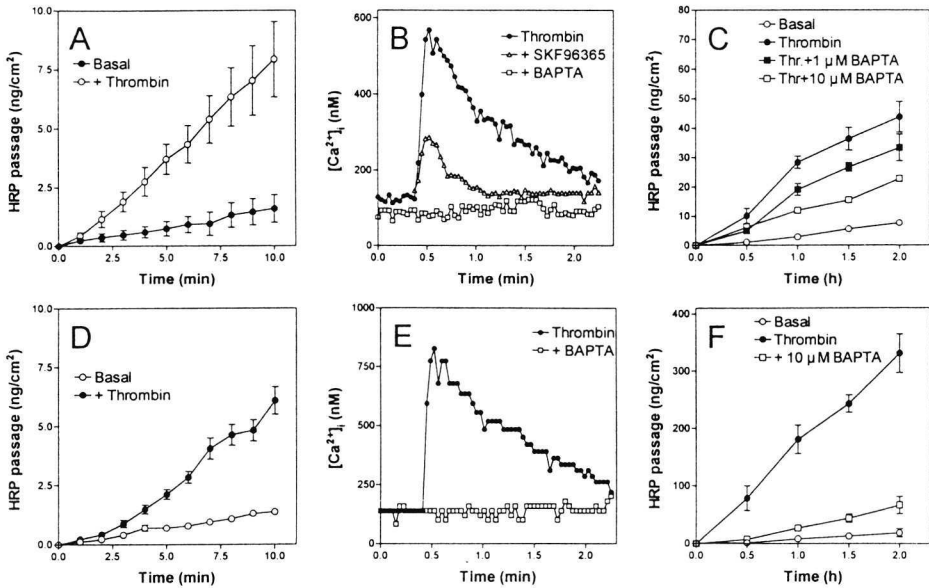


Figure 1. Graphs showing effects of thrombin on the $[Ca^{2+}]_i$ and permeability of human umbilical vein (A through C) and human aortic (D through F) endothelial cell monolayers. A and D: Early time courses show the passage of horseradish peroxidase (HRP) under basal conditions (●) and after stimulation with 1 U/ml thrombin (○), which is added at t=0 (mean ± SEM of six determinations). The thrombin-induced permeability is significantly different from the basal permeability after 3 min ($p < 0.05$). Passage of HRP was determined as described in 'Materials and Methods'.

B and E: The increase in $[Ca^{2+}]_i$ after addition of 1 U/ml thrombin (●) was prevented by addition of the intracellular Ca^{2+} chelator BAPTA-AM (10 μM, □). In the presence of the Ca^{2+} entry blocker SKF96365 (100 μM, ▢) $[Ca^{2+}]_i$ was markedly reduced. Each graph represents the mean of three representative recordings with different batches of umbilical vein endothelial cells and one representative recording with aortic endothelial cells. Similar results were obtained with 25 μM EGTA in calcium-free buffer instead of SKF96365 (not shown).

C and F: Time courses show the passage of HRP in hours under basal conditions (○) and after stimulation with 1 U/ml thrombin (●). The thrombin-induced passage of HRP through endothelial cell monolayers was partly prevented in monolayers, that were preincubated for 1 hour with BAPTA-AM (1 μM, ■ and 10 μM, □) (mean ± SEM of triplicate cultures).

trans-endothelial electrical resistance (40-60% reduction; not shown). Thrombin also rapidly enhanced the passage rate of HRP fivefold through monolayers of human aorta endothelial cells (Fig. 1D).

Thrombin induced an immediate rise in $[Ca^{2+}]_i$ in both endothelial cell types (Fig. 1B, 1E). This increase was abolished by the intracellular Ca^{2+} chelator BAPTA. The elevation of the $[Ca^{2+}]_i$ was caused by a rapid release of calcium ions from intracellular stores and an influx of extracellular Ca^{2+} (Fig. 1B), since $[Ca^{2+}]_i$ accumulation was reduced by the calcium entry blocker SKF96365³⁹ and by incubation in Ca^{2+} -free

medium supplemented with EGTA (not shown). Further evidence that elevation of the $[Ca^{2+}]_i$ is also important for the prolonged thrombin-mediated increase in endothelial permeability was obtained using the intracellular Ca^{2+} chelator BAPTA. BAPTA reduced the thrombin-mediated increase in permeability in a concentration-dependent manner (Fig. 1C, 1F). In the presence of 10 μ M BAPTA the thrombin-induced increase in permeability was reduced to $50 \pm 9\%$ in umbilical vein endothelial cells (five independent cultures, $p < 0.05$) and to $53 \pm 20\%$ in aortic endothelial cells (three independent experiments with cells from two different donors).

Table 1. Effect of 8-bromo-cGMP (1 mM) on the passage of horseradish peroxidase (HRP) through human umbilical vein and human aorta endothelial cell monolayers under basal conditions and after stimulation with 1 U/ml thrombin.

| Endothelial cells | Addition | HRP Passage ($ng \cdot cm^{-2} \cdot h^{-1}$) | |
|-------------------|----------|---|------------------|
| | | Control | 8-Br-cGMP |
| Umbilical vein EC | None | 10 ± 2 (22) | 7 ± 2 (15)* |
| | Thrombin | 71 ± 14 (22)# | 48 ± 7 (22)* |
| Aorta EC | None | 43 ± 14 (7) | 31 ± 12 (7) |
| | Thrombin | 193 ± 57 (7)# | 90 ± 29 (7)* |

Endothelial permeability was determined in Medium199 supplemented with 1% human serum albumin and with or without 1 mM 8-Br-cGMP. HRP passage was determined after an one hour time interval as described in the Materials and Methods section. Values are mean \pm SEM of the number of experiments (in parentheses). * $p < 0.05$ vs corresponding control value; # $p < 0.001$ (umbilical vein EC) and $p < 0.05$ (aortic EC) vs corresponding EC not stimulated with thrombin.

cGMP induces a simultaneous reduction of thrombin-enhanced permeability and rise of $[Ca^{2+}]_i$ in aortic endothelial cells. The thrombin-enhanced permeability was reduced in human umbilical vein and aorta endothelial cell monolayers by the cell membrane-permeant cGMP analogue 8-Br-cGMP (Table 1). Under basal conditions 8-Br-cGMP was less or not effective on endothelial permeability. When another cGMP-analogue, 8-PCPT-cGMP, was used, the thrombin-increased permeability was reduced in aorta endothelial cell monolayers to 50 ± 3 and $33 \pm 8\%$ in the presence of 0.1 mM and 1 mM 8-PCPT-cGMP, respectively (four experiments), but was not affected in umbilical endothelial cell monolayers (with 1 mM 8-PCPT-cGMP $101 \pm 14\%$ of thrombin-stimulated counterparts; seven experiments). The cGMP analogues activate

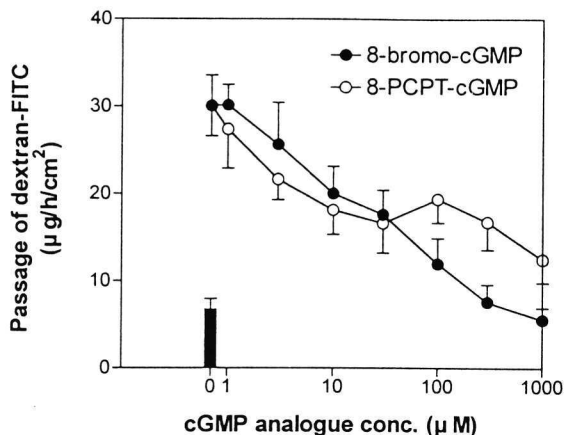


Figure 2. Graph showing the passage of a FITC-labeled dextran (38 900 D) through human aorta endothelial cell monolayers after stimulation with 1 U/ml thrombin, measured in the presence of different concentrations of 8-bromo-cGMP (●) or 8-PCPT-cGMP (○). The basal passage (bar) increased fourfold after thrombin stimulation. The elevated passage was concentration-dependently reduced by the cGMP analogues. The passage of HRP was reduced similarly (not shown). Data are mean of two different cultures, performed in duplicate.

cGMP-dependent protein kinase with a similar potency, but have relatively little effect on cAMP-dependent protein kinase.^{40,41} In addition, 8-PCPT-cGMP acts selectively on cGMP-dependent protein kinase as compared to cGMP-regulated phosphodiesterases, whereas 8-Br-cGMP is less specific in this respect.⁴⁰

Both 8-PCPT-cGMP and 8-Br-cGMP decreased the thrombin-enhanced permeability for macromolecules at low concentrations (1-30 μM) in aortic endothelial cells (Fig. 2). This suggests that activation of cGMP-dependent protein kinase is indeed involved. Determination of the $[Ca^{2+}]_i$ in fura-2-loaded endothelial cells revealed that the thrombin-induced elevation of $[Ca^{2+}]_i$ was markedly reduced by a preincubation with 8-PCPT-cGMP in aorta endothelial cells. On the other hand, the $[Ca^{2+}]_i$ rise was only marginally attenuated by 8-PCPT-cGMP in umbilical vein endothelial cells (Table 2; Fig. 3). The cAMP-analogue 8-Br-cAMP (0.1-1 mM) did not change the thrombin-induced elevation of the $[Ca^{2+}]_i$ in either cell type (not shown).

cGMP-inhibited cAMP phosphodiesterase activity in umbilical vein endothelial cells.

The discrepancy between the effects of 8-PCPT-cGMP and 8-Br-cGMP on thrombin-enhanced permeability of human umbilical vein endothelial cells suggests the existence of an additional regulatory target by which cGMP may affect permeability. Therefore, we investigated whether a cGMP-inhibited cAMP phosphodiesterase activity (PDE III) contributed, additionally, to the reducing effect of cGMP on the passage of macromolecules through thrombin-stimulated endothelial cell monolayers. SKF94120 and Indolidan, two specific inhibitors of the phosphodiesterase type III (cGMP-inhibited cAMP PDE) were used. When cAMP levels were measured after thrombin-stimulation in umbilical vein endothelial cells, cAMP increased from $1.2 \pm$

Table 2. Reduction of thrombin-induced rise in the $[Ca^{2+}]_i$ in endothelial cells by 8-PCPT-cGMP.

| Endothelial cells | $[Ca^{2+}]_i$ (nM) | | |
|--------------------------|--------------------|---------------------------|-----------|
| | basal | thrombin + 8-PCPT-cGMP | thrombin |
| Umbilical vein EC (n=10) | | | |
| peak value | 120 ± 6 | 899 ± 85 | 726 ± 85 |
| after 1 min | | 388 ± 57 | 269 ± 22 |
| Aortic EC (n=7) | | | |
| peak value | 111 ± 5 | 761 ± 188 | 228 ± 29* |
| after 1 min | | 486 ± 102 | 167 ± 20* |

The intracellular calcium concentration $[Ca^{2+}]_i$ was determined as described in the Materials and Methods section. Peak value and values 1 min after stimulation with 1 U/ml thrombin of $[Ca^{2+}]_i$ is presented with and without a 15 min preincubation of 100 μ M 8-PCPT-cGMP in aortic and umbilical vein endothelial cells. Values are mean \pm SEM of the number of determinations (n). * $p < 0.05$ vs. control.

0.2 pmol in the absence of PDE III inhibitors to 1.9 ± 0.4 pmol/ 3.5×10^5 cells in the presence of thrombin and SKF94120 ($p < 0.05$) and tended to increase to 1.9 ± 0.5 pmol in the presence of thrombin and Indolidan (eight different cell cultures). In the absence of thrombin both inhibitors slightly increased cAMP approximately 30% compared to the control value. SKF94120 and Indolidan, as well as Rolipram, an inhibitor of the PDE type IV (cAMP-specific phosphodiesterase), inhibited the thrombin-induced increase of the passage of macromolecules through umbilical vein endothelial cell monolayers (Fig. 4). SKF94120 slightly reduced the thrombin-induced HRP passage in aorta endothelial cells to $89 \pm 7\%$ (four cultures). The basal permeability was not changed by SKF94120 in either cell type.

Inhibition of NO synthesis by L-NAME intensifies the thrombin-induced elevation of endothelial permeability. The rise in $[Ca^{2+}]_i$ after addition of thrombin stimulates the constitutive Ca^{2+} /calmodulin-dependent NO synthase. NO activates guanylate cyclase, which leads to cGMP generation. In agreement with observations by other authors,⁴² we found that thrombin augmented the intracellular cGMP concentration in tight endothelial cell monolayers of umbilical vein from 1.3 ± 0.2 to 2.4 ± 0.4 pmol/ 3.5×10^5 cells ($p < 0.01$; 11 different cultures, assayed after 15 min in the presence of

Appendix

IBMX). This increase in cGMP concentration is apparently due to NO generation, because (pre)incubation of the cells with the competitive NO synthase inhibitor L-NAME (100 μ M) prevented the thrombin-induced increase in these cells (1.4 ± 0.2 pmol cGMP/ 3.5×10^5 cells; $p < 0.05$ as compared to thrombin-stimulated cells).

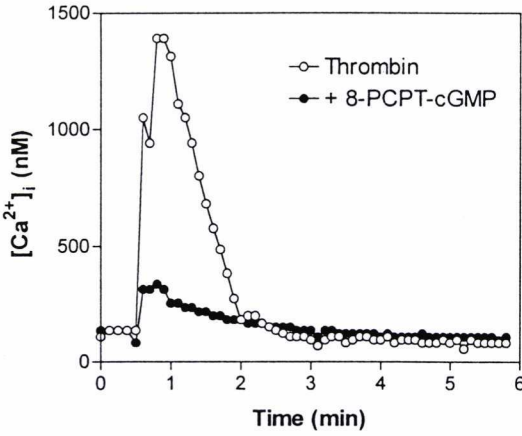
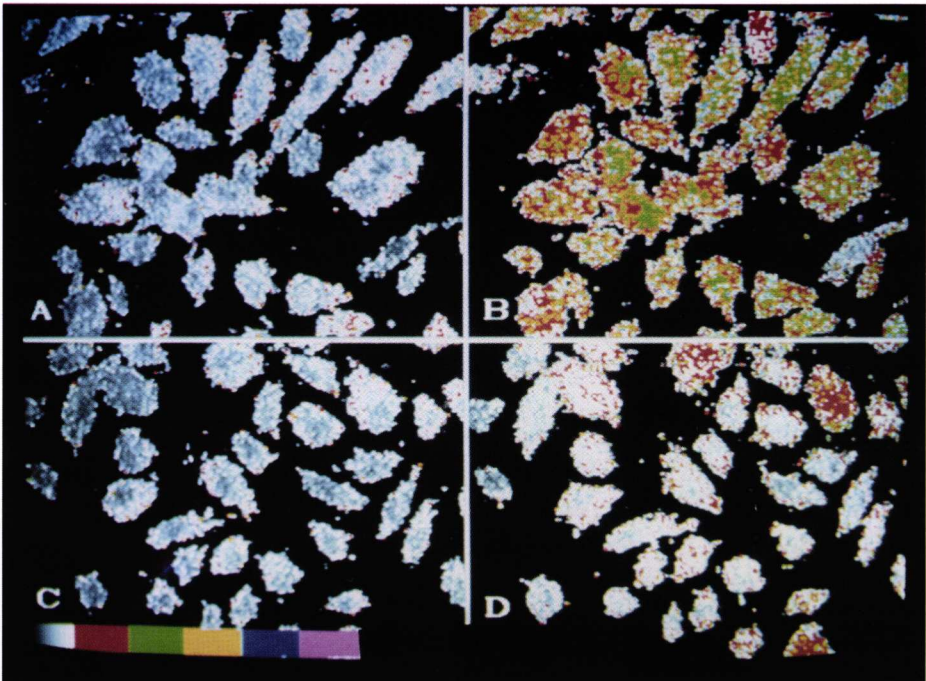


Figure 3. Effect of 8-(4-chlorophenylthio)-cGMP (8-PCPT-cGMP) on the $[Ca^{2+}]_i$ in thrombin-stimulated human aortic endothelial cells. Top: Graph showing that preincubation of endothelial cells with 100 μ M 8-PCPT-cGMP (\bullet) reduced the increase in $[Ca^{2+}]_i$ induced by 1 U/ml thrombin (\circ). Bottom: Video microscope image of a part of the culture before (A and C) and 10 seconds after stimulation with thrombin (B and D). The intensity of the fluorescence ratio 340/380 nm, which is represented in pixels, is reduced by

15 min preincubation of the cells with 8-PCPT-cGMP (C and D). The fluorescence intensity bar represents, from left to right, an increase in $[Ca^{2+}]_i$.



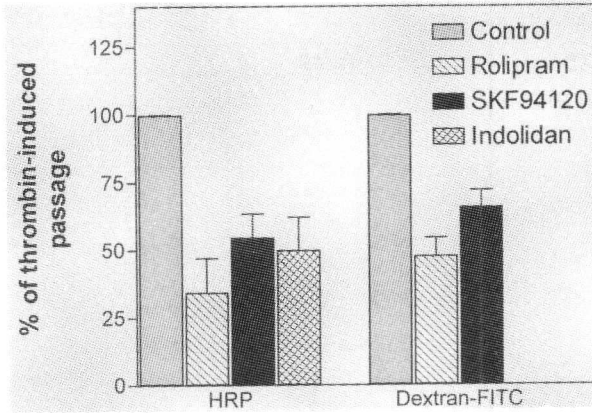


Figure 4. Bar graph showing the effect of phosphodiesterase inhibitors on the passage of HRP and FITC-dextran (35,600 D) through monolayers of umbilical vein endothelial cells. The endothelial cells were stimulated with 1 U/ml thrombin in the presence of Rolipram (100 μ M), SKF94120 (100 μ M) or Indolidan (100 μ M), or without addition of PDE inhibitors (Control). Permeability values after stimulation with thrombin

(= 100%) were $76 \pm 19 \mu\text{g}\cdot\text{cm}^{-2}\cdot\text{h}^{-1}$ for HRP and $7.6 \pm 0.7 \text{mg}\cdot\text{cm}^{-2}\cdot\text{h}^{-1}$ for FITC-dextran. All conditions reduced the passage of both tracer molecules ($p < 0.05$ for Rolipram and Indolidan, $p < 0.01$ for SKF94120). Data are mean \pm SEM of the indicated number of different cultures.

cGMP was not significantly altered when these cells were (pre)incubated with L-NAME alone ($1.6 \pm 0.2 \text{pmol cGMP}/3.5 \times 10^5 \text{ cells}$). Therefore, we wondered whether the thrombin-induced increase in permeability was partly attenuated/counteracted by the generation of NO. If so, addition of L-NAME would be expected to increase thrombin-induced permeability. In 37 different cultures of human endothelial cell monolayers the thrombin-enhanced permeability increased by $51 \pm 13\%$ after preincubation of the cells for one hour with $100 \mu\text{M}$ L-NAME ($p < 0.005$). Although this effect is highly significant, considerable variation was observed between cultures. In Fig. 5 the effect of L-NAME on the thrombin-enhanced permeability is plotted as a function of the thrombin-enhanced permeability. The effect of L-NAME was significant in 23 cultures, which had a thrombin-enhanced permeability for HRP that was $< 100 \text{ng}\cdot\text{cm}^{-2}\cdot\text{h}^{-1}$ ($42 \pm 4 \text{ng}\cdot\text{cm}^{-2}\cdot\text{h}^{-1}$ vs. $69 \pm 9 \text{ng}\cdot\text{cm}^{-2}\cdot\text{h}^{-1}$). This effect could not be demonstrated in the cultures, which displayed a relatively high permeability after thrombin-stimulation (14 cultures with a mean permeability of $217 \pm 21 \text{ng}\cdot\text{cm}^{-2}\cdot\text{h}^{-1}$). In the latter cultures, the thrombin-induced increase in permeability could still be reduced by an elevation of the intracellular cGMP content by 8-Br-cGMP or ANP (not shown). In the responsive cultures, L-NAME enhanced the thrombin-induced increase in permeability in a concentration-dependent manner (Fig. 6). Furthermore, the additional increase caused by L-NAME was completely prevented by agents that raised cGMP: ANP, sodium nitroprusside (SNP) and 8-Br-cGMP (Fig. 7). This was also observed in human pulmonary artery endothelial cells (Fig. 7b). Additionally, a significant increase of the passage of HRP through umbilical vein endothelial cell monolayers after thrombin stimulation by L-NAME from 100 (thrombin)

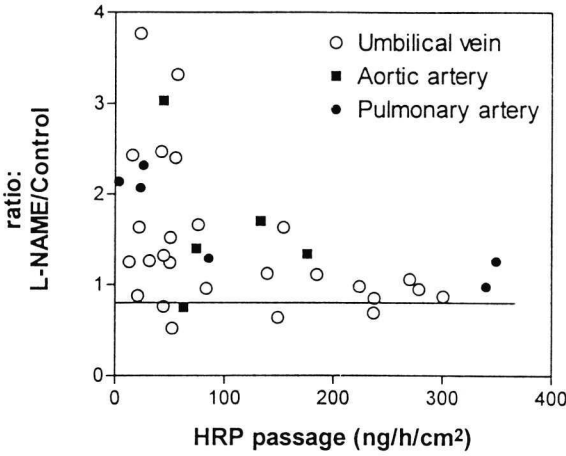


Figure 5. Graph showing the effect of L-NAME on thrombin-stimulated endothelial permeability in cultures of three endothelial cell types. The ratio of the passage of HRP after 1 U/ml thrombin stimulation with and without the nitric oxide synthase inhibitor L-NAME (100 μ M) is plotted against the HRP passage in $\text{ng}\cdot\text{cm}^{-2}\cdot\text{h}^{-1}$ after thrombin stimulation without L-NAME. No additional effect of L-NAME upon the thrombin-induced passage is marked with a horizontal line at a ratio of one. The passage is shown 1 hour

after thrombin-stimulation for umbilical vein (○), aortic (■) and pulmonary artery (●) endothelial cell monolayers. The response to L-NAME is inversely correlated to the permeability of HRP in the presence of thrombin. Each point represents the mean of a triplicate determination.

to $130 \pm 18\%$ (thrombin with L-NAME) was decreased by SNP to $105 \pm 12\%$ (thrombin with L-NAME and SNP; 7 cultures of different donors). L-NAME was ineffective on the basal permeability regardless of the basal passage rate. To evaluate whether the observed lack of response to L-NAME was associated with an impaired formation of NO and/or cGMP, cGMP and thrombin-enhanced permeability were determined in 10 independent cultures of umbilical vein endothelial cells. The cGMP concentration was increased after thrombin stimulation from 0.8 ± 0.1 to 2.5 ± 0.4 $\text{pmol}/3.5 \times 10^5$ cells in cultures with a low thrombin-induced permeability ($p < 0.05$, five different cultures), but remained unchanged in cultures with a high permeability (0.6 ± 0.1 vs. 0.9 ± 0.4 $\text{pmol}/3.5 \times 10^5$ cells, respectively, five different cultures).

To obtain further mechanistic information, cyclic nucleotides and $[\text{Ca}^{2+}]_i$ were assayed after addition of thrombin and L-NAME in aortic and umbilical vein endothelial cells, in the absence of IBMX. A transient (50-100%) increase in cGMP was observed, which peaked at 5-6 min after addition of thrombin. In aortic endothelial cells, the cGMP concentration increased from 0.39 ± 0.09 to 0.62 ± 0.06 pmol cGMP/ 3.5×10^5 cells 5 min after thrombin addition. Preincubation of the cells with L-NAME reduced the cellular cGMP concentration to 0.24 ± 0.13 pmol in those cells. In the same aortic endothelial cell culture, the peak value of $[\text{Ca}^{2+}]_i$ after stimulation by thrombin (606 ± 170 nM) was additionally increased to 1015 ± 184 nM by preincubation of the cells with L-NAME ($p < 0.05$; 24 determinations). These observations are consistent with the suggestion that NO-mediated cGMP generation partially reduces the accumulation of $[\text{Ca}^{2+}]_i$ after stimulation of aortic endothelial cells by thrombin.

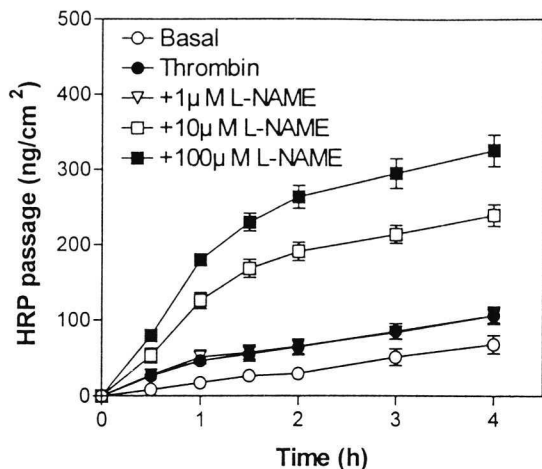


Figure 6. Graph showing the effect of L-NAME on the thrombin-induced increase in endothelial permeability. The time courses of the HRP passage through human umbilical vein endothelial cell monolayers are presented, under basal condition (Medium 199 supplemented with 1% human serum albumin) or after stimulation with 1 U/ml thrombin, in the presence or absence of L-NAME. The basal HRP passage (○) is increased upon addition of thrombin (●) and is further elevated in combination with L-NAME (1 µM ▽; 10 µM □; and 100 µM ■). Data are mean ± SEM of triplicate filters.

In umbilical vein endothelial cells no change in $[Ca^{2+}]_i$ was observed. On the other hand, in the absence of IBMX, cAMP increased after stimulation with thrombin from 1.9 ± 0.5 to 2.6 ± 0.2 pmol/ 3.5×10^5 cells (three different cultures). The thrombin-induced increase in cAMP was reduced by L-NAME to 2.1 ± 0.1 pmol/ 3.5×10^5 cells.

Discussion

In this study we have presented evidence that endogenous production of NO attenuates the thrombin-induced increase in permeability by a cGMP-dependent mechanism. Elevation of the cGMP concentration acts on the regulation of permeability by suppressing the elevation of $[Ca^{2+}]_i$ via cGMP-dependent kinase and by elevation of the cellular cAMP concentration via the cGMP-dependent inhibition of PDE III. The relative contribution of these mechanisms is different in human aortic and umbilical vein endothelial cells.

Mechanisms involved in cGMP-dependent reduction of thrombin-stimulated endothelial permeability. Previous reports have shown that elevation of the cellular cGMP concentration reduces the increase in endothelial permeability induced by thrombin.^{16,19} Our data confirm these observations and identify two mechanisms by which cGMP acts on endothelial permeability: 1) reduction of the increase in $[Ca^{2+}]_i$ induced by thrombin, and 2) elevation of the cellular cAMP concentration by inhibition of PDE III. Ca^{2+} is involved in the induction of endothelial contraction.^{4,8,17}

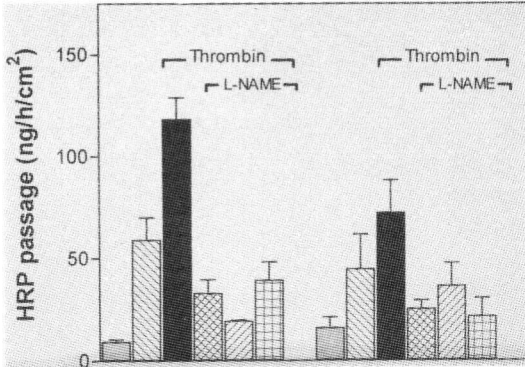


Figure 7. Bar graphs showing that cGMP-elevating agents reduce the L-NAME-dependent enhancement of thrombin-stimulated permeability of human aortic and pulmonary arterial endothelial cell monolayers. L-NAME (100 μ M, hatched bars) enhanced the increase in permeability induced by 1 U/ml thrombin (open bars); the permeability under control conditions is indicated by filled bars. Simultaneous addition of the cGMP-elevating agents atrial natriuretic peptide (ANP, 10^{-7} M), sodium

nitroprusside (SNP, 10^{-4} M) and 8-Br-cGMP (1 mM) reduced the increased permeability induced by thrombin and L-NAME. Left half: human aortic endothelial cell monolayers (two different cultures). Right half: human pulmonary arterial endothelial cell monolayers (three different cultures). Data are mean \pm SEM.

Our data with the intracellular Ca^{2+} ion chelator BAPTA demonstrate a direct relation between the rise in $[\text{Ca}^{2+}]_i$ and a rapid and prolonged increase in endothelial permeability after exposure to thrombin. The sustained elevation of the permeability, after $[\text{Ca}^{2+}]_i$ has returned to basal level, suggests the onset of other intracellular events.⁶ Two lines of evidence indicate that cGMP interferes with the Ca^{2+} -dependent increase in permeability, in particular in human aortic endothelial cells. First, the increase in permeability induced by thrombin was reduced by 8-PCPT-cGMP and 8-Br-cGMP at concentrations at which they selectively activate cGMP-dependent protein kinase compared to the activation of the cAMP-dependent protein kinase.^{40,41} We recently found that endothelial cells from human aorta, but not of the umbilical vein contain a considerable amount of cGMP-dependent protein kinase (Draijer *et al.*, manuscript in preparation). Second, direct assay of $[\text{Ca}^{2+}]_i$ in fura-2-loaded endothelial cells demonstrated a reduced accumulation of Ca^{2+} ions in the presence of 8-PCPT-cGMP. Reduction of $[\text{Ca}^{2+}]_i$ by activation of cGMP-dependent protein kinase is expected to reduce the Ca^{2+} /calmodulin-dependent phosphorylation of the myosin light chain kinase and the subsequent actin-nonmuscle myosin interaction.^{5,8,9} It is unlikely that cGMP reduces the Ca^{2+} response via interaction with the regulatory subunit of the cAMP-dependent protein kinase,⁴³ because 1 mM 8-Br-cAMP did not influence the thrombin-stimulated Ca^{2+} response. This observation is in accordance with the inability of cAMP-elevating agents to reduce accumulation of cytoplasmic Ca^{2+} ions induced by histamine.⁴⁴ The mechanism by which cGMP affects the accumulation of Ca^{2+} ions in aortic endothelial cells is not known. Analogous with findings in smooth muscle cells it may be expected that the cyclic nucleotide can induce a decrease in Ca^{2+} influx or an

increase in Ca^{2+} efflux.^{45,46} Ca^{2+} efflux from vascular smooth muscle cells was found to be stimulated by cGMP via $\text{Na}^+/\text{Ca}^{2+}$ -exchange.⁴⁷ Alternatively, it has been suggested that cGMP-dependent protein kinase activity causes reduction of cytoplasmic Ca^{2+} via suppression of inositol-1,4,5-trisphosphate formation⁴⁸ or via the stimulation of Ca^{2+} -ATPase pumps.^{22,23} Further studies are needed to elucidate whether one or several of these mechanisms are involved in the cGMP-dependent reduction of $[\text{Ca}^{2+}]_i$ in endothelial cells.

In addition to reducing cytoplasmic Ca^{2+} accumulation, cGMP also affects endothelial cell permeability by inhibiting cGMP-inhibited cAMP-phosphodiesterase (PDE III). PDE III has been demonstrated previously in endothelial cells^{49,50} and has been implicated in the control of endothelial permeability.⁴⁹ Inhibition of PDE III lowers the cellular breakdown of cAMP and enhances the steady state level of cAMP. Many studies have demonstrated that elevation of the cAMP concentration in endothelial cells can reduce endothelial permeability *in vivo*^{10,11,51} and *in vitro*.^{14,15} cAMP activates the cAMP-dependent protein kinase, which interferes with endothelial contraction by several mechanisms including reduction of the phosphorylation of the myosin light chain.⁹ Involvement of PDE III in cGMP-dependent reduction of the increased permeability mediated by thrombin was demonstrated in our study using two specific PDE III inhibitors, Indolidan and SKF94120.^{52,53} PDE III inhibition was found in human umbilical vein endothelial cells in particular, whereas only a small effect of the PDE III inhibitors was observed in human aortic endothelial cells. Thus, the PDE III activity may be different in various endothelial cell types. Alternatively, the PDE III activity of endothelial cells from aorta and umbilical vein may have been altered to a different degree during subculturing of the cells. In umbilical vein endothelial cells 8-PCPT-cGMP did not decrease the thrombin-induced permeability and in parallel reduced the thrombin-stimulated $[\text{Ca}^{2+}]_i$ rise only slightly. The fact that 8-Br-cGMP reduced the permeability of these cells can be explained by an inhibitory action of 8-Br-cGMP on PDE III, a property that is less prominent for 8-PCPT-cGMP.^{40,41}

NO acts as an endogenous modulator of endothelial cell function. The notion that cGMP can modulate endothelial $[\text{Ca}^{2+}]_i$ puts forward the question: Does NO, which induces cGMP generation by activation of soluble guanylate cyclase not only in smooth muscle cells and platelets^{54,55} but also in endothelial cells,^{56,57} act as an endogenous counter-regulatory molecule? Under normal noninflammatory conditions, NO is generated in endothelial cells by the constitutive NO synthase, the activity of which depends amongst others on Ca^{2+} /calmodulin.^{58,59} Thrombin evokes a rapid increase in $[\text{Ca}^{2+}]_i$ in endothelial cells. In accordance with the aforementioned feature of the constitutive NO synthase, thrombin causes a rapid and sustained elevation of NO generation⁶⁰ and an increase of the cGMP level (Reference 42 and the present

study) in human endothelial cells. Inhibition of NO synthase by L-NAME^{61,62} prevented cGMP accumulation. The enhancement of the thrombin-induced increase of endothelial permeability caused by preincubation of the cells with L-NAME suggests that the NO/cGMP generation indeed modulates endothelial contraction, at least partly by attenuating the cytoplasmic Ca^{2+} accumulation. This suggestion is further strengthened by the observation that the L-NAME-induced increase in permeability was abolished by adding agents that increase the cellular cGMP production independently of NO synthase. Furthermore, a preincubation with L-NAME caused an additional increase of the thrombin-induced $[\text{Ca}^{2+}]_i$ accumulation. Shin *et al.*⁵⁶ obtained comparable results with bovine aorta endothelial cells, in which ATP-induced $[\text{Ca}^{2+}]_i$ accumulation was enhanced by the NO-synthesis inhibitor N^G -monomethyl-L-arginine. Thrombin-induced NO/cGMP formation may, in umbilical vein endothelial cells, increase intracellular cAMP via inhibition of cAMP degradation. This was suggested by cAMP accumulation after thrombin stimulation in the presence of the PDE III-inhibitors SKF94120 and Indolidan. Additionally, thrombin-induced cAMP accumulation was blocked by L-NAME. A counter-regulatory role of NO/cGMP is probably to be found not only in the regulation of endothelial permeability, but also in other Ca^{2+} -dependent processes in the endothelial cells such as the generation of prostacyclin,⁶³ platelet activating factor⁶⁴ and NO itself,⁵⁹ and the release of von Willebrand factor and tissue-type plasminogen activator.⁶⁵ Indeed, Buga *et al.*⁶⁶ reported recently that NO is able to modulate its own generation.

Our observation that those endothelial cell monolayers that displayed a rather high permeability after exposure to thrombin (permeability coefficient $>5.5 \times 10^{-6}$ cm/s) were not affected by L-NAME was surprising but not contrary to our previous findings. These cells, for unknown reasons, are probably defective in the generation of NO and/or cGMP. This suggestion is favored by the observations that thrombin did not enhance the cellular cGMP concentration in such cells and that the thrombin-induced increase in permeability is excessively high. It further strengthens the hypothesis that Ca^{2+} -regulated NO production prevents excessive contraction of endothelial cells and impairment of their barrier function.

In conclusion, cGMP elevation attenuates the thrombin-induced increase in permeability of endothelial monolayers *in vitro*. cGMP can act via two pathways: cGMP reduces elevation of thrombin-stimulated $[\text{Ca}^{2+}]_i$ and reduces cAMP-degradation by inhibition of the PDE III activity. We postulate that autocrine nitric oxide can act as a permeability-counter-regulatory agent in endothelial cells.

Acknowledgement

We would like to thank Bea van der Vecht and Annette Seffelaar for excellent technical assistance.

This study was supported by the Netherlands Heart Foundation by grants 90.085 (R. Draijer) and 90.089 (D. E. Atsma).

References

1. Majno G, Gilmore V, Leventhal M. On the mechanism of vascular leakage caused by histamine-type mediators. *Circ Res.* 1967;21:833-847.
2. Grega GJ, Persson CGA, Svensjö E. Endothelial cell reactions to inflammatory mediators assessed in vivo by fluid and solute flux analysis, in Ryan US (ed): *Endothelial Cells vol. III.* Boca Raton, CRC Press, Inc., 1988, pp 103-119.
3. Laposata M, Dohnansky DK, Shin HS. Thrombin-induced gap formation in confluent endothelial cell monolayers in vitro. *Blood.* 1983;62:549-556.
4. Rotrosen D, Gallin JI. Histamine type I receptor occupancy increases endothelial cytosolic calcium, reduces F-actin, and promotes albumin diffusion across cultured endothelial monolayers. *J Cell Biol.* 1986;103:2379-2387.
5. Schnittler H-J, Wilke A, Gress T, Suttorp N, Drenckhahn D. Role of actin and myosin in the control of paracellular permeability in pig, rat and human vascular endothelium. *J Physiol. (Lond)* 1990;431:379-401.
6. Lum H, Andersen TT, Siflinger-Birnboim A, Tirupathi C, Goligorsky MS, Fenton II JW, Malik AB. Thrombin receptor peptide inhibits thrombin-induced increase in endothelial permeability by receptor desensitization. *J Cell Biol.* 1993;120:1491-1499.
7. Svensjö E, Grega GJ. Evidence for endothelial cell-mediated regulation of macromolecular permeability by postcapillary venules. *Federation Proc.* 1986;45:89-95.
8. Wysolmerski RB, Lagunoff D. Involvement of myosin light-chain kinase in endothelial cell retraction. *Proc Natl Acad Sci USA.* 1990;87:16-20.
9. Moy AB, Shasby SS, Scott BD, Shasby DM. The effect of histamine and cyclic adenosine monophosphate on myosin light chain phosphorylation in human umbilical vein endothelial cells. *J Clin Invest.* 1993;92:1198-1206.
10. Kobayashi H, Kobayashi T, Fukushima M. Effects of dibutyryl cAMP on pulmonary air embolism-induced lung injury in awake sheep. *J Appl Physiol.* 1987;63:2201-2207.
11. Inagaki N, Miura T, Daikoku H, Nagai H, Koda A. Inhibitory effects of Beta-adrenergic stimulants on increased vascular permeability caused by passive cutaneous anaphylaxis, allergic mediators, and mediator releasers in rats. *Pharmacology.* 1989;39:19-27.
12. Doorenbos CJ, Van Es A, Valentijn RM, Van Es LA. Systemic capillary leak syndrome. Preventive treatment with terbutaline. *Neth J Med.* 1988;32:178-184.
13. Droder RM, Kyle RA, Greipp PR. Control of systemic capillary leak syndrome with aminophylline and terbutaline. *Am J Med.* 1992;92:523-526.
14. Stelzner TJ, Weil JV, O'Brien RF. Role of cyclic adenosine monophosphate in the induction of endothelial barrier properties. *J Cell Physiol.* 1989;139:157-166.

Appendix

15. Langelier EG, Van Hinsbergh VWM. Norepinephrine and iloprost improve barrier function of human endothelial cell monolayers: role of cAMP. *Am J Physiol*. 1991;260:C2052-2059.
16. Baron DA, Lofton CE, Newman WH, Currie MG. Atriopeptin inhibition of thrombin-mediated changes in the morphology and permeability of endothelial monolayers. *Proc Natl Acad Sci U S A*. 1989;86:3394-3398.
17. Yamada Y, Furumichi T, Furui H, Yokoi T, Ito T, Yamauchi K, Yokota M, Hayashi H, Saito H. Roles of calcium, cyclic nucleotides, and protein kinase C in regulation of endothelial permeability. *Arteriosclerosis*. 1990;10:410-420.
18. Westendorp RGJ, Draijer R, Meinders AE, Van Hinsbergh VWM. Cyclic GMP mediated decrease in permeability of human umbilical and pulmonary artery endothelial cell monolayers. *J Vasc Res*. 1994;31:42-52
19. Lofton CE, Newman WH, Currie MG. Atrial natriuretic peptide regulation of endothelial permeability is mediated by cGMP. *Biochem Biophys Res Commun*. 1990;172:793-799.
20. Lofton CE, Baron DA, Heffner JE, Currie MG, Newman WH. Atrial natriuretic peptide inhibits oxidant-induced increases in endothelial permeability. *J Mol Cell Cardiol*. 1991;23:919-927.
21. Popescu LM, Panoiu C, Hinescu M, Nutu O. The mechanism of cGMP-induced relaxation in vascular smooth muscle. *Eur J Pharmacol*. 1985;107:393-394.
22. Vrolix M, Raeymaekers L, Wuytack F, Hofmann F, Casteels R. Cyclic GMP-dependent protein kinase stimulates the plasmalemmal Ca^{2+} pump of smooth muscle via phosphorylation of phosphatidylinositol. *Biochem J*. 1988;255:855-863.
23. Yoshida Y, Sun H-T, Cai J-Q, Imai S. Cyclic GMP-dependent protein kinase stimulates the plasma membrane Ca^{2+} pump ATPase of smooth muscle via phosphorylation of a 240-kDa protein. *J Biol Chem*. 1991;266:19819-19825.
24. Beavo JA, Reifsnnyder DH. Primary sequence of cyclic nucleotide phosphodiesterase isozymes and the design of selective inhibitors. *TIPS*. 1990;11:150-155.
25. Nicholson CD, Challiss RAJ, Shahid M. Differential modulation of tissue function and therapeutic potential of selective inhibitors of cyclic nucleotide phosphodiesterase isoenzymes. *TIPS*. 1991;12:19-27.
26. Bredt DS, Hwang PM, Snyder SH. Localization of nitric oxide synthase indicating a neural role for nitric oxide. *Nature*. 1990;347:768-769.
27. Lowenstein CJ, Snyder SH. Nitric oxide, a novel biologic messenger. *Cell*. 1992;70:705-707.
28. Maciag T, Cerundolo J, Ilsley S, Kelley PR, Forand R. An endothelial growth factor from bovine hypothalamus: identification and partial characterization. *Proc Natl Acad Sci U S A*. 1979;76:5674-5678.
29. Jaffe EA, Nachman RL, Becker CG, Minick CR. Culture of human endothelial cells derived from umbilical veins. Identification by morphologic and immunologic criteria. *J Clin Invest*. 1973;52:2745-2746.
30. Van Hinsbergh VWM, Mommaas-Kienhuis AM, Weinstein R, Maciag T. Propagation and morphologic phenotypes of human umbilical cord artery endothelial cells. *Eur J Cell Biol*. 1986;42:101-110.
31. Van Hinsbergh VWM, Binnema D, Scheffer MA, Sprengers ED, Kooistra T, Rijken DC. Production of plasminogen activators and inhibitors by serially propagated endothelial cells from adult human blood vessels. *Arteriosclerosis*. 1987;7:389-400.
32. Langelier EG, Van Hinsbergh VWM. Characterization of an in vitro model to study the permeability of human arterial endothelial cell monolayers. *Thromb Haemostas*. 1988;60:240-246.

33. Langelier EG, Snelting-Havinga I, Van Hinsbergh VWM. Passage of low density lipoproteins through monolayers of human arterial endothelial cells. Effects of vasoactive substances in an in vitro model. *Arteriosclerosis*. 1989;9:550-559.
34. Deelder AM, Koper G, De Water R, Tanke HJ, Rotmans JP, Ploem JS. Automated measurement of immunogalactosidase reactions with a fluorogenic substrate by the aperture defined microvolume measurement method and its potential application to *Schistosoma mansoni* immunodiagnosis. *J Immunol Meth*. 1980;36:269-283.
35. Steiner AL, Parker CW, Kipnis DM. Radioimmunoassay for cyclic nucleotides. Preparation of antibodies and iodinated cyclic nucleotides. *J Biol Chem*. 1972;247:1106-1113.
36. Ince C, Van Dissel JT, Disselhof-den Dulk MMC. A teflon culture dish for high magnification observations and measurements from single cells. *Eur J Physiol*. 1985;403:240-244.
37. Atsma DE, Bastiaanse EML, Ince C, Van der Laarse A. A novel two-compartment culture dish allows microscopic evaluation of two different treatments in one cell culture simultaneously: Influence of external pH on $\text{Na}^+/\text{Ca}^{2+}$ exchanger activity in cultured rat cardiomyocytes. *Pflügers Arch*. 1994;3-4:296-299.
38. Gryniewicz G, Poenie M, Tsien RY. A new generation of Ca^{2+} indicators with greatly improved fluorescence properties. *J Biol Chem*. 1985;260:3440-3450.
39. Merritt JE, Armstrong WP, Benham CD, Hallam TJ, Jacob R, Jaxa-Chamiec A, Leigh BK, McCarthy SA, Moores KE, Rink TJ. SK&F96365, a novel inhibitor of receptor-mediated calcium entry. *Biochem J*. 1990;271:515-522.
40. Butt E, Nolte C, Schulz S, Beltman J, Beavo J, Jastorff B, Walter U. Analysis of the functional role of cGMP-dependent protein kinase in intact human platelets using a specific activator 8-PCPT-cGMP. *Biochem Pharmacol*. 1992;43:2591-2600.
41. Francis SH, Noblett BD, Todd BW, Wells JN, Corbin JD. Relaxation of vascular and tracheal smooth muscle by cyclic nucleotide analogs that preferentially activate purified cGMP-dependent protein kinase. *Mol Pharmacol*. 1988;34:506-517.
42. Adams Brotherton AF. Induction of prostacyclin biosynthesis is closely associated with increased guanosine 3'-5'-cyclic monophosphate accumulation in cultured human endothelium. *J Clin Invest*. 1986;78:1253-1260.
43. Buchan KW, Martin W. Modulation of barrier function of bovine aortic and pulmonary artery endothelial cells: dissociation from cytosolic calcium content. *Br J Pharmacol*. 1992;107:932-938.
44. Carson MR, Shasby SS, Shasby DM. Histamine and inositol phosphate accumulation in endothelium: cAMP and a G protein. *Am J Physiol*. 1989;257:L259-L264.
45. McDaniel NL, Chen X-L, Singer HA, Murphy RA, Rembold CM. Nitrovasodilators relax arterial smooth muscle by decreasing $[\text{Ca}^{2+}]_i$ and uncoupling stress from myosin phosphorylation. *Am J Physiol*. 1992;263:C461-C467.
46. Chen X-L, Rembold CM. Cyclic nucleotide-dependent regulation of Mn^{2+} influx, $[\text{Ca}^{2+}]_i$, and arterial smooth muscle relaxation. *Am J Physiol*. 1992;263:C468-C473.
47. Furukawa K-I, Ohshima N, Tawada-Iwata Y, Shigekawa M. Cyclic GMP stimulates $\text{Na}^+/\text{Ca}^{2+}$ exchange in vascular smooth muscle cells in primary culture. *J Biol Chem*. 1991;266:12337-12341.
48. Ruth P, Wang G-X, Boekhoff I, May B, Pfeifer A, Penner R, Korth M, Breer H, Hofmann F. Transfected cGMP-dependent protein kinase suppresses calcium transients by inhibition of inositol 1,4,5-triphosphate production. *Proc Natl Acad Sci USA*. 1993;90:2623-2627.
49. Suttorp N, Weber U, Welsch T, Schudt C. Role of phosphodiesterases in the regulation of endothelial permeability in vitro. *J Clin Invest*. 1993;91:1421-1428.

Appendix

50. Tani T, Sakurai K, Kimura Y, Ishikawa T, Hidaka H. Pharmacological manipulation of tissue cyclic AMP by inhibitors: effects of phosphodiesterase inhibitors on the function of platelets and vascular endothelial cells. *Adv Sec Mess Phosphoprot Res.* 1992;25:215-227.
51. Warren JB, Wilson AJ, Loi RK, Coughlan ML. Opposing roles of cyclic AMP in the vascular control of edema formation. *FASEB J.* 1993;7:1394-1400.
52. Simpson AWM, Reeves ML, Rink TJ. Effects of SK&F94120, an inhibitor of cyclic nucleotide phosphodiesterase type III, on human platelets. *Biochem Pharmacol.* 1988;37:2315-2320.
53. Kaufmann RF, Crowe VG, Utterback BG, Robertson DW. LY195115: inhibition of membrane-bound cAMP phosphodiesterase. *Mol Pharmacol.* 1987;30:609-616.
54. Ignarro LJ. Haem-dependent activation of cytosolic guanylate cyclase by nitric oxide: a widespread signal transduction mechanism. *Biochem Soc Trans.* 1992;20:465-469.
55. Geiger J, Nolte C, Butt E, Sage SO, Walter U. Role of cGMP and cGMP-dependent protein kinase in nitrovasodilator inhibition of agonist-evoked calcium elevation in human platelets. *Proc Natl Acad Sci U S A.* 1992;89:1031-1035.
56. Shin WS, Sasaki T, Kato M, Hara K, Seko A, Yang W-D, Shimamoto N, Sugimoto T, Toyo-oka T. Autocrine and paracrine effects of endothelium-derived relaxing factor on intracellular Ca^{2+} of endothelial cells and vascular smooth muscle cells. Identification by two-dimensional image analysis in coculture. *J Biol Chem.* 1992;267:20377-20382.
57. Boulanger C, Schini VB, Moncada S, Vanhoutte PM. Stimulation of cyclic GMP production in cultured endothelial cells of the pig by bradykinin, adenosine diphosphate, calcium ionophore A23187 and nitric oxide. *Br J Pharmacol.* 1990;101:152-156.
58. Schini VB, Vanhoutte PM. Inhibitors of calmodulin impair the constitutive but not the inducible nitric oxide synthase activity in the rat aorta. *J Pharmacol Exp Ther.* 1992;261:553-559.
59. Förstermann U, Pollock JS, Schmidt HHHW, Heller M, Murad F. Calmodulin-dependent endothelium-derived relaxing factor/nitric oxide synthase activity is present in the particulate and cytosolic fractions of bovine aortic endothelial cells. *Proc Natl Acad Sci U S A.* 1991;88:1788-1792.
60. Tsukahara H, Gordienko DV, Goligorsky MS. Continuous monitoring of nitric oxide release from human umbilical vein endothelial cells. *Biochem Biophys Res Commun.* 1993;193:722-729.
61. Rees DD, Palmer RMJ, Schulz R, Hodson HF, Moncada S. Characterization of three inhibitors of endothelial nitric oxide synthase in vitro and in vivo. *Br J Pharmacol.* 1990;101:746-752.
62. Randall MD, Griffith TD. Differential effects of L-arginine on the inhibition by N^G -nitro-L-arginine methyl ester of basal and agonist-stimulated EDRF activity. *Br J Pharmacol.* 1991;104:743-749.
63. Adams Brotherton AFA, Hoak JC. Role of Ca^{2+} and cAMP in the regulation of the production of prostacyclin by the vascular endothelium. *Proc Natl Acad Sci U S A.* 1982;79:495-499.
64. Brock TA, Gimbrone Jr MA. Platelet activating factor alters calcium homeostasis in cultured vascular endothelial cells. *Am J Physiol.* 1986;250:H1086-H1092.
65. Tranquille N, Emeis JJ. The simultaneous acute release of tissue-type plasminogen activator and von Willebrand factor in the perfused rat hindleg region. *Thromb Haemostas.* 1990;63:454-458.
66. Buga GM, Griscavage JM, Rogers NE, Ignarro LJ. Negative feedback regulation of endothelial cell function by nitric oxide. *Circ Res.* 1993;73:808-812.